Cellular responses to replication problems

Magdalena Budzowska

Cellular Responses to Replication Problems

Cellulaire respons na replicatie problemen

Proefschrift

ter verkrijging van de graad van doctor aan de
Erasmus Universiteit Rotterdam
op gezag van de
rector magnificus

Prof.dr. S.W.J. Lamberts

en volgens besluit van het College voor Promoties

De openbare verdediging zal plaatsvinden op
woensdag 26 maart 2008 om 11:45 uur

door

Magdalena Budzowska

geboren te Krakow, Poland

ERASMUS UNIVERSITEIT ROTTERDAM
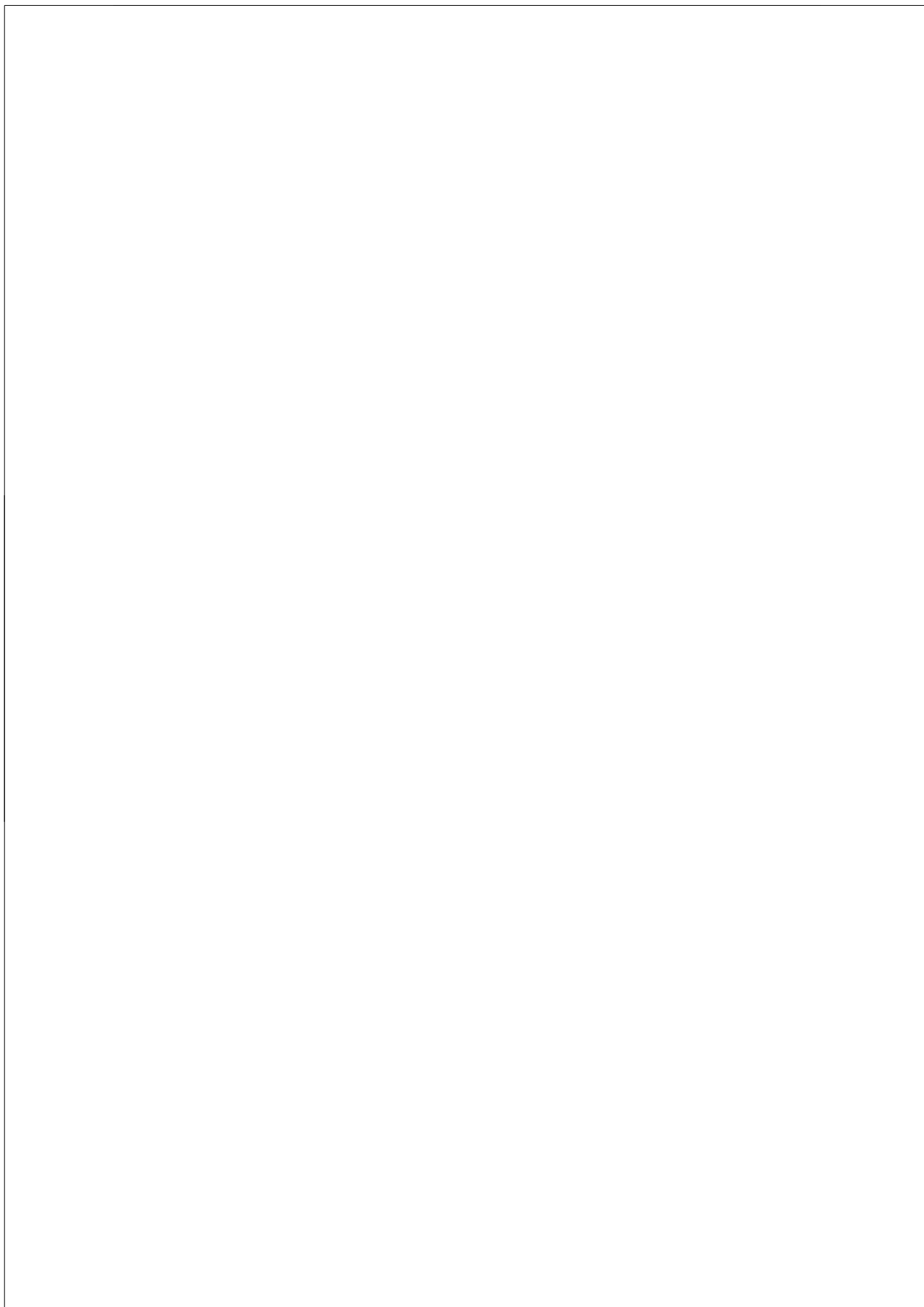
Promotiecommissie

Promotoren:	Prof.dr. R. Kanaar
	Prof.dr. J.H.J. Hoeijmakers
Overige leden:	Prof.dr. T.K. Sixma
	Dr. C. Wyman
	Dr. H. Vrieling
Copromotor:	Dr. A. Maas

Contents

Aim of the thesis

During every S-phase cells need to duplicate their genomes so that both daughter cells inherit complete copies of genetic information. It is a tremendous task, given the large sizes of mammalian genomes and the required precision of DNA replication. A major threat to the accuracy and efficiency of DNA synthesis is the presence of damaged DNA, e.g. abasic sites, single stranded DNA breaks, DNA crosslinks and adducts. This damage can be caused by exogenous agents, e.g. UV light, ionizing radiation, or environmental carcinogens, but is also an inevitable consequence of normal cellular metabolism. Replicative DNA polymerases, which carry out the bulk of DNA synthesis, evolved to do their job extremely precisely and efficiently. However, they are unable to use damaged DNA as templates, and, consequently, are stopped at most DNA lesions. Failure to restart such stalled forks can result in major chromosomal aberrations and lead to cell dysfunction or death. Therefore, a well-coordinated response to replication perturbation is essential for cell survival and wellbeing. It involves adjusting cell cycle progression to the emergency situation, and the use of specialized pathways promoting replication recovery. The aim of this thesis was to contribute to our understanding of the mechanisms the cell employs to deal with replication problems.

Chapter 1 briefly summarizes the current knowledge of how cells sense DNA damage and/or stalled replication, and how they subsequently activate intricate signaling cascades called DNA damage checkpoints. Checkpoint signaling can inhibit cell cycle at G1/S and G2/M transitions, and slow down progression of S-phase, to allow the affected cell sufficient time for repair and/or overcoming replication blocks. Two main mechanisms that promote replication recovery: homologous recombination and translesion synthesis are described in the second part of chapter 1.

Efficient checkpoint signaling is required for survival of mammalian cells. **Chapter 2** examines the consequences of deletion or N-terminal truncation of mouse Rad17 on the survival of organisms and cells. It shows that Rad17 is required for correct response to a wide range of DNA-damaging agents. Surprisingly, the data presented in this chapter suggest that, in addition to its role in checkpoint signaling, Rad17 is also directly involved in DNA metabolism. The responses of cells expressing truncated Rad17 to agents that directly interfere with DNA replication are further analyzed in **chapter 3**.

Slower progression through S-phase and delayed entry into mitosis give the cells the opportunity to solve replication problems. However, restarting stalled forks might, in some cases, be a rather difficult task. When cells are treated with crosslinking agents, particularly toxic DNA lesions are created. Interstrand crosslinks (ICLs) covalently bind two complementary DNA strands and thus block DNA unwinding, required for DNA replication. Since ICLs affect both DNA strands, their removal and subsequent restart of the stalled forks is a complex process, during which DNA double strand break (DSB) intermediates can be created. **Chapter 4** presents evidence that Mus81/Eme1 endonuclease is the enzyme responsible for generating DSB in response to crosslinking agents and describes how these potentially dangerous intermediates can promote subsequent repair processes and cell survival. In **chapter 5** the response of Mus81-deficient cells to replication inhibitors is analyzed in order

to discriminate whether Mus81 is involved in crosslink-specific repair pathways, or responds to stalled replication in general. Furthermore, the consequences of loss of Mus81 function on replication recovery are examined.

Stalled or collapsed replication forks are suitable substrates for homologous recombination. RAD51-mediated recombination promotes reestablishing of the intact fork, therefore allowing DNA synthesis to continue. This function makes homologous recombination essential for cell survival. However, uncontrolled or incorrect recombination reactions can be dangerous, since they can cause i.e. deletions, insertions, translocations and loss of heterozygosity. A strict control of homologous recombination is necessary to promote its beneficial actions and avoid its potentially detrimental effects. Mammalian cells have a number of essential proteins called recombination mediators that regulate every step of the recombination reaction. **Chapter 6** presents a novel mediator protein RAD51AP1, and provides evidence that it directly influences RAD51-mediated strand exchange *in vitro*, and affects recombination reactions *in vivo*.

Chapter 1

Introduction

1. The cell cycle machinery

During every cell cycle genomic DNA has to be faithfully and completely replicated and correctly separated so that both daughter cells inherit intact copies of the genetic material. To ensure the proper timing and coordination of these events, the cell cycle machinery is controlled by a complex web of regulatory pathways. They converge on cyclin-dependent protein kinases (CDKs), which are responsible for triggering the major transitions of the eukaryotic cell cycle. The CDK levels remain constant during normal cell cycle, and their catalytic activity is regulated mainly post-translationally, by several conserved mechanisms.

Activation of all CDKs requires the binding of a positive regulatory subunit known as a cyclin (1) (Fig 1). Each phase of the cell cycle is characterized by expression of a specific type of cyclin, and oscillation in cyclin levels represents the primary mechanism by which CDK activity is regulated. The first cyclins to be expressed in G1 phase are D-type cyclins (D1, D2 and D3), which bind CDK4 and CDK6 (2). The major substrates of cylin D-CDK4/6 complexes are proteins from the retinoblastoma (Rb) family, which bind and inhibit several growth-stimulating proteins. The CDK-mediated phosphorylation of Rb proteins abolishes this association, releases the stimulating proteins, and activates progression through the cell cycle (3). Next, cyclin E is expressed in mid to late G1-phase (4,5). The kinase activity of cyclin
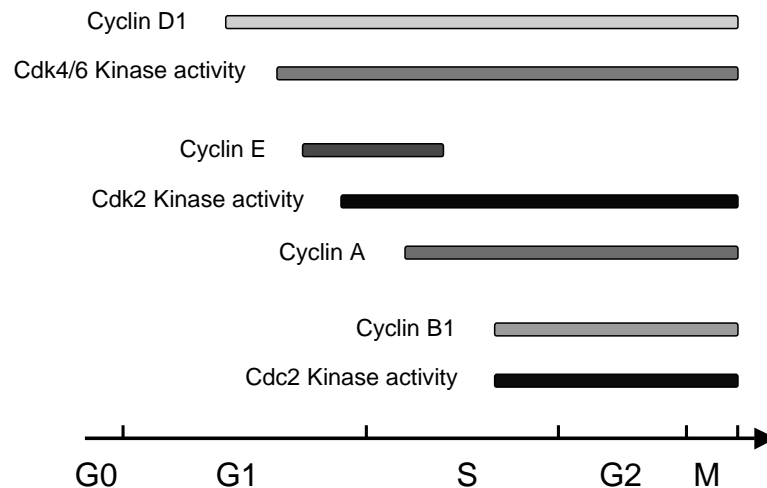

Figure 1. Expression patterns of cyclins and CDKs during the cell cycle.
Adapted from ref. (11). See text for details.

E/CDK2 complex is required for S-phase entry and the initiation of DNA replication (6,7). Cyclin A is expressed soon after cyclin E at the G1/S boundary, and also forms a complex with CDK2 and, to a lesser extent, with CDC2 (8). The activity of cyclin A/CDC2 is required for S-phase transition and the control of DNA replication (9). Cyclin B associates with CDC2 and is expressed in late S and G2 phases; however, cyclin B/CDC2 complexes remain inactive until late G2, when their activation triggers entry into mitosis (10). Targets of cyclin B/CDC2 include both structural proteins involved in execution of mitotic events, and regulatory proteins that are necessary for the control and timing of these processes.

In addition to cyclin binding, CDK activation requires the phosphorylation of a conserved threonine residue by the CDK-activating kinase (CAK), whose activity is also cyclin-dependent. The active cyclin-CDK complexes can be inhibited by phosphorylation of residues near the N-terminus. The enzymes responsible for phosphorylating CDK2 are the dual-specificity kinases Wee1 and Myt1, whose activities are regulated by phosphorylation and subcellular localization. The inhibitory phosphates are removed from CDKs by CDC25 phosphatases. Another mechanism of regulating cyclin/CDK activity involves CDK inhibitors (CKIs), which bind and inactivate cyclin-CDK complexes (11).

2. DNA damage checkpoints

The cell cycle checkpoints monitor the cell cycle progression and ensure that the cell proceeds to the next step only after completion of the previous one. They act by regulating the core cell cycle machinery briefly described above. The consequences of dysfunction of these control mechanisms may be catastrophic, e.g. entering mitosis before DNA replication has been finished will cause chromosomal breakage, which could result in chromosomal aberrations and cell death. Therefore, correct coordination of the cell cycle events is essential for cell viability during normal growth conditions.

This regulation becomes even more critical in the presence of DNA damage. DNA is constantly injured by a variety of damaging agents. The threat comes from inside a cell in the form of by-products of normal metabolism, e.g. reactive oxygen species and free radicals. DNA damage can also be caused by exogenous sources, e.g. UV light, ionizing radiation, and toxic chemicals. DNA lesions also arise spontaneously, e.g. depurinations. Cells are equipped with a number of repair pathways that remove the damage and restore the intact DNA, but they are not sufficient to fully protect the cells against DNA lesions. The efficient response to the dangerous situation requires the presence of DNA damage checkpoints. In response to DNA damage these checkpoints activate signaling cascades that regulate the activity of different components of the cell cycle machinery. The resulting delay or temporal arrest of the cell cycle progression gives the affected cells time to repair the damage (12). The damage signaling can stop the cell cycle at the G1/S and G2/M transitions and slow down progression through S-phase. The principal mechanisms by which this regulation is achieved are briefly described below.

2.1. G1/S checkpoint

Replication of damaged DNA is likely to cause stalling of replication forks and accumulation of potentially dangerous mutations. To protect genomic integrity it is important to repair the damaged DNA before it is used as a template for DNA synthesis. Damage-induced G1/S checkpoint causes cell cycle arrest before the onset of DNA synthesis, thus giving the cell time to repair the damaged DNA before an attempt to replicate it. The main player of this checkpoint is a tumor suppressor protein and a transcription factor p53. In undamaged cells p53 forms a complex with ubiquitin ligase MDM2. The constitutive ubiquitination of p53 targets it for proteosomal degradation, ensuring rapid turnover of p53 (13). DNA damage activates signaling cascades, which act to stabilize and activate p53 via multiple redundant mechanisms (see below), thus allowing p53 to activate transcription of many genes including the gene encoding CDK inhibitor p21 (Fig 2). Increase in p21 expression suppresses cyclin E and cyclin A-associated CDK activities, and thereby prevents progression to S-phase (14). Alternatively, in case of severe DNA damage p53 can induce expression of Puma, Noxa and Bax to activate caspases and induce apoptosis (15).

2.2. Intra-S checkpoint

Despite the action of the G1/S checkpoint it is not always possible to avoid the presence of damaged DNA templates during DNA replication, since DNA damage can be introduced during S-phase. Additionally, some types of DNA lesions, e.g. interstrand DNA crosslinks, cause only mild distortion of the DNA helix and often remain unrecognized and unrepaired until they interfere with replication and/or transcription (16). Moreover, natural replication pause sites caused by e.g. convergent transcription or DNA secondary structures, can lead to replication fork stalling. Intra-S checkpoint signaling helps to protect the cells experiencing such problems, and promotes their survival. The main role of this checkpoint is to inhibit firing of late origins and to stabilize stalled replication forks (17) (Fig 2). The inhibition of late origin firing reduces the level of ongoing replication. It also leads to extended duration of S-phase, which may provide additional time to restart the stalled and/or collapsed replication forks. The stabilization of stalled replication forks helps to prevent accumulation of unusual DNA structures at the forks, which could lead to irreversible fork collapse and subsequent cell death. Consistently, yeast *Saccharomyces cerevisiae*, defective in intra-S checkpoint signaling due to lack of mec1 (upstream checkpoint component, homolog of human ATR), cannot complete DNA replication in the presence of DNA damage (18). In contrast, cells expressing the hypomorphic mec1 allele (mec1-100) are unable to inhibit late origin firing in response to DNA damage, but can complete replication of damaged DNA (19). These results show that the two functions of the intra-S checkpoint can be separated, at least in *S. cerevisiae*, and suggest that the main, life-saving role of this checkpoint is to protect and stabilize the replication forks stalled at lesions.

2.3. G2/M checkpoint

The role of the G2/M checkpoint is to ensure that chromosomes are intact and ready for separation before the cell is allowed to enter mitosis. This control point is

very important for genomic stability, since an attempt to segregate partially replicated chromosomes will result in DNA breakage and lead to chromosomal aberrations and aneuploidy. The main cell cycle protein targeted by this checkpoint is CDC2. The activation of CDC2 is regulated by inhibitory phosphorylation of Tyr15 by Wee1 and activating de-phosporylation of this residue by CDC25 phosphatases (Fig 2). So, in order to prevent activation of CDC2 and subsequent entry into mitosis, the cells need to maintain its phosphorylation by either increasing Wee1 activity or inhibiting CDC25. In response to DNA damage both Wee1 and CDC25 are phosphorylated in a checkpoint-dependent manner in yeast *Saccharomyces pombe* and both events contribute to the efficient cell cycle arrest. Wee1 phosphorylation results in its stabilization. The damage-induced phosphorylation of CDC25 leads to changes in its activity and subcellular localization.

The essential role of the checkpoint acting in G2 is to prevent segregation of partially replicated or damaged DNA. However, several lines of evidence suggest that cells might in fact lack efficient and/or absolute control mechanisms that would delay mitosis in the presence of aberrant DNA structures. It has been shown recently that in yeast cells lacking functional Smc6 protein replication forks are still present as cells enter mitosis (20). Chromosomal aberrations observed in many repair-deficient cell lines, e.g. Ercc1 or Mus81 knockout cells arise as a result of segregating unrepaired DNA (21,22). Fragile sites may represent late-replicating regions, at which DNA replication might not be finished before the subsequent mitosis. Such partially replicated DNA molecules will then be torn as chromosomes are pulled apart by the mitotic spindle. Since these events should in principle be prevented by the G2 checkpoint, it has been suggested that the cells do not check whether the chromosomes are ready to be segregated. However, it seems more likely that the control in G2 phase does exists, although it is not as strict as proposed before. This idea is supported by the recent discovery that ultrafine DNA fibers connecting two daughter genomes can be found in a remarkably high percentage of anaphase cells (23). This data shows that a large number of cells enter mitosis with low levels of incompletely separated DNA. However, the cells appear to have mechanisms able to resolve such structures before cytokinesis and presumably prevent chromosomal aberrations.

The picture emerging form these studies shows that the cells appear to ignore low levels of DNA damage. The reasons for such tolerance are not completely clear. It has been suggested that cells have limited time (measured in a replication-independent manner) to finish DNA replication and divide (24,25). Such mechanism could serve to prevent cells from staying in the G2 phase, which might lead to the formation of polyploid cells in organs where they normally do not arise.

2.4. DNA damage checkpoints are controlled by ATM and ATR

ATM and ATR are two main proteins, which activate checkpoint signaling in response to DNA damage. They belong to a structurally conserved family, which in mammalian cells includes SMG-1, mTOR and DNA-PK$_{CS}$. The members of this family contain catalytic domains resembling those found in lipid kinase phosphatidylinositol 3-kinase (PI3K), and are therefore called 'PI3K-like protein kinases' (PIKKs). Although related to a lipid kinase, they phosporylate proteins on serine and threonine residues.
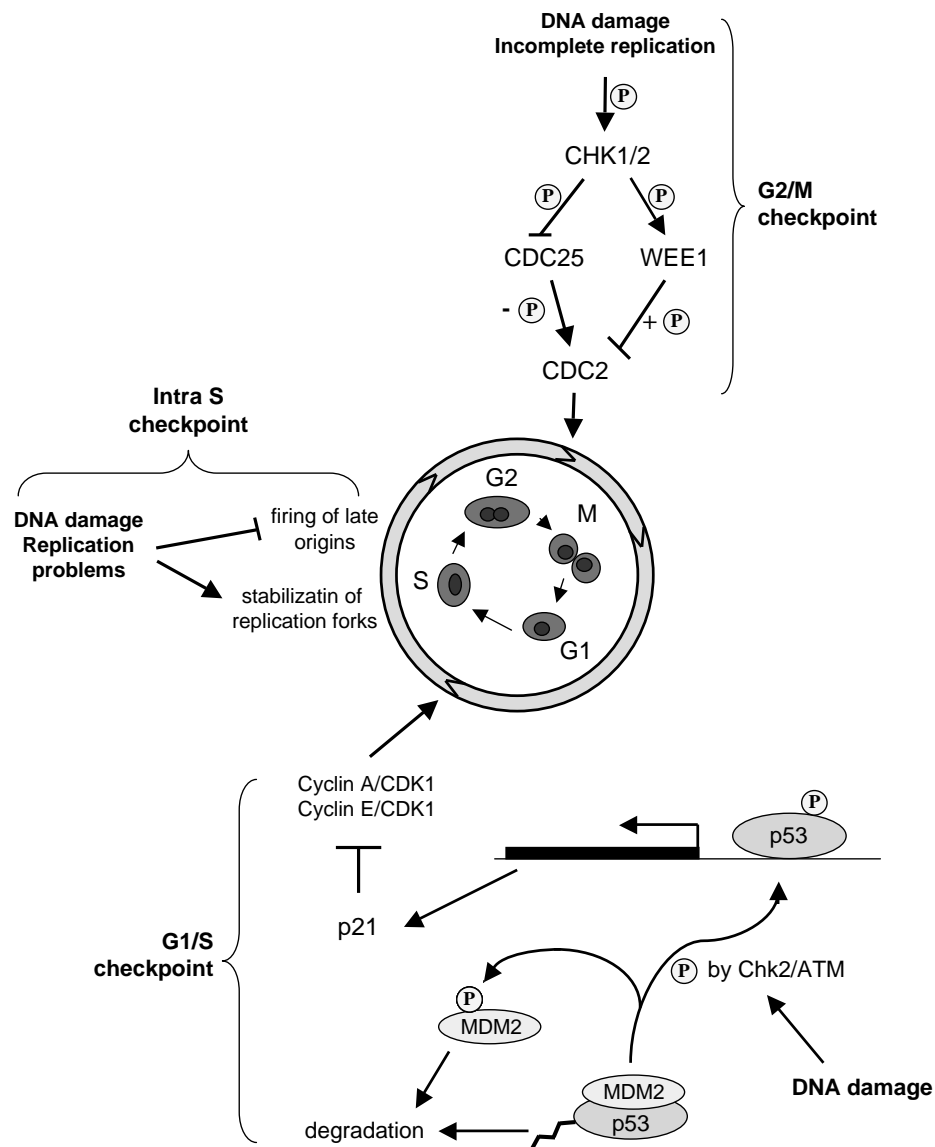
Figure 2. Schematic representation of the cell cycle proteins and processes targeted by different DNA damage checkpoints.
DNA damage can arrest cell cycle progression at the G1/S and G2/M transitions, and slow down S-phase progression. The main target of the G1/S checkpoint is the tumor suppressor protein p53, which is stabilized and activated by the damage signaling. The S-phase checkpoint promotes stabilization of replication forks and inhibition of late origin firing. The entry into mitosis is controlled by the Cyclin B/CDC2 kinase, which is inhibited by the G2/M checkpoint.

Their preferred substrates contain SQ/TQ motifs, in which the serine or threonine is directly followed by glutamine (26). Such motifs are often found in clusters, and SQ/TQ-rich domains are especially common in proteins involved in checkpoint signaling and DNA repair, e.g. in BRCA1 and CHK1.

The PIKKs are very large polypetides, ranging from 270 to 450 kDa. Their conserved kinase domain occupies only 5-10% of the protein, and is located at the C-terminus (Fig 3). It is flanked by FAT and FATC domains, which span approximately 500 and 35 amino acids, respectively (27). Although these domains have no catalytic activity, they are essential for kinase activity of the protein, probably by promoting its correct folding. The N-termini of ATM and ATR are composed of a large number of HEAT repeats (Huntingtin, Elongation factor 3, A subunit of protein phosphatase 2A, and mTOR repeats), which are involved in protein-protein interactions (28) (Fig 3). Such an abundance of potential interaction sites indicates that both kinases are likely to be engaged in various dynamic complexes. It is not surprising, considering their central position in checkpoint signaling cascades.

ATM and ATR have distinct, although partially overlapping functions. ATM responds primarily to DSBs, while ATR is activated by replication stress and a wide range of DNA damaging agents, including UV light, alkylating agents, and DSBs. ATM and ATR share many substrates, and accumulating evidence shows that there is crosstalk between ATR- and ATM-controlled pathways. However, the different phenotypes of ATM- and ATR-deficient mice and cells indicate that these kinases are not completely redundant.
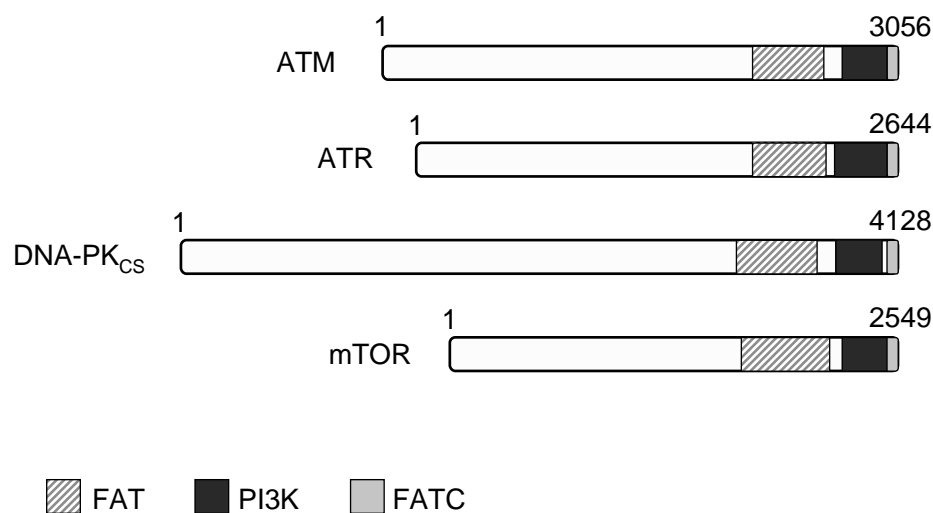

Figure 3. The domain organization of PI3KK family members.
The three common motifs of the PI3K-like kinases: FAT, PI3K-like catalytic domain, and FATC are indicated. The N-terminal parts of the proteins consist of a large number of HEAT repeats, involved in protein-protein interactions.

2.4.1. ATM-dependent checkpoint signaling

The ATM protein was identified as the product of a gene mutated in the severe human genetic disorder ataxia telangiectasia (A-T). A-T is characterized by cerebellar degeneration (which causes progressive neuromotor dysfuntion), immunodeficiency, genomic instability, a striking predisposition to lymphorecticular malignancies, and extreme sensitivity to ionizing radiation and DSB-inducing agents (29,30). Consistently, cultured cells from A-T patients show defects in almost all of the known branches of the DSB response (31). Such a broad defect places ATM at the central position of the damage response pathway.

Activation of ATM

ATM is specifically activated by DSBs *in vivo*. Consistent with its upstream position in the signaling cascade, ATM responds very quickly to DSB induction. Within seconds after irradiation ATM kinase activity rapidly increases. However, the actual stimulus required to initiate the signaling cascade, the exact requirements for ATM activation, and the precise order of the events remain elusive. It is clear that at least three events are important for ATM activation: (1) ATM autophosporylation, (2) the recruitment of ATM to the sites of DSBs and its interaction with the MRE11/RAD50/NBS1 (MRN) complex and (3) the action of acetyltransferases, which cause DSB-induced changes of chromatin structure and acetylation of ATM itself (Fig 4).

ATM autophosporylation

A critical event in damage-induced ATM activation is its autophosphorylation, leading to the dissociation of an inactive dimer, in which the kinase domain of each molecule is blocked by the FAT domain of the other, to active monomers, which are in turn free to phosphorylate a range of substrates (32) (Fig 4). Almost maximal ATM autophosphorylation occurs within minutes, even after very low radiation doses. The first identified autophosphorylation site was S1981, but subsequent analysis revealed at least two more sites, S367 and S1893 (33). The phosphorylation mutants (S367A, S1893A and S1981A) failed to correct radio sensitivity, genome instability and cell cycle checkpoint defects in A-T cells, showing that all three sites are physiologically important for ATM-controlled damage response (33).

The S1981A mutant tranfected into A-T cells failed to support phosphorylation of p53 on S15, and its expression had a dominant negative effect on wild type ATM signaling (32). It was therefore surprising that mice expressing S1987A ATM mutant (corresponding to human S1981A mutation) showed normal ATM-dependent responses (34). This discrepancy can be caused by inherent differences between species - it is possible that autophosphorylation is dispensable for ATM activation in mice, and that other post-transcriptional modifications might be of primary importance. Alternatively, the regulation by autophosphorylation may be conserved, but the relative importance of different phosphorylation sites may differ between mouse and human cells.

ATM dephosphorylation

Since autophosphorylation plays a vital role in ATM activation, it is likely that dephosphorylation will affect ATM signaling as well. Indeed, at least three phosphatases influence ATM-dependent signaling. The PP2A phosphatase co-immunoprecipitates with ATM in unirradiated cells, but not in cells exposed to radiation, and this interaction depends on ATM kinase activity (35). It has been proposed that the PP2A-ATM interaction serves to suppress the inherent tendency of ATM molecules to undergo phosphorylation on S1981. Radiation-induced dissociation of this complex would favour ATM autophosphorylation and subsequent interaction with the MRN complex at the sites of DSBs, as part of the activation process.

PP5, another protein serine phosphatase, also co-immunoprecipitates with ATM. An obvious prediction would be that PP5 would also have an inhibitory role in ATM signaling. Surprisingly, in contrast to PP2A-ATM interaction, binding of PP5 to ATM is induced by DNA damage. Down regulation of PP5, or expressing the catalytically inactive PP5, inhibited damage-induced ATM activation (36), suggesting that PP5 promotes ATM activation. The PP5-deficient mouse embryonic fibroblasts display defects in G2/M DNA damage checkpoint caused by attenuated ATM signaling (37). The mechanism by which PP5 affects ATM signaling remains to be discovered.

The PP2C phosphatase Wip1 (PPM1D) can dephosphorylate S1981 of ATM both *in vivo* and *in vitro*. Overexpression of PPM1D inhibited damage-induced ATM activation (38). PPM1D also dephosphorylates p53 and CHK1, thus inhibiting DNA-damage-induced checkpoint signaling (39).

The MRN complex

The MRN complex, composed of MRE11, RAD50 and NBS1, is proposed to be a sensor of DSBs, as it directly binds DNA ends and immediately localizes to the sites of DSB *in vivo* in an ATM-independent manner (40-43). The complex is thought to be required for optimal activation of ATM, as both ATM autophosporylation and phosphorylation of ATM downstream substrates are significantly reduced in MRN-deficient cells (44). However, the residual autophosphorylation detected in these cells raised doubts about whether MRN was absolutely necessary for this process. Since MRE11, RAD50 and NBS1 are essential genes, they are studied mainly in cells expressing hypomorphic alleles. So, these cells probably retain enough of MRN activity to promote low levels of ATM autophosphorylation. Indeed, infection of cells with adenovirus, which results in efficient degradation of Mre11 by viral proteins, causeed a near-complete loss of ATM autophosphorylation and checkpoint signaling (45). On the other hand, ATM is readily autophosphorylated in NBS1-deficient cells, although it fails to localize to radiation-induced foci (46). ATM is also recruited to DNA ends by MRN *in vitro* (42). These results suggest that the main role of the MRN complex in activation of the ATM pathway can be to recruit already activated ATM to the sites of DSB (Fig 4). This recruitment may not be necessary for ATM activation per se, but it can place ATM in the vicinity of its partners and/or substrates, and therefore facilitate the rapid and efficient response to DSBs (46).

The dependence of ATM autophoshporylation on the MRN complex could also be an indirect effect, e.g. localization of ATM to the sites of damage could help to sustain its activation. Alternatively, MRN-mediated processing of DSBs could
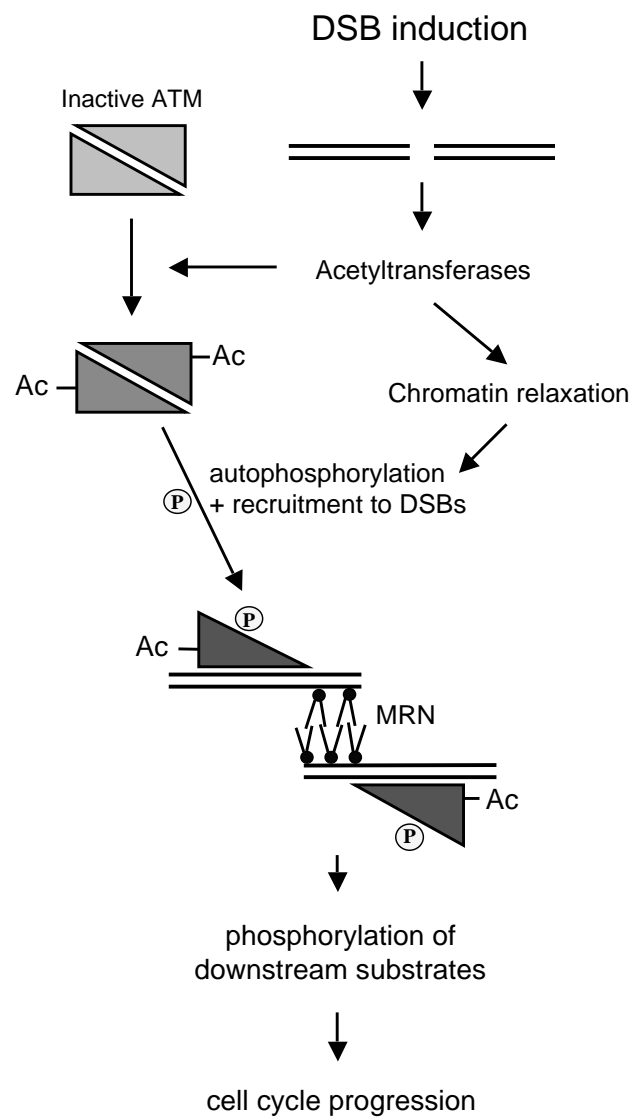
Figure 4. A model of ATM activation
In undamaged cells ATM exists as an inactive dimer. DSBs induce several events that cooperate to activate ATM and ATM-dependent checkpoint signaling. The activation of several acetyltransferases influences the chromatin structure and induces acetylation of ATM. Both of these processes are thought to contribute to ATM activation. Next, ATM autophosphorylation results in an increase in its kinase activity, and ATM is recruited to DSBs in an MRN-dependent manner. The exact order of these events and their mutual dependencies remain unclear. Finally, ATM phosphorylates a number of cell cycle proteins that in turn regulate cell cycle progression.

contribute to DSB-induced changes in the chromatin structure. It has been proposed that ATM activation is triggered by chromatin alterations rather than the presence of DSBs (32). Consistent with this hypothesis, it appears that the presence of the intact MRN complex is not sufficient for ATM activation, since MRE11 mutants lacking endonuclease activity failed to complement the defective signaling in MRE11-deficient cells (44).

Taken together, the exact role and position of MRN in the ATM pathway remains controversial. Phosphorylation of Nbs1, required for efficient response to radiation-induced damage, is dependent on ATM *in vivo* (47-49), which indicates that MRN acts both upstream and downstream of ATM. This is perhaps not surprising and could indicate that the damage signaling is not a simple linear pathway, but rather a complex web of interdependent events.

Chromatin structure and acetyltransfereases

The hypothesis that DSBs first have to be accessible before they can activate signaling and repair events (50) places changes in chromatin structure upstream of ATM-mediated signaling (Fig 4). Although the exact structures of the chromatin are ill defined, it is clear that eukaryotic DNA is wound around nucleosomes, forming 10 nm fibers. These fibers are compacted to create higher-order structures. An introduced DSB would locally alter the chromatin structure. In addition to these changes, which do not require any enzymatic activities, in response to DSBs chromatin structure is actively modulated by a number of chromatin remodeling complexes. Interestingly, ATM autophosphorylation, which results in its dissociation into active monomers, occurs not only after irradiation, but also after treatment with mildly-hypotonic buffers, which alter chromatin structure, or chromatin-remodeling drugs. It suggests that the chromatin structure, rather then the direct contact of ATM with the broken DNA could be the main trigger of ATM activation (32).

While changes in chromatin structure appear to be critical for ATM activation, recently it became clear that the histone acetyltransferase Tip60 directly targets and activates ATM. DNA damage stimulates the activity of Tip60, which acetylates ATM on a conserved lysine residue K3016. This modification likely activates the kinase activity of ATM, since suppression of acetylation inhibits ATM autophosphorylation and conversion into active monomers, prevents phosphorylation of ATM targets, and sensitizes the cells to radiation. This suggests that acetylation is an upstream and essential part of ATM activation (51,52).

Another histone acetyltransferase, hMoF, also interacts with ATM and influences its damage-induced activation (53). However, it is unclear whether ATM is a direct substrate of hMoF, or whether hMoF influenced ATM indirectly, e.g. by acetylating K16 of histone H4 hMoF might induce chromatin changes necessary for ATM activation.

ATM substrates

The number of ATM substrates identified so far indicates that ATM controls a remarkably broad range of cellular responses to DSBs. It regulates cell cycle progression at G1/S, in S phase, and at the G2/M transition and ATM-deficient cells display significant defects in all of these checkpoints.

p53 is the key protein involved in controlling the G1/S transition and the key target of ATM signaling. ATM directly phosphorylates p53 on S15 which stabilizes p53, and enhances its activity as a transcription factor (54-56). In addition, ATM indirectly stabilizes p53 by phosphorylating CHK2 and MDM2. In undamaged cells p53 interacts with its inhibitor MDM2, which serves as a ubiquitin ligase for p53 and targets it for proteosomal degradation. CHK2-mediated phosphorylation of p53 on S20 interferes with MDM2 interaction. Additionally, phosporylation of MDM2 by ATM inhibits nuclear export of p53-MDM2 complex and hence the degradation of p53 (57).

ATM regulates the intra-S checkpoint by phosphorylating a number of proteins controlling S-phase progression and protecting stalled replication forks: NBS1, SMC1 and FANCD2, a member of a multi-protein complex dysfunction of which causes the rare genomic instability syndrome – Fanconi Anaemia (47-49,58-60). These phosphorylation events are required for the S-phase checkpoint, although their exact roles are not fully understood.

Another ATM substrate, BRCA1, is a tumor suppressor protein involved in DNA repair, as well as in S-phase and G2/M checkpoints (61,62). By phosphorylating BRCA1 on distinct sites ATM controls its participation in different branches of damage signaling: BRCA1 phosphorylated on S1387 acts in intra-S checkpoint (63), while phosphorylation on S1423 engages it in G2/M checkpoint (64).

ATM affects the cell cycle machinery also by phosphorylating and activating two other protein kinases: CHK2 and CHK1. Both of them subsequently phosphorylate the CDC25A phosphatase, marking it for degradation (65,66). CDC25A dephosphorylates and activates the cyclin-dependent kinases CDK1, which promotes G2/M transition, and CDK2, regulating G1/S transition and S-phase progression. Therefore CDC25A degradation contributes to G1/S, intra-S phase, and G2/M checkpoints. In addition, CHK2 phosphorylates CDC25C - another phosphatase acting on CDK1. CDC25C phosphorylation results in the retention of CDC25C in the cytoplasm, away from its substrate CDK1.

ATM has also been directly implicated in DSB repair by influencing Artemis, a nuclease required to cleave the DNA hairpin intermediates generated during V(D)J recombination and implicated in the non-homologous end joining pathway of DSB repair. ATM mediates phosphorylation of Artemis and is required for rejoining of a subfraction of DSBs that requires Artemis nuclease activity (67).

2.4.2. ATR-dependent checkpoint signaling

The ATR protein kinase plays a central role in the cellular response to replication stress and DNA damage. ATR participates in an elaborate, step-wise accumulation of the checkpoint signaling machinery at the DNA lesions that leads to activation of the effector proteins (Fig 5). A critical function of the ATR-dependent signaling is the activation of a downstream kinase CHK1, which subsequently imposes cell cycle arrest and promotes stabilization of the stalled forks (68). The ATR-dependent branch of damage signaling is essential for cell viability. ATR-deficient mice die early during embryogenesis, and ATR^{-/-} cells accumulate chromosomal breaks prior to apoptosis. Deletion of other proteins involved in the ATR pathway, e.g. RAD17, RAD1, and CHK1 also results in embryonic lethality in mice (68-71). It indicates that ATR-dependent signaling is required not only to protect the cells against external DNA damage, but

also to deal with spontaneous damage, e.g. oxidative base damage, or abnormal DNA structures arising during DNA replication.

The role of RPA in ATR activation

In human cells, ATR exists in a stable complex with its indispensable partner ATRIP (ATR-interacting protein). Mec1 and Rad3, the *S. cervisiae* and *S. pombe* homologs of ATR, also form similar complexes with Ddc2 and Rad26, respectively. The presence of ATR and ATRIP proteins is mutually dependent, suggesting that formation of the complex is important for the stability of both proteins (72).

ATR is activated by a wide variety of DNA damaging agents, which produce different DNA lesions. It was therefore unclear whether these lesions are sensed by distinct sensors, or whether they are processed to a common intermediate that is detected by a single sensor, which in turn transmits the damage signal to ATR. The question was addressed by experiments showing that the key structure required for activating ATR is ssDNA coated with RPA, a common structural intermediate produced at stalled replication forks and by repair reactions (73). Since RPA stimulates binding of ATRIP to ssDNA *in vitro*, it was proposed that interaction between ATRIP and the RPA-coated ssDNA brings ATR/ATRIP complex to the sites of damage (Fig 5). This recruitment, which presumably places ATR in the vicinity of its substrates and other essential components of the checkpoint cascade, is likely to contribute to the activation of ATR-dependent signaling. Another critical factor in the activation of ATR is a conserved protein called TopBP1 (topoisomerase IIβ binding protein 1). TopBP1 possesses multiple BRCA1 C-terminal (BRCT) domains, which are implicated in binding phosphorylated serines and threonine residues and which are present in numerous proteins implicated in the response to DNA damage (74). TopBP1 specifically and directly interacts with ATR, and this interaction induces a large increase in the kinase activity of ATR (75).

RAD17 and the 9-1-1 complex

The recruitment of ATR/ATRIP to RPA-coated ssDNA is necessary, but not sufficient for the activation of checkpoint signaling. Another required event involves RAD17-mediated loading of the RAD1-RAD9-HUS1 (9-1-1) complex onto damaged DNA.

RAD1, RAD9 and HUS1 share structural similarity with PCNA and are predicted to form a PCNA-like heterotrimeric ring (76). This data is consistent with yeast two hybrid assays and gel filtration experiments indicating that the three proteins form a complex *in vivo* in undamaged cells (77-79).

RAD17 shares homology with RFC1 – a subunit of the complex that loads PCNA onto primer/template junctions during replication. RAD17 forms a complex with four small subunits of the replicative RFC complex: RFC2-5. RAD17 is recruited to the sites of damage independently of ATR/ATRIP complex by means of its interaction with RPA-coated ssDNA (80-82). RAD17 recognizes and binds the transitions from dsDNA to ssDNA and catalyzes loading of the 9-1-1 complex onto the transitions in an ATP-dependent manner (Fig 5), a reaction similar to RFC-mediated loading of PCNA (77,83). Disruption of RAD17 function blocks damage-induced 9-1-1 chromatin binding (78,81). When naked DNA substrates are used, RAD17 acts on both 3' and
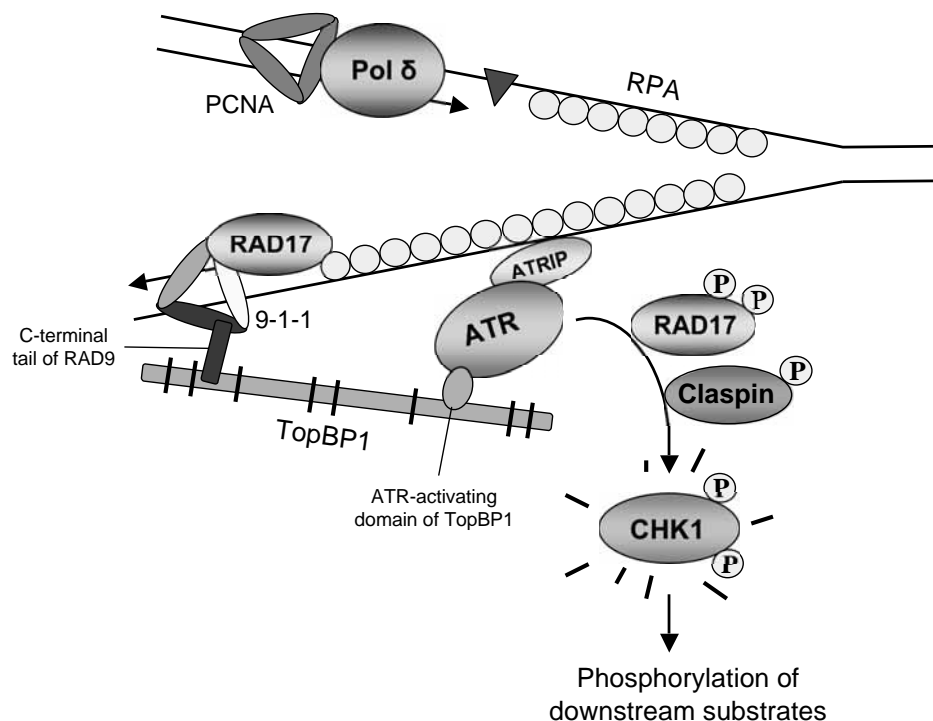
Figure 5. A model for activation of the ATR-signaling pathway.
The assembly of distinct protein complexes at the site of damage is required for activation of ATR-dependent signaling. RPA-coated ssDNA produced at the lesion site serves to recruit ATR/ATRIP and RAD17. RAD17 in turn loads the 9-1-1 complex onto 5' junctions. Next, binding of TopBP1 to RAD9, mediated by the C-terminal part of RAD9, places TopBP1 in the proximity of ATR and allows it to activate ATR kinase activity. ATR then phosphorylates RAD17. Claspin localizes at the replication forks via its interaction with CDC54 (not shown) and, together with phosphorylated RAD17, is required for ATR-mediated CHK1 phosphorylation and activation.

5' junctions, but the presence of RPA limits the loading specificity of a *S. cerevisiae* homolog of RAD17 to 5' junctions (83,84). However, since the 9-1-1 complex is able to slide across dsDNA *in vitro*, its exact position at the damage site is still unclear.

TopBP1 and Claspin

Binding of the ATR/ATRIP complex and the loading of the 9-1-1 complex occur independently of one another, but both events are essential for optimal activation of the downstream effectors. The mechanism by which the chromatin-bound 9-1-1 complex promotes ATR-dependent signaling remained unclear until recently, when two groups (85,86) independently showed that TopBP1, an essential activator of ATR,

binds both ATR and RAD9. The interaction of TopBP1 with the 9-1-1 complex serves to recruit TopBP1 to the site of damage so that it can bind and activate ATR. It appears that the recruitment of TopBP1 is the main role of the 9-1-1 complex in the checkpoint signaling, since the fusion of the ATR-activating domain of TopBP1 to PCNA, which places it close to ATR, bypasses the requirement for the 9-1-1 clamp.

ATR-mediated activation of CHK1 requires yet another protein, named Claspin. Claspin is phosphorylated in response to DNA damage and replication stress. These phosphorylation events are essential for the direct Claspin-CHK1 interaction, which subsequently enables phosphorylation of CHK1 by ATR, resulting in CHK1 activation.

Claspin associates with replication forks. Its binding to DNA depends on the pre-replication complex (consisting of the origin recognition complex, CDC6, CDT1, and MCM2-7 complex) and Cdc45 and is independent of RPA, ATR/ATRIP and RAD17/9-1-1 complexes. The question how Claspin, ATR/ATRIP and RAD17/9-1-1 complexes interact to regulate CHK1 phosphorylation was at least partially answered by a recent discovery (87) implicating RAD17 in the regulation of Claspin phosphorylation.

Activated ATR mediates damage-induced phosphorylation of RAD17 on two serine residues (Ser635 and Ser645). This reaction is HUS-1 dependent, consistent with the participation of the 9-1-1 clamp in the upstream checkpoint activation steps involving TopBP1. ATR phosphorylates RAD17 *in vitro,* which suggests that RAD17 is its direct substrate (88). Phosphorylated RAD17 interacts with Claspin and promotes its phosphorylation, which presumably promotes CHK1 recruitment to Claspin and ultimately phosphorylation and activation of CHK1 by ATR (87).

ATR substrates

Although ATR may directly regulate many proteins, several studies suggest that its critical function involves phosphorylation and activation of the downstream checkpoint effector kinase CHK1. CHK1 has several SQ/TQ motifs in the regulatory C-terminus and two of them (Ser345 and Ser317) appear to be particularly important for the DNA damage response. The mechanisms by which phosphorylation regulates CHK1 activity are not fully understood. Several studies indicated that phosphorylated CHK1 has increased kinase activity (89,90). The underlying molecular mechanism might involve the C-terminal part of CHK1. It has been suggested that the C-terminus may play an inhibitory role and that phosphorylation may release this inhibition (91,92). It is also possible that CHK1 phosphorylation enables CHK1 to interact with its substrates and/or other proteins regulating its activity. CHK1 associates with chromatin, and its phosphorylation releases this association. Inhibiting this release by fusing CHK1 to histone H2B impaired the damage-induced checkpoint response (93). This data suggests that CHK1 phosphorylation might help CHK1 to spread the damage signal throughout the nucleus and reach substrates e.g. cell cycle proteins, that are likely not present at the damage site.

Activated CHK1 slows down cell cycle progression during S-phase and prohibits the G2/M transition as long as damaged or incompletely replicated DNA is present in the cell by phosphorylating downstream cell cycle proteins such as

CDC25A, CDC25C and WEE1 (see above).

In addition to regulating Cyclin B/CDC2 activity via CDC25 and WEE1, the ATR pathway affects other cell cycle kinases: Cyclin E/CDK2 and CDC7/DBF4, which are necessary for origin firing. CDK2 activity is regulated by CDC25 and WEE1, similarly to CDC2 (94). ATR-mediated checkpoint activation results in dissociation of CDC7 from its activating subunit DBF4 (95). CDC7 is required for initiation of DNA replication, since it promotes the phosphorylation of the MCM complex and subsequent binding of CDC45 to pre-replication complexes, which leads to origin firing (96,97). Therefore, inhibition of CDC7 activity helps to inhibit origin firing in response to replication stress and DNA damage.

Another way by which ATR influences the damage response involves phosphorylation of p53 on Ser15, which leads to p53 stabilization and increased transcriptional activator activity. One of the genes up regulated by p53 is p21, which in turn inhibits CDKs and blocks cell cycle progression.

Checkpoint-independent roles of RAD17 and the 9-1-1 complex

Several lines of evidence indicate that, in addition to participating in checkpoint signaling, both RAD17 and the 9-1-1 complex might be more directly involved in damage repair and/or damage bypass. Studies in yeast *S. cerevisiae* and *S. pombe* have implicated the 9-1-1 complex in regulation of mutagenic translesion DNA synthesis (TLS). TLS employs specialized, error-prone polymerases to bypass DNA lesions that stall the high fidelity replicative polymerases (see below for a more detailed description of this pathway). A critical step in the TLS process is the switch between a replicative and a translesion polymerase and there is a wealth of evidence that PCNA is responsible for controlling this process. However, the structural similarity between PCNA and the 9-1-1 complex, as well as the presence of 9-1-1 at the sites of damage, raised a tempting speculation that 9-1-1 could also be involved in polymerase switch and/or recruiting TLS polymerases to the damaged template. To date there is little evidence supporting this possibility. The *S. cerevisiae* homologs of RAD1, HUS1 and RAD17 are required for UV-induced mutagenesis that requires one of the TLS polymerases (Pol ζ) (98). Similarly, in *S. pombe* RAD17 was required for chromatin binding of TLS Pol κ and for Pol κ-dependent mutagenesis (99). However, the involvement of RAD17 and the 9-1-1 complex in TLS in mammalian cells has not been confirmed.

It has been shown recently that RAD17 and each of the 9-1-1 subunits interact with DNA ligase I and this association between these proteins increases in S phase following DNA damage or replication stress. Moreover, RAD17 stimulates joining of Okazaki fragments by DNA ligase I (100). Although the consequences and the significance of these findings are not fully understood, these results suggest that RAD17 and the 9-1-1 complex might play a role in DNA replication.

Studies in yeast demonstrate that the 9-1-1 complex is involved in the repair of DSBs. Deletion of the *S. cerevisiae* homologs of RAD17 and RAD1 resulted in hypersensitivity to enzymatically-produced DSBs, which was not reversed when the cell cycle progression was slowed down (101). These results indicate that the decreased survival was caused by a defect in processing and/or repair of the breaks. Interestingly, some reports suggested that RAD1 and RAD9 have a 3'-5' exonuclease activity (102,103). Since other studies did not confirm it (104,105), the enzymatic

activity of RAD1 remains uncertain. However, it is worth noting that the gel filtration analysis of the components of the 9-1-1 complex revealed that in human cells approximately half of the cellular RAD1 pool is engaged in the 9-1-1 complex, while the whole RAD9 and HUS1 pools are present in the 9-1-1 complex. The presence of free RAD1 in the cells raises the possibility that RAD1 can have distinct, 9-1-1-independent roles (78).

Similarly, RAD17 could also be more directly involved in DNA repair processes, in addition to its checkpoint function. As will be described in the second and third chapters of this thesis, an N-terminal truncation of mouse Rad17 results in hypersensitivity to a wide range of DNA damaging agents and replication inhibitors, although this does not confer defects in checkpoint signaling.

2.5. Turning the checkpoint off

Activation of checkpoint signaling is critical for an efficient response to DNA damage and replication problems. However, once DNA repair has been completed, it is equally important to switch the checkpoint off to allow progression of the cell cycle. The mechanisms attenuating checkpoint signaling are still poorly understood, but it is clear that re-entering the cell cycle is an active and highly regulated process. ATM and ATR-dependent damage signaling converge on CHK2 and CHK1 effector kinases, respectively. Therefore, it is not unexpected that these two kinases appear to be the main targets of the mechanisms regulating checkpoint recovery.

The role of phosphatases in checkpoint recovery

Since activation of CHK1 and CHK2 is induced by ATM/ATR-dependent phosphorylation, it could be envisioned that their dephosphorylation would inhibit checkpoint signaling. Indeed, several reports implicated phosphatases in promoting checkpoint recovery. A screen for *S. pombe* genes that, when overexpressed, cause premature mitotic entry in the presence of DNA damage, identified a type I protein phosphatase Dis2. Dis2 can abrogate Chk1 phosphorylation and activation both *in vivo* and *in vitro* and Dis2-deficient cells have a prolonged, Chk1-dependent cell cycle arrest induced by DNA damage (106). The *S. cerevisiae* homolog of CHK2, Rad53, is also negatively regulated by dephosphorylation. Both *in vivo* and *in vitro* evidence suggests that phosphorylated forms of two PP2C-like phosphatases Ptc2 and Ptc3 specifically bind to Rad53 and inactivate Rad53-dependent pathways during checkpoint recovery by dephosphorylating Rad53. Cells deficient in Ptc2 and Ptc3 were defective in recovering from a repairable DSB (107). Affecting checkpoint signaling via dephosphorylation appears to be evolutionary conserved, since the human PPM1D (also known as Wip1) type 2C serine/threonine phosphatase can also bind to and dephosphorylate activated CHK2 (108,109). Interestingly, in addition to targeting CHK2, PPM1D acts directly on ATM. PPM1D dephosphorylates Ser1981, a site critical for ATM monomerization and activation, and is critical for resetting ATM phosphorylation after the cells have completed repair (38). PPM1D can also dephosphorylate p53 and CHK1. Such a collection of substrates, which include main checkpoint activating proteins, suggests a critical role of PPM1D in regulating responses to DNA damage. This possibility is supported by the finding that PPM1D is amplified and overexpressed in a subset of human breast cancers (110).

The role of Claspin in checkpoint recovery

Another possible way to influence checkpoint signaling is to prevent checkpoint activation. Recent discoveries have shown that Claspin plays an important role in controlling checkpoint activation. As mentioned above, Claspin is required for ATR-mediated phosphorylation and activation of CHK1. In undamaged cells Claspin is continuously turned over by the proteasome system, but after induction of DNA damage e.g. by UV light, ionizing radiation, and in response to replication stress, Claspin levels transiently increase (111). The protein responsible for damage-induced Claspin stabilization is a deubiquitinating enzyme USP28 (112). The increased abundance of Claspin promotes CHK1 phosphorylation. After the initial stabilization Claspin levels decrease at later time points after damage induction in a proteosome-dependent manner. The degradation of Claspin is dependent on the phosphorylation of a phospho-degron motif at the N-terminus of Claspin, which depends on Polo-like kinase 1 (PLK1) (111,113,114). Consistent with the role of Claspin in mediating Chk1 activation and cell cycle arrest, inhibition of Claspin degradation prohibits mitotic entry during checkpoint recovery.

3. DNA Replication in Eukaryotes

DNA replication is initiated at specific sites named replication origins. Simple organisms, such as bacteria, have only one origin per genome. Relatively large genomes of eukaryotic cells are replicated from multiple origins located throughout each chromosome. Initiation of DNA replication requires an ordered and highly regulated sequence of events. It begins with the formation of the pre-replication complexes (pre-RC) at the origins prior to S-phase. This process, known as origin licensing, involves the assembly of the origin recognition complex (ORC), followed by binding of the two essential factors: Cdc6 and Cdt1. These proteins promote loading of the putative replicative helicase - the Mcm2-7 complex onto the origins (115).

The transition from G1 to S phase involves the conversion of pre-RC into replication forks (origin firing) and requires unwinding of the DNA at the origin site, stabilization of the ssDNA, and the assembly of the multi-protein replication machinery, which includes replicative DNA polymerases. These processes are supported by a second set of replication factors and controlled by the activity of at least two cell cycle-regulated kinases: CDK (Cyclin dependent kinase) and a Dbf-dependent kinase Cdc7 (DDK) (116). The earliest initiation factor recruited to pre-RC is Mcm10. It is required for the recruitment of Cdc45 (117). Both the presence of Mcm2-7 and Cdc45 loading are essential for subsequent origin unwinding (118). Several lines of evidence indicate that Mcm2-7 functions as a replicative helicase during S-phase (119). Cdk45 likely activates the helicase activity of Mcm2-7, since formation of a Cdc45-Mcm complex closely correlates with helicase activation (120). The stabilization of the ssDNA by RPA further stimulates origin unwinding (118). Cdc45 is also required for the subsequent loading of the replicative polymerases. Additionally, the *S. cerevisiae* protein Dpb11 (Cut5 in *S. pombe*, TopBP1 in mammals) forms a complex with pol ε, and is required for recruiting pol ε and pol α to origins after Cdc45 and RPA binding (121).

Maintaining genomic integrity requires that the entire genome is duplicated exactly once per cell cycle. This is achieved by a two-step, cell cycle-regulated mechanism. First, origin licensing can only occur during the low CDK, high APC/C period from late mitosis through early G1 phase. Origin licensing is strictly controlled by redundant pathways, which involve CDKs and geminin. These pathways regulate degradation, subcellular localization and DNA binding of different pre-RC components. Second, origin firing (the initiation of replication) can only occur during S-phase, after the anaphase promoting complex has been inactivated and CDKs re-accumulate (122).

Origins fire at specific times during S-phase. The replication timing is associated with local chromatin environment, since early-replicating regions are present in euchromatin, while the late-replicating regions are localized in heterochromatin. Changes in origin localization or the local chromatin structure are sufficient to alter the timing of origin firing (123,124).

The final step in replication initiation is the loading of the replicative polymerases: Pol α, Pol δ and Pol ε. All are essential for DNA replication, although they are specialized in different tasks (125). After origin unwinding stimulated by Cdc45 and RPA binding, Pol α is recruited to the origins. Pol α is unique among eukaryotic polymerases, since in addition to DNA polymerase activity, it has DNA primase activity. Therefore it is the only DNA polymerase that can initiate synthesis *de novo* on ssDNA, whereas Pol δ and Pol ε require a primed template. Pol α synthesizes short RNA/DNA hybrid primers of approximately 10 RNA nucleotides followed by 20-30 DNA nucleotides. Since all DNA polymerases catalyze DNA synthesis in the 5'–3' direction, and the two DNA strands to be replicated are antiparallel, DNA replication occurs continuously only on the leading strand. The lagging strand is replicated discontinuously by synthesizing short, about 200 base pairs long DNA pieces called Okazaki fragments. Therefore, Pol α has to synthesize one primer per origin for the leading strand, and one primer per Okazaki fragment in the lagging strand. After primer synthesis, polymerase switching occurs, which replaces Pol α with Pol δ and/or Pol ε. Both Pol δ and Pol ε display greater processivity and have proofreading exonuclease activity, which makes them better suited for synthesizing long stretches of DNA.

The polymerase switch is coordinated by RFC and involves a complex network of interactions among Pol α, Pol δ, RFC and RPA. It has been proposed that RFC induces the polymerase switching by sequestering the 3'-OH DNA end from Pol α and subsequently recruiting PCNA to DNA (126,127). Processive DNA synthesis requires that Pol δ and Pol ε associate with the ring-shaped processivity factor PCNA (128). PCNA forms a homotrimeric ring that encircles DNA and by physical interaction with Pol δ and Pol ε topologically links these polymerases to DNA, allowing them to synthesize long DNA fragments without dissociating from the template. PCNA is loaded onto the primed DNA template by the clamp loader, RFC. This heteropentameric complex uses the energy of ATP binding to open the PCNA ring and load it onto the DNA (129). Upon ATP hydrolysis RFC dissociates from PCNA.

Both Pol δ and Pol ε are essential for replication and perform non redundant functions (130). Pol δ functions as a dimer and, therefore, may be responsible for replicating both leading and lagging strands. It was suggested that Pol δ and Pol ε are responsible for synthesizing the leading and the lagging DNA strands, respectively, since proofreading-defective mutants of Pol δ and Pol ε accumulate mismatches on

different DNA strands (131,132). However, the N-terminus of Pol ε, containing the catalytic domain, is dispensable for viability, while the C-terminal region involved in protein-protein interactions and checkpoint activation is required for cell survival. This does not necessarily mean that the catalytic activity of Pol ε is not involved in DNA replication, but suggests that this activity can be functionally replaced by Pol δ, in contrast to other, non-calalytic functions of Pol ε. Since its C-terminus is involved in checkpoint control, Pol ε may monitor replication fork progression by augmenting the action of the other polymerases. This idea is supported by recent genetic studies that have implicated Pol ε in correcting errors made by Pol α and Pol δ. Pol ε loading occurs prior to Pol α loading, suggesting that it may play a role in replication initiation after pre-RC formation.

The discontinuous synthesis of the lagging strand results in the formation of many Okazaki fragments, which need to be joined to form an intact DNA strand. Pol δ - catalyzed extension of the upstream Okazaki fragment displaces the downstream RNA/DNA primer into a flap. This flap has to be removed by a nuclease before the adjacent Okazaki fragments can be ligated by DNA ligase I to generate the continuous dsDNA. Short flaps (10 nucleotides) displaced by Pol δ are processed efficiently by a 5' structure-specific endonuclease FEN1, which cleaves the base of the flap (133,134), generating a nick for ligation (135,136). If a longer flap (> 27 nucleotides) is produced, it is coated with RPA, which inhibits FEN1, but stimulates the helicase/nuclease Dna2 (137). Since Dna2 is unable to cleave at the base of the flap, it cleaves the ssDNA region of the flap (138). The resulting short flap is then processed by FEN1.

4. Repair of Stalled Replication Forks

Faithful DNA replication requires an extremely precise and efficient replication machinery. The replicative DNA polymerases insert correct bases in the growing DNA molecule, making a mistake as rarely as 1 per every 10^6 nucleotides copied. However, they cannot replicate over unusual DNA structures, since their active sites are designed to fit regular DNA bases and would not accommodate bigger elements, e.g. pyrimidine dimers or intrastrand crosslinks.

Exogenous and endogenous agents frequently cause DNA lesions, which impede progression of replication forks, and can introduce mutations and chromosomal aberrations. Therefore, to ensure the most efficient and precise genome duplication it would be ideal to repair the damaged template before starting to replicate it. Cells are equipped with a number of repair and checkpoint mechanisms designed to achieve this, but it is impossible to completely avoid the presence of DNA lesions during S-phase. First, DNA damage can be introduced during S-phase. Second, some types of DNA lesions often escape detection until the replication fork collides with them. Other lesions are inherent to the replication process, e.g. DSBs formed at fragile replication sites. So, in order to complete DNA replication and divide, cells need mechanisms that would promote the progression of replication forks stalled at various DNA lesions. Two main pathways responsible for dealing with such forks, homologous recombination and translesion synthesis, are discussed below.

4.1. Homologous Recombination

Homologous recombination (HR) is a process of exchange of genetic information between homologous DNA molecules. It is responsible for generating genetic diversity during meiosis and during development of the immune system. It is also essential for DNA replication, and is involved in repair of DSB and other DNA lesions.

A recombination reaction is initiated as RAD51 protomers assemble into a filament on the single stranded (ss) DNA overhang generated by the resection of the DSB. The RAD51 nucleoprotein filament is an active structure that supports homology recognition and strand exchange, leading to the formation of a joint molecule (D-loop). The 3'-ended ssDNA end invaded into a homologous DNA duplex can then serve as a primer for DNA synthesis. The subsequent branch migration and resolution of the joint molecule restores intact DNA molecules, and is presumably accompanied by dissociation of RAD51 from DNA (Fig. 6).

4.1.1. RAD51 – the Core Protein of Homologous Recombination

RAD51 is the main protein catalyzing the strand exchange reaction of homologous recombination. It assembles on ssDNA to form a polymer – the RAD51 nucleoprotein filament. This structure is responsible for aligning homologous sequences and driving strand exchange between the ssDNA in the filament and homologous double-stranded DNA (dsDNA).

The human RAD51 protein belongs to the RecA-like family of recombinases, which includes bacterial RecA, archeal RadA, *S. cerevisiae* Rad51, human DMC1, etc (139). All of them are DNA-dependent ATPases and require ATP binding, but not hydrolysis, for filament formation and catalyzing strand exchange (140-142). Although they are considered structural and functional homologs, their amino acid sequence conservation is limited to the core ATP-binding domain (143,144). Despite limited sequence homology, the recombinases form structurally similar nucleoprotein filaments, as visualized by electron microscopy (145). The filaments are right-handed helical structures, with the DNA bound within the filament extended approximately 50% relative to the regular B-form helix. However, biochemical and biophysical experiments, as well as single molecule imaging techniques indicate that nucleoprotein filaments are dynamic structures, with monomers being exchanged, redistributed, and forming discontinuous patches (146-148). The properties of the filaments may also change depending on whether they are formed on ss or dsDNA (149). The dynamic nature of the filaments is likely to be critical for performing complex DNA transactions required during homology search and strand exchange.

The exact mechanism by which the filament finds homologous sequences is unclear, and at least two scenarios can be envisioned. It might randomly probe the target dsDNA molecule, retract if the homology was not found, and repeat these cycles until it encounters the homologous sequence. Alternatively, the invaded ssDNA could processively translocate along the recipient DNA until it finds the homologous sequence, upon which the joint molecule can be stabilized and extended. The recent advances in single molecule and imaging techniques may help to test these purely hypothetical possibilities.

The biochemical activities of RecA and RAD51 are qualitatively similar, but RAD51 appears to be a less potent enzyme: the rate of ATP hydrolysis, homologous pairing, and subsequent strand exchange promoted by RAD51 have been reported to be less than 1/10 those of RecA (150,151). In addition, while ATP hydrolysis is not required for the basic strand exchange activity of RecA, it confers several new properties to the RecA-mediated reaction. ATP hydrolysis renders DNA strand exchange catalyzed by RecA unidirectional, greatly increases the lengths of the created heteroduplex, and permits the bypass of heterologous DNA insertions in one or both DNA substrates (152,153). In contrast, the activity of RAD51 is not augmented in this manner by ATP hydrolysis. Together, this data indicates that RAD51 is a less proficient and less independent enzyme, and might require additional proteins to modulate and/or stimulate its action during recombination reactions. Paradoxically, such apparent attenuation of activity may be evolutionary beneficial, as it may provide additional levels for regulating the recombination machinery.

4.1.2. A Model of DSB Repair by Homologous Recombination

The first necessary step in the DSB-induced recombination reaction is the resection of the blunt ends to produce the 3' ssDNA overhangs (Fig 6a). In bacteria, this reaction is catalyzed by the multi-functional RecBCD complex (154). In eukaryotes DSB resection requires MRE11/RAD50/NBS1 (MRN) complex (155,156), although it is not clear whether the nuclease activity of MRE11 is directly responsible for generating the overhang, or whether MRN is indirectly involved in the reaction. A mammalian protein, CtIP, is required for DSB resection. CtIP is recruited to DSBs only in S and G2 phases of the cell cycle, which is consistent with its involvement in HR (157). The *S. pombe* homolog of CtIP, Ctp1, appears to have similar functions. It is recruited to DSBs and is essential for HR repair and efficient formation of RPA-coated single-strand DNA adjacent to DSBs (158). CtIP physically interacts with the MRN complex and affects its enzymatic activity, suggesting that CtIP might regulate and/or activate the DSB resection by the MRN complex. However, direct evidence to support this hypothesis is currently missing.

In the next step of DSB repair by HR RAD51 monomers assemble on the ssDNA tail to form a nucleoprotein filament, which then searches for homology and invades the homologous dsDNA template (first strand invasion) (Fig. 6b), forming a joint molecule, also called a displacement loop (D-loop). The invaded end then serves as a primer for DNA synthesis and information lost at the site of the break is retrieved using the homologous DNA molecule as a template (Fig. 6c). The recombination reaction can then proceed via alternative paths leading to a repaired intact duplex (159).

The second ssDNA tail, derived from the other end of the DSB, may also invade the dsDNA (second-strand invasion). It can also anneal to the displaced DNA strand that is produced by DNA synthesis from the 3'-end of the first ssDNA (second end capture). These pathways can eventually produce cross-stranded structures, called double Holliday Junctions (HJs) (Fig. 6d). Branch migration and resolution of HJs occurs during late stages of HR (160). In bacteria, branch migration and HJ resolution of are catalyzed by the RuvABC complex (161). RuvAB dimer specifically binds HJs and drives branch migration by "pumping out" the DNA in the opposite directions. RuvC resolves the HJs by endonucleolytic cleavage, producing nicked
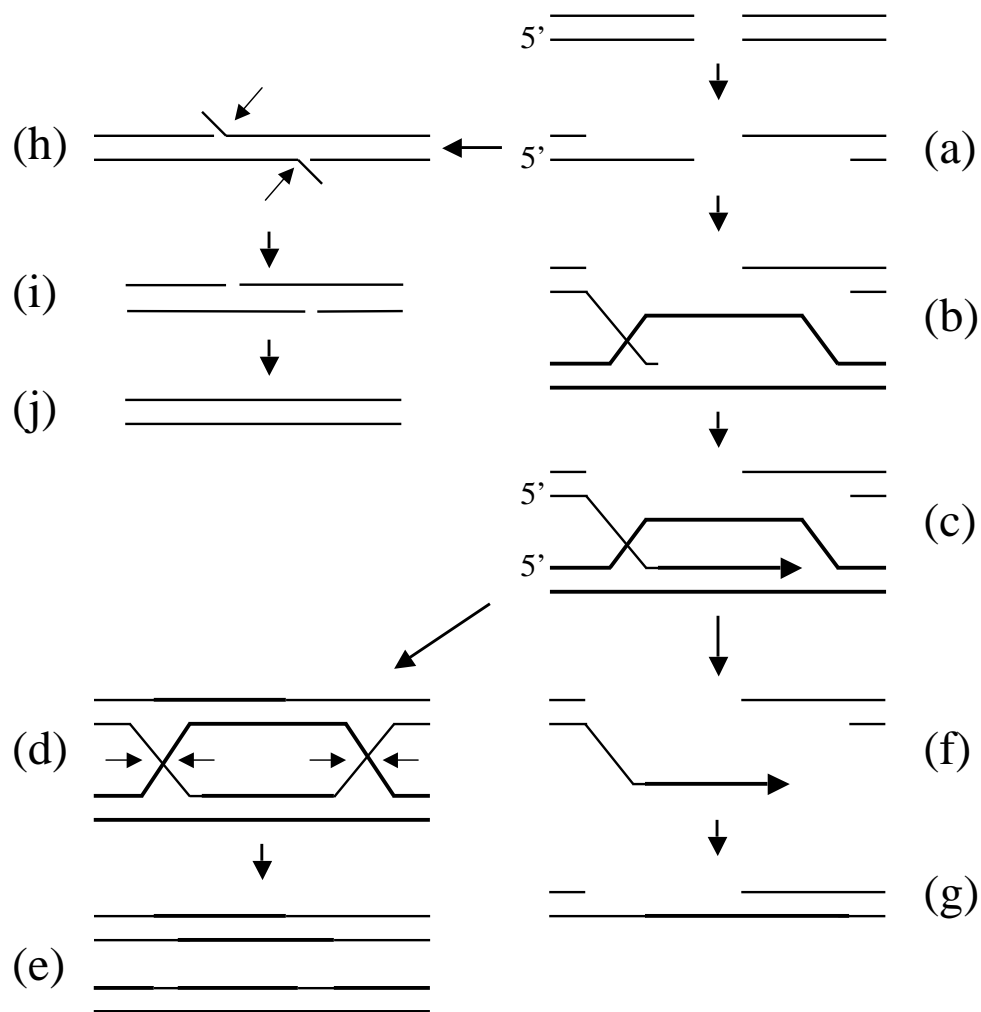
Figure 6. A model of DSB repair by homologous recombination
A DSB is resected to produce a 3' ssDNA overhang (a), which is subsequently bound by RAD51. RAD51 catalyzes homology search and the invasion of the first end into the homologous DNA duplex, leading to the formation of a joint molecule (b). The 3' end then serves as a primer for DNA synthesis (c). After the extension of the invading end the reaction can be channeled into different paths. The second end may also invade the homologous template in a RAD51-mediated reaction, or it can simply anneal to the displaced strand of the homologous duplex. This process is promoted by single strand annealing activity of Rad52. Engagement of the second end leads to the formation of a double Holliday Junction (d), which in somatic cells is predominantly resolved to produce non crossovers (e). Alternatively, the first end extended by a DNA polymerase can be displaced from the joint molecule (f) and re-anneal with the second end of the break in a process called synthesis-dependent strand annealing (SDSA) (g). Since the information lost at the site of the break is recovered, the resulting gap can be filled to restore the intact DNA molecule. If repeated sequences are uncovered by the DSB resection, they can be processed by the single strand annealing pathway (SSA) (h). Since the non-homologous fragments are displaced and removed, this reaction results in a deletion at the site of the break (i,j).

duplexes that are repaired by DNA ligase. The activities similar to those of RuvABC enzyme have been observed in fractionated human cell extracts (162), but despite extensive search, the identity of the enzyme/enzymes responsible for cleaving HJs in eukaryotic cells remains unknown. The extended joint molecules can also be processed by the BLM helicase and topoisomerase IIIα, (163).

In an alternative pathway, called synthesis-dependent strand annealing (SDSA) (Fig. 6f-g), the 3' invaded end extended by a DNA polymerase can be displaced from the joint molecule and re-anneal with the complementary strand of the second end. SDSA is an error-free mechanism. (164).

One type of homology-directed DSB repair - single-strand annealing (SSA) (Fig. 6h-j), does not require RAD51 and does not involve strand invasion. Since a large part of the mammalian genomes consists of repeated sequences, DSB resection will often produce ssDNA tails with complementary sequences. They can be annealed in a reaction catalyzed by Rad52 and RPA (165,166) (Fig. 6h), followed by removing the displaced non-complementary DNA flaps by the action of ERCC1/XPF endonuclease (167,168) (Fig. 6h-i). SSA results in a deletion at the site of the DSB.

4.1.3. Repair of Stalled Replication Forks by Homologous Recombination

The presence of damaged DNA templates, as well as proteins bound to DNA may interfere with the progression of replication forks. It has been estimated that as many as 15 – 20% of all replication forks stall or collapse in one generation of a single *Escherichia coli* cell (169). Since completion of genome duplication is necessary for cell survival, it is evident that the cells must have the means to resume blocked replication. As mentioned above, two pathways are involved in rescuing stalled forks: TLS and HR. As described in more detail below, during TLS specialized, low-fidelity DNA polymerases temporarily gain access to the primer terminus and insert nucleotides opposite the lesion. Therefore TLS polymerases allow bypassing a damage site, but, at the same time, they often introduce mutations. HR uses the intact sister chromatid as a template for repair, and is therefore essentially an error-free pathway. Which of these two pathways will deal with a given stalled fork likely depends on the type of the lesion and the structure that is created at the fork.

Replicative DNA polymerases will be stalled once they encounter a lesion in a DNA strand, e.g. an abasic site or a cyclobutane pyrimidine dimer (Fig. 7a). However, the replicative DNA helicase will continue unwinding the DNA duplex, and DNA replication can proceed normally at the other site of the fork (Fig. 7b,e). Such replication fork can be rescued in several ways. First, TLS polymerases can be recruited to replicate over the damaged site (Fig. 7b-d). At least *in vitro* DNA replication is restarted downstream the lesion (170). The gap left behind (Fig. 7b) is later filled by the combined action of TLS and replicative polymerases (Fig. 7c,d). Alternatively, the gap might also be repaired by recombination-based mechanisms (Fig.7e-j). Another structure that can be created at a stalled fork (Fig. 7a) is a so-called chicken foot – a four-way junction that is formed as a result of fork regression and re-annealing of the nascent DNA strands (Fig. 7f). Forming a chicken foot at the fork places the lesion site back in the ds DNA region. Consequently, the homologous stand is then available as a template for repair of the damage. After the repair is completed, branch migration could lead to a structure from which replication can be resumed (Fig. 7k). In
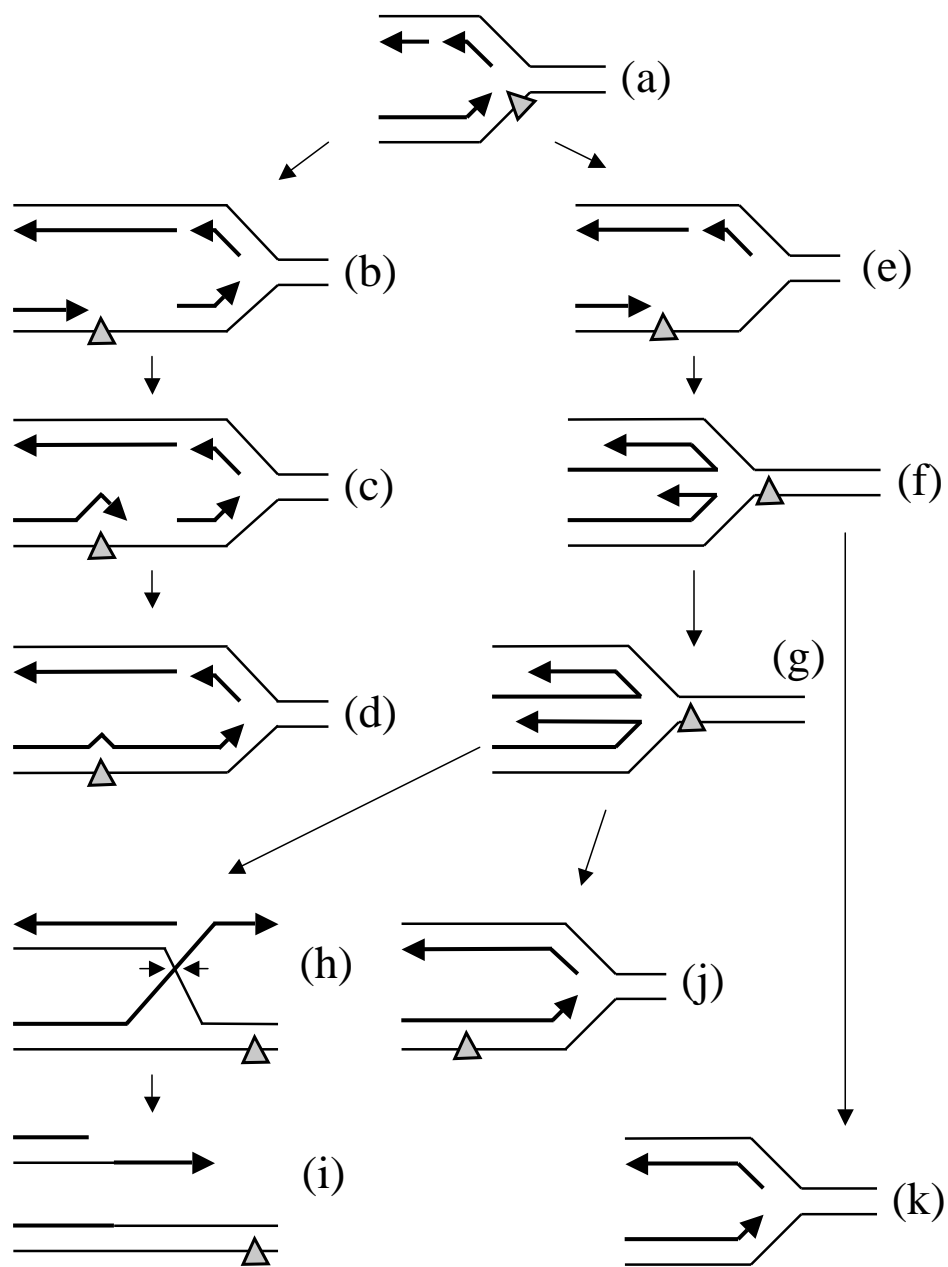
Figure 7. Pathways of restarting stalled replication forks.
Stalling of a replication fork at a lesion in the DNA template (a) in most cases does not stop
replicative helicase, which continues to unwind DNA (b,e). Often, DNA synthesis is re-initiated
downstream of the lesion, leaving a gap behind (b). The gap can be filled by the combined
action of a translesion polymerase, which inserts nucleotides opposite the lesion (c), and a
replicative polymerase, which extends the DNA fragment (d). The gap can also be repaired by
HR (not shown). The replication fork stalled at the lesion (e) can also regress to form a four-way
junction named 'chicken foot' (f). This places the lesion back in dsDNA region (f,g). Therefore,

another scenario the longer nascent DNA strand, synthesized using the undamaged DNA strand, can be used as the alternative template for the nascent strand that was blocked by the lesion (Fig. 7f,g). DNA synthesis using this new template strand and subsequent branch migration will result in error-free bypassing of the lesion (Fig. 7j). This scenario is very similar to the template switch mechanism, during which the undamaged sister chromadid, instead of the damaged homologous DNA strand, is used as a template for replicating DNA. Alternatively, a chicken foot could be cut by a structure-specific endonuclease. The resulting one-ended DSB can invade the homologous DNA duplex to re-establish the active replication fork (Fig. 7h,i).

Another possible scenario of processing a replication fork stalled at a lesion (Fig. 7a) involves cleavage of the fork by a structure-specific endonuclease, which results in the formation of a one-ended DSB. Replication forks stalled by lesions that affect only one DNA strand, by inhibitors of DNA polymerases, or by depleting cellular dNTP pools can be converted to DSBs, although it is difficult to estimate which fraction of the affected forks is processed in this way, and which fraction is rescued via other pathways. In contrast, replication forks stalled at interstrand crosslinks, appear to require processing into DSBs in order to be restarted. Additionally, DSBs will inevitably be created once an advancing replication fork encounters a SSB in the template (Fig. 8a). Irrespective of the way they were created at the fork, such one-ended DSB are substrates for HR machinery. Initiation of recombination reaction requires the presence of ssDNA overhang, which is likely present at the fork due to DNA unwinding by replicative DNA helicase. The ssDNA-RAD51 complex can then invade the intact homologous DNA molecule to reestablish the replication fork (Fig. 8b-e).

DSBs created at the stalled forks are dangerous DNA lesions, but their formation might facilitate subsequent repair processes and replication restart. In bacteria, the DSBs introduced by the RuvABC complex are suggested to recruit replication proteins to recombination intermediates, and therefore promote origin-independent replication restart (171). Introducing DSBs could serve similar purposes in eukaryotic cells. The induction of DSBs in response to DNA damaging agents has been observed in eukaryotes, but until recently the identity of the enzyme/enzymes catalyzing this reaction was unknown. The data presented in Chapter 4 and Chapter 5 of this thesis indicates, that the structure-specific endonuclease Mus81/Eme1 is

the homologous DNA strand can serve as a template for repairing the damage. After the damage is removed and the nascent strands re-anneal with their original template strands, the active replication fork can be restored (k). Alternatively, the chicken foot can be cut by structure-specific endonucleases (h) to generate a one-ended DSB (i), which, after being coated with RAD51, can invade the homologous DNA molecule. If the damage has been removed from the DNA before the invasion (not shown), this pathway will restore the intact replication fork. If the damage is still present (i), the restored fork will face the same obstacle that halted it originally and will require other pathways to be restarted.
DNA replication is likely to proceed at the damage-free strand (e). The chicken foot structure allows the nascent DNA strand, synthesized at the other site of the stalled fork, to serve as an alternative template for the strand whose synthesis was blocked by the lesion (f,g). If thus replicated DNA fragment is long enough, it will cover the lesion site once the fork adapts its original conformation (j). This will result in an error-free damage bypass.
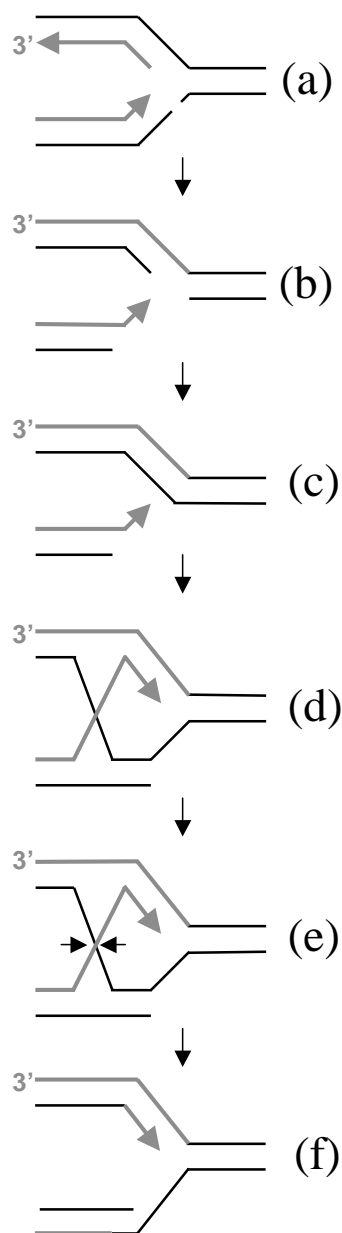
involved in generating DSB intermediates at stalled forks (22,172). Mus81/Eme1 preferentially cleaves branched DNA substrates, which resemble recombination and replication intermediates. Such *in vitro* substrate specificity as well as genetic experiments in *S. cerevisiae* suggest that Mus81/Eme1 might also act after the stalled replication forks have been processed to DSBs, e.g. by cleaving the DNA structure generated by HR-mediated repair of collapsed forks.

It is worth noting that the recombination sub pathways described above do not, by definition, remove the damage that caused fork stalling. Only in some cases, e.g. when a SSB is encountered, or when the progression of the fork is hindered by shortage of dNTPs or presence of replication inhibitors, can the recombination machinery restore the intact, undamaged DNA molecule. When the fork is halted by an obstacle in the DNA template, e.g. benzo[a]pyrene adduct, or interstrand crosslink, HR can help to re-establish the fork, and, depending on the pathway employed, can bypass the damage, but will not remove it. Therefore restarting of the stalled forks may in some cases require support of other DNA repair pathways.

Figure 8. A pathways of restarting collapsed replication forks.
Introducing a DSB at a stalled fork converts it to a collapsed fork. The DSB can be made by a structure-specific endonuclease (not shown), or can be passively formed when the replication fork encounters a SSB in the template (a). Initiation of HR requires the presence of ssDNA overhang. Depending on the lesion, the structure and the amount of ssDNA at the stalled fork, the overhang can be already present or has to be produced by end resection (b). After the intact template molecule is restored (c), it can be invaded by the broken DNA fragment (d). The invasion leads to the re-establishment of the active fork and leaves a single Holliday Junction behind (e), which is resolved by a structure-specific endonuclease (f).

4.1.4. The recombination proteins

RAD51 is the main protein catalyzing stand exchange reactions and the core player of HR. However, it requires assistance of other proteins to efficiently promote recombination reactions. Additionally, regulatory proteins are needed to ensure that HR occurs properly. HR is essential for maintaining genomic integrity (173), but it is also potentially dangerous. If HR occurs in an uncontrolled or incorrect way, it can cause deletions, gene amplifications and loss of heterozygosity. All of these events can contribute to genomic instability and increase the risk of malignant transformation. Therefore, to promote beneficial actions and limit potentially detrimental effects, HR must be precisely regulated.

A number of accessory proteins, or mediators, have been identified and shown to guide RAD51 and control its action during each phase of HR. The main role of early recombination factors is to facilitate assembly of RAD51 nucleoprotein filaments. Two proteins involved in this process, RAD52 and BRCA2 are discussed below. The accessory proteins acting at later recombination steps assist in the formation of the joint molecule, affect its stability, and regulate branch migration within the joint molecule. An example of a protein acting at this step is RAD51AP1. Finally, the mediator proteins could also influence the processing of joint molecules, i.e. channel them into distinct recombination sub pathways described above. The complexity of HR control is further underscored by the fact that the same accessory protein often influences the recombination reactions at several distinct steps via different mechanisms. The many roles of RAD54 in HR are briefly introduced below.

During the last decades significant progress has been made in understanding how HR is controlled, but many unanswered questions remain. It is not fully understood how the many recombination mediators interact and whether or how they act together to influence the choice of the recombination pathway. Moreover, the activities of some mediators have been difficult to uncover. For example, the five proteins known as RAD51 paralogs play important roles in recombination reactions, as proven by cellular phenotypes caused by their deletion (174). However, until now their mechanism of action remains elusive.

Formation of RAD51 filament: roles of RPA, Rad52 and BRCA2

RPA has both inhibitory and stimulatory effect on RAD51-mediated strand exchange *in vitro*. Its stimulatory role relies on its ability to disrupt secondary DNA structures (175). Since RAD51 can bind to dsDNA (176), its association with secondary structures hinders the formation of active, extended nucleoprotein filaments (177,178). Promoting the assembly of the RAD51-coated filaments by RPA is essential for recombination reactions *in vivo*, as well as for *in vitro* assays when long DNA substrates are used.

On the other hand, RPA inhibits DNA strand exchange when it is allowed to bind ssDNA before the addition of Rad51. Such *in vitro* conditions likely mimic the *in vivo* situation. Both bacterial and eukaryotic ssDNA binding proteins (SSB and RPA, respectively) bind ssDNA with higher affinity than the recombinases do and therefore may inhibit the formation of the active nucleoprotein filaments. In bacteria this problem is overcome by the action of the RecBCD complex which, in addition to generating the ssDNA tail during DSB resection, directly loads RecA monomers onto

the ssDNA it produces (179). Since eukaryotic cells do not have a RecBCD function, the ssDNA produced by the resection will likely be bound by RPA. Since RPA has higher affinity for ssDNA than RAD51, its displacement from ssDNA by RAD51 is a slow process. This process can be accelerated by accessory proteins, which include i.e. Rad52, BRCA2 and RAD51 paralogs.

Rad52 mutants in *S. cerevisiae* show extreme radiation sensitivity and defects in recombination (180). Surprisingly, Rad52 knockout mice are alive and healthy. They are not hypersensitive to DSB-inducing agents, although they do show slightly reduced frequency of HR. This data suggests that recombination pathways that do not require RAD52 could be more active in mammalian cells than in yeast, and/or there are other proteins that can substitute for the loss of Rad52 (181).

Rad52 interacts with both RPA and Rad51 in a species-specific manner (166,182) and stimulates RAD51-mediated strand exchange *in vitro* (183,184). Biochemical experiments indicate that Rad52 itself does not remove RPA. Instead, it binds the RPA-ssDNA complex, recruits Rad51 to ssDNA, and stimulates RPA displacement by Rad51 (185).

In addition to promoting strand exchange by Rad51, Rad52 also has ssDNA binding and annealing activities (186) and is therefore involved in the SSA pathway. Together with RPA it also mediates second end capture during HR, i.e. annealing of the displaced DNA strand that is produced by Rad51-mediated DNA strand exchange with a second ssDNA end (187).

BRCA2 can be one of the proteins that have taken over RAD52 function in higher eukaryotes, as it is involved in regulating the assembly of the RAD51 nucleoprotein filament, and is required for efficient recombination-mediated repair of DSBs. In the absence of functional BRCA2, cells use alternative, more error-prone or less efficient forms of DNA repair. This leads to accumulation of DNA breaks and chromosomal rearrangements, which, in the long term, can promote malignant transformation. Consistently, BRCA2 mutations strongly predispose to breast and/or ovarian cancer (188).

BRCA2 has two regions involved in RAD51 binding: six out of eight BRC repeats (35-amino acid motifs) located in the central part of the protein, and a BRC-unrelated C-terminal region. The BRC repeats disrupt RAD51 oligomers and facilitate the formation of a BRCA2–RAD51 complex with RAD51 monomers binding BRC repeats (189). It has been suggested that this interaction may keep RAD51 inactive until it is needed, i.e. after DNA damage. Since BRCA2 interacts directly with ssDNA, it may recruit RAD51 to sites of damage, and possibly facilitate loading of the RAD51 monomers onto the ssDNA, thus promoting the assembly of the active nucleoprotein filament (190). The C-terminal region interacting with RAD51 (the TR2 region) appears to have different characteristics. In contrast to the BRC repeats, TR2 does not interact with RAD51 monomers. Instead, it binds the oligomeric form of RAD51 that is present in the context of a RAD51-ssDNA filament. Therefore, the TR2 region of BRCA2 can serve to protect this oligomeric RAD51 form from disassembly, and thus stimulate strand invasion (191,192). However, it worth noting that the data described above is based on experiments with BRCA2 fragments. Since the full-length BRCA2 has not been purified yet, the exact mechanism of BRCA2 action remains uncertain.

RAD51AP1 stimulates joint molecule formation

RAD51AP1 was identified as a protein interacting with RAD51, which suggested that it might play a role in HR. Its down regulation resulted in hypersensitivity to crosslinking agents and ionizing radiation, a hallmark phenotype of recombination deficiency. The detailed analysis of RAD51AP1, described in Chapter 5 of this thesis, revealed that it promotes recombination reactions both *in vivo* and *in vitro*. However, unlike BRCA1 and RAD52, RAD51AP1 most likely does not influence the formation of the RAD51 nucleoprotein filament. Instead, it specifically stimulates joint molecule formation through the combination of structure-specific DNA binding and physical contact with RAD51 (147).

RAD54 – a recombination protein with many functions

The efficiency of RAD51-mediated strand invasion, as measured *in vitro* by the stability of the resultant joint molecule, is stimulated by RAD54, a protein belonging to the SWI2/SNF2 family of chromatin-remodeling proteins (193). Mutations in the Rad54 gene strongly impair HR in both yeast and higher eukaryotes (180,194,195), but the mechanisms by which RAD54 stimulates HR are unclear. It is possible that it affects the reaction at different stages. RAD54 binds to the assembled RAD51 nucleoprotein filament and this interaction is thought to recruit RAD54 to the joint molecule (196). As shown by ChIP experiments, RAD54 is recruited to a DSB *in vivo* during early steps of recombination. Both *in vivo* and *in vitro* data indicate that RAD54 facilitates the formation of the joint molecule (197,198). RAD54 is a dsDNA dependent ATPase (199,200), which uses the energy of ATP hydrolysis to translocate on dsDNA. This can lead to introducing negative supercoils into the recipient duplex DNA and positive supercoils on the other side, and could favor the invasion of the incoming single strand (201,202), and/or promote the extension of the formed heterodupex (203). Interestingly, RAD54 can dissociate Rad51 from nucleoprotein filaments formed on dsDNA, and this activity might help to recycle RAD51 that is bound to duplex DNA (204). Recently, it has also been shown that Rad54 specifically binds HJs and promotes their bidirectional branch migration in an ATPase-dependent manner (205). Interestingly, the Rad54 branch migration activity was shown to be involved in dissociating DNA joint molecules (D-loops) (206), which might channel the recombination reaction into the SDSA pathway.

4.2. Translesion synthesis

As mentioned above, two mechanisms allow overcoming the replication blocks imposed by DNA lesions. Homologous recombination (HR), including the template switch pathway, uses the intact sister chromatid as a template for repair, and is therefore mostly error-free (207). Translesion synthesis (TLS) employs a specialized set of DNA polymerases to replicate over damaged DNA (208,209). However, neither TLS, nor template switch recombination actually remove the damage, and therefore they are referred to as the damage tolerance systems.

The common characteristics of TLS polymerases are more open active sites which allow them to accommodate irregular template structures (210), and the lack of 3'–5' exonuclease proofreading activity (211). These features allow the

TLS polymerases to copy lesion-containing DNA, but, at the same time, make them intrinsically error-prone. TLS polymerases frequently introduce mutations by incorporating incorrect nucleotides on both damaged and undamaged templates, and therefore have to be precisely controlled.

Replication of damaged DNA is regulated by the genes in the RAD6 epistasis group in *S. cerevisiae* (212). Some members of this group encode enzymes involved in ubiquitin conjugation: RAD6 is an E2 ubiquitin conjugating enzyme, which acts together with RAD18, a RING finger-containing E3 ubiquitin ligase (213). Another pair of E2/E3 enzymes consists of a RING finger ubiquitin ligase RAD5, and a ubiquitin-conjugating enzyme MMS2/UBC13. This dimer is unusual in that the poly-ubiquitin chains it forms are linked via internal lysine K63 of ubiquitin, rather than the more common K48 used for targeting proteins for proteasomal degradation (214,215).

Recent discoveries showed that the main target of these enzymes in the damage tolerance pathway is the replication processivity factor PCNA (213). In response to DNA damage RAD6 and RAD18 catalyze binding of a single ubiquitin moiety to the conserved K164 of PCNA. Multiple ubiquitin molecules can be subsequently added, forming a K63-linked poly-ubiquitin chain, in a reaction promoted by RAD5 and MMS2/UBC13. Interestingly, the two modifications have different outcomes (216). Poly-ubiquitination promotes error-free, recombination-mediated rescue of stalled replication forks. This process, and the mechanisms of its regulation by PCNA poly-ubiquitination are poorly understood. In contrast, PCNA mono-ubiquitination activates TLS. Recent discoveries uncovered the basic mechanisms of this regulation, as two independent groups (217,218) showed that TLS polymerase η preferentially interacts with the mono-ubiquitinated form of PCNA. This interaction was proposed to recruit Pol η to the stalled forks, where it can carry out lesion bypass. This process appears to be a common way of promoting polymerase switch, since Pol ι and REV1 also interact with mono-ubiquitinated PCNA, and this interaction is necessary for their localization to the damage-induced local accumulation of proteins, named foci, which also contain PCNA. All Y-family TLS polymerases (REV1, Pol η, Pol ι and Pol κ) have two evolutionary conserved ubiquitin-binding domains. These domains are required for the interaction of Pol η and Pol ι (and possibly other Y-family members) with mono-ubiquitinated PCNA (219) (Fig 9).

However, the molecular details of how exactly the recruitment of TLS polymerases to the template DNA occurs are still unclear. It is conceivable that the TLS polymerases are constitutively associated with the replication machinery at the moving replication fork. The ability of TLS polymerases to bind PCNA, as well as co-localization studies showing that some TLS polymerases are present in replication factories are consistent with this possibility (220). Mono-ubiquitination of PCNA at the stalled fork would increase its affinity for the TLS polymerases, which could induce protein re-arrangements at the fork, resulting in a TLS polymerase gaining access to the 3' OH primer terminus. Alternatively, mono-ubiquitinated PCNA could also attract free TLS polymerases to the replication machinery. The absence of Pol η foci in Rad18-deficient cells favors this possibility (218) .

Although the precise mechanism of polymerase switch is unknown, it is clear that the main event triggering it is the ubiquitination of PCNA. Ubiquitination is induced by UV light and benzo[a]pyrene (217,221), which generate replication-stalling DNA
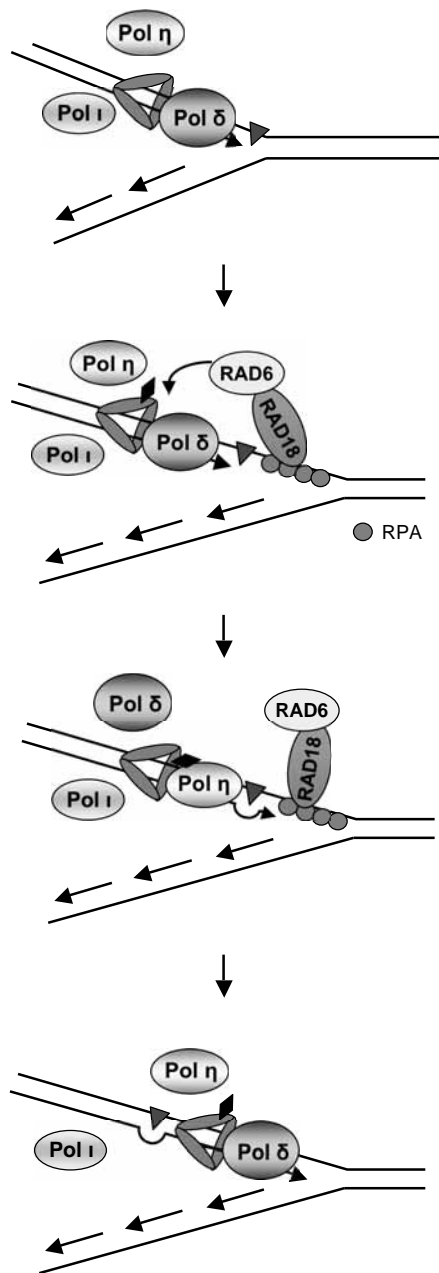
Figure 9. Model of translesion synthesis
A replicative polymerase (e.g. Pol δ stalls at a lesion in the DNA template. The RPA-coated ssDNA generated at the damage site might help to recruit RAD18/RAD6, which in turn ubiquitinate PCNA. PCNA ubiquitination induces polymerase switch, as a result of which a TLS polymerase (e.g. Pol η)gains access to the template and synthesizes a short fragment of DNA opposite the lesion. The second polymerase switch places a replicative polymerase at the primer terminus and allows it to continue high fidelity DNA synthesis.

lesions. Ubiquitination is induced also by hydroxyurea, which hinders replication by depleting nucleotide pools, and not by introducing any physical damage to the DNA template (217). This indicates that PCNA mono-ubiquitination is primarily activated by the presence of stalled replication forks. As mentioned above, TLS is an inherently error-prone process, and its rigorous control is critical to prevent unwanted mutations. Therefore, it would be very interesting to know whether PCNA ubiquitination is a direct and passive consequence of arresting replication forks, or whether it is actively regulated, e.g. by damage signaling pathways. RAD18, the ubiquitin ligase catalyzing mono-ubiquitination of PCNA, interacts not only with RAD6 and PCNA, but also with ssDNA (222). As increased amount of ssDNA is present at a stalled replication fork, this interaction might be involved in recruiting RAD18 and RAD6 to its PCNA target.

Recently, it has been shown that levels of mono-ubiquitinated PCNA are also regulated by a de-ubiquitinating enzyme USP1. UV-induced auto-cleavage of USP1 leads to the accumulation of modified PCNA and activates TLS. Consistently, USP1 down regulation resulted in increased mutation frequency following UV irradiation (223). It remains unknown how UV triggers inactivation of USP1. Neither ATM- and ATR-controlled damage response pathways, nor the nucleotide excision repair (NER) proteins seem to be involved in this process. At present, there is no evidence for the regulation of TLS activity by checkpoint pathways. PCNA mono-ubiquitination is unaffected in cells deficient in Rad3 (*S. pombe* homolog of human ATR) and checkpoint signaling is normally activated in cells expressing PCNA K164R mutant (224).

Another yet unanswered question concerns the choice of the TLS polymerase that will bypass a specific lesion. Eukaryotic cells express a number of TLS polymerases, which have different properties and different substrate preferences (summarized in Table 1). The current 'trial and error' model predicts that they simply compete for binding to ubiquitinated PCNA and either insert nucleotides or fall off if they cannot cope with the damage, leaving the stage for another candidate (208).

The choice of the polymerase is even more complicated by the fact that cooperation of two different enzymes is often needed to overcome certain lesions. The two-step model of lesion bypass comprises incorporation of a limited number of nucleotides directly opposite the damage by the first TLS polymerase, followed by extension from the inserted nucleotides by the second TLS polymerase (225,226). Because the damage is present in the template DNA, the insertion will likely generate a mismatched or distorted primer terminus. Replicative DNA polymerases are not able to extend such a structure and will degrade it using their 3'-5' exonuclease activity. Therefore, extension by a second TLS polymerase, which lacks the exonuclease activity and can tolerate abnormal primer termini, is probably critical for efficient TLS. However, this scenario poses another question: whether or how are the polymerases programmed to act in a specific order? The ways of controlling their reorganizations remain to be found, but it is conceivable that ubiquitination of TLS polymerases themselves (219,227) could be involved in this process. As proposed before, ubiquitinated PCNA serves to attract the first TLS polymerase, which will insert nucleotides opposite the damage site. The subsequent ubiquitination of the first polymerase would create the binding site for the ubiquitin-binding domain of the second TLS polymerase, which could then extend the DNA molecule past the lesion.

REV1, a dCMP transferase belonging to the Y-family of TLS polymerases, could also be involved in controlling and/or facilitating polymerase switching. REV1 physically interacts with all main TLS polymerases: Pol η, Pol ι, Pol κ, and REV7 subunit of Pol ζ, and therefore it was proposed to form a platform for recruiting and/ or rearranging the polymerases at the stalled forks. Consistently, REV1, but not its catalytic activity, is required for damage-induced mutagenesis (228-230).

Once the DNA fragment opposite the lesion has been extended enough not to be susceptible to removal by exonucleolytic proofreading, the high-fidelity replicative polymerases should take over DNA synthesis (Fig 9). This leads to another important question of how the action of a TLS polymerase at the replication fork is terminated, and how do replicative polymerases regain access to the 3' OH end of the growing DNA molecule? Since TLS is activated by ubiquitination of PCNA, one could expect that, by analogy, it would be switched off by removing ubiquitin. However, levels of ubiquitinated PCNA increase after UV irradiation, and stay elevated for more then 24 hours (217). At present it is unknown whether this reflects the duration of PCNA ubiquitination at an individual fork, or whether this represents the equilibrium between de-ubiquitination at the already restarted forks and ubiquitination at the forks that have just encountered a lesion. The latter possibility is perhaps more likely, because it seems rather dangerous to maintain the modification that attracts error-prone polymerases to the template.

It is also possible that TLS polymerases dissociate from the template because of their inherently poor processivity. TLS polymerases generally synthesize short DNA fragments, e.g. pol η inserts only 1-8 nucleotides on any template (231) So, after synthesizing such a short piece, they could simply fall off the DNA. It is unclear though how the "falling off" happens – do the TLS polymerases dissociate, or are they still attached to PCNA, and only re-group within the replication complex? It is also unknown what happens to the replicative polymerases during the TLS process. As yet there is no direct evidence whether or not their affinity for PCNA is affected by its mono-ubiquitination.

Y family	Pol η	efficiently inserts correct nucleotides opposite UV-induced cyclobutane thymine dimers (but not 6-4 photoproducts (6-4 PP), and is responsible for their accurate bypass *in vivo* (232). Its deficiency results in the variant form of xeroderma pigmentosum, characterized by extreme sensitivity to sunlight and increased incidence of skin cancer (233). Pol η is constitutively localized in replication factories (234). It also plays a role in HR by extending the invading strand in a D-loop structure (235,236).
Y family	Pol ι	has very low processivity and very high error rate. It inserts bases opposite some types of damage, e.g 6-4 PP and abasic sites, but is unable to extend from the inserted base (237). Pol ι is found in replication factories (220). Its precise function is unknown.

Y family	Pol κ	can extend terminal mismatches on undamaged templates and bypass benzo[a]pyrene adducts (238,239) and has been proposed to function as an extender in bypass of UV-induced lesions (225). Pol κ-deficient cells are sensitive to benzo[a]pyrene and methyl methanesulfonate (240). Pol κ is localized to replication factories only in a fraction of S-phase cells (241).
Y family	Rev1	is a dCMP transferase (242). It inserts dCMPs opposite either guanines or abasic sites, and is able bypass of 6-4 PP and abasic sites. REV1 protein, but not its catalytical activity, is required for damage-induced mutagenesis. Via its C-terminal region REV1 interacts with other Y-family polymerases and with REV7 (228-230)
B family	Polζ	is composed of REV3 (catalytic) and REV7 (regulatory) subunits (243). It is required for damage-induced mutagenesis and for bypass of 6-4 PP and abasic sites. It is efficient in extending terminally mismatched primers or primer termini opposite lesions, and therefore is supposed to be involved in the extension step of TLS (225)

Table 1. Summary of properties of TLS polymerases present in higher eukaryotes.
In addition to polymerases listed here, other, yet uncharacterized TLS polymerases (Pol θ, Pol υ, Pol λ, and Pol μ) could also be involved in lesion bypass.

4.3. TLS versus HR

The damage tolerance systems consist of error-prone TLS and error-free recombination-mediated pathways, activated by mono- and poly-ubiquitination, respectively. While the components and activities of these two pathways are relatively conserved, their relative contributions to overcoming replication blocks differ significantly among eukaryotes. In yeast both mono- and poly-ubiquitination are readily detectable. In mammalian cells mono-ubiquitination is the main UV- induced PCNA modification. Poly-ubiquitination is detectable at significantly lower levels. As in yeast, poly-ubiquitination is involved in the error-free pathway of lesion bypass (244,245). It might be surprising that mammalian cells seem to favor the error-prone option. On the other hand, HR also potentially poses a threat to genome stability. It does not induce point mutations, but, if misregulated, can cause more dangerous types of damage, e.g. DNA DSBs breaks, deletions, duplications, and translocations. Since mammalian genomes are much larger that those of bacteria or yeast, and contain many more repetitive sequences, HR in mammalian cells might be associated with relatively higher risk and therefore be much more limited.

RecA-mediated HR is the main pathway dealing with stalled replication forks in bacteria. However, in addition to its mechanistic role during homology search, RecA also plays a crucial role in inducing a global damage response, termed the SOS response, which includes TLS-mediated mutagenesis. The presence of damage-induced RecA filaments assembled on ssDNA is the main trigger for autodigestion of the transcription repressor LexA. Inactivation of LexA results in the up regulation of more then 40 genes involved in DNA repair and regulation of the cell cycle, the so-called SOS response (246). UmuD and UmuC, whose expression is thus induced, form a $UmuD_2C$ complex. Its RecA-induced autocleavage leads to the formation of a catalytically active $UmuD_2'C$, which is the main bacterial TLS polymerase - Pol V (247). Strikingly, not only the formation of active Pol V enzyme depends on RecA. Both genetic and biochemical experiments proved that the presence of RecA is required for lesion bypass activity of Pol V (248-250). The finding that over expression of $UmuD_2'C$ inhibits RecA-catalyzed recombination suggests that the dependence might be mutual, and that the interaction between Pol V and RecA could act to favour the TLS pathway (251,252). Interestingly, RecA expression is induced very rapidly, while $UmuD_2'C$ levels increase relatively late during the SOS response (253). This difference in timing suggests an elegant way of regulating the order in which TLS and HR act: the RecA-mediated recombination is the preferred mechanism, and is active early during the SOS response. In case it cannot cope with the damage, TLS is subsequently activated and, by inhibiting HR, it takes over the task of rescuing the stalled forks.

Similar links between TLS and HR might exist in mammalian cells, although to date there is no evidence that TLS polymerases require RAD51 or assembled RAD51 filament for lesion bypass activity. However, the fact that RAD51 is an essential gene whose deletion is lethal (254,255) makes such dependency, if it exists, difficult to discover and to investigate. Interestingly though, recent findings indicate that in vertebrate cells TLS and HR are indeed related. TLS polymerase η was shown to be involved in the extension of the invading strand of the D-loop structure both *in vitro* and *in vivo* (235,236). Moreover, studies in chicken DT40 cells revealed that Rev1 and Pol ζ play a role in HR-dependent DSB repair, and that deletion of Pol ζ resulted in decreased gene targeting efficiency (256). Clearly, we are only beginning to understand the interplay and the interdependency of the damage avoidance pathways. An important part of the future research will likely focus on the mechanisms deciding which pathway will deal with a specific lesion.

5. Summary

During every S-phase replication forks are stalled at lesions in the DNA template. Such forks have to be detected and restarted in order for the cell to divide and survive. The essential function of the checkpoint machinery is to sense and signal the presence of DNA damage and replication problems and stop or delay cell cycle progression to allow sufficient time for repair. Additionally, checkpoint signaling helps to protect stalled replication forks from irreversible collapse. The restart of stalled replication forks is promoted by two pathways: homolgous recombination and translesion synthesis. Homologous recombination uses an intact sister chromatid as a template for repair and is therefore essentially error-free. Translesion synthesis

employs specialized polymerases to bypass the lesions and often induces mutations. Despite progress in understanding the molecular mechanisms of these pathways, it is still unclear how the choice between them is made. It also remains to be discovered whether or how checkpoint signaling is involved in activating and/or regulating the recombination restart.

References:

1. Solomon, M.J., Glotzer, M., Lee, T.H., Philippe, M. and Kirschner, M.W. (1990) Cyclin activation of p34cdc2. *Cell*, **63**, 1013-1024.
2. Sherr, C.J. (1995) D-type cyclins. *Trends Biochem Sci*, **20**, 187-190.
3. Beijersbergen, R.L. and Bernards, R. (1996) Cell cycle regulation by the retinoblastoma family of growth inhibitory proteins. *Biochim Biophys Acta*, **1287**, 103-120.
4. Geng, Y., Eaton, E.N., Picon, M., Roberts, J.M., Lundberg, A.S., Gifford, A., Sardet, C. and Weinberg, R.A. (1996) Regulation of cyclin E transcription by E2Fs and retinoblastoma protein. *Oncogene*, **12**, 1173-1180.
5. Botz, J., Zerfass-Thome, K., Spitkovsky, D., Delius, H., Vogt, B., Eilers, M., Hatzigeorgiou, A. and Jansen-Durr, P. (1996) Cell cycle regulation of the murine cyclin E gene depends on an E2F binding site in the promoter. *Mol Cell Biol*, **16**, 3401-3409.
6. Koff, A., Giordano, A., Desai, D., Yamashita, K., Harper, J.W., Elledge, S., Nishimoto, T., Morgan, D.O., Franza, B.R. and Roberts, J.M. (1992) Formation and activation of a cyclin E-cdk2 complex during the G1 phase of the human cell cycle. *Science*, **257**, 1689-1694.
7. Dulic, V., Lees, E. and Reed, S.I. (1992) Association of human cyclin E with a periodic G1-S phase protein kinase. *Science*, **257**, 1958-1961.
8. Elledge, S.J., Richman, R., Hall, F.L., Williams, R.T., Lodgson, N. and Harper, J.W. (1992) CDK2 encodes a 33-kDa cyclin A-associated protein kinase and is expressed before CDC2 in the cell cycle. *Proc Natl Acad Sci U S A*, **89**, 2907-2911.
9. van den Heuvel, S. and Harlow, E. (1993) Distinct roles for cyclin-dependent kinases in cell cycle control. *Science*, **262**, 2050-2054.
10. Nurse, P. (1990) Universal control mechanism regulating onset of M-phase. *Nature*, **344**, 503-508.
11. Obaya, A.J. and Sedivy, J.M. (2002) Regulation of cyclin-Cdk activity in mammalian cells. *Cell Mol Life Sci*, **59**, 126-142.
12. Zhou, B.B. and Elledge, S.J. (2000) The DNA damage response: putting checkpoints in perspective. *Nature*, **408**, 433-439.
13. Yang, Y., Li, C.C. and Weissman, A.M. (2004) Regulating the p53 system through ubiquitination. *Oncogene*, **23**, 2096-2106.
14. Bartek, J. and Lukas, J. (2001) Pathways governing G1/S transition and their response to DNA damage. *FEBS Lett*, **490**, 117-122.
15. Schuler, M. and Green, D.R. (2001) Mechanisms of p53-dependent apoptosis. *Biochem Soc Trans*, **29**, 684-688.
16. Dronkert, M.L. and Kanaar, R. (2001) Repair of DNA interstrand cross-links. *Mutat Res*, **486**, 217-247.
17. Lambert, S. and Carr, A.M. (2005) Checkpoint responses to replication fork barriers. *Biochimie*, **87**, 591-602.
18. Tercero, J.A. and Diffley, J.F. (2001) Regulation of DNA replication fork progression through damaged DNA by the Mec1/Rad53 checkpoint. *Nature*, **412**, 553-557.
19. Tercero, J.A., Longhese, M.P. and Diffley, J.F. (2003) A central role for DNA replication forks in checkpoint activation and response. *Mol Cell*, **11**, 1323-1336.
20. Torres-Rosell, J., Machin, F., Farmer, S., Jarmuz, A., Eydmann, T., Dalgaard, J.Z. and Aragon, L. (2005) SMC5 and SMC6 genes are required for the segregation of repetitive chromosome regions. *Nat Cell Biol*, **7**, 412-419.
21. Niedernhofer, L.J., Odijk, H., Budzowska, M., van Drunen, E., Maas, A., Theil, A.F., de Wit, J., Jaspers, N.G., Beverloo, H.B., Hoeijmakers, J.H. *et al.* (2004) The structure-specific endonuclease Ercc1-Xpf is required to resolve DNA interstrand cross-link-induced double-strand breaks. *Mol Cell Biol*, **24**, 5776-5787.

22. Hanada, K., Budzowska, M., Davies, S.L., van Drunen, E., Onizawa, H., Beverloo, H.B., Maas, A., Essers, J., Hickson, I.D. and Kanaar, R. (2007) The structure-specific endonuclease Mus81 contributes to replication restart by generating double-strand DNA breaks. *Nat Struct Mol Biol*, **14**, 1096-1104.

23. Chan, K.L., North, P.S. and Hickson, I.D. (2007) BLM is required for faithful chromosome segregation and its localization defines a class of ultrafine anaphase bridges. *Embo J*, **26**, 3397-3409.

24. Kelly, T.J., Martin, G.S., Forsburg, S.L., Stephen, R.J., Russo, A. and Nurse, P. (1993) The fission yeast cdc18+ gene product couples S phase to START and mitosis. *Cell*, **74**, 371-382.

25. Toyn, J.H., Johnson, A.L. and Johnston, L.H. (1995) Segregation of unreplicated chromosomes in Saccharomyces cerevisiae reveals a novel G1/M-phase checkpoint. *Mol Cell Biol*, **15**, 5312-5321.

26. Abraham, R.T. (2001) Cell cycle checkpoint signaling through the ATM and ATR kinases. *Genes Dev*, **15**, 2177-2196.

27. Bosotti, R., Isacchi, A. and Sonnhammer, E.L. (2000) FAT: a novel domain in PIK-related kinases. *Trends Biochem Sci*, **25**, 225-227.

28. Perry, J. and Kleckner, N. (2003) The ATRs, ATMs, and TORs are giant HEAT repeat proteins. *Cell*, **112**, 151-155.

29. Becker-Catania, S.G. and Gatti, R.A. (2001) Ataxia-telangiectasia. *Adv Exp Med Biol*, **495**, 191-198.

30. Crawford, T.O. (1998) Ataxia telangiectasia. *Semin Pediatr Neurol*, **5**, 287-294.

31. Shiloh, Y. and Kastan, M.B. (2001) ATM: genome stability, neuronal development, and cancer cross paths. *Adv Cancer Res*, **83**, 209-254.

32. Bakkenist, C.J. and Kastan, M.B. (2003) DNA damage activates ATM through intermolecular autophosphorylation and dimer dissociation. *Nature*, **421**, 499-506.

33. Kozlov, S.V., Graham, M.E., Peng, C., Chen, P., Robinson, P.J. and Lavin, M.F. (2006) Involvement of novel autophosphorylation sites in ATM activation. *Embo J*, **25**, 3504-3514.

34. Pellegrini, M., Celeste, A., Difilippantonio, S., Guo, R., Wang, W., Feigenbaum, L. and Nussenzweig, A. (2006) Autophosphorylation at serine 1987 is dispensable for murine Atm activation in vivo. *Nature*, **443**, 222-225.

35. Goodarzi, A.A., Jonnalagadda, J.C., Douglas, P., Young, D., Ye, R., Moorhead, G.B., Lees-Miller, S.P. and Khanna, K.K. (2004) Autophosphorylation of ataxia-telangiectasia mutated is regulated by protein phosphatase 2A. *Embo J*, **23**, 4451-4461.

36. Ali, A., Zhang, J., Bao, S., Liu, I., Otterness, D., Dean, N.M., Abraham, R.T. and Wang, X.F. (2004) Requirement of protein phosphatase 5 in DNA-damage-induced ATM activation. *Genes Dev*, **18**, 249-254.

37. Yong, W., Bao, S., Chen, H., Li, D., Sanchez, E.R. and Shou, W. (2007) Mice lacking protein phosphatase 5 are defective in ataxia telangiectasia mutated (ATM)-mediated cell cycle arrest. *J Biol Chem*, **282**, 14690-14694.

38. Shreeram, S., Demidov, O.N., Hee, W.K., Yamaguchi, H., Onishi, N., Kek, C., Timofeev, O.N., Dudgeon, C., Fornace, A.J., Anderson, C.W. *et al.* (2006) Wip1 phosphatase modulates ATM-dependent signaling pathways. *Mol Cell*, **23**, 757-764.

39. Lu, X., Nannenga, B. and Donehower, L.A. (2005) PPM1D dephosphorylates Chk1 and p53 and abrogates cell cycle checkpoints. *Genes Dev*, **19**, 1162-1174.

40. Maser, R.S., Monsen, K.J., Nelms, B.E. and Petrini, J.H. (1997) hMre11 and hRad50 nuclear foci are induced during the normal cellular response to DNA double-strand breaks. *Mol Cell Biol*, **17**, 6087-6096.

41. Mirzoeva, O.K. and Petrini, J.H. (2001) DNA damage-dependent nuclear dynamics of the Mre11 complex. *Mol Cell Biol*, **21**, 281-288.

42. Lee, J.H. and Paull, T.T. (2005) ATM activation by DNA double-strand breaks through the Mre11-Rad50-Nbs1 complex. *Science*, **308**, 551-554.

43. de Jager, M., van Noort, J., van Gent, D.C., Dekker, C., Kanaar, R. and Wyman, C. (2001) Human Rad50/Mre11 is a flexible complex that can tether DNA ends. *Mol Cell*, **8**, 1129-1135.

44. Uziel, T., Lerenthal, Y., Moyal, L., Andegeko, Y., Mittelman, L. and Shiloh, Y. (2003) Requirement of the MRN complex for ATM activation by DNA damage. *Embo J*, **22**, 5612-5621.

45. Carson, C.T., Schwartz, R.A., Stracker, T.H., Lilley, C.E., Lee, D.V. and Weitzman, M.D. (2003) The Mre11 complex is required for ATM activation and the G2/M checkpoint. *Embo J*, **22**, 6610-6620.

46. Kitagawa, R., Bakkenist, C.J., McKinnon, P.J. and Kastan, M.B. (2004) Phosphorylation of SMC1 is a critical downstream event in the ATM-NBS1-BRCA1 pathway. *Genes Dev*, **18**, 1423-1438.

47. Wu, X., Ranganathan, V., Weisman, D.S., Heine, W.F., Ciccone, D.N., O'Neill, T.B., Crick, K.E., Pierce, K.A., Lane, W.S., Rathbun, G. *et al.* (2000) ATM phosphorylation of Nijmegen breakage syndrome protein is required in a DNA damage response. *Nature*, **405**, 477-482.

48. Gatei, M., Young, D., Cerosaletti, K.M., Desai-Mehta, A., Spring, K., Kozlov, S., Lavin, M.F., Gatti, R.A., Concannon, P. and Khanna, K. (2000) ATM-dependent phosphorylation of nibrin in response to radiation exposure. *Nat Genet*, **25**, 115-119.

49. Lim, D.S., Kim, S.T., Xu, B., Maser, R.S., Lin, J., Petrini, J.H. and Kastan, M.B. (2000) ATM phosphorylates p95/nbs1 in an S-phase checkpoint pathway. *Nature*, **404**, 613-617.

50. Gontijo, A.M., Green, C.M. and Almouzni, G. (2003) Repairing DNA damage in chromatin. *Biochimie*, **85**, 1133-1147.

51. Sun, Y., Jiang, X., Chen, S., Fernandes, N. and Price, B.D. (2005) A role for the Tip60 histone acetyltransferase in the acetylation and activation of ATM. *Proc Natl Acad Sci U S A*, **102**, 13182-13187.

52. Sun, Y., Xu, Y., Roy, K. and Price, B.D. (2007) DNA damage induced acetylation of lysine 3016 of ATM activates ATM kinase activity. *Mol Cell Biol*.

53. Gupta, A., Sharma, G.G., Young, C.S., Agarwal, M., Smith, E.R., Paull, T.T., Lucchesi, J.C., Khanna, K.K., Ludwig, T. and Pandita, T.K. (2005) Involvement of human MOF in ATM function. *Mol Cell Biol*, **25**, 5292-5305.

54. Banin, S., Moyal, L., Shieh, S., Taya, Y., Anderson, C.W., Chessa, L., Smorodinsky, N.I., Prives, C., Reiss, Y., Shiloh, Y. *et al.* (1998) Enhanced phosphorylation of p53 by ATM in response to DNA damage. *Science*, **281**, 1674-1677.

55. Canman, C.E., Lim, D.S., Cimprich, K.A., Taya, Y., Tamai, K., Sakaguchi, K., Appella, E., Kastan, M.B. and Siliciano, J.D. (1998) Activation of the ATM kinase by ionizing radiation and phosphorylation of p53. *Science*, **281**, 1677-1679.

56. Ashcroft, M., Kubbutat, M.H. and Vousden, K.H. (1999) Regulation of p53 function and stability by phosphorylation. *Mol Cell Biol*, **19**, 1751-1758.

57. Ryan, K.M., Phillips, A.C. and Vousden, K.H. (2001) Regulation and function of the p53 tumor suppressor protein. *Curr Opin Cell Biol*, **13**, 332-337.

58. Kim, S.T., Xu, B. and Kastan, M.B. (2002) Involvement of the cohesin protein, Smc1, in Atm-dependent and independent responses to DNA damage. *Genes Dev*, **16**, 560-570.

59. Taniguchi, T., Garcia-Higuera, I., Xu, B., Andreassen, P.R., Gregory, R.C., Kim, S.T., Lane, W.S., Kastan, M.B. and D'Andrea, A.D. (2002) Convergence of the fanconi anemia and ataxia telangiectasia signaling pathways. *Cell*, **109**, 459-472.

60. Yazdi, P.T., Wang, Y., Zhao, S., Patel, N., Lee, E.Y. and Qin, J. (2002) SMC1 is a downstream effector in the ATM/NBS1 branch of the human S-phase checkpoint. *Genes Dev*, **16**, 571-582.

61. Gatei, M., Scott, S.P., Filippovitch, I., Soronika, N., Lavin, M.F., Weber, B. and Khanna, K.K. (2000) Role for ATM in DNA damage-induced phosphorylation of BRCA1. *Cancer Res*, **60**, 3299-3304.

62. Cortez, D., Wang, Y., Qin, J. and Elledge, S.J. (1999) Requirement of ATM-dependent phosphorylation of brca1 in the DNA damage response to double-strand breaks. *Science*, **286**, 1162-1166.

63. Xu, B., O'Donnell, A.H., Kim, S.T. and Kastan, M.B. (2002) Phosphorylation of serine 1387 in Brca1 is specifically required for the Atm-mediated S-phase checkpoint after ionizing irradiation. *Cancer Res*, **62**, 4588-4591.

64. Xu, B., Kim, S. and Kastan, M.B. (2001) Involvement of Brca1 in S-phase and G(2)-phase checkpoints after ionizing irradiation. *Mol Cell Biol*, **21**, 3445-3450.

65. Mailand, N., Falck, J., Lukas, C., Syljuasen, R.G., Welcker, M., Bartek, J. and Lukas, J. (2000) Rapid destruction of human Cdc25A in response to DNA damage. *Science*, **288**, 1425-1429.

66. Falck, J., Mailand, N., Syljuasen, R.G., Bartek, J. and Lukas, J. (2001) The ATM-Chk2-Cdc25A checkpoint pathway guards against radioresistant DNA synthesis. *Nature*, **410**, 842-847.

67. Riballo, E., Kuhne, M., Rief, N., Doherty, A., Smith, G.C., Recio, M.J., Reis, C., Dahm, K., Fricke, A., Krempler, A. *et al.* (2004) A pathway of double-strand break rejoining dependent upon ATM, Artemis, and proteins locating to gamma-H2AX foci. *Mol Cell*, **16**, 715-724.

68. Liu, Q., Guntuku, S., Cui, X.S., Matsuoka, S., Cortez, D., Tamai, K., Luo, G., Carattini-Rivera, S., DeMayo, F., Bradley, A. *et al.* (2000) Chk1 is an essential kinase that is regulated by Atr and required for the G(2)/M DNA damage checkpoint. *Genes Dev*, **14**, 1448-1459.

69. Brown, E.J. and Baltimore, D. (2000) ATR disruption leads to chromosomal fragmentation and early embryonic lethality. *Genes Dev*, **14**, 397-402.

70. Budzowska, M., Jaspers, I., Essers, J., de Waard, H., van Drunen, E., Hanada, K., Beverloo, B., Hendriks, R.W., de Klein, A., Kanaar, R. *et al.* (2004) Mutation of the mouse Rad17 gene leads to embryonic lethality and reveals a role in DNA damage-dependent recombination. *Embo J*, **23**, 3548-3558.

71. de Klein, A., Muijtjens, M., van Os, R., Verhoeven, Y., Smit, B., Carr, A.M., Lehmann, A.R. and Hoeijmakers, J.H. (2000) Targeted disruption of the cell-cycle checkpoint gene ATR leads to early embryonic lethality in mice. *Curr Biol*, **10**, 479-482.

72. Cortez, D., Guntuku, S., Qin, J. and Elledge, S.J. (2001) ATR and ATRIP: partners in checkpoint signaling. *Science*, **294**, 1713-1716.

73. Zou, L. and Elledge, S.J. (2003) Sensing DNA damage through ATRIP recognition of RPA-ssDNA complexes. *Science*, **300**, 1542-1548.

74. Garcia, V., Furuya, K. and Carr, A.M. (2005) Identification and functional analysis of TopBP1 and its homologs. *DNA Repair (Amst)*, **4**, 1227-1239.

75. Kumagai, A., Lee, J., Yoo, H.Y. and Dunphy, W.G. (2006) TopBP1 activates the ATR-ATRIP complex. *Cell*, **124**, 943-955.

76. Venclovas, C. and Thelen, M.P. (2000) Structure-based predictions of Rad1, Rad9, Hus1 and Rad17 participation in sliding clamp and clamp-loading complexes. *Nucleic Acids Res*, **28**, 2481-2493.

77. St Onge, R.P., Udell, C.M., Casselman, R. and Davey, S. (1999) The human G2 checkpoint control protein hRAD9 is a nuclear phosphoprotein that forms complexes with hRAD1 and hHUS1. *Mol Biol Cell*, **10**, 1985-1995.

78. Burtelow, M.A., Roos-Mattjus, P.M., Rauen, M., Babendure, J.R. and Karnitz, L.M. (2001) Reconstitution and molecular analysis of the hRad9-hHus1-hRad1 (9-1-1) DNA damage responsive checkpoint complex. *J Biol Chem*, **276**, 25903-25909.

79. Singh, V.K., Nurmohamed, S., Davey, S.K. and Jia, Z. (2007) Tri-cistronic cloning, overexpression and purification of human Rad9, Rad1, Hus1 protein complex. *Protein Expr Purif*, **54**, 204-211.

80. Kondo, T., Matsumoto, K. and Sugimoto, K. (1999) Role of a complex containing Rad17, Mec3, and Ddc1 in the yeast DNA damage checkpoint pathway. *Mol Cell Biol*, **19**, 1136-1143.

81. Zou, L., Cortez, D. and Elledge, S.J. (2002) Regulation of ATR substrate selection by Rad17-dependent loading of Rad9 complexes onto chromatin. *Genes Dev*, **16**, 198-208.

82. Kondo, T., Wakayama, T., Naiki, T., Matsumoto, K. and Sugimoto, K. (2001) Recruitment of Mec1 and Ddc1 checkpoint proteins to double-strand breaks through distinct mechanisms. *Science*, **294**, 867-870.

83. Majka, J. and Burgers, P.M. (2004) The PCNA-RFC families of DNA clamps and clamp loaders. *Prog Nucleic Acid Res Mol Biol*, **78**, 227-260.

84. Majka, J., Binz, S.K., Wold, M.S. and Burgers, P.M. (2006) Replication protein A directs loading of the DNA damage checkpoint clamp to 5'-DNA junctions. *J Biol Chem*, **281**, 27855-27861.

85. Lee, J., Kumagai, A. and Dunphy, W.G. (2007) The Rad9-Hus1-Rad1 checkpoint clamp regulates interaction of TopBP1 with ATR. *J Biol Chem*, **282**, 28036-28044.

86. Delacroix, S., Wagner, J.M., Kobayashi, M., Yamamoto, K. and Karnitz, L.M. (2007) The Rad9-Hus1-Rad1 (9-1-1) clamp activates checkpoint signaling via TopBP1. *Genes Dev*, **21**, 1472-1477.

87. Wang, X., Zou, L., Lu, T., Bao, S., Hurov, K.E., Hittelman, W.N., Elledge, S.J. and Li, L. (2006) Rad17 phosphorylation is required for claspin recruitment and Chk1 activation in response to replication stress. *Mol Cell*, **23**, 331-341.

88. Post, S., Weng, Y.C., Cimprich, K., Chen, L.B., Xu, Y. and Lee, E.Y. (2001) Phosphorylation of serines 635 and 645 of human Rad17 is cell cycle regulated and is required for G(1)/S checkpoint activation in response to DNA damage. *Proc Natl Acad Sci U S A*, **98**, 13102-13107.

89. Zhao, H. and Piwnica-Worms, H. (2001) ATR-mediated checkpoint pathways regulate phosphorylation and activation of human Chk1. *Mol Cell Biol*, **21**, 4129-4139.

90. Capasso, H., Palermo, C., Wan, S., Rao, H., John, U.P., O'Connell, M.J. and Walworth, N.C. (2002) Phosphorylation activates Chk1 and is required for checkpoint-mediated cell cycle arrest. *J Cell Sci*, **115**, 4555-4564.

91. Chen, P., Luo, C., Deng, Y., Ryan, K., Register, J., Margosiak, S., Tempczyk-Russell, A., Nguyen, B., Myers, P., Lundgren, K. *et al.* (2000) The 1.7 A crystal structure of human cell cycle checkpoint kinase Chk1: implications for Chk1 regulation. *Cell*, **100**, 681-692.

92. Oe, T., Nakajo, N., Katsuragi, Y., Okazaki, K. and Sagata, N. (2001) Cytoplasmic occurrence of the Chk1/Cdc25 pathway and regulation of Chk1 in Xenopus oocytes. *Dev Biol*, **229**, 250-261.

93. Smits, V.A., Reaper, P.M. and Jackson, S.P. (2006) Rapid PIKK-dependent release of Chk1 from chromatin promotes the DNA-damage checkpoint response. *Curr Biol*, **16**, 150-159.

94.   Donzelli, M. and Draetta, G.F. (2003) Regulating mammalian checkpoints through Cdc25 inactivation. *EMBO Rep*, **4**, 671-677.

95.   Costanzo, V., Shechter, D., Lupardus, P.J., Cimprich, K.A., Gottesman, M. and Gautier, J. (2003) An ATR- and Cdc7-dependent DNA damage checkpoint that inhibits initiation of DNA replication. *Mol Cell*, **11**, 203-213.

96.   Jares, P., Donaldson, A. and Blow, J.J. (2000) The Cdc7/Dbf4 protein kinase: target of the S phase checkpoint? *EMBO Rep*, **1**, 319-322.

97.   Masai, H., You, Z. and Arai, K. (2005) Control of DNA replication: regulation and activation of eukaryotic replicative helicase, MCM. *IUBMB Life*, **57**, 323-335.

98.   Paulovich, A.G., Armour, C.D. and Hartwell, L.H. (1998) The Saccharomyces cerevisiae RAD9, RAD17, RAD24 and MEC3 genes are required for tolerating irreparable, ultraviolet-induced DNA damage. *Genetics*, **150**, 75-93.

99.   Kai, M. and Wang, T.S. (2003) Checkpoint activation regulates mutagenic translesion synthesis. *Genes Dev*, **17**, 64-76.

100.   Song, W., Levin, D.S., Varkey, J., Post, S., Bermudez, V.P., Hurwitz, J. and Tomkinson, A.E. (2007) A conserved physical and functional interaction between the cell cycle checkpoint clamp loader and DNA ligase I of eukaryotes. *J Biol Chem*, **282**, 22721-22730.

101.   Aylon, Y. and Kupiec, M. (2003) The checkpoint protein Rad24 of Saccharomyces cerevisiae is involved in processing double-strand break ends and in recombination partner choice. *Mol Cell Biol*, **23**, 6585-6596.

102.   Bessho, T. and Sancar, A. (2000) Human DNA damage checkpoint protein hRAD9 is a 3' to 5' exonuclease. *J Biol Chem*, **275**, 7451-7454.

103.   Parker, A.E., Van de Weyer, I., Laus, M.C., Oostveen, I., Yon, J., Verhasselt, P. and Luyten, W.H. (1998) A human homologue of the Schizosaccharomyces pombe rad1+ checkpoint gene encodes an exonuclease. *J Biol Chem*, **273**, 18332-18339.

104.   Freire, R., Murguia, J.R., Tarsounas, M., Lowndes, N.F., Moens, P.B. and Jackson, S.P. (1998) Human and mouse homologs of Schizosaccharomyces pombe rad1(+) and Saccharomyces cerevisiae RAD17: linkage to checkpoint control and mammalian meiosis. *Genes Dev*, **12**, 2560-2573.

105.   Majka, J. and Burgers, P.M. (2003) Yeast Rad17/Mec3/Ddc1: a sliding clamp for the DNA damage checkpoint. *Proc Natl Acad Sci U S A*, **100**, 2249-2254.

106.   den Elzen, N.R. and O'Connell, M.J. (2004) Recovery from DNA damage checkpoint arrest by PP1-mediated inhibition of Chk1. *Embo J*, **23**, 908-918.

107.   Leroy, C., Lee, S.E., Vaze, M.B., Ochsenbien, F., Guerois, R., Haber, J.E. and Marsolier-Kergoat, M.C. (2003) PP2C phosphatases Ptc2 and Ptc3 are required for DNA checkpoint inactivation after a double-strand break. *Mol Cell*, **11**, 827-835.

108.   Oliva-Trastoy, M., Berthonaud, V., Chevalier, A., Ducrot, C., Marsolier-Kergoat, M.C., Mann, C. and Leteurtre, F. (2007) The Wip1 phosphatase (PPM1D) antagonizes activation of the Chk2 tumour suppressor kinase. *Oncogene*, **26**, 1449-1458.

109.   Fujimoto, H., Onishi, N., Kato, N., Takekawa, M., Xu, X.Z., Kosugi, A., Kondo, T., Imamura, M., Oishi, I., Yoda, A. *et al.* (2006) Regulation of the antioncogenic Chk2 kinase by the oncogenic Wip1 phosphatase. *Cell Death Differ*, **13**, 1170-1180.

110.   Lu, X., Nguyen, T.A. and Donehower, L.A. (2005) Reversal of the ATM/ATR-mediated DNA damage response by the oncogenic phosphatase PPM1D. *Cell Cycle*, **4**, 1060-1064.

111.   Mamely, I., van Vugt, M.A., Smits, V.A., Semple, J.I., Lemmens, B., Perrakis, A., Medema, R.H. and Freire, R. (2006) Polo-like kinase-1 controls proteasome-dependent degradation of Claspin during checkpoint recovery. *Curr Biol*, **16**, 1950-1955.

112.   Gewurz, B.E. and Harper, J.W. (2006) DNA-damage control: Claspin destruction turns off the checkpoint. *Curr Biol*, **16**, R932-934.

113.   Mailand, N., Bekker-Jensen, S., Bartek, J. and Lukas, J. (2006) Destruction of Claspin by SCFbetaTrCP restrains Chk1 activation and facilitates recovery from genotoxic stress. *Mol Cell*, **23**, 307-318.

114.   Peschiaroli, A., Dorrello, N.V., Guardavaccaro, D., Venere, M., Halazonetis, T., Sherman, N.E. and Pagano, M. (2006) SCFbetaTrCP-mediated degradation of Claspin regulates recovery from the DNA replication checkpoint response. *Mol Cell*, **23**, 319-329.

115.   Bell, S.P. and Dutta, A. (2002) DNA replication in eukaryotic cells. *Annu Rev Biochem*, **71**, 333-374.

116.   Takeda, D.Y. and Dutta, A. (2005) DNA replication and progression through S phase. *Oncogene*, **24**, 2827-2843.

117. Sawyer, S.L., Cheng, I.H., Chai, W. and Tye, B.K. (2004) Mcm10 and Cdc45 cooperate in origin activation in Saccharomyces cerevisiae. *J Mol Biol*, **340**, 195-202.

118. Walter, J. and Newport, J. (2000) Initiation of eukaryotic DNA replication: origin unwinding and sequential chromatin association of Cdc45, RPA, and DNA polymerase alpha. *Mol Cell*, **5**, 617-627.

119. Labib, K. and Diffley, J.F. (2001) Is the MCM2-7 complex the eukaryotic DNA replication fork helicase? *Curr Opin Genet Dev*, **11**, 64-70.

120. Masuda, T., Mimura, S. and Takisawa, H. (2003) CDK- and Cdc45-dependent priming of the MCM complex on chromatin during S-phase in Xenopus egg extracts: possible activation of MCM helicase by association with Cdc45. *Genes Cells*, **8**, 145-161.

121. Masumoto, H., Sugino, A. and Araki, H. (2000) Dpb11 controls the association between DNA polymerases alpha and epsilon and the autonomously replicating sequence region of budding yeast. *Mol Cell Biol*, **20**, 2809-2817.

122. Diffley, J.F. (2004) Regulation of early events in chromosome replication. *Curr Biol*, **14**, R778-786.

123. Friedman, K.L., Diller, J.D., Ferguson, B.M., Nyland, S.V., Brewer, B.J. and Fangman, W.L. (1996) Multiple determinants controlling activation of yeast replication origins late in S phase. *Genes Dev*, **10**, 1595-1607.

124. Stevenson, J.B. and Gottschling, D.E. (1999) Telomeric chromatin modulates replication timing near chromosome ends. *Genes Dev*, **13**, 146-151.

125. Hubscher, U., Maga, G. and Spadari, S. (2002) Eukaryotic DNA polymerases. *Annu Rev Biochem*, **71**, 133-163.

126. Maga, G., Stucki, M., Spadari, S. and Hubscher, U. (2000) DNA polymerase switching: I. Replication factor C displaces DNA polymerase alpha prior to PCNA loading. *J Mol Biol*, **295**, 791-801.

127. Stucki, M., Stagljar, I., Jonsson, Z.O. and Hubscher, U. (2001) A coordinated interplay: proteins with multiple functions in DNA replication, DNA repair, cell cycle/checkpoint control, and transcription. *Prog Nucleic Acid Res Mol Biol*, **65**, 261-298.

128. Jonsson, Z.O. and Hubscher, U. (1997) Proliferating cell nuclear antigen: more than a clamp for DNA polymerases. *Bioessays*, **19**, 967-975.

129. Ellison, V. and Stillman, B. (2001) Opening of the clamp: an intimate view of an ATP-driven biological machine. *Cell*, **106**, 655-660.

130. Fukui, T., Yamauchi, K., Muroya, T., Akiyama, M., Maki, H., Sugino, A. and Waga, S. (2004) Distinct roles of DNA polymerases delta and epsilon at the replication fork in Xenopus egg extracts. *Genes Cells*, **9**, 179-191.

131. Karthikeyan, R., Vonarx, E.J., Straffon, A.F., Simon, M., Faye, G. and Kunz, B.A. (2000) Evidence from mutational specificity studies that yeast DNA polymerases delta and epsilon replicate different DNA strands at an intracellular replication fork. *J Mol Biol*, **299**, 405-419.

132. Shcherbakova, P.V. and Pavlov, Y.I. (1996) 3'-->5' exonucleases of DNA polymerases epsilon and delta correct base analog induced DNA replication errors on opposite DNA strands in Saccharomyces cerevisiae. *Genetics*, **142**, 717-726.

133. Harrington, J.J. and Lieber, M.R. (1995) DNA structural elements required for FEN-1 binding. *J Biol Chem*, **270**, 4503-4508.

134. Harrington, J.J. and Lieber, M.R. (1994) The characterization of a mammalian DNA structure-specific endonuclease. *Embo J*, **13**, 1235-1246.

135. Ayyagari, R., Gomes, X.V., Gordenin, D.A. and Burgers, P.M. (2003) Okazaki fragment maturation in yeast. I. Distribution of functions between FEN1 AND DNA2. *J Biol Chem*, **278**, 1618-1625.

136. Jin, Y.H., Ayyagari, R., Resnick, M.A., Gordenin, D.A. and Burgers, P.M. (2003) Okazaki fragment maturation in yeast. II. Cooperation between the polymerase and 3'-5'-exonuclease activities of Pol delta in the creation of a ligatable nick. *J Biol Chem*, **278**, 1626-1633.

137. Rossi, M.L. and Bambara, R.A. (2006) Reconstituted Okazaki fragment processing indicates two pathways of primer removal. *J Biol Chem*, **281**, 26051-26061.

138. Kao, H.I., Veeraraghavan, J., Polaczek, P., Campbell, J.L. and Bambara, R.A. (2004) On the roles of Saccharomyces cerevisiae Dna2p and Flap endonuclease 1 in Okazaki fragment processing. *J Biol Chem*, **279**, 15014-15024.

139. Lusetti, S.L. and Cox, M.M. (2002) The bacterial RecA protein and the recombinational DNA repair of stalled replication forks. *Annu Rev Biochem*, **71**, 71-100.

140. Kowalczykowski, S.C. and Krupp, R.A. (1995) DNA-strand exchange promoted by RecA protein in the absence of ATP: implications for the mechanism of energy transduction in protein-promoted nucleic acid transactions. *Proc Natl Acad Sci U S A*, **92**, 3478-3482.
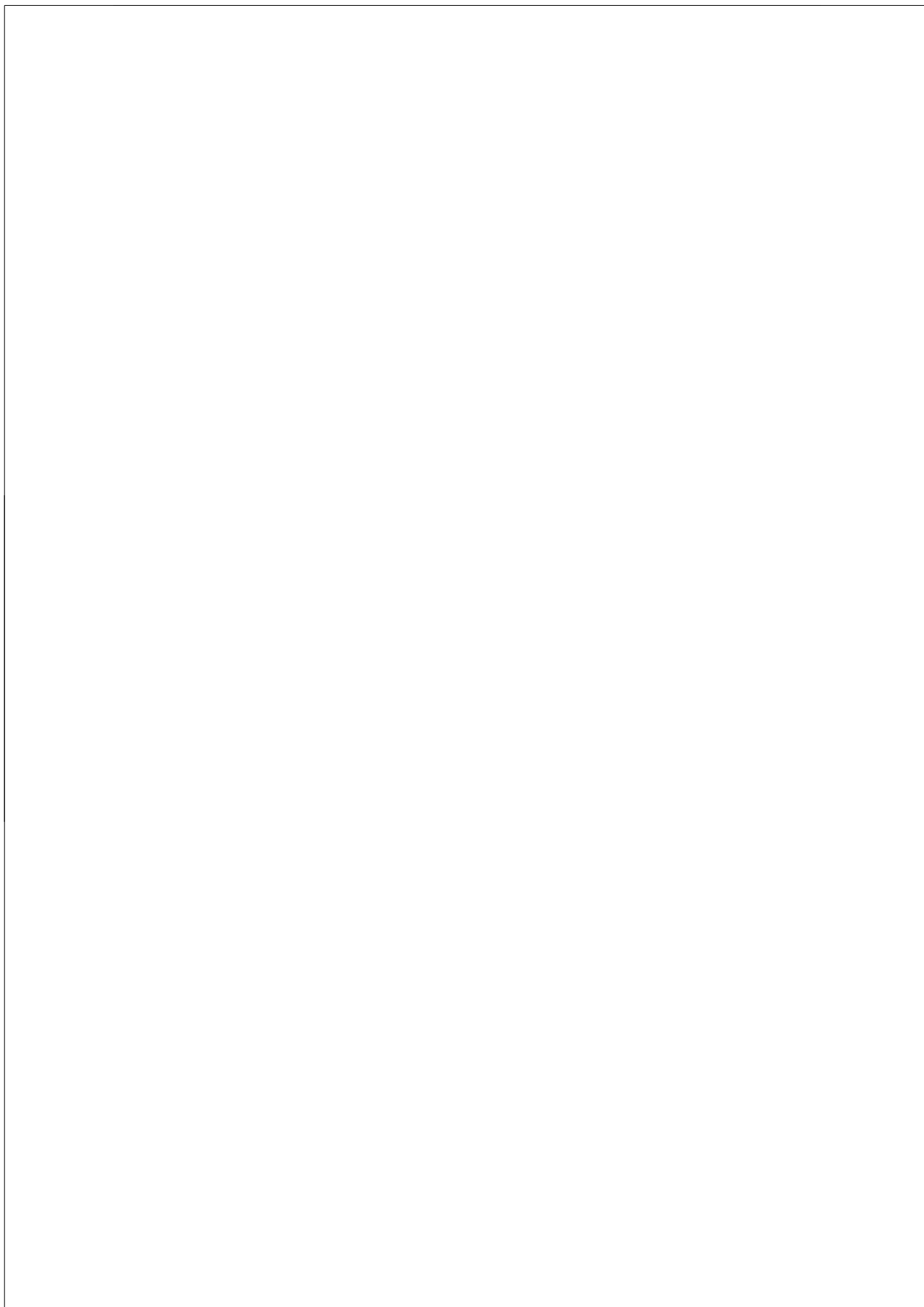
141. Sung, P. and Stratton, S.A. (1996) Yeast Rad51 recombinase mediates polar DNA strand exchange in the absence of ATP hydrolysis. *J Biol Chem*, **271**, 27983-27986.

142. Chi, P., Van Komen, S., Sehorn, M.G., Sigurdsson, S. and Sung, P. (2006) Roles of ATP binding and ATP hydrolysis in human Rad51 recombinase function. *DNA Repair (Amst)*, **5**, 381-391.

143. Conway, A.B., Lynch, T.W., Zhang, Y., Fortin, G.S., Fung, C.W., Symington, L.S. and Rice, P.A. (2004) Crystal structure of a Rad51 filament. *Nat Struct Mol Biol*, **11**, 791-796.

144. Brendel, V., Brocchieri, L., Sandler, S.J., Clark, A.J. and Karlin, S. (1997) Evolutionary comparisons of RecA-like proteins across all major kingdoms of living organisms. *J Mol Evol*, **44**, 528-541.

145. Benson, F.E., Stasiak, A. and West, S.C. (1994) Purification and characterization of the human Rad51 protein, an analogue of E. coli RecA. *Embo J*, **13**, 5764-5771.

146. Mameren, J., Modesti, M., Kanaar, R., Wyman, C., Wuite, G.J. and Peterman, E.J. (2006) Dissecting elastic heterogeneity along DNA molecules coated partly with Rad51 using concurrent fluorescence microscopy and optical tweezers. *Biophys J*, **91**, L78-80.

147. Modesti, M., Ristic, D., van der Heijden, T., Dekker, C., van Mameren, J., Peterman, E.J., Wuite, G.J., Kanaar, R. and Wyman, C. (2007) Fluorescent human RAD51 reveals multiple nucleation sites and filament segments tightly associated along a single DNA molecule. *Structure*, **15**, 599-609.

148. Shan, Q. and Cox, M.M. (1997) RecA filament dynamics during DNA strand exchange reactions. *J Biol Chem*, **272**, 11063-11073.

149. Shan, Q. and Cox, M.M. (1996) RecA protein dynamics in the interior of RecA nucleoprotein filaments. *J Mol Biol*, **257**, 756-774.

150. Gupta, R.C., Bazemore, L.R., Golub, E.I. and Radding, C.M. (1997) Activities of human recombination protein Rad51. *Proc Natl Acad Sci U S A*, **94**, 463-468.

151. Tombline, G. and Fishel, R. (2002) Biochemical characterization of the human RAD51 protein. I. ATP hydrolysis. *J Biol Chem*, **277**, 14417-14425.

152. MacFarland, K.J., Shan, Q., Inman, R.B. and Cox, M.M. (1997) RecA as a motor protein. Testing models for the role of ATP hydrolysis in DNA strand exchange. *J Biol Chem*, **272**, 17675-17685.

153. Jain, S.K., Cox, M.M. and Inman, R.B. (1994) On the role of ATP hydrolysis in RecA protein-mediated DNA strand exchange. III. Unidirectional branch migration and extensive hybrid DNA formation. *J Biol Chem*, **269**, 20653-20661.

154. Anderson, D.G. and Kowalczykowski, S.C. (1997) The recombination hot spot chi is a regulatory element that switches the polarity of DNA degradation by the RecBCD enzyme. *Genes Dev*, **11**, 571-581.

155. Lee, S.E., Moore, J.K., Holmes, A., Umezu, K., Kolodner, R.D. and Haber, J.E. (1998) Saccharomyces Ku70, mre11/rad50 and RPA proteins regulate adaptation to G2/M arrest after DNA damage. *Cell*, **94**, 399-409.

156. Tauchi, H., Kobayashi, J., Morishima, K., van Gent, D.C., Shiraishi, T., Verkaik, N.S., vanHeems, D., Ito, E., Nakamura, A., Sonoda, E. *et al.* (2002) Nbs1 is essential for DNA repair by homologous recombination in higher vertebrate cells. *Nature*, **420**, 93-98.

157. Sartori, A.A., Lukas, C., Coates, J., Mistrik, M., Fu, S., Bartek, J., Baer, R., Lukas, J. and Jackson, S.P. (2007) Human CtIP promotes DNA end resection. *Nature*, **450**, 509-514.

158. Limbo, O., Chahwan, C., Yamada, Y., de Bruin, R.A., Wittenberg, C. and Russell, P. (2007) Ctp1 is a cell-cycle-regulated protein that functions with Mre11 complex to control double-strand break repair by homologous recombination. *Mol Cell*, **28**, 134-146.

159. Paques, F. and Haber, J.E. (1999) Multiple pathways of recombination induced by double-strand breaks in Saccharomyces cerevisiae. *Microbiol Mol Biol Rev*, **63**, 349-404.

160. Szostak, J.W., Orr-Weaver, T.L., Rothstein, R.J. and Stahl, F.W. (1983) The double-strand-break repair model for recombination. *Cell*, **33**, 25-35.

161. West, S.C. (1997) Processing of recombination intermediates by the RuvABC proteins. *Annu Rev Genet*, **31**, 213-244.

162. Constantinou, A., Davies, A.A. and West, S.C. (2001) Branch migration and Holliday junction resolution catalyzed by activities from mammalian cells. *Cell*, **104**, 259-268.

163. Wu, L. and Hickson, I.D. (2003) The Bloom's syndrome helicase suppresses crossing over during homologous recombination. *Nature*, **426**, 870-874.

164. Wyman, C. and Kanaar, R. (2006) DNA double-strand break repair: all's well that ends well. *Annu Rev Genet*, **40**, 363-383.

165. Shinohara, A., Shinohara, M., Ohta, T., Matsuda, S. and Ogawa, T. (1998) Rad52 forms ring structures and co-operates with RPA in single-strand DNA annealing. *Genes Cells*, **3**, 145-156.

166. Sugiyama, T., New, J.H. and Kowalczykowski, S.C. (1998) DNA annealing by RAD52 protein is stimulated by specific interaction with the complex of replication protein A and single-stranded DNA. *Proc Natl Acad Sci U S A*, **95**, 6049-6054.

167. Sargent, R.G., Meservy, J.L., Perkins, B.D., Kilburn, A.E., Intody, Z., Adair, G.M., Nairn, R.S. and Wilson, J.H. (2000) Role of the nucleotide excision repair gene ERCC1 in formation of recombination-dependent rearrangements in mammalian cells. *Nucleic Acids Res*, **28**, 3771-3778.

168. Sargent, R.G., Rolig, R.L., Kilburn, A.E., Adair, G.M., Wilson, J.H. and Nairn, R.S. (1997) Recombination-dependent deletion formation in mammalian cells deficient in the nucleotide excision repair gene ERCC1. *Proc Natl Acad Sci U S A*, **94**, 13122-13127.

169. Cox, M.M., Goodman, M.F., Kreuzer, K.N., Sherratt, D.J., Sandler, S.J. and Marians, K.J. (2000) The importance of repairing stalled replication forks. *Nature*, **404**, 37-41.

170. Heller, R.C. and Marians, K.J. (2006) Replication fork reactivation downstream of a blocked nascent leading strand. *Nature*, **439**, 557-562.

171. Seigneur, M., Bidnenko, V., Ehrlich, S.D. and Michel, B. (1998) RuvAB acts at arrested replication forks. *Cell*, **95**, 419-430.

172. Hanada, K., Budzowska, M., Modesti, M., Maas, A., Wyman, C., Essers, J. and Kanaar, R. (2006) The structure-specific endonuclease Mus81-Eme1 promotes conversion of interstrand DNA crosslinks into double-strands breaks. *Embo J*, **25**, 4921-4932.

173. Sonoda, E., Takata, M., Yamashita, Y.M., Morrison, C. and Takeda, S. (2001) Homologous DNA recombination in vertebrate cells. *Proc Natl Acad Sci U S A*, **98**, 8388-8394.

174. Takata, M., Sasaki, M.S., Tachiiri, S., Fukushima, T., Sonoda, E., Schild, D., Thompson, L.H. and Takeda, S. (2001) Chromosome instability and defective recombinational repair in knockout mutants of the five Rad51 paralogs. *Mol Cell Biol*, **21**, 2858-2866.

175. Sugiyama, T., Zaitseva, E.M. and Kowalczykowski, S.C. (1997) A single-stranded DNA-binding protein is needed for efficient presynaptic complex formation by the Saccharomyces cerevisiae Rad51 protein. *J Biol Chem*, **272**, 7940-7945.

176. Mazin, A.V., Zaitseva, E., Sung, P. and Kowalczykowski, S.C. (2000) Tailed duplex DNA is the preferred substrate for Rad51 protein-mediated homologous pairing. *Embo J*, **19**, 1148-1156.

177. Sung, P. and Robberson, D.L. (1995) DNA strand exchange mediated by a RAD51-ssDNA nucleoprotein filament with polarity opposite to that of RecA. *Cell*, **82**, 453-461.

178. McIlwraith, M.J., Van Dyck, E., Masson, J.Y., Stasiak, A.Z., Stasiak, A. and West, S.C. (2000) Reconstitution of the strand invasion step of double-strand break repair using human Rad51 Rad52 and RPA proteins. *J Mol Biol*, **304**, 151-164.

179. Anderson, D.G. and Kowalczykowski, S.C. (1997) The translocating RecBCD enzyme stimulates recombination by directing RecA protein onto ssDNA in a chi-regulated manner. *Cell*, **90**, 77-86.

180. Game, J.C. (1993) DNA double-strand breaks and the RAD50-RAD57 genes in Saccharomyces. *Semin Cancer Biol*, **4**, 73-83.

181. Rijkers, T., Van Den Ouweland, J., Morolli, B., Rolink, A.G., Baarends, W.M., Van Sloun, P.P., Lohman, P.H. and Pastink, A. (1998) Targeted inactivation of mouse RAD52 reduces homologous recombination but not resistance to ionizing radiation. *Mol Cell Biol*, **18**, 6423-6429.

182. Sung, P. (1997) Function of yeast Rad52 protein as a mediator between replication protein A and the Rad51 recombinase. *J Biol Chem*, **272**, 28194-28197.

183. Shinohara, A. and Ogawa, T. (1998) Stimulation by Rad52 of yeast Rad51-mediated recombination. *Nature*, **391**, 404-407.

184. New, J.H., Sugiyama, T., Zaitseva, E. and Kowalczykowski, S.C. (1998) Rad52 protein stimulates DNA strand exchange by Rad51 and replication protein A. *Nature*, **391**, 407-410.

185. Sugiyama, T. and Kowalczykowski, S.C. (2002) Rad52 protein associates with replication protein A (RPA)-single-stranded DNA to accelerate Rad51-mediated displacement of RPA and presynaptic complex formation. *J Biol Chem*, **277**, 31663-31672.

186. Mortensen, U.H., Bendixen, C., Sunjevaric, I. and Rothstein, R. (1996) DNA strand annealing is promoted by the yeast Rad52 protein. *Proc Natl Acad Sci U S A*, **93**, 10729-10734.

187. Sugiyama, T., Kantake, N., Wu, Y. and Kowalczykowski, S.C. (2006) Rad52-mediated DNA annealing after Rad51-mediated DNA strand exchange promotes second ssDNA capture. *Embo J*, **25**, 5539-5548.

188. Gudmundsdottir, K. and Ashworth, A. (2006) The roles of BRCA1 and BRCA2 and associated proteins in the maintenance of genomic stability. *Oncogene*, **25**, 5864-5874.

189. Davies, A.A., Masson, J.Y., McIlwraith, M.J., Stasiak, A.Z., Stasiak, A., Venkitaraman, A.R. and West, S.C. (2001) Role of BRCA2 in control of the RAD51 recombination and DNA repair protein. *Mol Cell*, **7**, 273-282.

190. Yang, H., Jeffrey, P.D., Miller, J., Kinnucan, E., Sun, Y., Thoma, N.H., Zheng, N., Chen, P.L., Lee, W.H. and Pavletich, N.P. (2002) BRCA2 function in DNA binding and recombination from a BRCA2-DSS1-ssDNA structure. *Science*, **297**, 1837-1848.

191. Esashi, F., Galkin, V.E., Yu, X., Egelman, E.H. and West, S.C. (2007) Stabilization of RAD51 nucleoprotein filaments by the C-terminal region of BRCA2. *Nat Struct Mol Biol*, **14**, 468-474.

192. Davies, O.R. and Pellegrini, L. (2007) Interaction with the BRCA2 C terminus protects RAD51-DNA filaments from disassembly by BRC repeats. *Nat Struct Mol Biol*, **14**, 475-483.

193. Thoma, N.H., Czyzewski, B.K., Alexeev, A.A., Mazin, A.V., Kowalczykowski, S.C. and Pavletich, N.P. (2005) Structure of the SWI2/SNF2 chromatin-remodeling domain of eukaryotic Rad54. *Nat Struct Mol Biol*, **12**, 350-356.

194. Essers, J., Hendriks, R.W., Swagemakers, S.M., Troelstra, C., de Wit, J., Bootsma, D., Hoeijmakers, J.H. and Kanaar, R. (1997) Disruption of mouse RAD54 reduces ionizing radiation resistance and homologous recombination. *Cell*, **89**, 195-204.

195. Bezzubova, O., Silbergleit, A., Yamaguchi-Iwai, Y., Takeda, S. and Buerstedde, J.M. (1997) Reduced X-ray resistance and homologous recombination frequencies in a RAD54-/- mutant of the chicken DT40 cell line. *Cell*, **89**, 185-193.

196. Mazin, A.V., Bornarth, C.J., Solinger, J.A., Heyer, W.D. and Kowalczykowski, S.C. (2000) Rad54 protein is targeted to pairing loci by the Rad51 nucleoprotein filament. *Mol Cell*, **6**, 583-592.

197. Sugawara, N., Wang, X. and Haber, J.E. (2003) In vivo roles of Rad52, Rad54, and Rad55 proteins in Rad51-mediated recombination. *Mol Cell*, **12**, 209-219.

198. Wolner, B., van Komen, S., Sung, P. and Peterson, C.L. (2003) Recruitment of the recombinational repair machinery to a DNA double-strand break in yeast. *Mol Cell*, **12**, 221-232.

199. Swagemakers, S.M., Essers, J., de Wit, J., Hoeijmakers, J.H. and Kanaar, R. (1998) The human RAD54 recombinational DNA repair protein is a double-stranded DNA-dependent ATPase. *J Biol Chem*, **273**, 28292-28297.

200. Petukhova, G., Stratton, S. and Sung, P. (1998) Catalysis of homologous DNA pairing by yeast Rad51 and Rad54 proteins. *Nature*, **393**, 91-94.

201. Petukhova, G., Van Komen, S., Vergano, S., Klein, H. and Sung, P. (1999) Yeast Rad54 promotes Rad51-dependent homologous DNA pairing via ATP hydrolysis-driven change in DNA double helix conformation. *J Biol Chem*, **274**, 29453-29462.

202. Van Komen, S., Petukhova, G., Sigurdsson, S., Stratton, S. and Sung, P. (2000) Superhelicity-driven homologous DNA pairing by yeast recombination factors Rad51 and Rad54. *Mol Cell*, **6**, 563-572.

203. Solinger, J.A., Lutz, G., Sugiyama, T., Kowalczykowski, S.C. and Heyer, W.D. (2001) Rad54 protein stimulates heteroduplex DNA formation in the synaptic phase of DNA strand exchange via specific interactions with the presynaptic Rad51 nucleoprotein filament. *J Mol Biol*, **307**, 1207-1221.

204. Solinger, J.A., Kiianitsa, K. and Heyer, W.D. (2002) Rad54, a Swi2/Snf2-like recombinational repair protein, disassembles Rad51:dsDNA filaments. *Mol Cell*, **10**, 1175-1188.

205. Bugreev, D.V., Mazina, O.M. and Mazin, A.V. (2006) Rad54 protein promotes branch migration of Holliday junctions. *Nature*, **442**, 590-593.

206. Bugreev, D.V., Hanaoka, F. and Mazin, A.V. (2007) Rad54 dissociates homologous recombination intermediates by branch migration. *Nat Struct Mol Biol*, **14**, 746-753.

207. Cox, M.M. (2002) The nonmutagenic repair of broken replication forks via recombination. *Mutat Res*, **510**, 107-120.

208. Pages, V. and Fuchs, R.P. (2002) How DNA lesions are turned into mutations within cells? *Oncogene*, **21**, 8957-8966.

209. Lehmann, A.R. (2002) Replication of damaged DNA in mammalian cells: new solutions to an old problem. *Mutat Res*, **509**, 23-34.

210. Yang, W. (2003) Damage repair DNA polymerases Y. *Curr Opin Struct Biol*, **13**, 23-30.

211. Kunkel, T.A., Pavlov, Y.I. and Bebenek, K. (2003) Functions of human DNA polymerases eta, kappa and iota suggested by their properties, including fidelity with undamaged DNA templates. *DNA Repair (Amst)*, **2**, 135-149.

212. Lawrence, C. (1994) The RAD6 DNA repair pathway in Saccharomyces cerevisiae: what does it do, and how does it do it? *Bioessays*, **16**, 253-258.

213. Hoege, C., Pfander, B., Moldovan, G.L., Pyrowolakis, G. and Jentsch, S. (2002) RAD6-dependent DNA repair is linked to modification of PCNA by ubiquitin and SUMO. *Nature*, **419**, 135-141.

214. Ulrich, H.D. and Jentsch, S. (2000) Two RING finger proteins mediate cooperation between ubiquitin-conjugating enzymes in DNA repair. *Embo J*, **19**, 3388-3397.

215. Hofmann, R.M. and Pickart, C.M. (1999) Noncanonical MMS2-encoded ubiquitin-conjugating enzyme functions in assembly of novel polyubiquitin chains for DNA repair. *Cell*, **96**, 645-653.

216. Stelter, P. and Ulrich, H.D. (2003) Control of spontaneous and damage-induced mutagenesis by SUMO and ubiquitin conjugation. *Nature*, **425**, 188-191.

217. Kannouche, P.L., Wing, J. and Lehmann, A.R. (2004) Interaction of human DNA polymerase eta with monoubiquitinated PCNA: a possible mechanism for the polymerase switch in response to DNA damage. *Mol Cell*, **14**, 491-500.

218. Watanabe, K., Tateishi, S., Kawasuji, M., Tsurimoto, T., Inoue, H. and Yamaizumi, M. (2004) Rad18 guides poleta to replication stalling sites through physical interaction and PCNA monoubiquitination. *Embo J*, **23**, 3886-3896.

219. Bienko, M., Green, C.M., Crosetto, N., Rudolf, F., Zapart, G., Coull, B., Kannouche, P., Wider, G., Peter, M., Lehmann, A.R. *et al.* (2005) Ubiquitin-binding domains in Y-family polymerases regulate translesion synthesis. *Science*, **310**, 1821-1824.

220. Kannouche, P., Fernandez de Henestrosa, A.R., Coull, B., Vidal, A.E., Gray, C., Zicha, D., Woodgate, R. and Lehmann, A.R. (2003) Localization of DNA polymerases eta and iota to the replication machinery is tightly co-ordinated in human cells. *Embo J*, **22**, 1223-1233.

221. Bi, X., Barkley, L.R., Slater, D.M., Tateishi, S., Yamaizumi, M., Ohmori, H. and Vaziri, C. (2006) Rad18 regulates DNA polymerase kappa and is required for recovery from S-phase checkpoint-mediated arrest. *Mol Cell Biol*, **26**, 3527-3540.

222. Bailly, V., Lauder, S., Prakash, S. and Prakash, L. (1997) Yeast DNA repair proteins Rad6 and Rad18 form a heterodimer that has ubiquitin conjugating, DNA binding, and ATP hydrolytic activities. *J Biol Chem*, **272**, 23360-23365.

223. Huang, T.T., Nijman, S.M., Mirchandani, K.D., Galardy, P.J., Cohn, M.A., Haas, W., Gygi, S.P., Ploegh, H.L., Bernards, R. and D'Andrea, A.D. (2006) Regulation of monoubiquitinated PCNA by DUB autocleavage. *Nat Cell Biol*, **8**, 339-347.

224. Frampton, J., Irmisch, A., Green, C.M., Neiss, A., Trickey, M., Ulrich, H.D., Furuya, K., Watts, F.Z., Carr, A.M. and Lehmann, A.R. (2006) Postreplication repair and PCNA modification in Schizosaccharomyces pombe. *Mol Biol Cell*, **17**, 2976-2985.

225. Prakash, S. and Prakash, L. (2002) Translesion DNA synthesis in eukaryotes: a one- or two-polymerase affair. *Genes Dev*, **16**, 1872-1883.

226. Bridges, B.A. and Woodgate, R. (1985) The two-step model of bacterial UV mutagenesis. *Mutat Res*, **150**, 133-139.

227. Guo, C., Tang, T.S., Bienko, M., Parker, J.L., Bielen, A.B., Sonoda, E., Takeda, S., Ulrich, H.D., Dikic, I. and Friedberg, E.C. (2006) Ubiquitin-binding motifs in REV1 protein are required for its role in the tolerance of DNA damage. *Mol Cell Biol*, **26**, 8892-8900.

228. Ohashi, E., Murakumo, Y., Kanjo, N., Akagi, J., Masutani, C., Hanaoka, F. and Ohmori, H. (2004) Interaction of hREV1 with three human Y-family DNA polymerases. *Genes Cells*, **9**, 523-531.

229. Guo, C., Fischhaber, P.L., Luk-Paszyc, M.J., Masuda, Y., Zhou, J., Kamiya, K., Kisker, C. and Friedberg, E.C. (2003) Mouse Rev1 protein interacts with multiple DNA polymerases involved in translesion DNA synthesis. *Embo J*, **22**, 6621-6630.

230. Tissier, A., Kannouche, P., Reck, M.P., Lehmann, A.R., Fuchs, R.P. and Cordonnier, A. (2004) Co-localization in replication foci and interaction of human Y-family members, DNA polymerase pol eta and REVI protein. *DNA Repair (Amst)*, **3**, 1503-1514.

231. Masutani, C., Kusumoto, R., Iwai, S. and Hanaoka, F. (2000) Mechanisms of accurate translesion synthesis by human DNA polymerase eta. *Embo J*, **19**, 3100-3109.

232. Yagi, Y., Ogawara, D., Iwai, S., Hanaoka, F., Akiyama, M. and Maki, H. (2005) DNA polymerases eta and kappa are responsible for error-free translesion DNA synthesis activity over a cis-syn thymine dimer in Xenopus laevis oocyte extracts. *DNA Repair (Amst)*, **4**, 1252-1269.

233. Lehmann, A.R., Kirk-Bell, S., Arlett, C.F., Paterson, M.C., Lohman, P.H., de Weerd-Kastelein, E.A. and Bootsma, D. (1975) Xeroderma pigmentosum cells with normal levels of excision repair have a defect in DNA synthesis after UV-irradiation. *Proc Natl Acad Sci U S A*, **72**, 219-223.

234. Kannouche, P., Broughton, B.C., Volker, M., Hanaoka, F., Mullenders, L.H. and Lehmann, A.R. (2001) Domain structure, localization, and function of DNA polymerase eta, defective in xeroderma pigmentosum variant cells. *Genes Dev*, **15**, 158-172.

235. McIlwraith, M.J., Vaisman, A., Liu, Y., Fanning, E., Woodgate, R. and West, S.C. (2005) Human DNA polymerase eta promotes DNA synthesis from strand invasion intermediates of homologous recombination. *Mol Cell*, **20**, 783-792.

236. Kawamoto, T., Araki, K., Sonoda, E., Yamashita, Y.M., Harada, K., Kikuchi, K., Masutani, C., Hanaoka, F., Nozaki, K., Hashimoto, N. *et al.* (2005) Dual roles for DNA polymerase eta in homologous DNA recombination and translesion DNA synthesis. *Mol Cell*, **20**, 793-799.

237. Johnson, R.E., Washington, M.T., Haracska, L., Prakash, S. and Prakash, L. (2000) Eukaryotic polymerases iota and zeta act sequentially to bypass DNA lesions. *Nature*, **406**, 1015-1019.

238. Zhang, Y., Wu, X., Guo, D., Rechkoblit, O. and Wang, Z. (2002) Activities of human DNA polymerase kappa in response to the major benzo[a]pyrene DNA adduct: error-free lesion bypass and extension synthesis from opposite the lesion. *DNA Repair (Amst)*, **1**, 559-569.

239. Suzuki, N., Ohashi, E., Kolbanovskiy, A., Geacintov, N.E., Grollman, A.P., Ohmori, H. and Shibutani, S. (2002) Translesion synthesis by human DNA polymerase kappa on a DNA template containing a single stereoisomer of dG-(+)- or dG-(-)-anti-N(2)-BPDE (7,8-dihydroxy-anti-9,10-epoxy-7,8,9,10-tetrahydrobenzo[a]pyrene). *Biochemistry*, **41**, 6100-6106.

240. Ogi, T., Shinkai, Y., Tanaka, K. and Ohmori, H. (2002) Polkappa protects mammalian cells against the lethal and mutagenic effects of benzo[a]pyrene. *Proc Natl Acad Sci U S A*, **99**, 15548-15553.

241. Ogi, T., Kannouche, P. and Lehmann, A.R. (2005) Localisation of human Y-family DNA polymerase kappa: relationship to PCNA foci. *J Cell Sci*, **118**, 129-136.

242. Nelson, J.R., Lawrence, C.W. and Hinkle, D.C. (1996) Deoxycytidyl transferase activity of yeast REV1 protein. *Nature*, **382**, 729-731.

243. Nelson, J.R., Lawrence, C.W. and Hinkle, D.C. (1996) Thymine-thymine dimer bypass by yeast DNA polymerase zeta. *Science*, **272**, 1646-1649.

244. Chiu, R.K., Brun, J., Ramaekers, C., Theys, J., Weng, L., Lambin, P., Gray, D.A. and Wouters, B.G. (2006) Lysine 63-polyubiquitination guards against translesion synthesis-induced mutations. *PLoS Genet*, **2**, e116.

245. Langie, S.A., Knaapen, A.M., Ramaekers, C.H., Theys, J., Brun, J., Godschalk, R.W., van Schooten, F.J., Lambin, P., Gray, D.A., Wouters, B.G. *et al.* (2007) Formation of lysine 63-linked poly-ubiquitin chains protects human lung cells against benzo[a]pyrene-diol-epoxide-induced mutagenicity. *DNA Repair (Amst)*, **6**, 852-862.

246. Courcelle, J., Khodursky, A., Peter, B., Brown, P.O. and Hanawalt, P.C. (2001) Comparative gene expression profiles following UV exposure in wild-type and SOS-deficient Escherichia coli. *Genetics*, **158**, 41-64.

247. Sutton, M.D. and Walker, G.C. (2001) Managing DNA polymerases: coordinating DNA replication, DNA repair, and DNA recombination. *Proc Natl Acad Sci U S A*, **98**, 8342-8349.

248. Tang, M., Bruck, I., Eritja, R., Turner, J., Frank, E.G., Woodgate, R., O'Donnell, M. and Goodman, M.F. (1998) Biochemical basis of SOS-induced mutagenesis in Escherichia coli: reconstitution of in vitro lesion bypass dependent on the UmuD'2C mutagenic complex and RecA protein. *Proc Natl Acad Sci U S A*, **95**, 9755-9760.

249. Reuven, N.B., Arad, G., Maor-Shoshani, A. and Livneh, Z. (1999) The mutagenesis protein UmuC is a DNA polymerase activated by UmuD', RecA, and SSB and is specialized for translesion replication. *J Biol Chem*, **274**, 31763-31766.

250. Schlacher, K., Cox, M.M., Woodgate, R. and Goodman, M.F. (2006) RecA acts in trans to allow replication of damaged DNA by DNA polymerase V. *Nature*, **442**, 883-887.

251. Sommer, S., Bailone, A. and Devoret, R. (1993) The appearance of the UmuD'C protein complex in Escherichia coli switches repair from homologous recombination to SOS mutagenesis. *Mol Microbiol*, **10**, 963-971.

252. Rehrauer, W.M., Bruck, I., Woodgate, R., Goodman, M.F. and Kowalczykowski, S.C. (1998) Modulation of RecA nucleoprotein function by the mutagenic UmuD'C protein complex. *J Biol Chem*, **273**, 32384-32387.

253. Opperman, T., Murli, S., Smith, B.T. and Walker, G.C. (1999) A model for a umuDC-dependent prokaryotic DNA damage checkpoint. *Proc Natl Acad Sci U S A*, **96**, 9218-9223.

254. Lim, D.S. and Hasty, P. (1996) A mutation in mouse rad51 results in an early embryonic lethal that is suppressed by a mutation in p53. *Mol Cell Biol*, **16**, 7133-7143.

255. Tsuzuki, T., Fujii, Y., Sakumi, K., Tominaga, Y., Nakao, K., Sekiguchi, M., Matsushiro, A., Yoshimura, Y. and MoritaT. (1996) Targeted disruption of the Rad51 gene leads to lethality in embryonic mice. *Proc Natl Acad Sci U S A*, **93**, 6236-6240.

256. Okada, T., Sonoda, E., Yoshimura, M., Kawano, Y., Saya, H., Kohzaki, M. and Takeda, S. (2005) Multiple roles of vertebrate REV genes in DNA repair and recombination. *Mol Cell Biol*, **25**, 6103-6111.
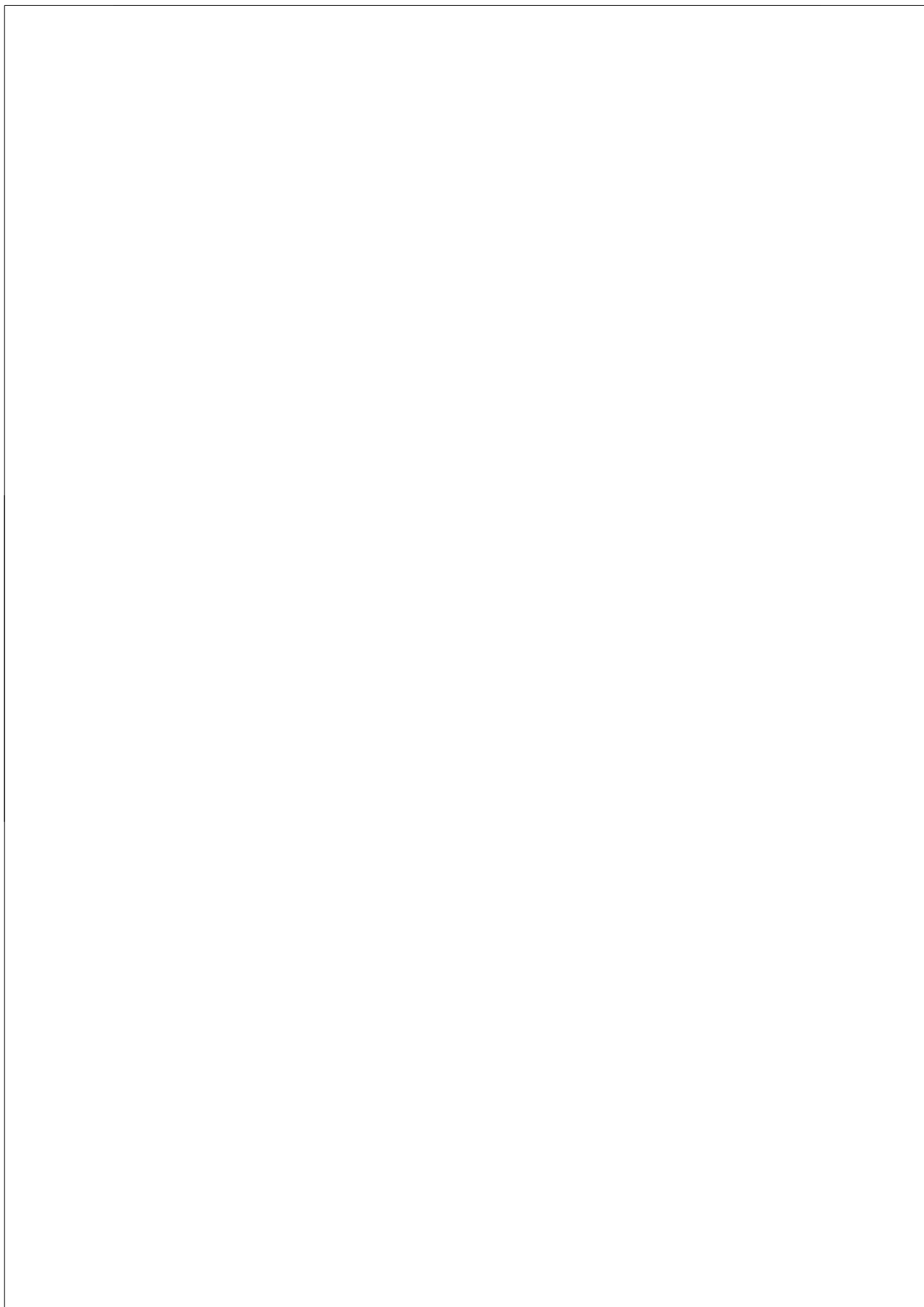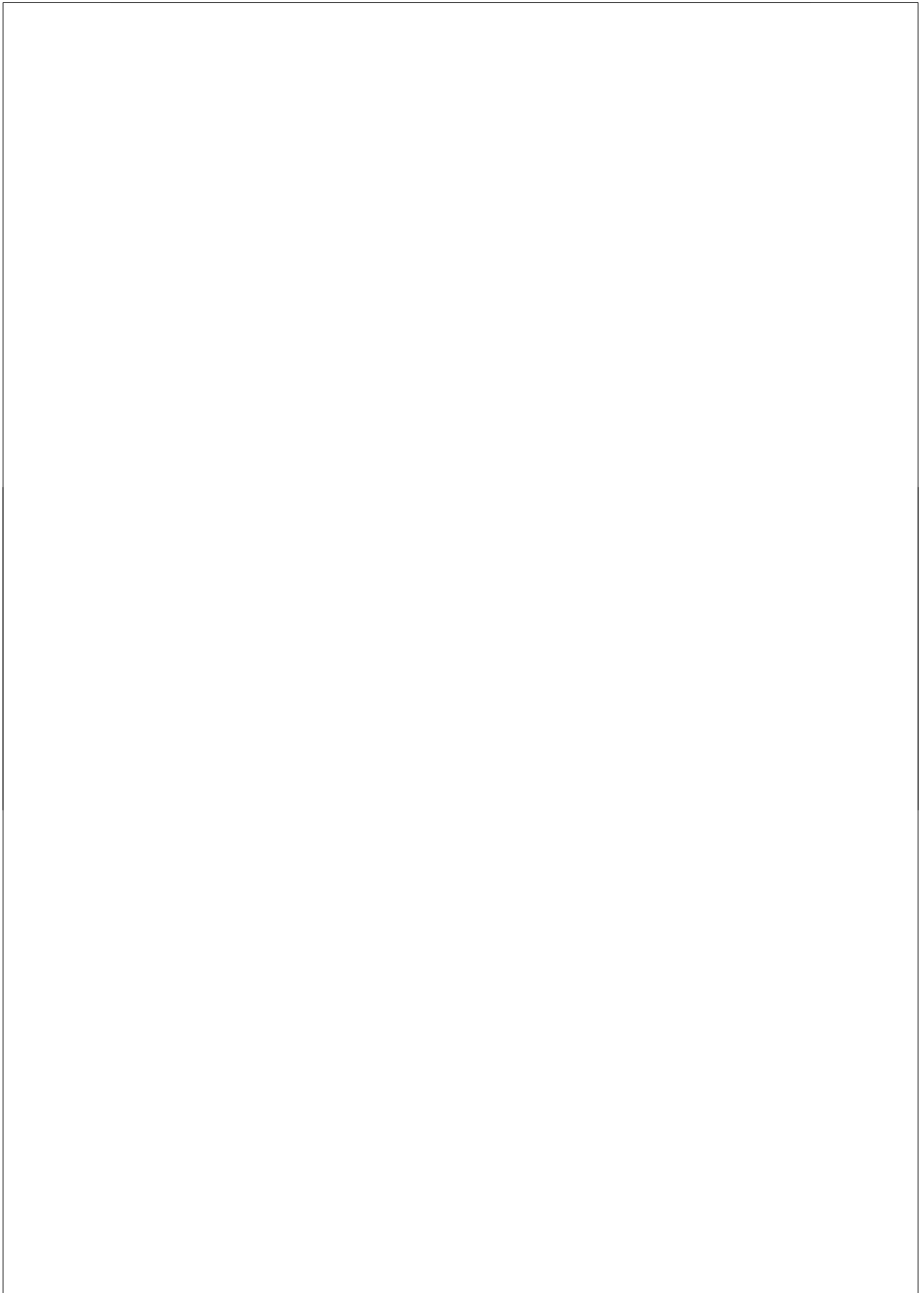
Chapter 2

Mutation of the mouse Rad17 gene
leads to embryonic lethality
and reveals a role
in DNA damage-dependent
recombination

Mutation of the mouse *Rad17* gene leads to embryonic lethality and reveals a role in DNA damage-dependent recombination

Magda Budzowska[1], Iris Jaspers[1], Jeroen Essers[1], Harm de Waard[1], Ellen van Drunen[1], Katsuhiro Hanada[1], Berna Beverloo[1,2], Rudolf W Hendriks[3], Annelies de Klein[2], Roland Kanaar[1,4], Jan H Hoeijmakers[1] and Alex Maas[1,*]

[1]MGC-Department of Cell Biology and Genetics, Center for Biomedical Genetics, Erasmus MC, DR Rotterdam, The Netherlands, [2]MGC-Department of Clinical Genetics, Erasmus MC, DR Rotterdam, The Netherlands, [3]Department of Immunology, Erasmus MC, DR Rotterdam, The Netherlands and [4]Department of Radiation Oncology, Erasmus MC-Daniel, DR Rotterdam, The Netherlands

Genetic defects in DNA repair mechanisms and cell cycle checkpoint (CCC) genes result in increased genomic instability and cancer predisposition. Discovery of mammalian homologs of yeast CCC genes suggests conservation of checkpoint mechanisms between yeast and mammals. However, the role of many CCC genes in higher eukaryotes remains elusive. Here, we report that targeted deletion of an N-terminal part of *mRad17*, the mouse homolog of the *Schizosaccharomyces pombe* Rad17 checkpoint clamp-loader component, resulted in embryonic lethality during early/mid-gestation. In contrast to mouse embryos, embryonic stem (ES) cells, isolated from *mRad17*$^{5'\Delta/5'\Delta}$ embryos, produced truncated mRad17 and were viable. These cells displayed hypersensitivity to various DNA-damaging agents. Surprisingly, *mRad17*$^{5'\Delta/5'\Delta}$ ES cells were able to arrest cell cycle progression upon induction of DNA damage. However, they displayed impaired homologous recombination as evidenced by a strongly reduced gene targeting efficiency. In addition to a possible role in DNA damage-induced CCC, based on sequence homology, our results indicate that mRad17 has a function in DNA damage-dependent recombination that may be responsible for the sensitivity to DNA-damaging agents.

*Corresponding author. MGC-Department of Cell Biology and Genetics, Center for Biomedical Genetics, Erasmus MC, PO Box 1738, 3000 DR Rotterdam, The Netherlands. Tel.: + 31 10 408 7202; Fax: + 31 10 408 9468; E-mail: a.maas.1@erasmusmc.nl

Introduction

Accurate transmission of genetic information from a dividing cell to its daughters is essential for the survival of organisms. To minimize the number of irreversible mutations, extreme accuracy in DNA replication and equal distribution of chromosomes between daughter cells are critical. In addition, maintaining genome stability requires accurate repair of physiologically and environmentally induced DNA damage. Throughout the cell cycle, DNA integrity is monitored by checkpoint pathways, which arrest cell cycle progression upon the presence of DNA damage or unreplicated DNA (Hartwell and Weinert, 1989; Zhou and Elledge, 2000). This arrest in cell cycle progression, often referred to as DNA damage-induced cell cycle checkpoint (CCC), provides a window of opportunity for DNA damage repair or causes irreversible withdrawal from the cell cycle. Loss of these CCCs can result in genomic instability, which is linked to an increase in cancer susceptibility.

The importance of DNA damage-induced CCC is illustrated by the human disorder ataxia telangiectasia (AT), caused by mutations in the *ATM* gene (Savitsky *et al*, 1995) and characterized by increased sensitivity to DNA damage, high frequency of chromosomal aberrations and elevated risk of cancer. Most notably, *ATM* shares significant homology with *Rad3* from the fission yeast *Schizosaccharomyces pombe* and with *TEL1* from the budding yeast *Saccharomyces cerevisiae* (Savitsky *et al*, 1995). These sequence similarities and those of other CCC genes between the two distantly related yeast species and the identification of mammalian homologs strongly suggest that CCC mechanisms are highly conserved among eukaryotic cells.

In response to DNA damage, different putative CCC pathways can be identified. The mitotic cell cycle can be inhibited before commitment to S phase DNA replication at the G1/S transition (G1/S checkpoint; Siede *et al*, 1993), during S phase (intra-S checkpoint; Paulovich and Hartwell, 1995) and upon entry into mitosis from G2 (G2/M checkpoint; Hartwell and Weinert, 1989). In recent years, a variety of genes have been identified that, when defective, lead to hypersensitivity to agents causing DNA damage or replication stalling, such as UV light, γ-radiation and hydroxyurea (HU), and to disturbed cell cycle response upon genome damage. In *S. pombe*, the products of *Rad1*, *Rad3*, *Rad9*, *Rad17*, *Rad26* and *Hus1* have been identified as essential components of DNA damage-induced CCC pathways. Mutants of these checkpoint genes fail to undergo a dose-dependent cell cycle arrest in response to DNA damage or incomplete DNA replication. In *S. cerevisiae*, a similar group of checkpoint genes *RAD9*, *RAD17*, *RAD24*, *TEL1*, *MEC1*, *MEC3* and *DDC1* is found to be required for DNA damage-induced mitotic cell cycle arrest.

In *S. pombe*, Rad17 is indispensable for S phase and G2/M arrest in response to both DNA damage and incomplete DNA

61

replication. The structural counterpart in *S. cerevisiae* is RAD24. In both human and mouse, homologs of the *Rad17* gene, *hRAD17* and *mRad17*, respectively, have been identified and characterized (Bluyssen *et al*, 1999; von Deimling *et al*, 1999). Homology is also detected between the Rad17 homologs and proteins of mammalian replication factor C (RFC). RFC consists of five structurally related subunits (RFC$_{1-5}$; Lee *et al*, 1991), which all contain intrinsic DNA-dependent ATPase activity and together act as a 'clamp loader' for proliferating cell nuclear antigen (PCNA). PCNA operates as a sliding clamp complex along DNA and is involved in recruiting replicative DNA polymerases δ and ε onto primed DNA templates (Hubscher *et al*, 2002). A recent study has demonstrated that Rad17 associates specifically with members 2–5 of the RFC complex (Green *et al*, 2000; Ellison and Stillman, 2003), suggesting that Rad17 and RFC1 are competing for interaction with the other four RFC subunits. The homology of Rad17 with RFC and the interaction with the PCNA-like Rad9–Rad1–Hus1 (9-1-1) complex suggests a role for Rad17 in the recruitment of this complex to DNA lesions in a manner similar to PCNA loading by RFC (Zou *et al*, 2002; Ellison and Stillman, 2003). Consistent with this notion, the 9-1-1 complex is less extractable from the nucleus upon DNA damage induction, suggesting a DNA damage-induced association to chromatin stimulated by Rad17 (Burtelow *et al*, 2000). Hus1 is phosphorylated after the induction of DNA damage and this modification requires other CCC Rad proteins, including the ATM/ATR-related kinase Rad3 (Kostrub *et al*, 1998). In *S. pombe*, Rad3 phosphorylates its tightly bound partner Rad26 after ionizing radiation treatment, independent of Rad17 and the 9-1-1 complex (Edwards *et al*, 1999), suggesting that the Rad3–Rad26 complex might directly respond to certain types of DNA damage. The recent identification of ATRIP (ATR-interacting protein), the human homolog of Rad26, suggests a similar, Rad17- and 9-1-1 complex-independent, mechanism for detection of certain types of DNA lesions in human cells (Cortez *et al*, 2001). However, the phosphorylation of Rad17 by ATR, both in different complexes, is stimulated by Hus1 (Zou *et al*, 2002). These data indicate that the 9-1-1 complex recruited by Rad17 upon DNA damage induction enables ATR to recognize its substrates on the chromatin and thereby combine two independent sensory pathways to activate the DNA-damage response fully.

Although our understanding of DNA damage-induced CCC mechanisms is improving, many aspects of CCC function in mammals remain elusive. To determine the role of mRad17 in mouse development and mouse CCC function, we produced a targeted disruption of *mRad17*. Here we report that deletion of mRad17 leads to death in early- to mid-gestation embryos. Although no damage-induced CCC defects could be detected, our analyses of viable *mRad17$^{5'\Delta/5'\Delta}$* embryonic stem (ES) cells, producing truncated mRad17, reveal the involvement of mRad17 in DNA damage-dependent recombination.

Results

Deletion of mRad17 results in embryonic lethality during early/mid-gestation

For targeting the *mRad17* gene, we constructed a targeting vector with a 110 bp deletion in exon 3. Due to this deletion, the reading frame is shifted, resulting in the formation of
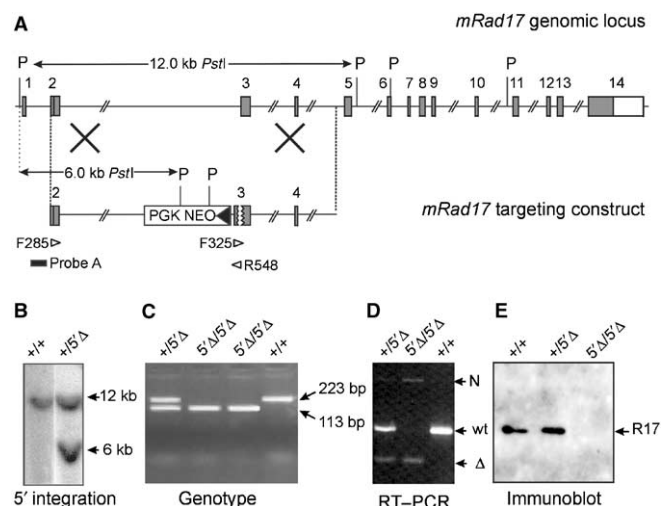

Figure 1 Generation of *mRad17* mutant mice. (**A**) Targeting vector design and screening strategy. Numbered gray boxes represent exons. The positions of *Pst*I (P) restriction sites, size of the *Pst*I restriction fragments and the position of probe A used for DNA blot screening of digested ES cell DNA are indicated. The open arrowheads indicate the position and direction of primers used for PCR. (**B**) DNA blot analysis of *Pst*I-digested ES cell DNA using probe A. The positions of wild type (+;12 kb) and 5'Δ (6 kb) are indicated. (**C**) Analysis of genotype by PCR using primers F325 and R548. The positions of wt (223 bp) and 5'Δ (113 bp) bands are indicated. (**D**) RT–PCR on E8.5 embryos using a poly-dT primer and primers F285 and R548. The positions of 'wt', 'Δ' and 'N' bands are indicated. (**E**) Immunoblot analysis of E8.5 embryos. The position of mRad17 protein is indicated. Each lane contained half of the total E8.5 embryo lysate.

three immediate stop codons in the new reading frame. A neomycin selection cassette, driven by the PGK promoter, was cloned in antisense orientation in intron 2 (Figure 1A). Because the region deleted in the targeting vector is present in all different splice variants of mRad17 and the frameshift results in the presence of multiple stop codons, we anticipated that homologous integration of this targeting vector would result in an *mRad17* null allele. The linearized targeting construct was electroporated into E14 ES cells and, after G418 selection, resistant clones were screened by DNA blotting of *Pst*I-digested genomic DNA (Figure 1B). Three clones that had undergone homologous recombination events were obtained out of 240 clones tested. These clones were karyotyped and further analyzed for correct 3′ integration of the targeting vector by PCR (data not shown). Two of the clones, F17 and F24, were injected into C57bl/6 blastocysts to produce chimeric mice that transmitted the targeted *mRad17* allele through the germ line. No differences between the two independent mouse lines were detected in the experiments described below, indicating that the resulting mouse mutant represents a 'bona fide' outcome of the genetic modification. Male chimeras were bred to C57bl/6 females to produce $mRad17^{+/5'\Delta}$ heterozygous offspring. Heterozygous $mRad17^{+/5'\Delta}$ mice were normal and fertile, and no aberrant phenotype has been observed for up to 1 year of age. However, when heterozygous $mRad17^{+/5'\Delta}$ mice were intercrossed to produce homozygous mutant *mRad17* mice, $mRad17^{5'\Delta/5'\Delta}$ mice were absent from the large number of offspring analyzed (Table I). Both $mRad17^{+/5'\Delta}$ and wild-type mice were present, suggesting that the homozygous mutant *mRad17* results in embryonic lethality. As $mRad17^{+/5'\Delta}$ pups were born in normal numbers and

showed no abnormal phenotype, a dominant-negative effect of the targeted allele is not likely.

Transcription of the targeted *mRad17* allele was examined using RT–PCR on RNA isolated from E8.5 embryos, using primers F285 in exon 2 and R548 in exon 3 (Figure 1A). The RT–PCR experiment revealed the presence of three differently sized *mRad17* mRNAs, designated 'wt', 'Δ' and 'N', respectively, in wild-type, $mRad17^{+/5'\Delta}$ or $mRad17^{5'\Delta/5'\Delta}$ embryos (Figure 1D). Sequence analysis of the three bands showed that the 'wt' band, present in the +/+ and +/5′Δ lanes, was derived from the wild-type *mRad17* allele, whereas the smaller 'Δ' band, present in lower quantities in the +/5′Δ and 5′Δ/5′Δ lanes, was derived from the targeted *mRad17* allele (data not shown). Sequencing confirmed the reading frameshift and the presence of three immediate stop codons in the 'Δ' RT–PCR product. The third, weak 'N' band in the +/5′Δ and 5′Δ/5′Δ lanes contained sequences of the disrupted *mRad17* allele and part of the inverted *Neo* gene with stop codons in all reading frames (data not shown). When mRad17 protein expression was investigated on immunoblot, no mRad17 could be detected in lysates of $mRad17^{5'\Delta/5'\Delta}$ embryos (Figure 1E), supporting our prediction that the targeted disruption would result in an *mRad17* null mutant allele.

To characterize the timing and nature of the embryonic lethality caused by the absence of mRad17, we analyzed early/mid-gestation embryos from heterozygous $mRad17^{+/5'\Delta}$ matings. Up to E8.5, no obvious differences were detected between wild-type, $mRad17^{+/5'\Delta}$ and $mRad17^{5'\Delta/5'\Delta}$ embryos (Table I; Figure 2A and B; data not shown). At E8.5, the majority of the mRad17-deficient embryos appeared normal. Only a small fraction of the homozygous $mRad17^{5'\Delta/5'\Delta}$ embryos showed growth retardation, morphological defects or had an inviable appearance (Table I; Figure 2C and D). At days E9.5 and E10.5, a larger proportion of the $mRad17^{5'\Delta/5'\Delta}$ embryos showed morphological abnormalities, but still most embryos were essentially normal (Table I; Figure 2E and H). At E11.5, the majority showed numerous and heterogeneous morphological abnormalities. The most striking were growth retardation, reduction in the number of somites, bleedings in rhomencephalon, mesencephalon and prosencephalon, failure to close the head folds, delays and abnormalities in the development of the neural tube and pharyngeal arches, bleedings and morphological abnormalities of heart and liver (Table I; Figure 2I and J). Viable mRad17-deficient embryos were not detected at later stages of gestation (Table I). In conclusion, deletion of *mRad17* results in a wide range and extensive heterogeneity of defects over a relative long period of embryonic development.

Generation of mRad17-deficient mouse cell lines

The results described above suggest that $mRad17^{5'\Delta/5'\Delta}$ embryos are viable up to E8.5 of gestation. Metaphase spreads from such E8.5 embryos did not show obvious genomic instability and no endoreplication (Table II). This is in contrast to $Rad17^{flox/-}$ human colon epithelial cells, which exhibited acute chromosomal aberrations and underwent endoreplication at high rate upon Rad17 deletion (Wang *et al*, 2003). Therefore, we attempted to derive mouse embryonic fibroblasts (MEFs) from E8.5 embryos. Out of 40 embryos isolated from $mRad17^{+/5'\Delta}$ heterozygous matings, three $mRad17^{5'\Delta/5'\Delta}$ primary MEF cultures were obtained.

Table I Genotyping of offspring and embryos from matings of heterozygous $mRad17^{+/5'\Delta}$ mice

Stage (E)	Genotype			Total
	+/+	+/5′Δ	5′Δ/5′Δ	
3.5	4	12	5	21
6.5	4	4	4	12
7.5	1	8	6	15
8.5	7	41	18 (4A)[a]	66
9.5	6	19	9 (3A)	34
10.5	14 (1A)	24 (3A)	17 (6A)	55 + 2ND[b]
11.5	7	6 (1A)	8 (5A)	21
12.5	2	5	1 (1A)	8
13.5	4	9	0	13 + 7ND
15.5	3	4	0	7 + 2ND
Total early/ mid-embryos	52 (1.9%)[c]	132 (3%)	68 (23.5%)	252
(expected)	(63)[d]	(126)	(63)	
Offspring (F2)	56	86	0	142
(expected)	(47)	(94)	(47)	

For each developmental stage, defined by embryonic day post-conception (E), the number of embryos/offspring of the indicated genotype is listed.
[a]Abnormal embryo, defined by small size, morphological defects, resorptions or developmental delay. The number in parentheses is included in the total number of the specific genotype and in the total number of embryos analyzed.
[b]ND indicates not determined, due to the high level of resorption.
[c]The percentage of abnormal embryos.
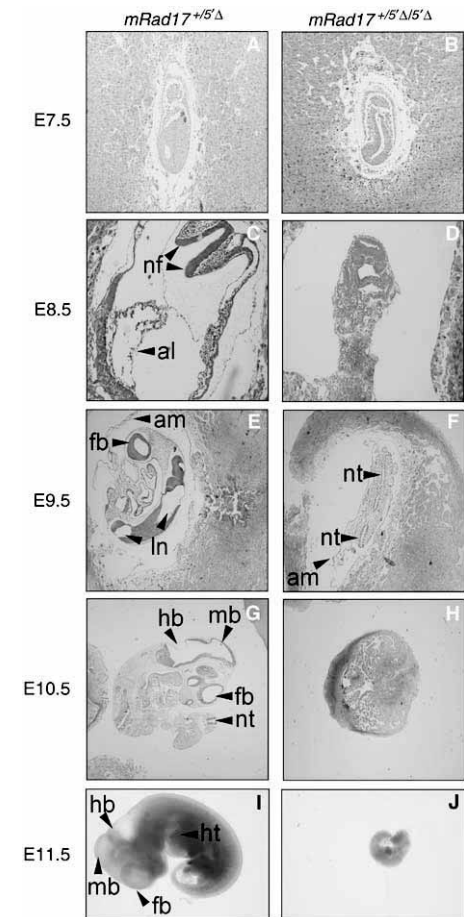[d]The expected number of embryos based on Mendelian inheritance.

Figure 2 Development of $mRad17^{+/5'\Delta}$ and $mRad17^{5'\Delta/5'\Delta}$ embryos. Examples of hematoxylin–eosin-stained sections (**A–H**) and whole embryos (**I–J**). Original magnifications are $\times 100$ for (**A–D**) and $\times 40$ for (**E–J**). Genotypes of embryos are given at the top. Developmental stage, in embryonic days (E), is indicated on the left. al: allantois; am: amnion; nf: neural fold (head fold); nt: neural tube; ln: lumen neural tube; ht: hart; fb: forebrain; mb: midbrain; hb: hindbrain.

Table II Karyotype of cells from embryos

Genotype	No. of metaphases counted	Loss of 1–2 chrom.	40 chrom.	Gain of 1–2 chrom.	Tetraploid	ND[a]
Wild type	15	5	9	0	0	1
	15	2	11	0	0	2
	15	2	9	0	2	2
	15	2	13	0	0	0
$5'\Delta/+$	16	2	13	0	0	1
	15	0	0	0	14	1
	15	3	10	0	0	2
	15	0	11	0	0	4
	15	2	11	0	0	2
	15	3	8	0	1	3
	15	1	13	0	0	1
	15	0	10	0	4	1
$5'\Delta/5'\Delta$	16	2	7	0	0	7
	14	1	10	1	1	1

[a]ND indicates nondeterminable.

However, in contrast to wild-type and $mRad17^{+/5'\Delta}$ MEFs, which did not show culture abnormalities, all homozygous $mRad17^{5'\Delta/5'\Delta}$ MEFs grew poorly and became senescent around passage 5, from which they failed to recover, even when grown under low (3%) oxygen conditions (data not shown).

Next we tried to generate ES cells from E3.5 blastocysts of $mRad17^{+/5'\Delta}$ heterozygous matings. In contrast to the MEFs, we succeeded in establishing multiple ES cell lines. An $mRad17^{+/5'\Delta}$, three $mRad17^{5'\Delta/5'\Delta}$ together with a C57bl/6 wild-type control ES cell line were used for further experiments (Figure 3A). When mRad17 protein expression was investigated on immunoblots using an mRad17 antibody, unexpectedly, a smaller protein band could be detected in $mRad17^{+/5'\Delta}$ and $mRad17^{5'\Delta/5'\Delta}$ ES whole-cell extracts (WCE; Figure 3B). This is in contrast to $mRad17^{5'\Delta/5'\Delta}$ MEFs, in which no mRad17 could be detected (data not shown). Usage of a second, independent polyclonal mRad17 antibody confirmed these results (data not shown). Skipping of the natural start codon and usage of a second ATG in exon 3, which is out of frame in the natural *mRad17* sequence, could lead to production of truncated mRad17 protein because the 129 bp deletion and the addition of 19 bp cloning sequence results in a frameshift. Due to this frameshift, usage of the second ATG results in the loss of 78 N-terminal amino acids of the regular mRad17 frame and the addition of 16 N-terminal nonsense amino acids (Figure 3C). The wild-type and 5′Δ-mRad17 were expressed to a similar level, since no difference in the amount of the proteins was detected in WCE (Figure 3B). However, immunoblotting of subcellular fractions revealed that, compared to wild-type mRad17, less of the 5′Δ-mRad17 protein was present in the nucleus. This is evident from a reduction in the one-to-one ratio of the 5′Δ-mRad17 to wild-type mRad17 in the WCE compared to the nuclear fraction. This is observed when comparing extracts from wild-type cells with extracts from $mRad17^{5'\Delta/5'\Delta}$ cells and when directly comparing the amounts of wild-type and 5′Δ-mRad17 protein within extracts from $mRad17^{+/5'\Delta}$ cells. Importantly, the truncation of the mRad17 protein resulted in less efficient association of the protein with chromatin (Figure 3B). Using standard cell culture conditions, both $mRad17^{5'\Delta/5'\Delta}$ and $mRad17^{+/5'\Delta}$ ES cell lines showed growth characteristics comparable to wild-type ES cells and no genomic instability was detected between early and late passages (Table III).

$mRad17^{5'\Delta/5'\Delta}$ ES cells are sensitive to γ-radiation, UV light, mitomycin C, illudin-S, methyl methane sulfonate and hydroxyurea

S. pombe Rad17 and *S. cerevisiae RAD24* mutants are characterized by hypersensitivity to a wide variety of DNA-damaging agents. We therefore investigated the sensitivity of $mRad17^{5'\Delta/5'\Delta}$, $mRad17^{+/5'\Delta}$ and wild-type ES cells after
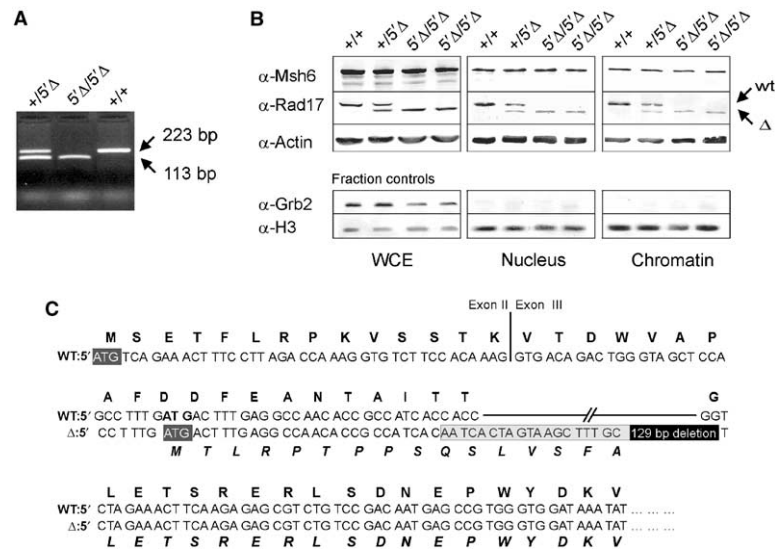
Figure 3 Generation of *mRad17* mutant ES cell lines. (A, B) Genotypes are indicated above the lanes. (**A**) PCR analysis of genotypes using primers F325 and R548 (see Figure 1A). The positions of wild-type (223 bp) and targeted (113 bp) *mRad17* bands are indicated. (**B**) Immunoblot analysis on ES cell lysates and cell fractions. The positions of wild-type mRad17 ($+$) and targeted mRad17 (Δ) are indicated. Actin and Msh6 were used as loading controls. Histone 3 (H3) and Grb2 were used as subcellular fractionation controls. (**C**) Sequence analysis of 'wt' and 'Δ' RT–PCR fragments. Bold capitals represent mRad17 amino acids, capitals represent nucleotides and bold italic capitals represent mutant mRad17 amino acids. II and III indicate exons 2 and 3, respectively. Dark gray boxes indicate translation start sites. In the 'Δ' sequence, the positions of the deletion (black box) and additional sequence due to cloning (light gray box) are indicated.

Table III Karyotype of ES cells

Genotype	Passage no.	No. of metaphases counted	39 chrom.		40 chrom.		41 chrom.	
			—	Marker[a]	—	Marker[a]	—	Marker[a]
Wild type	30	15	1	1	13	0	0	0
	53	15	0	1	14	0	0	0
$5'\Delta/5'\Delta$	17	15	0	0	0	13	2	0
	43	15	0	0	0	14	0	1

[a]Metacentric chromosome.

exposure to γ-rays by determining their colony forming ability. Upon γ-irradiation, $mRad17^{5'\Delta/5'\Delta}$ ES cell lines were found to be two- to three-fold more sensitive than wild-type ES cells. As a positive control for irradiation, γ-irradiation-sensitive ES cells deficient for the DNA repair protein Rad54 were used (Figure 4A; Essers *et al*, 1997).

To investigate whether $mRad17^{5'\Delta/5'\Delta}$ causes a general sensitivity to genotoxic stress, we tested cell survival after treatment with other DNA-damaging agents, producing different types of DNA lesions that are repaired by different pathways. $mRad17^{5'\Delta/5'\Delta}$ ES cells appeared ~1.5-fold more sensitive to UV light (Figure 4B). However, they are not as UV light sensitive as $Xpa^{-/-}$ ES cells, which are deficient in nucleotide excision repair. In addition, $mRad17^{5'\Delta/5'\Delta}$ ES cells displayed ~2-fold hypersensitivity to the DNA interstrand crosslinks-inducing agent mitomycin C (MMC), which

is not as high as crosslink repair-defective $Ercc1^{-/-}$ ES cells (Figure 4C; Niedernhofer *et al*, 2001). Moreover, $mRad17^{5'\Delta/5'\Delta}$ ES cells were ~2.5-fold more sensitive than wild-type ES cells but less sensitive than $Xpa^{-/-}$ ES cells to illudin-S, which induces lesions presumed to be removed by transcription-coupled repair and which are also detected by the DNA replication machinery (Figure 4D; Jaspers *et al*, 2002). Methyl methane sulfonate (MMS) exposure, inducing DNA lesions repaired by recombination and DNA translesion synthesis, revealed an ~1.5- to 2-fold increased sensitivity of $mRad17^{5'\Delta/5'\Delta}$ ES cells compared to wild-type ES cells, whereas $mRad17^{+/5'\Delta}$ ES cells showed an intermediate sensitivity (Figure 4E). Exposure to the replication inhibitor HU showed a very high sensitivity of the $mRad17^{5'\Delta/5'\Delta}$ ES cells compared to wild-type ES cells (Figure 4G). The observation that $mRad17^{5'\Delta/5'\Delta}$ ES cells are sensitive to agents causing
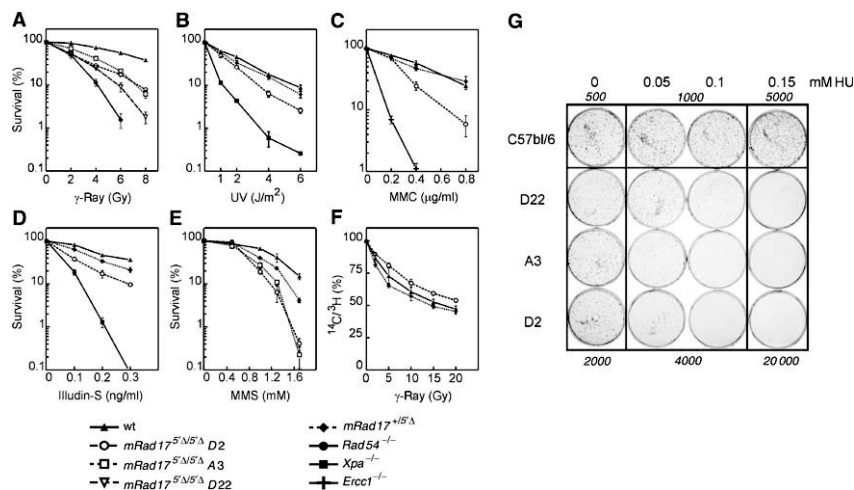
Figure 4 Effect of DNA-damaging agents on survival of $mRad17^{5'\Delta/5'\Delta}$, $mRad17^{+/5'\Delta}$ and wild-type ES cells. (**A**) Colony survival assay on ES cells after γ-irradiation, (**B**) UV irradiation, (**C**) MMC exposure, (**D**) illudin-S exposure and (**E**) MMS exposure. (**F**) RDS analysis on ES cells. (**G**) Colony survival assay after HU exposure. The numbers of seeded cells are indicated in italics.

a variety of different DNA lesions or replication stalling suggests that mRad17 is involved in a DNA damage processing or repair step that is shared between a number of distinct DNA repair or processing pathways, or that it harbors a defect in one or more CCCs.

Effect of $mRad17^{5'\Delta/5'\Delta}$ mutation on DNA damage-induced cell cycle arrest

We subsequently investigated whether γ-ray sensitivity of the $mRad17^{5'\Delta/5'\Delta}$ ES cells was due to a defect in the intra-S checkpoint. Surprisingly, we found that $mRad17^{5'\Delta/5'\Delta}$ ES cells did not display radiation-resistant DNA synthesis (RDS; Figure 4F). Because RDS is a hallmark of cells known to be defective in the induction of intra-S checkpoints, the results suggest that, in ES cells, deletion of the 5′ end of mRad17 has no detectable effect on this checkpoint or, alternatively, that mRad17 is not essential for it.

The absence of an overt RDS in $mRad17^{5'\Delta/5'\Delta}$ ES cells prompted us to analyze other CCCs. Asynchronously growing ES cultures were exposed to various DNA-damaging agents and at different time points DNA content was ascertained by propidium iodide staining and analyzed by flow cytometry. The responses to γ-irradiation and to MMC are presented in Figure 5. Wild-type ES cells responded initially (6 h) by accumulation in S phase and G2 leading to a depletion of cells in the G1 pool, followed by a strong increase in cells in the G2 fraction (at 12 h) and in the case of γ-rays normalization of the G1 pool at 24 h. At the dose of MMC used, cells accumulated in G2; however, at a lower dose (0.2 μg/ml), a similar recovery of the G1 fraction was noted as observed for the γ-ray response (data not shown). Similar findings were obtained with different doses of both DNA-damaging agents. All three independently isolated $mRad17^{5'\Delta/5'\Delta}$ ES cell lines behaved identical in these experiments (data not shown). Importantly, $mRad17^{+/5'\Delta}$ as well as $mRad17^{5'\Delta/5'\Delta}$ ES cells

behaved indistinguishable from the wild-type ES cells. Even in experiments using a phosphospecific histone 3 antibody, as described by Xu *et al* (2002), no differences in damage-induced CCC could be detected between wild-type, $mRad17^{+/5'\Delta}$ and $mRad17^{5'\Delta/5'\Delta}$ ES cells (data not shown). We also investigated the effect of 5′Δ-mRad17 on the apoptotic response upon DNA damage, but did not find any differences compared to wild-type ES cells (data not shown). We conclude that, at least in ES cells, deletion of the 5′ end of $mRad17$ has no detectable effect on DNA damage-induced CCC nor on apoptosis.

Effect of $mRad17^{5'\Delta/5'\Delta}$ on homologous recombination

Since lack of wild-type $mRad17$ expression does not lead to impairment of intra-S and G2/M cell cycle arrests, nor increased apoptosis upon exposure to DNA-damaging agents, we investigated whether there are differences in genomic stability after acquiring DNA damage between wild-type, $mRad17^{+/5'\Delta}$ and $mRad17^{5'\Delta/5'\Delta}$ ES cells. Therefore, we analyzed the ability of the cells to mediate sister chromatid exchanges (SCEs). No difference was observed in the level of spontaneous and MMC-induced SCE between wild-type, $mRad17^{+/5'\Delta}$ and $mRad17^{5'\Delta/5'\Delta}$ ES cells (data not shown). These results indicate that $mRad17^{5'\Delta/5'\Delta}$ ES cells have a normal capacity to perform SCE as observed cytologically. However, compared to wild-type and $mRad17^{+/5'\Delta}$ ES cells, only a low percentage of $mRad17^{5'\Delta/5'\Delta}$ ES cells were in second division after MMC treatment (data not shown). This indicates that these cells have a reduced capacity to repair or otherwise properly respond to interstrand DNA crosslinks.

The SCE analyses presented above suggest that homologous recombination between sister chromatids is unaffected in $mRad17^{5'\Delta/5'\Delta}$ ES cells. A similar observation has been made for mutants in the structure-specific endonuclease
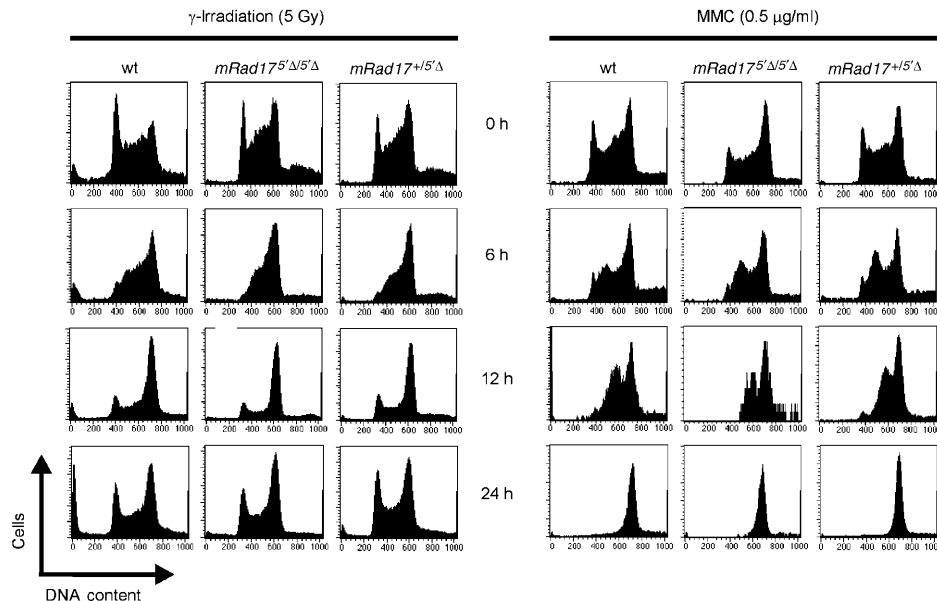
Figure 5 Fluorescent activated cell sorting (FACS) analysis of the effect of DNA damage on cell cycle progression of ES cells. Shown on the *x*-axis is the DNA content of the cells (stained with propidium iodide) and on the *y*-axis the number of cells. The left panel shows the effect after γ-irradiation, while the right panel displays the effect after MMC exposure. Genotypes of ES cells are shown on top. Time (h) is shown between the two panels.

Ercc1/Xpf (Niedernhofer *et al*, 2001). For *Ercc1*$^{-/-}$ ES cells, it has been demonstrated that although homologous recombination between identical DNAs, as measured by SCE, is unaffected, the cells are defective in homologous gene replacement. The difference between homologous recombination between sister chromatids and homologous gene replacement is that the former recombination occurs between identical sequences while in the latter the homology is interrupted by nonidentical sequences, for example, the selectable marker. We investigated the possibility that mRad17 is also involved in the homologous recombination subpathway that mediates homologous gene replacement. The capacity of wild-type and mutant cells to conduct gene targeting was assessed using a green fluorescent protein (GFP)-based gene targeting assay. ES cells were electroporated with a construct designed to introduce a GFP tag in the mouse *Rad54* locus. This targeting construct is referred to as *11.1hRad54GFP* knock-in construct (Figure 6A; Abraham *et al*, 2003). Targeted integration of the construct within the *Rad54* locus results in expression of GFP-tagged mRad54 from the endogenous *mRad54* promoter. Homologous integration can be scored in individual cells as green fluorescence, using FACS analysis, as established by DNA blot analysis of genomic DNA of individually sorted and expanded green fluorescent cells (data not shown). Random integration of the *Rad54-GFP* construct resulted in nonfluorescent cells.

Using this assay, transfection of the *Rad54-GFP* construct into the wild-type ES cells resulted in targeting efficiencies of ~23% (Figure 6B). Similar targeting efficiencies were ob-

tained with ES cells from both 129Sv and C57bl/6 genetic background, indicating that the genetic background does not influence the efficiency of targeted gene replacement at the *mRad54* locus (data not shown). The targeting efficiency is similar to that determined by DNA blotting analysis (Niedernhofer *et al*, 2001). As a negative control, we used *Ercc1*$^{-/-}$ ES cells that are completely deficient in targeted gene replacement (Niedernhofer *et al*, 2001). Transfection of the *Rad54-GFP* construct to *Ercc1*$^{-/-}$ ES cells resulted in 0.7% green fluorescent cells (Figure 6B), which is similar to the background level in this assay. We then examined the capability of *mRad17*$^{5'\Delta/5'\Delta}$ ES for targeted gene replacement. In experiments using the three independent *mRad17*$^{5'\Delta/5'\Delta}$ ES cells with the *Rad54-GFP* knock-in construct, the percentage of green fluorescent cells never exceeded background levels (Figure 6B). *Rad54* expression is not affected by the Rad17 mutation, as shown in the immunoblot (Figure 6C). Together, these data show that mRad17 plays an important role in recombination.

Discussion

S. pombe Rad17 is one of the components of the cellular machinery that responds to DNA damage and stalled DNA replication. In this study, we examined the role of the mouse homolog of *Rad17* by analyzing the consequences of a targeted deletion of mRad17. Our findings reveal an important role for *mRad17* in cell growth and/or differentiation at an early stage of embryonic development, as mRad17-deficient
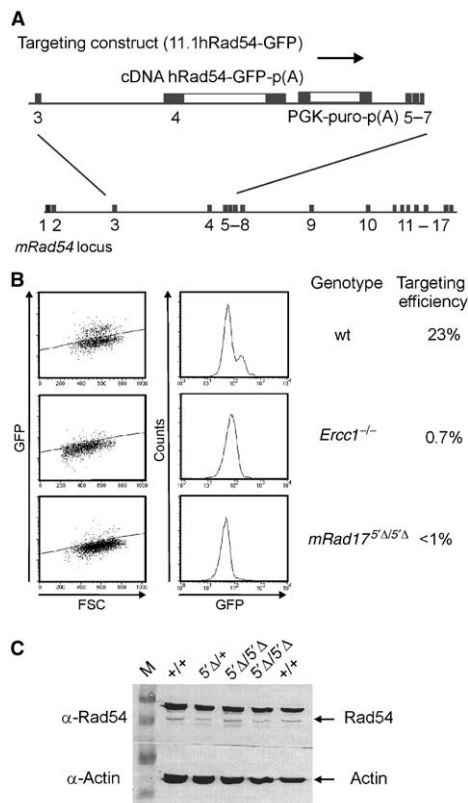
Figure 6 Targeted gene replacement is severely reduced in *mRad17*^{5'Δ/5'Δ} cells. (**A**) Schematic overview of the Rad54 targeting strategy. The *Rad54* targeting construct (11.1hRad54-GFP) and the *mRad54* gene locus are shown. Targeted gene replacement by the *Rad54-GFP* construct results in GFP expression, while random integration results in nonfluorescent cells. (**B**) (left) Cells of the indicated genotype were electroporated with the *Rad54-GFP* knock-in construct and 1×10^5 cells were analyzed by flow cytometry. Shown are green fluorescence (GFP) versus forward scatter (FSC) plots. Fluorescent cells appear above and nonfluorescent cells below the diagonal line (left panels). To determine the percentage of gene targeting efficiency, results were also plotted in a fluorescence (GFP) histogram (right panels). In wild-type ES cells, two peaks are visible, representing non-GFP- and GFP-expressing cells. *Ercc1*^{−/−} and *mRad17*^{5'Δ/5'Δ} cells show only one peak representing nonfluorescent cells. (**C**) Immunoblot using anti-Rad54, showing that mRad54 expression is not affected by the *mRad17* genotype (indicated on top). Actin was used as a loading control. The upper band in the Rad54 blot is a nonspecific band (Essers *et al*, 1997).

embryos die during early/mid-gestation. In contrast, *S. pombe Rad17* and *S. cerevisiae RAD24* mutants are viable under normal growth conditions (al-Khodairy and Carr, 1992). This may indicate that mRad17 has acquired functions not mediated by *S. pombe* Rad17 or *S. cerevisiae* RAD24. However, in view of the strong sequence conservation of the Rad17 protein between yeast and mammals and the notion that it is part of a larger complex, this option may not seem

very likely. A more plausible explanation is that fundamental physiological differences between yeast and mammalian cells increase the requirement for mRad17. During early embryogenesis, cells are constantly under mitotic stress as divisions in some regions of the embryo can occur as rapidly as every 2–3 h. Under these circumstances, correct ordering of cell cycle events and fast repair of DNA damage or resolution of replication stalling are crucial. Failures, caused by mitotic stress, may lead to random drop out of cells in early embryogenesis. This may lead to heterogeneous effects later in development and explains the observed heterogeneity in time and cause of embryonic lethality. In this respect, it is not surprising that targeted disruption of other mouse cell cycle genes, including *Atr* (Brown and Baltimore, 2000; de Klein *et al*, 2000), *Hus1* (Weiss *et al*, 2000) and *mRad1* (A Maas, unpublished results) also results in heterogeneity in early embryonic lethality. Conditional gene targeting therefore should give more insight into the role of mRad17 in adult tissue.

mRad17^{5'Δ/5'Δ} MEFs isolated from E8.5 embryos failed to grow beyond passage 5. This is consistent with *RAD17*^{flox/−} human HCT116 colon epithelial cells, of which >90% were unable to form colonies upon Ad-Cre infection and subsequent loss of Rad17 (Wang *et al*, 2003). However, in cells freshly isolated from *mRad17*^{5'Δ/5'Δ} embryos, we failed to observe detectable levels of chromosomal instability and endoreplication, as present in *RAD17*^{flox/−} epithelial cells (Wang *et al*, 2003). In the established Ad-Cre-infected *RAD17*^{flox/−} epithelial cells, inefficient apoptotic responses or DNA repair may result in chromosomal aberrations and endoreplication. Possibly, a more efficient apoptotic response in primary *mRad17*^{5'Δ/5'Δ} cells prevents the detection of chromosomal instability and endoreplication. Alternatively, the difference in the site of mutation in the mRad17 protein may be responsible for this phenotypic difference.

In contrast to more differentiated cells, as shown here, and to *Rad17*^{flox/−} human epithelial cells (Wang *et al*, 2003), *mRad17*^{5'Δ/5'Δ} ES cells appeared viable. Unexpectedly and in contrast to other more differentiated cell types, a shorter truncated mRad17 protein is produced in *mRad17*^{5'Δ/5'Δ} ES cells. The molecular mechanism for the observed discrepancy of truncated mRad17 expression between ES cells and somatic cells is not clear at this point, but might involve differences in translation initiation and/or protein stability between these cell types.

Although a mutant form of mRad17 is expressed in these ES cells, they show hypersensitivity to different types of DNA damage induced by γ-irradiation, UV light, MMC, MMS and illudin-S and replication stalling induced by HU treatment. Thus, like Rad17 in *S. pombe*, mouse Rad17 is involved in cellular responses to genotoxic stress. However, in striking contrast to *S. pombe* Rad17 and *S. cerevisiae* RAD24 mutants, cell cycle arrest during S phase and the G2/M transition upon induction of DNA damage is not affected in *mRad17*^{5'Δ/5'Δ} ES cells, expressing the shorter *mRad17* mutant form (Weinert *et al*, 1994; Lydall and Weinert, 1997). In addition, our results with mRad17 also differ from those obtained with other mammalian cell lines defective in CCC genes. For example, *ATM* and members of the DNA repair complex Rad50/Mre11/Nbs1 influence cell cycle progression. Cell lines with mutations in these components display RDS (de Jager and Kanaar, 2002; Falck *et al*, 2002). DNA synthesis in *mRad17*^{5'Δ/5'Δ} ES

cells is not significantly different after γ-irradiation treatment compared to wild-type and $mRad17^{+/5'\Delta}$ ES cells. The broad-spectrum DNA damage sensitivity combined with apparently normal DNA damage signaling and CCC exhibited by the $mRad17^{5'\Delta/5'\Delta}$ ES cells indicates a defect in DNA damage processing, likely in relation to replication of a damaged DNA template.

Our results in mouse ES cells lead us to consider that mRad17 may be involved in both CCC and DNA repair processes. This is not unprecedented because a similar dual function is found for the Rad50/Mre11/Nbs1 complex, which also has both DNA repair and CCC functions (Bender *et al*, 2002; Falck *et al*, 2002). It is possible that ES cells require only the contribution of mRad17 to DNA repair, while in more differentiated cells both functions of mRad17 are required, making it essential for cellular viability. This might also explain the fact that, in contrast to $mRad17^{5'\Delta/5'\Delta}$ ES cells, $mRad17^{5'\Delta/5'\Delta}$ MEFs fail to grow and become senescent. In contrast to MEFs, ES cells do not arrest at the G1/S transition (Aladjem *et al*, 1998; Schmidt-Kastner *et al*, 1998). DNA damage can trigger G1/S cell cycle arrest in $mRad17^{5'\Delta/5'\Delta}$ MEFs, which could lead to irreversible withdrawal from cell cycling. However, this cannot be the sole explanation as the ES cell CCCs for intra-S and G2 do not appear to be abnormal, except when the initial DNA damage signaling in ES cells is principally different for all CCCs when compared to other cell types. In this respect, it is interesting that deletion of *p21* can rescue poor growth of other cell cycle protein-deficient MEFs, including ATM$^{-/-}$ (Wang *et al*, 1997; Xu *et al*, 1998) and Hus1$^{-/-}$ cells (Weiss *et al*, 2000). However, a more plausible explanation is that the reduced amount of 5′Δ-mRad17 compared to wild-type mRad17, present in the nucleus and bound to chromatin, may be sufficient for $mRad17^{5'\Delta/5'\Delta}$ ES cell viability but not for DNA repair functions.

$mRad17^{5'\Delta/5'\Delta}$ ES cells are severely impaired in homologous gene targeting and show hypersensitivity to a variety of DNA-damaging agents. One conclusion from these findings is that the hypersensitive phenotype apparent in these $mRad17^{5'\Delta/5'\Delta}$ ES cells is not due to a compromised CCC function but is primarily derived from the defect in homologous recombination, most likely dependent on DNA damage. This opens the possibility that the hypersensitivity of other CCC genes is also caused by inefficient handling of DNA lesions. A common intermediate in homologous recombination and DNA damage repair is a single-stranded DNA gap. It is possible that mRad17 has a role in restoration of these single-stranded DNA gaps to duplex DNA, which requires the action of a DNA polymerase (Figure 7; Venclovas and Thelen, 2000; Ellison and Stillman, 2003). A docking site for DNA polymerase δ and ε on the chromatin is provided by PCNA, which is loaded by RFC$_{1-5}$ (Hubscher *et al*, 2002). Similarly, mRad17 can bind to the four small subunits of RFC (mRad17/RFC$_{2-5}$; Green *et al*, 2000; Ellison and Stillman, 2003). mRad17/RFC$_{2-5}$ may have a higher affinity for nicked or gapped DNA, resulting in the loading of the 9-1-1 trimer (Rauen *et al*, 2000). Rad9, Rad1 and Hus1 may be involved in further processing or stabilization of the DNA repair intermediate structures and/or provide a platform for other DNA repair enzymes, including DNA lesion bypass polymerases (Ellison and Stillman, 2003). CCC may be mediated by the mammalian homologs for the *S. pombe*
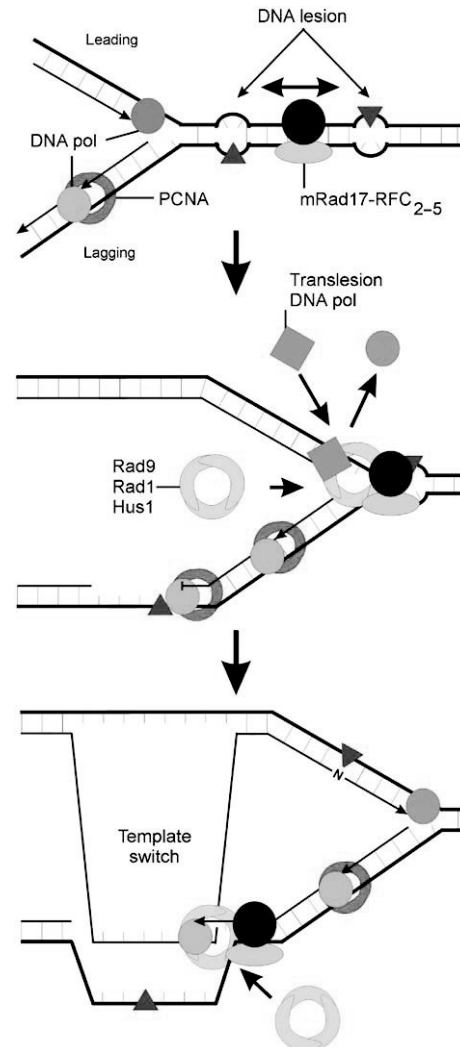

Figure 7 Schematic model of the role of mRad17 in DNA damage. In response to DNA damage, RFC$_1$ from the RFC$_{1-5}$ complex is replaced by mRad17 to form a Rad17–RFC$_{2-5}$ complex. If this complex has a higher affinity for damaged or gapped DNA than RFC$_{1-5}$, then this could result in the preferential loading of the Rad9–Rad1–Hus1 heterotrimer onto the site of damage compared to PCNA. Phosphorylation of mRad17, by ATR/ATRIP and stimulated by Hus1, may result in dissociation of Rad17–RFC$_{2-5}$ from Rad9–Rad1–Hus1, which then forms a docking site for translesion bypass DNA polymerases or may result in a template switch. In this model, CCC is not necessarily mediated by mRad17 but by other protein complexes, possibly ATR/ATRIP, binding to the site of damage independently of mRad17.

Rad3/Rad26 complex, ATR/ATRIP (Cortez *et al*, 2001), binding to the damaged DNA independently of Rad17.

Materials and methods

Construction of the mRad17 targeting vector

To construct an *mRad17* targeting vector, an *mRad17* genomic 4.8 kb *Xba*I fragment was used as the 3′ homologous fragment. This fragment, which contains 38 bp of the end of exon 3, was subcloned into the *Xba*I site of pGEM-9Zf (Promega), excised as an *Spe*I–*Sal*I fragment and cloned into *Spe*I–*Sal*I sites of pGem-5Zf (Promega). For the 5′ homologous fragment, a 5 kb PCR fragment, generated with primers F285 (5′-GTCAGAAACTTTCCTTAGACCAAAGGTGTC-3′) and R380 (5′-GTGATGGCGGTGTTGGC CTCAAAGTC-3′) and containing 55 bp of the beginning of exon 3, was cloned into pGem T easy (Promega). A pgk-Neo selection cassette was cloned in antisense orientation into a unique *Ava*I site in intron 2, approximately 200 bp 5′ of exon 3. The insert was then excised from the pGem T easy vector using a partial *Spe*I–*Sac*II digest and cloned into *Sac*II–*Spe*I sites of pGem-5Zf, which already contained the 3′ homologous fragment. In this way, a 110 bp deletion of exon 3 was generated. The targeting vector was linearized using a unique *Pme*I site that was generated 5′ of the insert.

ES cell culture, gene targeting and generation of mRad17 mutant mice

E14 ES cells (subclone IB10) were cultured in BRL-conditioned medium supplemented with 1000 U/ml leukemia inhibitory factor. A 20 µg portion of the *Pme*I-linearized targeting vector was electroporated into approximately 10^7 ES cells in 500 µl. Selection with 0.2 µg/ml G418 was started 24 h after electroporation. After 8–10 days, G418-resistant clones were isolated. Screening for homologous recombinants was performed using DNA blot analyses of *Pst*I-digested DNA with a 350 bp 5′ external probe. Correct integration of the 3′ end of the targeting construct was verified by PCR using a neomycin-specific primer (FNeo: 5′-AACCTGCGTG CAATCCAT-3′) and a primer outside the targeting vector in exon 5 (R348: 5′-GGTCGTTGTCTTTCCACAT CCAGG-3′). Out of 240 G418-resistant clones, three ES clones had a correctly targeted mRad17 allele. Two out of the three correctly targeted ES clones (designated F17 and F24) were injected into blastocysts of C57Bl/6 mice and transplanted into B10/CBA foster mothers. Chimeric offspring was mated to C57bl/6 females and resulted in mice heterozygous for the targeted mRad17 allele. These mice were further intercrossed, resulting in mice with a mixed 129Sv/C57bl/6 genetic background. Germline transmission and genotyping of offspring were carried out by PCR. Primers F325 (5′-GTGACAGACTGGGTAGCTCCAGCC-3′) and R548 (5′-GGCTCATTGTCGGACAGACGCT CTC-3′) encompassing the deletion in exon 3 were used.

Cell fractionation and immunoblotting

Cell fractionation was performed as described (Zou *et al*, 2002). For immunoblotting, α-Rad17 H-300 (Santa Cruz), α-histone H3 (Upstate), α-actin (Chemicon Int.), α-Grb2, α-Msh6 (Becton Dickinson) and α-hRad54 (Essers *et al*, 1997) were used.

Colony survival curves

Sensitivity of ES cells to increasing doses of DNA-damaging agents was determined as described previously (Essers *et al*, 1997). Briefly, cells were plated in 6 cm dishes, at various dilutions. After 12–16 h, cells were irradiated with a single dose in the range of 0–10 Gy using a ^{137}Cs source or UV (0–8 J/m^2) or treated for 1 h with MMC (0–0.8 µg/ml), illudin-S (0–0.3 ng/ml) or MMS (0–1.7 mM). Cells were grown for 4–6 days, fixed, stained and colonies were counted. For the HU colony survival assay, 500–20 000 ES cells were plated in a 6 cm dish 4 h prior to the addition of HU. After 5–7 days, cells were fixed and stained. All experiments were performed in triplicate.

Flow cytometric analysis

Confluent ES cells (60–70%) on 10 cm culture dishes were either irradiated with a single dose of γ-radiation (5 or 10 Gy) using a ^{137}Cs source or treated for 1 h with MMC (0.2 or 0.5 µg/ml). At different time points after treatment, cells were collected and fixed with 70% ethanol. After a minimum of 2 h on ice, cells were washed with phosphate buffered saline (PBS) and resuspended in 400 µl PBS containing 0.1% Triton X-100, 0.1 mg/ml propidium iodide and 0.1 mg/ml RNAse. Cells were incubated overnight and analyzed on a Facscan (Becton Dickinson).

Transfections and recombination assays

To quantitate the efficiency of homologous gene targeting, ES cells were transfected with a *Rad54-GFP* knock-in construct containing a puromycin selectable marker (Abraham *et al*, 2003). At 1 week after puromycin selection, plates were trypsinized, resuspended to single-cell suspensions in PBS and fixed with 1% paraformaldehyde. After permeabilization with 0.1% Triton X-100 and RNAse treatment, cells were analyzed in a Becton Dickinson FacsCalibur on a green fluorescence (FL1) versus forward scatter (FSC-H) plot (Figure 6). GFP-positive and -negative cells appeared in separate populations, above and below the diagonal line, respectively (Figure 6). Results were also plotted in a fluorescence (GFP) histogram (Figure 6). The expression level of mRad54 was analyzed using α-hRad54 antibodies (Essers *et al*, 1997).

References

Abraham J, Lemmers B, Hande MP, Moynahan ME, Chahwan C, Ciccia A, Essers J, Hanada K, Chahwan R, Khaw AK, McPherson P, Shehabeldin A, Laister R, Arrowsmith C, Kanaar R, West SC, Jasin M, Hakem R (2003) Eme1 is involved in DNA damage processing and maintenance of genomic stability in mammalian cells. *EMBO J* **22**: 6137–6147

Aladjem MI, Spike BT, Rodewald LW, Hope TJ, Klemm M, Jaenisch R, Wahl GM (1998) ES cells do not activate p53-dependent stress responses and undergo p53-independent apoptosis in response to DNA damage. *Curr Biol* **8**: 145–155

al-Khodairy F, Carr AM (1992) DNA repair mutants defining G2 checkpoint pathways in *Schizosaccharomyces pombe*. *EMBO J* **11**: 1343–1350

Bender CF, Sikes ML, Sullivan R, Huye LE, Le Beau MM, Roth DB, Mirzoeva OK, Oltz EM, Petrini JH (2002) Cancer predisposition and hematopoietic failure in Rad50(S/S) mice. *Genes Dev* **16**: 2237–2251

Bluyssen HA, Naus NC, van Os RI, Jaspers I, Hoeijmakers JH, de Klein A (1999) Human and mouse homologs of the *Schizosaccharomyces pombe* rad17 + cell cycle checkpoint control gene. *Genomics* **55**: 219–228

Brown EJ, Baltimore D (2000) ATR disruption leads to chromosomal fragmentation and early embryonic lethality. *Genes Dev* **14**: 397–402

Burtelow MA, Kaufmann SH, Karnitz LM (2000) Retention of the human Rad9 checkpoint complex in extraction-resistant nuclear complexes after DNA damage. *J Biol Chem* **275**: 26343–26348

Cortez D, Guntuku S, Qin J, Elledge SJ (2001) ATR and ATRIP: partners in checkpoint signaling. *Science* **294**: 1713–1716

de Jager M, Kanaar R (2002) Genome instability and Rad50(S): subtle yet severe. *Genes Dev* **16**: 2173–2178

de Klein A, Muijtjens M, van Os R, Verhoeven Y, Smit B, Carr AM, Lehmann AR, Hoeijmakers JH (2000) Targeted disruption of the cell-cycle checkpoint gene ATR leads to early embryonic lethality in mice. *Curr Biol* **10**: 479–482

Edwards RJ, Bentley NJ, Carr AM (1999) A Rad3–Rad26 complex responds to DNA damage independently of other checkpoint proteins. *Nat Cell Biol* **1**: 393–398
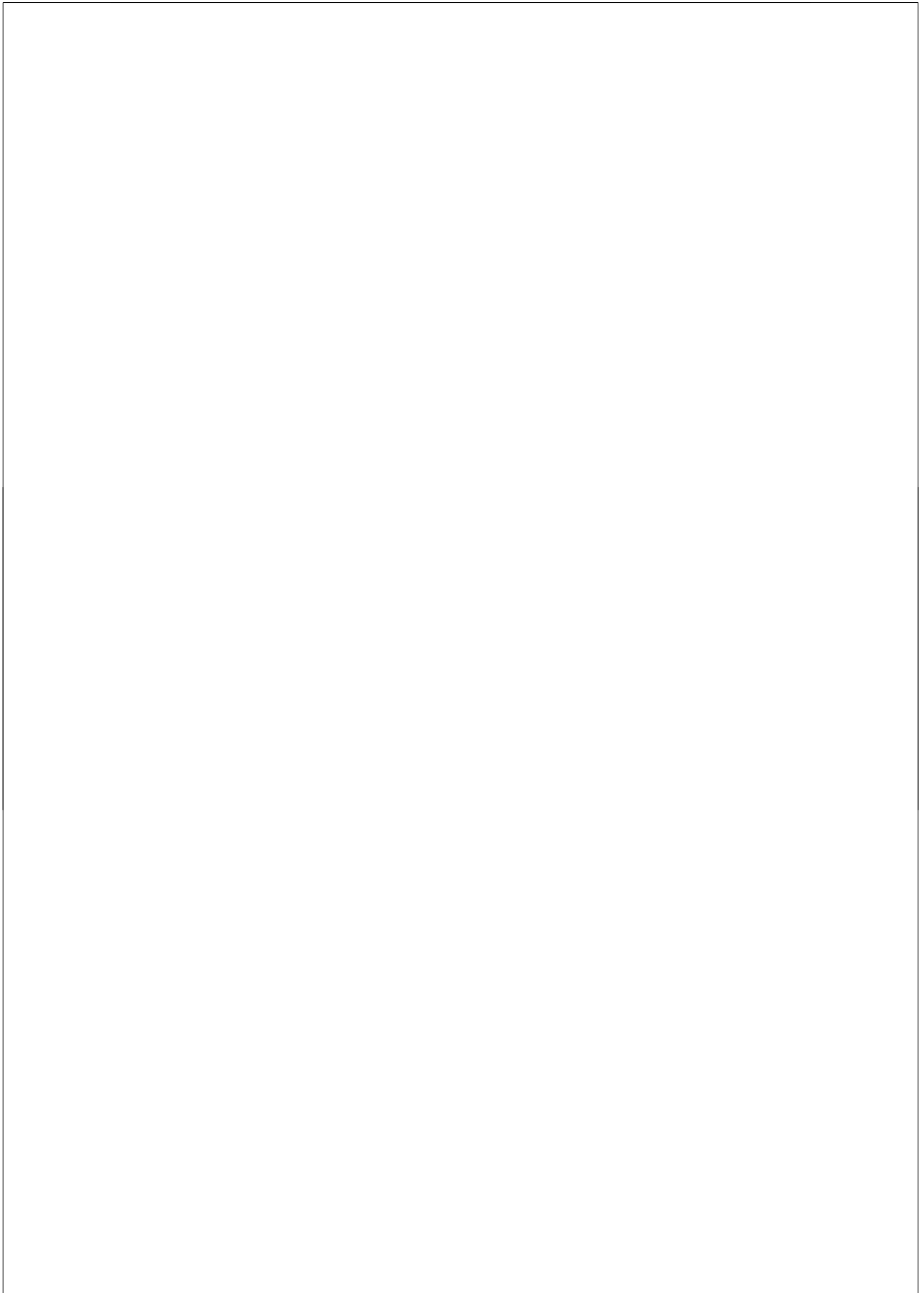
Ellison V, Stillman B (2003) Biochemical characterization of DNA damage checkpoint complexes: clamp loader and clamp complexes with specificity for 5′ recessed DNA. *PLoS Biol* **1**: E33

Essers J, Hendriks RW, Swagemakers SM, Troelstra C, de Wit J, Bootsma D, Hoeijmakers JH, Kanaar R (1997) Disruption of mouse RAD54 reduces ionizing radiation resistance and homologous recombination. *Cell* **89**: 195–204

Falck J, Petrini JH, Williams BR, Lukas J, Bartek J (2002) The DNA damage-dependent intra-S phase checkpoint is regulated by parallel pathways. *Nat Genet* **30**: 290–294

Green CM, Erdjument-Bromage H, Tempst P, Lowndes NF (2000) A novel Rad24 checkpoint protein complex closely related to replication factor C. *Curr Biol* **10**: 39–42

Hartwell LH, Weinert TA (1989) Checkpoints: controls that ensure the order of cell cycle events. *Science* **246**: 629–634

Hubscher U, Maga G, Spadari S (2002) Eukaryotic DNA polymerases. *Annu Rev Biochem* **71**: 133–163

Jaspers NG, Raams A, Kelner MJ, Ng JM, Yamashita YM, Takeda S, McMorris TC, Hoeijmakers JH (2002) Anti-tumour compounds illudin S and Irofulven induce DNA lesions ignored by global repair and exclusively processed by transcription- and replication-coupled repair pathways. *DNA Repair (Amst)* **1**: 1027–1038

Kostrub CF, Knudsen K, Subramani S, Enoch T (1998) Hus1p, a conserved fission yeast checkpoint protein, interacts with Rad1p and is phosphorylated in response to DNA damage. *EMBO J* **17**: 2055–2066

Lee SH, Kwong AD, Pan ZQ, Hurwitz J (1991) Studies on the activator 1 protein complex, an accessory factor for proliferating cell nuclear antigen-dependent DNA polymerase delta. *J Biol Chem* **266**: 594–602

Lydall D, Weinert T (1997) G2/M checkpoint genes of *Saccharomyces cerevisiae*: further evidence for roles in DNA replication and/or repair. *Mol Gen Genet* **256**: 638–651

Niedernhofer LJ, Essers J, Weeda G, Beverloo B, de Wit J, Muijtjens M, Odijk H, Hoeijmakers JH, Kanaar R (2001) The structure-specific endonuclease Ercc1-Xpf is required for targeted gene replacement in embryonic stem cells. *EMBO J* **20**: 6540–6549

Paulovich AG, Hartwell LH (1995) A checkpoint regulates the rate of progression through S phase in *S. cerevisiae* in response to DNA damage. *Cell* **82**: 841–847

Rauen M, Burtelow MA, Dufault VM, Karnitz LM (2000) The human checkpoint protein hRad17 interacts with the PCNA-like proteins hRad1, hHus1, and hRad9. *J Biol Chem* **275**: 29767–29771

Savitsky K, Bar-Shira A, Gilad S, Rotman G, Ziv Y, Vanagaite L, Tagle DA, Smith S, Uziel T, Sfez S, Ashkenazi M, Pecker I, Frydman M, Harnik R, Patanjali S, Simmons A, Clines G, Sartiel A, Gatti R, Chessa L, Sanal O, Lavin M, Jaspers N, Taylor A, Arlett C, Miki T, Weissman S, Lovett M, Collins F, Shiloh Y (1995) A single ataxia telangiectasia gene with a product similar to PI-3 kinase. *Science* **268**: 1749–1753

Schmidt-Kastner PK, Jardine K, Cormier M, McBurney MW (1998) Absence of p53-dependent cell cycle regulation in pluripotent mouse cell lines. *Oncogene* **16**: 3003–3011

Siede W, Friedberg AS, Friedberg EC (1993) RAD9-dependent G1 arrest defines a second checkpoint for damaged DNA in the cell cycle of *Saccharomyces cerevisiae*. *Proc Natl Acad Sci USA* **90**: 7985–7989

Venclovas C, Thelen MP (2000) Structure-based predictions of Rad1, Rad9, Hus1 and Rad17 participation in sliding clamp and clamp-loading complexes. *Nucleic Acids Res* **28**: 2481–2493

von Deimling F, Scharf JM, Liehr T, Rothe M, Kelter AR, Albers P, Dietrich WF, Kunkel LM, Wernert N, Wirth B (1999) Human and mouse RAD17 genes: identification, localization, genomic structure and histological expression pattern in normal testis and seminoma. *Hum Genet* **105**: 17–27

Wang X, Zou L, Zheng H, Wei Q, Elledge SJ, Li L (2003) Genomic instability and endoreduplication triggered by RAD17 deletion. *Genes Dev* **17**: 965–970

Wang YA, Elson A, Leder P (1997) Loss of p21 increases sensitivity to ionizing radiation and delays the onset of lymphoma in atm-deficient mice. *Proc Natl Acad Sci USA* **94**: 14590–14595

Weinert TA, Kiser GL, Hartwell LH (1994) Mitotic checkpoint genes in budding yeast and the dependence of mitosis on DNA replication and repair. *Genes Dev* **8**: 652–665

Weiss RS, Enoch T, Leder P (2000) Inactivation of mouse Hus1 results in genomic instability and impaired responses to genotoxic stress. *Genes Dev* **14**: 1886–1898

Xu B, Kim ST, Lim DS, Kastan MB (2002) Two molecularly distinct G(2)/M checkpoints are induced by ionizing irradiation. *Mol Cell Biol* **22**: 1049–1059

Xu Y, Yang EM, Brugarolas J, Jacks T, Baltimore D (1998) Involvement of p53 and p21 in cellular defects and tumorigenesis in Atm−/− mice. *Mol Cell Biol* **18**: 4385–4390

Zhou BB, Elledge SJ (2000) The DNA damage response: putting checkpoints in perspective. *Nature* **408**: 433–439

Zou L, Cortez D, Elledge SJ (2002) Regulation of ATR substrate selection by Rad17-dependent loading of Rad9 complexes onto chromatin. *Genes Dev* **16**: 198–208
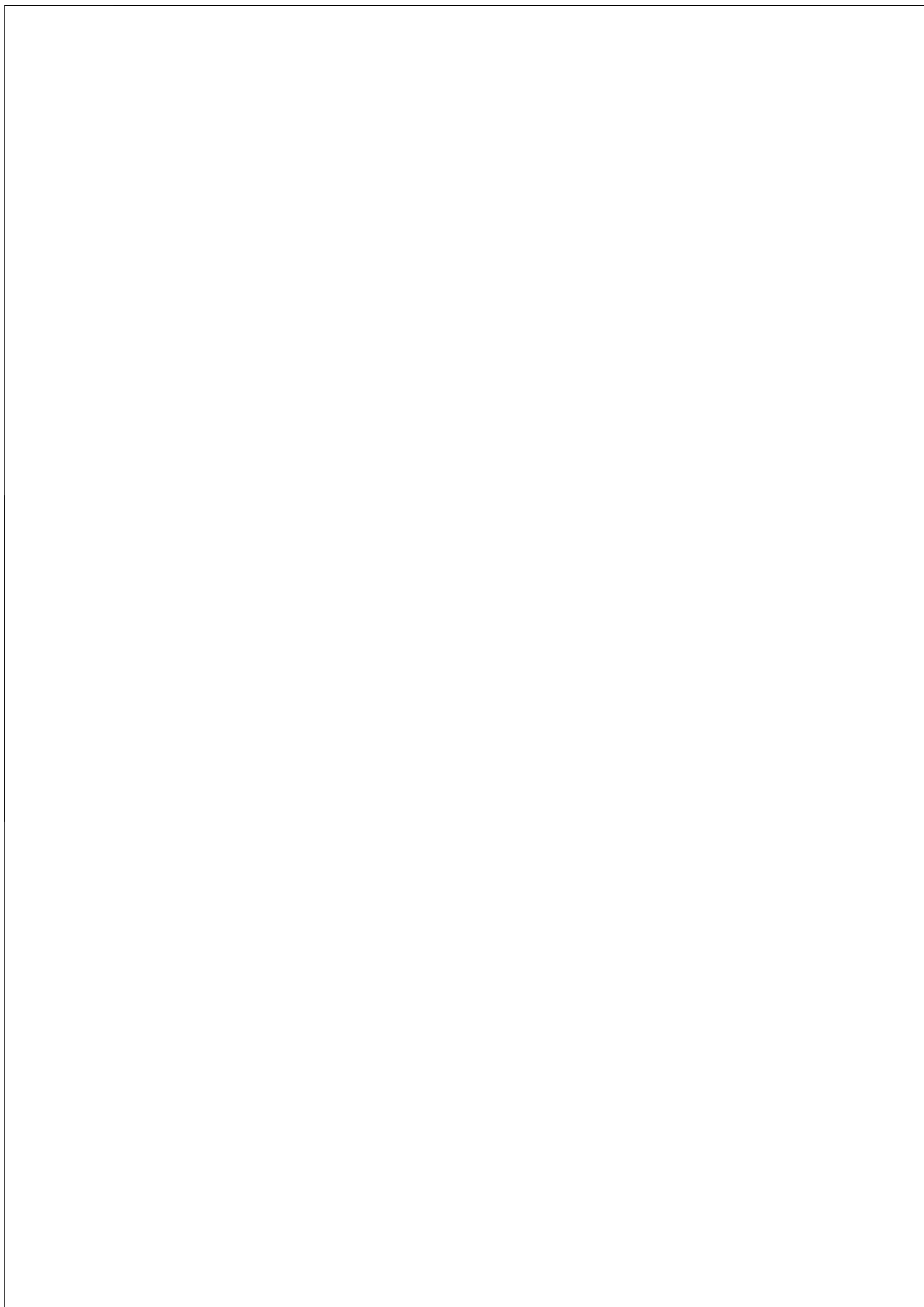
Chapter 3

The N-terminal domain of Rad17
is required for the cellular response
to replication-associated
DNA damage

The N-terminal domain of Rad17 is required for the cellular response to replication-associated DNA damage

Magda Budzowska[1], Alex Maas[1], and Roland Kanaar[1,2]

[1]Department of Cell Biology and Genetics and [2]Department of Radiation Oncology, Erasmus MC, PO Box 2040, 3000CA Rotterdam, The Netherland

Abstract

Checkpoint mechanisms help to protect cells and organisms against detrimental effects of DNA damage by triggering signaling cascades that regulate cell cycle progression, repair events and apoptosis. Rad17 is an essential protein in mammalian cells, involved in intra-S and G2/M checkpoints. It shares homology with Rfc1 – a subunit of the complex that loads PCNA onto primer/template junctions during replication. Similarly, Rad17 is part of the complex that loads the PCNA-like Rad9-Rad1-Hus1 heterotrimeric ring onto damaged DNA and promotes full activation of ATR-dependent damage signaling. Here, we found that ES cells expressing an N-terminally truncated version of Rad17 are hypersensitive to replication stress and, compared to wild type cells, show delayed cell cycle progression after treatment with replication inhibitors. They also accumulate increased levels of DSBs. We postulate that in addition to its role in imposing cell cycle delay in response to DNA damage, Rad17 is also more directly involved in processing stalled or collapsed replication forks.

Introduction

Agents generated during normal cellular metabolism or derived from environmental sources constantly damage cellular DNA at every cell cycle phase. DNA damage is especially dangerous during DNA replication, which by itself is a complex and difficult task. Replicating damaged DNA can cause loss or change in genetic information. Transmiting these genetic changes to daughter cells threatens genomic integrity and cell viability. Although cells are equipped with a number of specialized repair pathways recognizing and removing different types of DNA damage (1), some aberrant DNA structures e.g. interstrand crosslinks, are poorly recognized and therefore may be unnoticed until they interfere with replication or transcription (2). Additionally, DNA damage can be introduced during S-phase by exogenous agents, and is also inherent to the replication process, e.g. DNA double strand breaks (DSBs) generated at stalled replication forks. To avoid detrimental effects of DNA damage, cells have developed complex damage-response systems, named checkpoints, which sense and signal DNA damage and replication stress and coordinate cell cycle progression with repair processes or induce apoptosis or senescence (3).

Two checkpoint pathways are involved in dealing with damage encountered during DNA replication. The intra-S checkpoint is responsible for inhibition of firing of new origins. This checkpoint also stabilizes stalled or collapsed replication forks (4-7). The G2/M checkpoint ensures that DNA replication is finished before allowing a cell to enter mitosis (8,9). This helps to prevent chromosomal aberrations, which could arise after an attempt to segregate unreplicated or damaged DNA molecules.

Depending on the type of DNA damage, checkpoint responses can be conceptually divided into two main pathways, controlled by two phosphatidylinositol 3-kinase-related kinases: ATM and ATR. ATM is important primarily for the response to DSBs, while ATR responds to a broad spectrum of DNA damage and replication disruption (3,10). ATR-dependent signaling is activated by single stranded (ss) DNA, which is a common structural intermediate produced at stalled replication forks and by repair reactions. The exposed ssDNA is coated with the ssDNA-binding protein RPA, and this structure is thought to be the key damage mark (11), which recruits two protein complexes to the sites of damage: ATR/ATRIP (11), and the Rad17/Rad9-Rad1-Hus1 complex.

Rad17 is an RFC-related protein that forms a complex with the four smaller subunits of the replicative RFC complex. This complex presumably recognizes and binds to the transitions from double stranded (ds) DNA to ssDNA, which are generated at sites of DNA damage (12,13). Rad9, Rad1 and Hus1 are similar to PCNA and the 9-1-1 complex is predicted to form a PCNA-like heterotrimeric ring, which is loaded onto the primer/template junctions by the Rad17-RFC complex in an ATP-dependent manner (13-15). Rad17 is phosphorylated by ATR on Ser 635 and Ser 645, and this event is required for the propagation of checkpoint signaling (16). The chromatin-bound Rad1-Hus1-Rad9 complex facilitates ATR-mediated phosphorylation and activation of Chk1, the main effector kinase (17,18), and other downstream checkpoint proteins such as p53 and Brca1, which in turn regulate cell cycle progression and repair events (19).

Intact checkpoint responses are essential for cell well-being, as evidenced by genomic instability, increased sensitivity to DNA-damaging agents, and susceptibility to cancer development caused by defects in checkpoint signaling (20-22). Consistent with the important role of checkpoint signaling, Rad17 is essential for cell viability and chromosomal stability (23). We have previously found that deletion of Rad17 in mice is embryonically lethal, and that an N-terminal truncation of Rad17 causes hypersensitivity to a broad spectrum of DNA damaging agents. Here, we focused on agents inhibiting DNA replication and found that, in agreement with our previous results, Rad17 mutation resulted in hypersensitivity to replication stress. Surprisingly, our results indicated that the impaired survival of cells expressing the truncated protein was most likely not caused by a checkpoint dysfunction resulting in premature cell division, but rather by a defect in a repair process itself.

Materials and Methods

Cells and cell culture

Mouse ES cells used in this study were wild type (C57Bl/6) and $Rad17^{5'\Delta/5'\Delta}$ cells, which carry homozygous deletion of 78 N-terminal amino acids of *Rad17* (Budzowska, 2004). The cells were cultured on gelatinized dishes in a 1-to-1 mixture of DMEM and BRL (Buffalo Rat Liver) conditioned medium, supplemented with 10% fetal calf serum (Hyclone), 0.1 M non-essential amino acids (Biowhittaker™), penicillin/streptomycin, 50 μM ß-mercaptoethanol (Sigma) and 500 U/ml leukemia inhibitory factor, at 37 °C in an atmosphere containing 5% CO_2.

Detection of Chk1 phosphorylation

Cells were lysed directly with SDS sample buffer (2% SDS, 10% glycerol, 120 mM Tris-HCl, pH 6.8), After the protein concentration of the resulting extract was determined by the Lowry protein assay, the samples were supplemented with 0.5% ß-mercaptoethanol and 0.02% bromphenol blue. Phosphorylated Chk1 was detected using anti-phospho-Chk1 (S317) antibodies (Bethyl). Equal loading of proteins was verified by probing with anti-Grb2 antibodies (BD Transduction Laboratories).

Colony survival assays

The sensitivity of ES cells to increasing doses of DNA-damaging agents was determined by measuring their colony-forming ability. The cells were trypsinized and counted. 1000 cells (wild type) or 2000 cells ($Rad17^{5'\Delta/5'\Delta}$ cells) were seeded onto gelatinized 60 mm dishes, allowed to attach overnight, and incubated in drug-containing media. The cells were treated with aphidicolin (Sigma), hydroxyurea (Sigma), etoposide (Sigma) and camptothecin (Sigma) for 12 hrs. The cells were then washed twice with PBS and incubated in fresh medium for 6-9 days, after which the colonies were fixed, stained and counted. All measurements were performed in triplicate.

Detection of DSBs by pulsed-field gel electrophoresis

Sub-confluent cultures of ES cells were treated with hydroxyurea for 12 hrs, washed twice with PBS and incubated in fresh medium for the indicated time. Cells were harvested by trypsinization, and agarose plugs of 10^6 cells were prepared with a CHEF disposable plug Mold (BioRad). The plugs were incubated in lysis buffer (100 mM EDTA, 1% sodium lauryl sarcosyne, 0.2 % sodium deoxycholate, 1 mg/ml Proteinase K) at 37 ℃ for 48 hrs, and washed two times in TE buffer (10 mM Tris-HCl, pH 8.0, 100 mM EDTA) prior to loading onto an agarose gel. Electrophoresis was performed for 23 hrs at 13℃ in 0.9% agarose containing 250 mM Tris-Borate and 20 mM EDTA (TBE) using a Biometra Rotaphor apparatus with the following parameters: voltage 180 V to 120 V log; angle from 120° to 110° linear; interval 30 s to 5 s log. The gel was stained with ethidium bromide and analyzed using Typhoon 9200 scanner (Amersham).

Cell cycle analysis

Wild type and $Rad17^{5'\Delta/5'\Delta}$ cells were either mock-treated or treated with 0.75 mM hydroxyurea or 150 nM camptothecin for 12 hrs. They were washed twice with PBS and incubated in fresh medium. For BrdU/PI staining, before collection at the indicated time points, the cells were incubated with 10 μM BrdU for 5 min at 37°C, harvested

by trypsynization and fixed overnight with 70 % ethanol at 4°C (24). After the ethanol was washed away, the cells were treated with 0.1 N HCl containing 0.5 mg/ml pepsin (Merck) for 20 min at room temperature. Next, the cells were treated with 2 N HCl for 12 minutes at 37°C, followed by the addition of borate buffer (pH 8.5). The cells were washed with PBS containing 0.5 % Tween 20 and 0.1 % BSA and incubated with FITC-conjugated anti-BrdU antibodies (Becton Dickinson) for 1 hr at 4°C. After washing, the cells were counterstained with a solution containing PI (10 µg/ml) and RNAse (10 µg/ml) for 30 min at 37 °C. The cells were analyzed on a fluorescence-activated cell sorter (Becton Dickinson) using CellQuest software. For PI staining, the cells were harvested by trypsynization and fixed overnight with 70 % ethanol at 4°C. They were washed with PBS, stained with a solution containing PI (10 µg/ml) and RNase (10 µg/ml) for 30 min at 37 °C and analysed on a fluorescence-activated cell sorter (Becton Dickinson) using CellQuest software.

Measurement of relative DNA synthesis by ^{3}H- and ^{14}C-thymidine incorporation
The cells were seeded onto gelatinized 6-well plates and allowed to attach overnight. The regular medium was then replaced for 14 hrs with Ham's F10 (Biowhittaker^{TM}), supplemented with 10% fetal calf serum (Hyclone), 0.1 M non-essential amino acids (Biowhittaker^{TM}), penicillin/streptomycin, 50 µM ß-mercaptoethanol (Sigma) and 500 U/ml leukemia inhibitory factor, buffered with 20 mM Hepes-NaOH, pH 7.3. The medium contained [2-^{14}C] thymidine (0.05 µCi/ml, 1 µM; Amersham). Next, the cells were washed with PBS and incubated for 12 hrs in regular medium containing 0.75 mM hydroxyurea. The non-treated cells and the cells collected at 0 hrs after hydroxyurea release were then incubated for 1 hr in Ham's F10, supplemented with 10% fetal calf serum (Hyclone), 0.1 M non-essential amino acids (Biowhittaker^{TM}), penicillin/streptomycin, 50 µM ß-mercaptoethanol (Sigma) and 500 U/ml leukemia inhibitory factor, buffered with 20 mM Hepes-NaOH, pH 7.3 and containing [methyl-^{3}H] thymidine (2 µCi/ml, 1 µM; Amersham). The cells collected at later time points were incubated in regular medium for the indicated time, and treated with [methyl-^{3}H] thymidine-containing medium for 1 hr before collecting. The cells were washed once with ice-cold PBS and lysed in 0.2 N NaOH. Hionic-Fluor^{TM} (Perkin Elmer) was added to the lysate, and the samples were analyzed on TRI-CARB 2100TR Liquid Scintilation Analyser (Packard). The ^{3}H/^{14}C ratio represents the amount of DNA synthetized after release over the amount of DNA synthetized during unperturbed growth.

Results

***Rad17$^{5'\Delta/5'\Delta}$* cells are hypersensitive to replication stress**

We previously found that mouse ES cells expressing an N-terminally truncated Rad17 are hypersensitive to a wide spectrum of DNA damaging agents, including UV-light, ionizing radiation, mitomycin C and methyl methanesulfonate (25). The survival of *Rad17$^{5'\Delta/5'\Delta}$* cells was also severely affected by treating them with hydroxyurea, which inhibits DNA replication by depleting cellular dNTP pools. To test whether this response of *Rad17$^{5'\Delta/5'\Delta}$* cells was general to replication stress, we treated them with increasing doses of hydroxyurea, aphidicolin, camptothecin and etoposide. Aphidicolin is a

contact inhibitor of at least five DNA polymerases, including replicative polymerases α and ε (26). By inhibiting topoismerase I camptothecin induces S-phase specific DSBs, after advancing replication forks collide with and collapse at topoisomerase I-bound single-strand breaks (27). Etoposide inhibits topoisomerase II, which also leads to DSB formation during S-phase (28). Interestingly, we found that $Rad17^{5'\Delta/5'\Delta}$ cells were hypersensitive to all these agents, based on a colony forming assay (Figure 1). We conclude that $Rad17^{5'\Delta/5'\Delta}$ cells are hypersensitive to replication inhibition independent of the mechanism through which the inhibition is established.
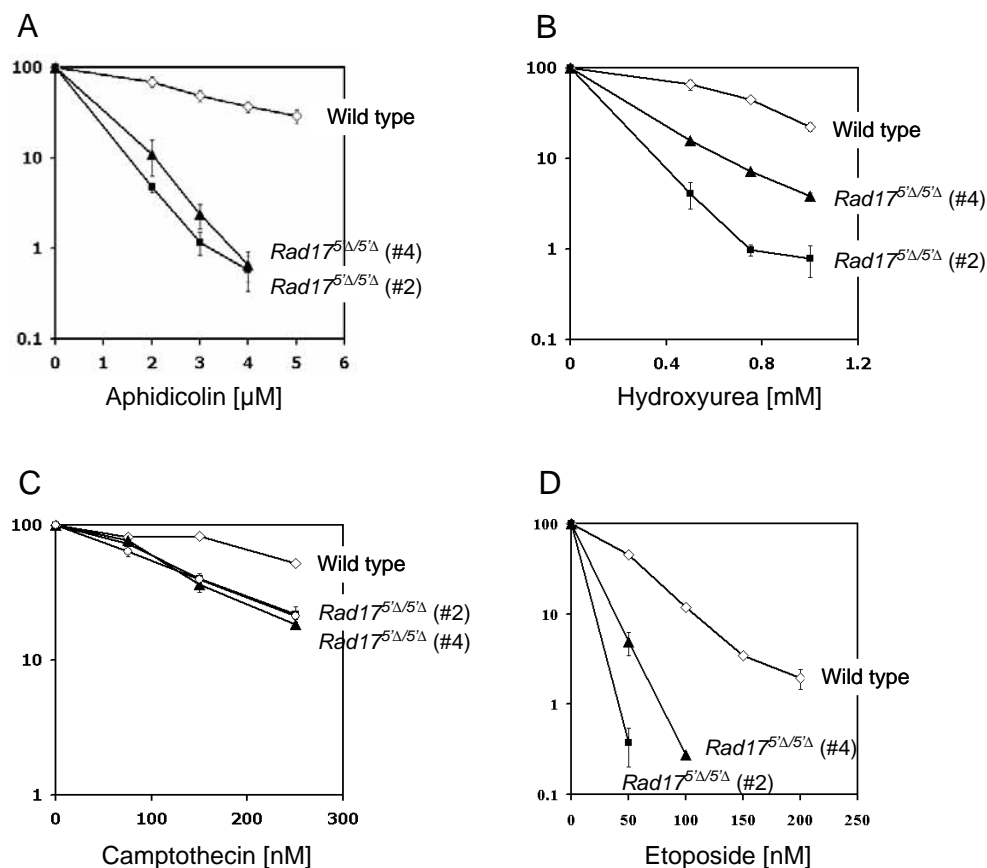
Figure 1. $Rad17^{5'\Delta/5'\Delta}$ cells are sensitive to replication inhibitors.
Wild type and independent $Rad17^{5'\Delta/5'\Delta}$ ES cell lines were treated with increasing doses of aphidicolin (A), hydroxyurea (B), camptothecin (C) and etoposide (D) for 12 hrs. The cells were incubated in fresh medium for 6-8 days, after which the colonies were fixed, stained and counted. Error bars represent standard error of the mean.

Cell cycle progression is delayed in *Rad17*$^{5'\Delta/5'\Delta}$ cells after treatment with replication inhibitors

Rad17 has been implicated in damage-induced checkpoint signaling (3,10,29). Therefore, we tested whether the Rad17 truncation affected cell cycle progression upon replication perturbation. We treated the cells with 150 nM camptothecin for 12 hrs, and allowed them to recover in fresh medium. The cells were collected at different time points and their cell cycle profiles were compared (Figure 2A). Incubation in camptothecin-containing medium resulted in the accumulation of the cells in late S-phase. Seven hrs after removing camptothecin the majority of both wild type and *Rad17*$^{5'\Delta/5'\Delta}$ cells had reached G2 phase. Interestingly, 11 hrs after drug release 15% of wild type cells were in G1 phase, while only 5-7% of *Rad17*$^{5'\Delta/5'\Delta}$ cells were in G1 (Figure 2B). A similar delay in cell cycle progression was observed in *Rad17*$^{5'\Delta/5'\Delta}$ cell lines after a 12 hrs treatment with 0.75 mM hydroxyurea and subsequent release of the cells into fresh medium (Figure 3A and data not shown), arguing that Rad17 is involved in promoting the recovery from replication inhibition.

The cell cycle profiles described above also showed that after release from replication-impeding drugs, *Rad17*$^{5'\Delta/5'\Delta}$ cells progressed through S-phase, suggesting that the restart of hydroxyurea- or camptothecin-stalled replication forks was not severely affected. To test this premise, we directly measured the relative amount of DNA synthesized at different time points after removing hydroxyurea. The cells were first incubated for 14 hrs in medium containing ^{14}C-thymidine, then treated with 0.75 mM hydroxyurea for 12 hrs and allowed to recover. Before collecting cells at different time points, they were incubated for 1 hr in ^{3}H-containing medium. The ^{3}H/^{14}C ratio represents the relative amount of DNA synthesized after hydroxyurea release. We found that three independently derived *Rad17*$^{5'\Delta/5'\Delta}$ cell lines did resume replication, although slightly slower than wild type cells, the difference being more pronounced at 12 hrs after the release. *Rad17*$^{5'\Delta/5'\Delta}$ cell line #2 was more severely delayed and until 12 hrs after release the cells did not restart replication (Fig 3B). This data suggests that the presence of truncated *Rad17* impairs replication restart to a limited extent.

Damage signaling induced by replication stress is prolonged in *Rad17*$^{5'\Delta/5'\Delta}$ cells

We have postulated (25) that the delayed entry into mitosis observed in *Rad17*$^{5'\Delta/5'\Delta}$ cells may be caused by the presence of incorrectly processed damage. To test this possibility we compared the level of hydroxyurea-induced Chk1 phosphorylation in whole cell extracts prepared from wild type and *Rad17*$^{5'\Delta/5'\Delta}$ cells (Figure 4A). We found that after 12 hrs of hydroxyurea treatment the levels of phopho-Chk1 increased in both wild type and mutant cells, but the increase was significantly higher in *Rad17*$^{5'\Delta/5'\Delta}$ cells. Six hrs after hydroxyurea was removed, Chk1 phosphorylation returned to background levels in wild type cells, while it stayed elevated for at least 12 hrs in *Rad17*$^{5'\Delta/5'\Delta}$ cells. This observation supports the notion that hydroxyurea-induced damage persists longer in *Rad17*$^{5'\Delta/5'\Delta}$ cells.
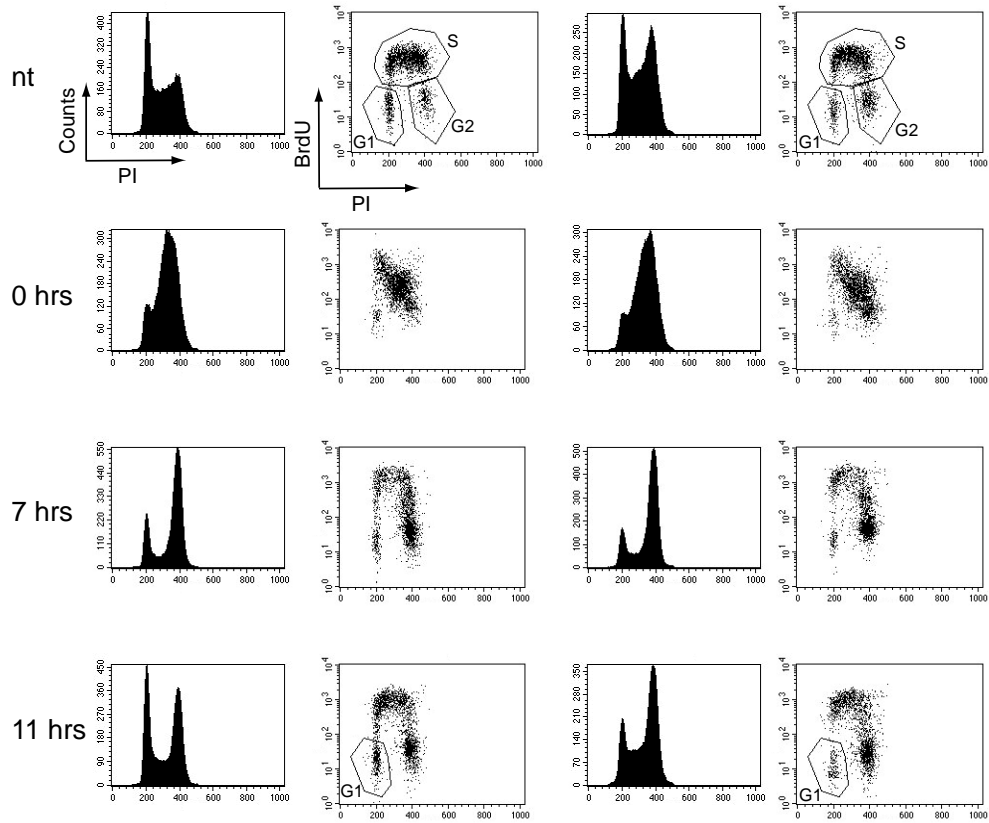
	Wild type	*Rad17*$^{5'\Delta/5'\Delta}$ (#2)	*Rad17*$^{5'\Delta/5'\Delta}$ (#3)	*Rad17*$^{5'\Delta/5'\Delta}$ (#4)
Cells in G1 phase (%)	15.3	7.3	5.2	6.9

Figure 2. Cell cycle progression of wild type and *Rad17*$^{5'\Delta/5'\Delta}$ cells after treatment with camptothecin.
(A) Wild type and *Rad17*$^{5'\Delta/5'\Delta}$ cells were treated with 150 nM camptothecin for 12 hrs, washed with PBS and incubated in fresh medium. At the indicated time points, they were pulse-labeled with BrdU and fixed. Their DNA content was determined by staining with propidium iodine (PI), and their replication status was assessed by staining with anti-BrdU antibodies. Shown are PI profiles in the panels on the left and BrdU incorporation (y-axis) versus PI-staining (x-axis) plots in the right panels. The gates in not treated samples indicate G1, S and G2 populations. (B) Number of wild type and *Rad17*$^{5'\Delta/5'\Delta}$ cells present in G1 phase 11 hrs after release from camptothecin treatment, shown as percentage of whole cell population.

Rad17$^{5'\Delta/5'\Delta}$ cells accumulate double strand breaks in response to hydroxyurea treatment

Replication forks stalled or collapsed by camptothecin or hydroxyurea can be processed in different ways (29). In one repair scenario affected forks are converted into single-ended DSBs, which in turn can serve to initiate homologous recombination repair (30). Elevated and prolonged Chk1 phosphorylation observed in *Rad17$^{5'\Delta/5'\Delta}$* cells after hydroxyurea treatment can be also explained by the presence of unrepaired damage, e.g. single stranded breaks or gaps, which can be converted into DSBs during subsequent S-phase. To test whether Rad17 truncation impairs proper processing of replication-associated damage, we analyzed the amount of DSBs induced by hydroxyurea in wild type and *Rad17$^{5'\Delta/5'\Delta}$* cells using pulsed field gel electrophoresis (PFGE). This electrophoresis method allows direct detection of broken DNA by separating intact chromosomal DNA, retained in the wells, from smaller DNA fragments, which can migrate into the gel (31). We found that 12 hrs of hydroxyurea treatment did not significantly induce DSB formation in wild type cells. In contrast, the amount of broken DNA was slightly higher in *Rad17$^{5'\Delta/5'\Delta}$* cells directly after release from hydroxyurea, gradually increased with time, and was still detectable 30 hrs after the release. We conclude that wild type Rad17 helps to prevent formation of hydroxyurea-induced DSBs.

Discussion

We have shown that murine ES cells expressing truncated Rad17 are hypersensitive to replication stress induced by treatment with hydroxyurea, aphidicolin, camptothecin and etoposide. Since Rad17 has been implicated in damage-induced checkpoint signaling in many organisms (23,32,33), it is possible that the hypersensitivity we observed is due to impaired checkpoint signaling. Such a defect could manifest itself by premature division of *Rad17$^{5'\Delta/5'\Delta}$* cells after treatment with hydroxyurea and camptothecin compared to wild type cells. However, we found that treated *Rad17$^{5'\Delta/5'\Delta}$* cells stayed longer in G2 phase, delayed cell division, and showed prolonged Chk1 phosphorylation. These results argue that, consistent with our previous observations (25), the truncation of Rad17 does not cause checkpoint dysfunction, which would result in premature entry into mitosis after DNA damage.

Figure 3. Cell cycle progression of wild type and *Rad17$^{5'\Delta/5'\Delta}$* cells after hydroxyurea treatment.
(A) Wild type and *Rad17$^{5'\Delta/5'\Delta}$* cells were treated for 12 hrs with 0.75 mM hydroxyurea, washed with PBS and incubated in fresh medium. At the indicated time points cells were fixed and their cell cycle profies were determined by PI staining. (B) Wild type and *Rad17$^{5'\Delta/5'\Delta}$* cells were incubated for 14 hrs with [2-^{14}C] thymidine-containing medium, washed with PBS and treated with 0.75 mM hydroxyurea for 12 hrs, after which the medium was refreshed. Before collecting at each time point the cells were incubated for 1hr in [methyl-^{3}H] thymidine-containing medium. The ^{3}H/^{14}C ratio represents relative DNA synthesis.
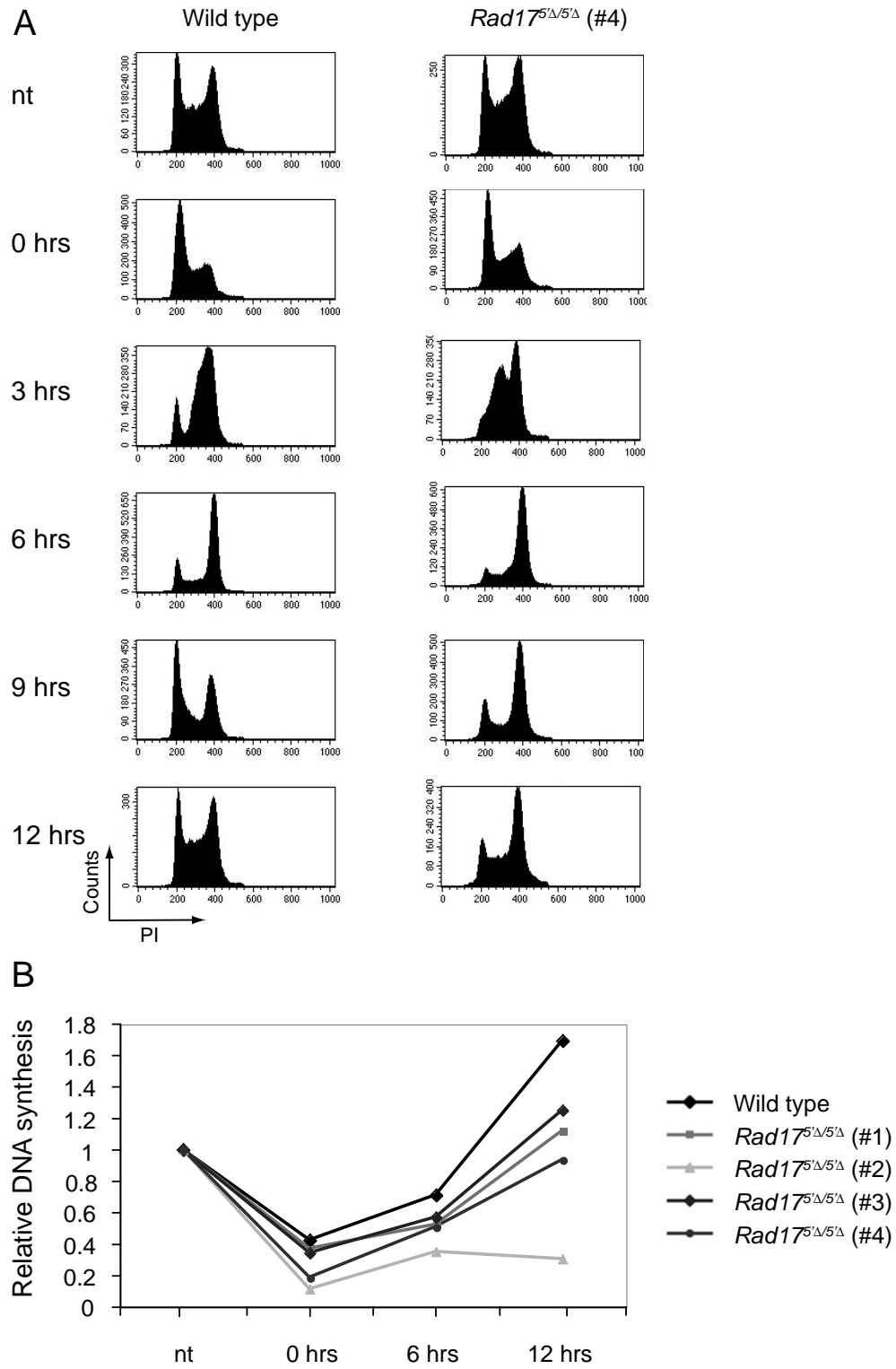
Different reasons for delayed cell cycle progression in $Rad17^{5'\Delta/5'\Delta}$ cells can be envisioned, one of them being that truncated Rad17 is able to activate checkpoint signaling more efficiently than the wild type protein, which would lead to prolonged Chk1 phosphorylation and will hold the cells longer in the G2 phase. In this case a dominant effect of the N-terminally truncated Rad17 protein would be expected. Since $Rad17^{+/5'\Delta}$ cells are not hypersensitive to DNA-damaging agents (25), we do not favor this explanation. Alternatively, Rad17 may be involved in promoting recovery from damage-induced cell cycle arrest and the truncation might impair this function.
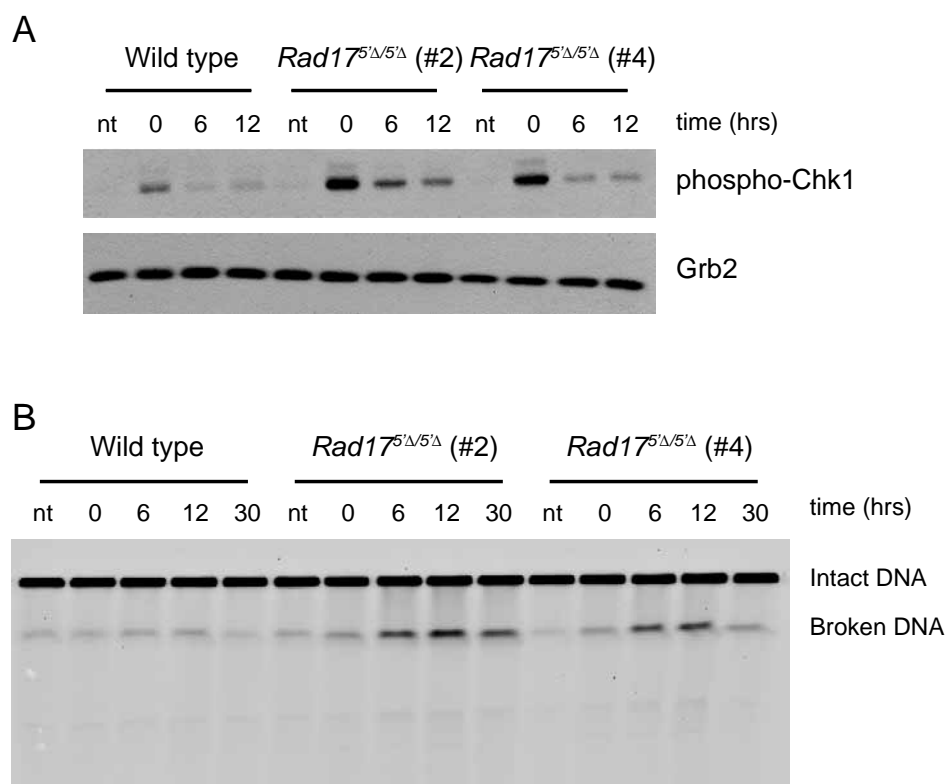
Figure 4. Prolonged damage signaling and increased DSB accumulation in Rad17 mutant cells following hydroxyurea treatment.
(A) Hydroxyurea – induced Chk1 phosphorylation. Wild type and $Rad17^{5'\Delta/5'\Delta}$ cells were treated for 12 hrs with 0.5 mM hydroxyurea and subsequently released into fresh medium. Whole cell extracts were prepared at the time of release (0 hr) and at the indicated time points and probed for phosporylated Chk1. (B) Hydroxyurea-induced DSB formation in wild type and $Rad17^{5'\Delta/5'\Delta}$ cells as analyzed by PFGE. After 12 hrs treatment with 0.5 mM hydroxyurea the cells were allowed to recover in fresh medium for the indicated time. They were fixed and lysed in agarose plugs, and their DNA was separated by size on an agarose gel. Under the electrophoresis conditions used intact genomic DNA remains in the well, while smaller DNA fragments (several Mbp to 500 kbp) migrate into the gel and are compacted into a single band.

The mechanisms controlling checkpoint recovery are not fully understood, and recent findings indicate that it is a complex and highly controlled process (34). However, the presence of physical damage i.e. the accumulation of DSBs in the hydroxyurea-treated $Rad17^{5'\Delta/5'\Delta}$ cells argues against a potential delay in checkpoint recovery and indicates that prolonged damage signaling and longer residence of $Rad17^{5'\Delta/5'\Delta}$ cells in G2 could be caused by the presence of unrepaired or incorrectly processed damage. This would imply that, in addition to its documented role in checkpoint signaling, Rad17 is more directly involved in DNA repair processes.

The sensitivity of $Rad17^{5'\Delta/5'\Delta}$ cells to replication inhibitors, as well as to all other DNA-damaging agents we tested (25) suggests that Rad17 truncation impairs a core repair/signaling event, common to distinct repair pathways. An example of such a step would be joining of DNA molecules by DNA ligase I, which is a necessary finishing step in base excision repair, nucleotide excision repair, HR, and TLS (1). Indeed, it has been reported recently that Rad17 physically interacts with DNA ligase I and stimulates its DNA joining activity (35). Strikingly, *in vitro* experiments show that the N-terminal part of Rad17 is involved in interaction with DNA ligase I (35). We can speculate that in $Rad17^{5'\Delta/5'\Delta}$ cells, expressing N-terminally truncated Rad17, this interaction might be impaired or abolished, rendering these cells hypersensitive to DNA-damaging agents due to less effective DNA ligation. However, it is also possible that the Rad17 truncation directly affects processing stalled or collapsed replication forks. Consistent with this possibility, we observed increased sensitivity of $Rad17^{5'\Delta/5'\Delta}$ cells to various replication inhibitors (Figure 1).

Two main pathways deal with hindered replication: translesion synthesis (TLS) and homologous recombination (HR) (29). DNA lesions, e.g. UV–induced pirymidine dimers, bulky adducts generated by polycyclic hydrocarbons and DNA crosslinks, can stall replicative DNA polymerases. TLS polymerases are less stringent in their template requirements and, due to their more permissive active sites and the lack of 3'-5' exonuclease activity, they are able to copy damaged DNA and therefore help overcoming replication blocks. However, TLS increases mutation frequency, since translesion polymerases are often error-prone (36,37). It is therefore essential that their access to replication forks is strictly controlled. It has recently become clear that TLS polymerases have increased affinity for monoubiquitinated PCNA, and that this PCNA modification acts as a switch between translesion and replicative polymerases (38,39). Rad17 is homologous to Rfc1, a subunit of PCNA clamp loader, and the 9-1-1 complex is structurally similar to PCNA (12,40). It is therefore tempting to speculate that, in addition to its role in checkpoint signaling, wild type Rad17 could be a part of an alternative clamp loader, that could also promote lesion bypass by recruiting translesion DNA polymerases. The N-terminal truncation of Rad17 could interfere with this putative clamp loading process and render the $Rad17^{5'\Delta/5'\Delta}$ cells hypersensitive to DNA-damaging agents. However, there is very limited evidence for Rad17 being directly involved in TLS (41,42). Moreover, the replication-impeding drugs used in this study generate mainly DSBs and single-stranded regions, breaks and gaps (26-28), and such damage is more likely to be dealt with by HR than by the translesion machinery.

In the process of HR genetic information blocked by a DNA lesion is retrieved from the undamaged sister chromatid. HR is needed to overcome spontaneously occurring replication problems and, consistently with such a vital role, it is essential for viability of mammalian cells (43). Many models for HR-mediated
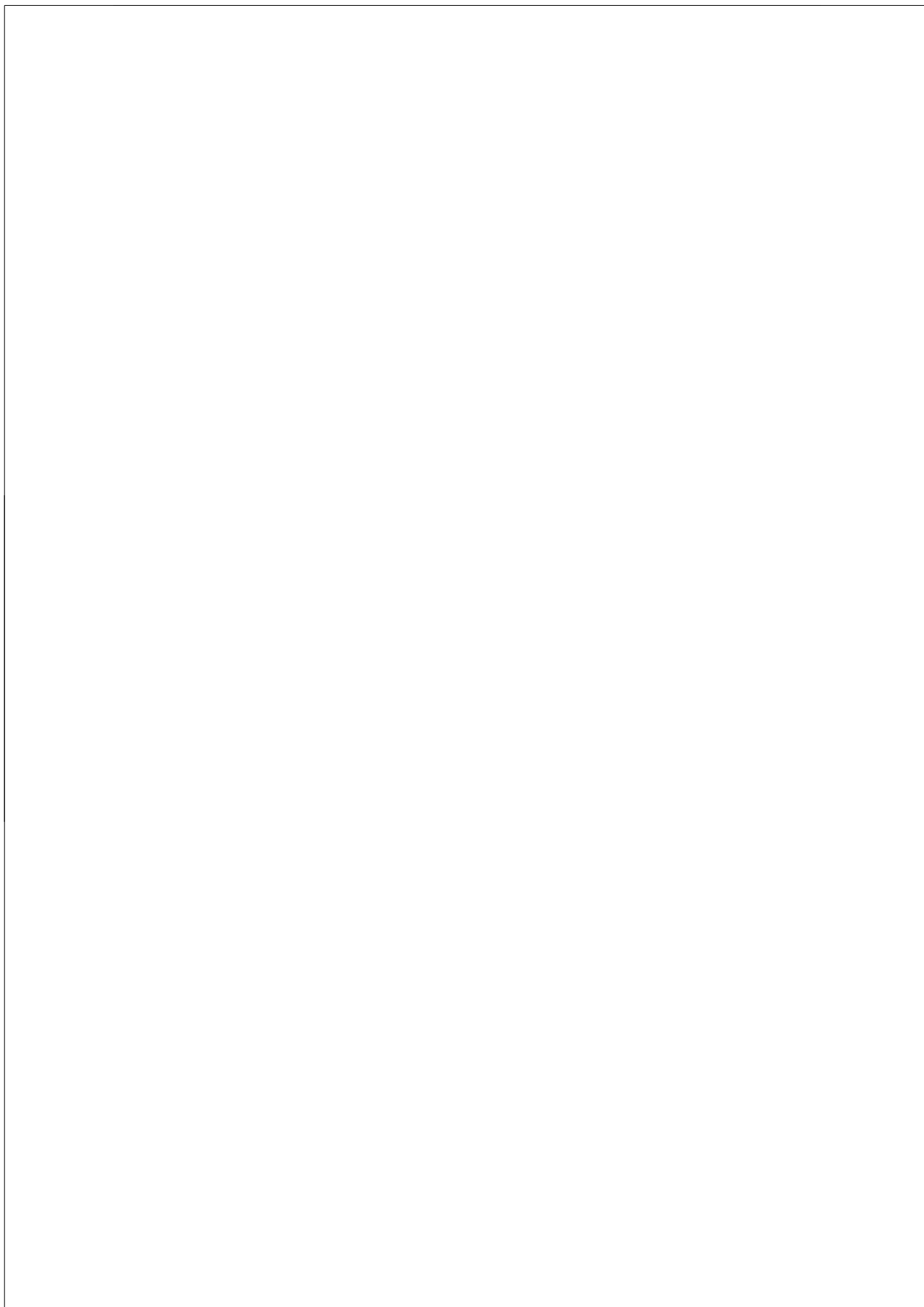
restart of stalled or collapsed replication forks have been proposed (30), but neither the exact mechanisms, nor the regulation of this process are fully understood. The data presented above and the significant reduction of homologous gene targeting in $Rad17^{5'\Delta/5'\Delta}$ cells that we have reported before (25) suggests that Rad17 might be involved in at least some scenarios of HR-mediated replication restart. However, we can only speculate which step of this process/these processes is affected by the truncation of Rad17. Based on the involvement of Rad17 in checkpoint signaling, Rad17 could play a regulatory role in HR, coordinating the signal from stalled replication forks with activating the HR machinery. Rad17 could also participate more directly in recombination processes. Translesion polymerase eta, in addition to its function in TLS, is involved in extending D-loop structures formed after strand invasion during HR (44,45). The requirement for pol eta in this process can be explained by difficulties replicative polymerases might have in starting DNA synthesis from a D-loop, which is structurally different from a regular primer/template junction. Based on its homology to Rfc1, Rad17 may be involved in loading pol eta or other yet unknown polymerase onto the invading strand, and thus promoting the DNA synthesis step of HR.

References

1.   Hoeijmakers, J.H. (2001) Genome maintenance mechanisms for preventing cancer. *Nature*, **411**, 366-374.
2.   Dronkert, M.L. and Kanaar, R. (2001) Repair of DNA interstrand cross-links. *Mutat Res*, **486**, 217-247.
3.   Abraham, R.T. (2001) Cell cycle checkpoint signaling through the ATM and ATR kinases. *Genes Dev*, **15**, 2177-2196.
4.   Paulovich, A.G. and Hartwell, L.H. (1995) A checkpoint regulates the rate of progression through S phase in S. cerevisiae in response to DNA damage. *Cell*, **82**, 841-847.
5.   Santocanale, C. and Diffley, J.F. (1998) A Mec1- and Rad53-dependent checkpoint controls late-firing origins of DNA replication. *Nature*, **395**, 615-618.
6.   Branzei, D. and Foiani, M. (2006) The Rad53 signal transduction pathway: Replication fork stabilization, DNA repair, and adaptation. *Exp Cell Res*, **312**, 2654-2659.
7.   Heffernan, T.P., Simpson, D.A., Frank, A.R., Heinloth, A.N., Paules, R.S., Cordeiro-Stone, M. and Kaufmann, W.K. (2002) An ATR- and Chk1-dependent S checkpoint inhibits replicon initiation following UVC-induced DNA damage. *Mol Cell Biol*, **22**, 8552-8561.
8.   Smits, V.A. and Medema, R.H. (2001) Checking out the G(2)/M transition. *Biochim Biophys Acta*, **1519**, 1-12.
9.   Nurse, P. (1994) Ordering S phase and M phase in the cell cycle. *Cell*, **79**, 547-550.
10.   Shiloh, Y. (2001) ATM and ATR: networking cellular responses to DNA damage. *Curr Opin Genet Dev*, **11**, 71-77.
11.   Zou, L. and Elledge, S.J. (2003) Sensing DNA damage through ATRIP recognition of RPA-ssDNA complexes. *Science*, **300**, 1542-1548.
12.   Majka, J. and Burgers, P.M. (2004) The PCNA-RFC families of DNA clamps and clamp loaders. *Prog Nucleic Acid Res Mol Biol*, **78**, 227-260.
13.   St Onge, R.P., Udell, C.M., Casselman, R. and Davey, S. (1999) The human G2 checkpoint control protein hRAD9 is a nuclear phosphoprotein that forms complexes with hRAD1 and hHUS1. *Mol Biol Cell*, **10**, 1985-1995.
14.   Majka, J., Binz, S.K., Wold, M.S. and Burgers, P.M. (2006) Replication protein A directs loading of the DNA damage checkpoint clamp to 5'-DNA junctions. *J Biol Chem*, **281**, 27855-27861.

15. Venclovas, C. and Thelen, M.P. (2000) Structure-based predictions of Rad1, Rad9, Hus1 and Rad17 participation in sliding clamp and clamp-loading complexes. *Nucleic Acids Res*, **28**, 2481-2493.

16. Wang, X., Zou, L., Lu, T., Bao, S., Hurov, K.E., Hittelman, W.N., Elledge, S.J. and Li, L. (2006) Rad17 phosphorylation is required for claspin recruitment and Chk1 activation in response to replication stress. *Mol Cell*, **23**, 331-341.

17. Zou, L., Cortez, D. and Elledge, S.J. (2002) Regulation of ATR substrate selection by Rad17-dependent loading of Rad9 complexes onto chromatin. *Genes Dev*, **16**, 198-208.

18. Chen, Y. and Sanchez, Y. (2004) Chk1 in the DNA damage response: conserved roles from yeasts to mammals. *DNA Repair (Amst)*, **3**, 1025-1032.

19. Osborn, A.J., Elledge, S.J. and Zou, L. (2002) Checking on the fork: the DNA-replication stress-response pathway. *Trends Cell Biol*, **12**, 509-516.

20. Bartek, J. and Lukas, J. (2003) Chk1 and Chk2 kinases in checkpoint control and cancer. *Cancer Cell*, **3**, 421-429.

21. Molinari, M. (2000) Cell cycle checkpoints and their inactivation in human cancer. *Cell Prolif*, **33**, 261-274.

22. Kastan, M.B. and Bartek, J. (2004) Cell-cycle checkpoints and cancer. *Nature*, **432**, 316-323.

23. Wang, X., Zou, L., Zheng, H., Wei, Q., Elledge, S.J. and Li, L. (2003) Genomic instability and endoreduplication triggered by RAD17 deletion. *Genes Dev*, **17**, 965-970.

24. Medema, R.H., Klompmaker, R., Smits, V.A. and Rijksen, G. (1998) p21waf1 can block cells at two points in the cell cycle, but does not interfere with processive DNA-replication or stress-activated kinases. *Oncogene*, **16**, 431-441.

25. Budzowska, M., Jaspers, I., Essers, J., de Waard, H., van Drunen, E., Hanada, K., Beverloo, B., Hendriks, R.W., de Klein, A., Kanaar, R. *et al.* (2004) Mutation of the mouse Rad17 gene leads to embryonic lethality and reveals a role in DNA damage-dependent recombination. *Embo J*, **23**, 3548-3558.

26. Dimitrova, D.S. and Gilbert, D.M. (2000) Temporally coordinated assembly and disassembly of replication factories in the absence of DNA synthesis. *Nat Cell Biol*, **2**, 686-694.

27. Pommier, Y. (2006) Topoisomerase I inhibitors: camptothecins and beyond. *Nat Rev Cancer*, **6**, 789-802.

28. Baldwin, E.L. and Osheroff, N. (2005) Etoposide, topoisomerase II and cancer. *Curr Med Chem Anticancer Agents*, **5**, 363-372.

29. Andreassen, P.R., Ho, G.P. and D'Andrea, A.D. (2006) DNA damage responses and their many interactions with the replication fork. *Carcinogenesis*, **27**, 883-892.

30. Helleday, T. (2003) Pathways for mitotic homologous recombination in mammalian cells. *Mutat Res*, **532**, 103-115.

31. Hanada, K., Budzowska, M., Modesti, M., Maas, A., Wyman, C., Essers, J. and Kanaar, R. (2006) The structure-specific endonuclease Mus81-Eme1 promotes conversion of interstrand DNA crosslinks into double-strands breaks. *Embo J*, **25**, 4921-4932.

32. Kobayashi, M., Hirano, A., Kumano, T., Xiang, S.L., Mihara, K., Haseda, Y., Matsui, O., Shimizu, H. and Yamamoto, K. (2004) Critical role for chicken Rad17 and Rad9 in the cellular response to DNA damage and stalled DNA replication. *Genes Cells*, **9**, 291-303.

33. Griffiths, D.J., Barbet, N.C., McCready, S., Lehmann, A.R. and Carr, A.M. (1995) Fission yeast rad17: a homologue of budding yeast RAD24 that shares regions of sequence similarity with DNA polymerase accessory proteins. *Embo J*, **14**, 5812-5823.

34. Gewurz, B.E. and Harper, J.W. (2006) DNA-damage control: Claspin destruction turns off the checkpoint. *Curr Biol*, **16**, R932-934.

35.   Song, W., Levin, D.S., Varkey, J., Post, S., Bermudez, V.P., Hurwitz, J. and Tomkinson, A.E. (2007) A conserved physical and functional interaction between the cell cycle checkpoint clamp loader and DNA ligase I of eukaryotes. *J Biol Chem*, **282**, 22721-22730.

36.   Ohmori, H., Friedberg, E.C., Fuchs, R.P., Goodman, M.F., Hanaoka, F., Hinkle, D., Kunkel, T.A., Lawrence, C.W., Livneh, Z., Nohmi, T. *et al.* (2001) The Y-family of DNA polymerases. *Mol Cell*, **8**, 7-8.

37.   Prakash, S., Johnson, R.E. and Prakash, L. (2005) Eukaryotic translesion synthesis DNA polymerases: specificity of structure and function. *Annu Rev Biochem*, **74**, 317-353.

38.   Watanabe, K., Tateishi, S., Kawasuji, M., Tsurimoto, T., Inoue, H. and Yamaizumi, M. (2004) Rad18 guides poleta to replication stalling sites through physical interaction and PCNA monoubiquitination. *Embo J*, **23**, 3886-3896.

39.   Kannouche, P.L., Wing, J. and Lehmann, A.R. (2004) Interaction of human DNA polymerase eta with monoubiquitinated PCNA: a possible mechanism for the polymerase switch in response to DNA damage. *Mol Cell*, **14**, 491-500.

40.   Caspari, T., Dahlen, M., Kanter-Smoler, G., Lindsay, H.D., Hofmann, K., Papadimitriou, K., Sunnerhagen, P. and Carr, A.M. (2000) Characterization of Schizosaccharomyces pombe Hus1: a PCNA-related protein that associates with Rad1 and Rad9. *Mol Cell Biol*, **20**, 1254-1262.

41.   Kai, M. and Wang, T.S. (2003) Checkpoint activation regulates mutagenic translesion synthesis. *Genes Dev*, **17**, 64-76.

42.   Sabbioneda, S., Minesinger, B.K., Giannattasio, M., Plevani, P., Muzi-Falconi, M. and Jinks-Robertson, S. (2005) The 9-1-1 checkpoint clamp physically interacts with polzeta and is partially required for spontaneous polzeta-dependent mutagenesis in Saccharomyces cerevisiae. *J Biol Chem*, **280**, 38657-38665.

43.   Cox, M.M. (2002) The nonmutagenic repair of broken replication forks via recombination. *Mutat Res*, **510**, 107-120.

44.   McIlwraith, M.J., Vaisman, A., Liu, Y., Fanning, E., Woodgate, R. and West, S.C. (2005) Human DNA polymerase eta promotes DNA synthesis from strand invasion intermediates of homologous recombination. *Mol Cell*, **20**, 783-792.

45.   Kawamoto, T., Araki, K., Sonoda, E., Yamashita, Y.M., Harada, K., Kikuchi, K., Masutani, C., Hanaoka, F., Nozaki, K., Hashimoto, N. *et al.* (2005) Dual roles for DNA polymerase eta in homologous DNA recombination and translesion DNA synthesis. *Mol Cell*, **20**, 793-799.

Chapter 4

The structure-specific endonuclease

Mus81-Eme1

promotes conversion of interstrand

DNA crosslinks into DSBs

The structure-specific endonuclease Mus81–Eme1 promotes conversion of interstrand DNA crosslinks into double-strands breaks

Katsuhiro Hanada[1,3], Magda Budzowska[1,3], Mauro Modesti[1], Alex Maas[1], Claire Wyman[1,2], Jeroen Essers[1,2] and Roland Kanaar[1,2,*]

[1]Department of Cell Biology & Genetics, Erasmus MC, Rotterdam, The Netherlands and [2]Department of Radiation Oncology, Erasmus MC, Rotterdam, The Netherlands

Repair of interstrand crosslinks (ICLs) requires multiple-strand incisions to separate the two covalently attached strands of DNA. It is unclear how these incisions are generated. DNA double-strand breaks (DSBs) have been identified as intermediates in ICL repair, but enzymes responsible for producing these intermediates are unknown. Here we show that Mus81, a component of the Mus81–Eme1 structure-specific endonuclease, is involved in generating the ICL-induced DSBs in mouse embryonic stem (ES) cells in S phase. Given the DNA junction cleavage specificity of Mus81–Eme1 *in vitro*, DNA damage-stalled replication forks are suitable *in vivo* substrates. Interestingly, generation of DSBs from replication forks stalled due to DNA damage that affects only one of the two DNA strands did not require Mus81. Furthermore, in addition to a physical interaction between Mus81 and the homologous recombination protein Rad54, we show that *Mus81*$^{-/-}$ *Rad54*$^{-/-}$ ES cells were as hypersensitive to ICL agents as *Mus81*$^{-/-}$ cells. We propose that Mus81–Eme1- and Rad54-mediated homologous recombination are involved in the same DNA replication-dependent ICL repair pathway.

Introduction

A DNA interstrand crosslink (ICL) covalently connects the two complementary strands of the DNA double helix, thereby blocking important DNA transactions, such as transcription and replication, that require unwinding of the two DNA strands. Because they cause such a dramatic block to acces-

*Corresponding author. Department of Cell Biology & Genetics, Erasmus University, Medical Genetics Center, Erasmus MC, PO Box 2040, 3000 CA Rotterdam, The Netherlands. Tel.: +31 10 408 7186; Fax: +31 10 408 9468; E-mail: r.kanaar@erasmusmc.nl
[3]These authors contributed equally to this work

sing genetic information, ICL-inducing agents are extremely cytotoxic (Dronkert and Kanaar, 2001). ICL-inducing agents, such as mitomycin C, nitrogen mustards, platinum compounds and psoralens, are more cytotoxic to proliferating cells compared to nondividing cells and therefore they are widely used in chemo- and phototherapy of cancers and skin diseases.

Owing to the nature of ICLs, mechanism(s) for their repair are complex. ICLs damage both DNA strands at the same, or very close, nucleotide positions. Therefore, repair mechanisms involving a simple excision followed by templated resynthesis are not sufficient. In *Escherichia coli* and *Saccharomyces cerevisiae*, ICL repair requires nucleotide excision repair (NER), homologous recombination and translesion DNA synthesis (Dronkert and Kanaar, 2001; McHugh *et al*, 2001). In these organisms, NER seems to be involved in generating the incision(s) near the ICL. Homologous recombination on the other hand has several roles in ICL repair (Dronkert and Kanaar, 2001). One important role for homologous recombination is the repair of DNA double-strand breaks (DSBs), which can result from ICL processing in *S. cerevisiae* cells (McHugh *et al*, 2001). Another role, documented for *E. coli* RecA-mediated homologous recombination *in vitro*, is the generation of the substrate for a second round of strand incisions by NER enzymes (Cheng *et al*, 1991). Alternative roles proposed for homologous recombination repair or homology-directed repair in ICL repair include mechanisms involving break-induced replication, single-strand annealing or the generation of substrates for translesion DNA synthesis (Dronkert and Kanaar, 2001; Niedernhofer *et al*, 2005).

In vertebrate cells, homologous recombination and translesion DNA synthesis are involved in ICL repair as well (Dronkert and Kanaar, 2001). However, an interesting difference between *S. cerevisiae* and higher eukaryotes is the role of the NER proteins in ICL repair. Most, if not all, NER proteins in *S. cerevisiae* cells are involved in ICL repair as deduced from the ICL hypersensitivity of the respective mutants. By contrast, in mammalian cells, mutations in *XPF* and *ERCC1* confer extreme ICL sensitivity, but mutations in other genes essential for NER, including *XPA*, *XPG* and *CSB*, are not dramatically ICL hypersensitive (Dronkert and Kanaar, 2001; De Silva *et al*, 2002). This suggests that XPF-ERCC1, a heterodimeric structure-specific endonuclease (de Laat *et al*, 1998), plays a central role in ICL repair that is largely independent of NER. In addition to an NER-independent role in ICL repair, XPF-ERCC1 functions in at least two subpathways of homology-directed DNA repair. Both in *S. cerevisiae* and mammalian cells, XPF-ERCC1 is involved in DSB repair, through single-strand annealing, and in homologous gene targeting (Paques and Haber, 1999; Adair *et al*, 2000; Sargent *et al*, 2000; Niedernhofer *et al*, 2001; Langston and Symington, 2005).

Unraveling the mechanism(s) of ICL repair requires answers to two central questions; what are the intermediates in ICL repair at the DNA level and how are they generated? Recently, it has become clear that one pivotal intermediate that can arise during the repair of an ICL is a DSB (Akkari *et al*, 2000; De Silva *et al*, 2000; Niedernhofer *et al*, 2004; Rothfuss and Grompe, 2004). The formation of this DSB intermediate requires DNA replication, suggesting that a stalled replication forks at the site of the ICL is recognized and processed by a structure-specific endonuclease into a DSB. Owing to the ICL hypersensitivity of cells mutated in the XPF–ERCC1 complex and the biochemical properties of this complex, it has been suggested that XPF–ERCC1 would convert ICLs to DSBs. However, recent studies have demonstrated that this conversion is XPF–ERCC1 independent (De Silva *et al*, 2000; Niedernhofer *et al*, 2004), thus leaving the question of how DSBs are generated from ICLs partially unanswered.

Recently, a structure-specific endonuclease, Mus81–Eme1, with amino-acid sequence similarity to XPF-ERCC1 has been identified in yeast and mammalian cells (Heyer, 2004). In yeast, *mus81* mutants exhibit sensitivity to hydroxyurea, UV-light and methyl methanesulfonate but not to ionizing radiation (Interthal and Heyer, 2000; Doe and Whitby, 2004; Doe *et al*, 2004). This sensitivity profile is consistent with a role for Mus81–Eme1 in processing stalled DNA replication forks. The biochemical properties of the enzyme complex are also consistent with its involvement in forming DSBs at DNA structures resembling replication forks. Like XPF–ERCC1, Mus81–Eme1 also cleaves branched DNA structures (Boddy *et al*, 2001; Chen *et al*, 2001; Constantinou *et al*, 2002; Kaliraman *et al*, 2001; Ciccia *et al*, 2003; Ogrunc and Sancar, 2003; Whitby *et al*, 2003). However, XPF–ERCC1 prefers three-way branched junctions containing two single-stranded DNA arms, whereas Mus81–Eme1 has a preference for three-way junctions that are more double-stranded in nature, such as 3′-flap and replication fork-like structures (Heyer, 2004). *Mus81* and *Eme1* mutant embryonic stem (ES) cells, which have recently become available, display hypersensitivity to ICL-inducing agents such as mitomycin C and cisplatin (Abraham *et al*, 2003; McPherson *et al*, 2004).

Results

Mus81 is involved in processing ICLs into DSBs

To test whether the Mus81–Eme1 structure-specific endonuclease is involved in processing ICLs into DSBs, we first constructed mouse ES cells lacking Mus81 (Supplementary Figure 1). Next, we analyzed ICL-induced DSB formation in Mus81-proficient and -deficient ES cells. Proliferating ES cells were treated with different doses of mitomycin C for 24 h and ICL-induced DSBs were detected using PFGE (Figure 1A). As we previously demonstrated, mitomycin C treatment resulted in an increase in broken DNA in wild-type ES cells (Niedernhofer *et al*, 2004). The increase was dose dependent (Figure 1A) and was not owing to DNA fragmentation during apoptosis (Supplementary Figure 2). In ES cells lacking ERCC1, mitomycin C-induced DSBs were observed (Figure 1A). However, cells lacking Mus81 mitomycin C failed to induce DSBs, even at the highest dose of mitomycin C used (Figure 1A). Similarly, in response to another ICL-inducing agent, cisplatin, wild-type ES cells showed a dose-dependent

increase in broken DNA that was not observed in *Mus81*$^{-/-}$ ES cells (Figure 2A). We conclude that the structure-specific endonuclease Mus81–Eme1 is involved in processing ICLs into DSBs.

Mus81 operates in S phase

Given the biochemical activity of Mus81–Eme1 on splayed arm DNA substrates and the lack of mitomycin C-induced DSBs in *Mus81*$^{-/-}$, the role of Mus81–Eme1 in ICL repair is likely the conversion of ICL-stalled replication forks into DSBs. Thus, Mus81–Eme1 would function during S phase. Consistent with this notion, culturing the cells in the continuous presence of mitomycin C or cisplatin resulted in their accumulation in S phase (Figures 1B and 2C, respectively). If Mus81–Eme1 acts in S phase on stalled replication forks, then the induction of DSBs by mitomycin C should be slow, in contrast to DSB induction by agents that directly act on DNA such as ionizing radiation. Indeed, in wild-type ES cells cultured in the presence of 1.0 μg/ml mitomycin C, DSB induction became apparent after around 12–18 h and subsequently increased over time (Figure 1C). Again, no DSBs were induced in *Mus81*$^{-/-}$ cells, even after 30 h of incubation with mitomycin C.

If Mus81–Eme1 functions on ICL-stalled replication forks, then active replication would be required to detect Mus81-dependent, ICL-dependent DSBs. To test this premise, we blocked replication by the addition of thymidine, which resulted in accumulation of the cells in S phase (Figure 3A and B). When mitomycin C was added, no increase in DSBs was detected, either in wild-type or *Mus81*$^{-/-}$ ES cells (Figure 3C). In normal growth conditions, without added thymidine to block replication, Mus81-dependent DSBs were detected upon the addition of mitomycin C. Furthermore, when cells treated with mitomycin C, under conditions of thymidine-blocked replication (Figure 4A), were allowed to resume replication by incubating them in media lacking thymidine and mitomycin C, Mus81-dependent DSBs were detected (Figure 4C, compare lanes 7 and 14). Based on the results of the PFGE analysis, the cell cycle analysis and the hypersensitivity of *Mus81*$^{-/-}$ cells to both mitomycin C and cisplatin (Figures 2B and 7C, respectively), we conclude that Mus81–Eme1 is involved in DSB formation when DNA replication forks are blocked by an ICL.

In the experiments described above, the cells were continuously incubated in the presence of mitomycin C. This resulted in accumulation of the cells in S phase (Figure 1B) and allowed us to observe the involvement of Mus81 in converting ICLs to DSBs. In contrast, when cells were incubated for 1 h in the presence of mitomycin C and subsequently placed in fresh media without mitomycin C, the cells did not accumulate in S phase, irrespective of their genotype (Figure 5A). Instead, 12 h after the mitomycin C pulse most cells were in late S phase, whereas G2, G1 and early S phase cells were detected by 36 h. Under these conditions, DNA breaks were observed in both wild-type and *Mus81*$^{-/-}$ ES cells (Figure 5B).

Mus81-mediated DSB formation is DNA lesion selective

Next, we asked whether Mus81–Eme1 is required, in general, to produce DSBs under conditions where DNA damage leads to replication fork stalling. Therefore, instead of using mitomycin C, UV light was used to stall replication through DNA
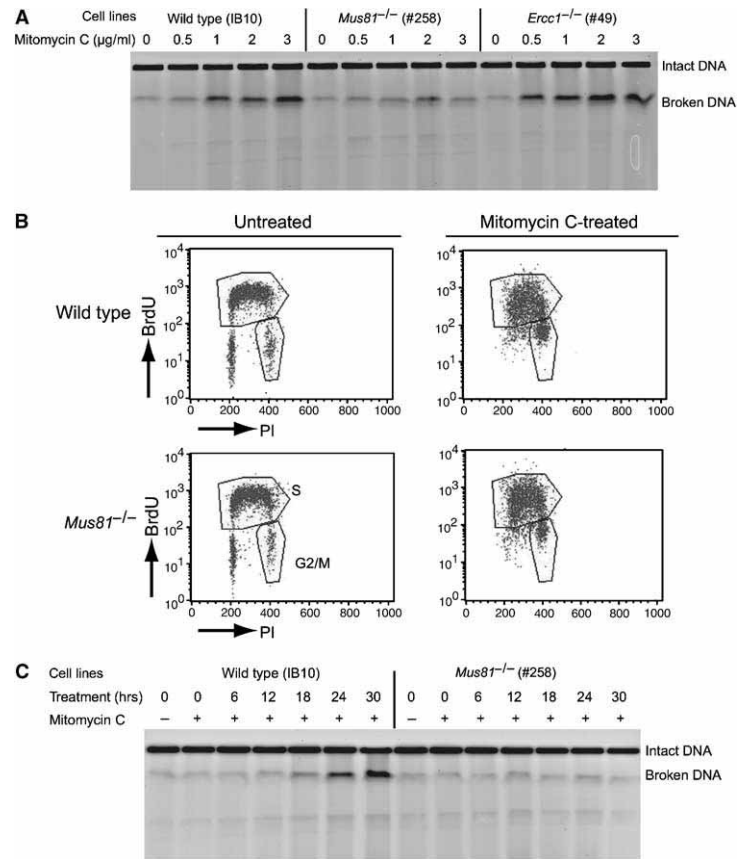
Figure 1 Analysis of mitomycin C-induced DSB formation in wild-type, $Ercc1^{-/-}$ and $Mus81^{-/-}$ ES cells. (**A**) Using PFGE, DSB formation was analyzed. Cells of the indicated genotype were treated with increasing concentrations of mitomycin C for 24 h, collected into agarose plugs and their DNA was separated by size on an agarose gel. Under the electrophoresis conditions used, high molecular weight genomic DNA remains in the well, whereas lower molecular weight DNA fragments (several Mbp to 500 kbp) migrate into the gel and are compacted into a single band. (**B**) Cell cycle profiles of wild-type and $Mus81^{-/-}$ ES cells after continuous treatment with mitomycin C for 24 h. Using a FACscan, the cell cycle profile of cells pulse labeled with BrdU was analyzed by total DNA content as determined by propidium iodide (PI) staining (x-axis) and replication status as determined by BrdU incorporation (y-axis). Cells were either untreated or incubated with 2.0 μg/ml mitomycin C. (**C**) Time course of mitomycin C-induced DSB formation in wild-type and $Mus81^{-/-}$ ES cells. Cells were treated with 1.0 μg/ml mitomycin C, indicated by (+). The untreated control sample is indicated by (−).

damage induction (Courcelle and Hanawalt, 2001; Branzei and Foiani, 2005). Wild-type, $Mus81^{+/-}$ and $Mus81^{-/-}$ ES cells were treated with increasing doses of UV light and the cells were analyzed for DSB formation after 4 h. After the treatment, the cells accumulated in S phase, just as was observed after treatment with the ICL-inducing agents (Figure 6C). A dose-dependent increase in broken DNA was observed, irrespective of whether Mus81 was functional (Figure 6A). Consistent with this observation, Mus81 was not required for cell survival in response to UV-light treatment (Figure 6B). By contrast, $Mus81^{-/-}$ cells were hypersensitive to ICL-inducing agents (Figures 2B and 7C, and McPherson et al, 2004; Dendouga et al, 2005). We conclude

that not all stalled replication forks are equivalent and that the replication fork cleavage activity of Mus81–Eme1 depends on the lesion that causes the stalling.

Physical and genetic interactions between Mus81 and Rad54

A one ended-DSB such as generated by Mus81–Eme1 from stalled replication forks is an ideal substrate for the initiation of homologous recombination as a next step in ICL repair. Consistent with this notion we observed a reduction of mitomcyin C-induced sister chromatid exchanges (SCEs) in $Mus81^{-/-}$ cells compared to wild-type ES cells. Wild-type cells treated with 0.2 μg/ml mitomycin C displayed 40.8 ± 4.0
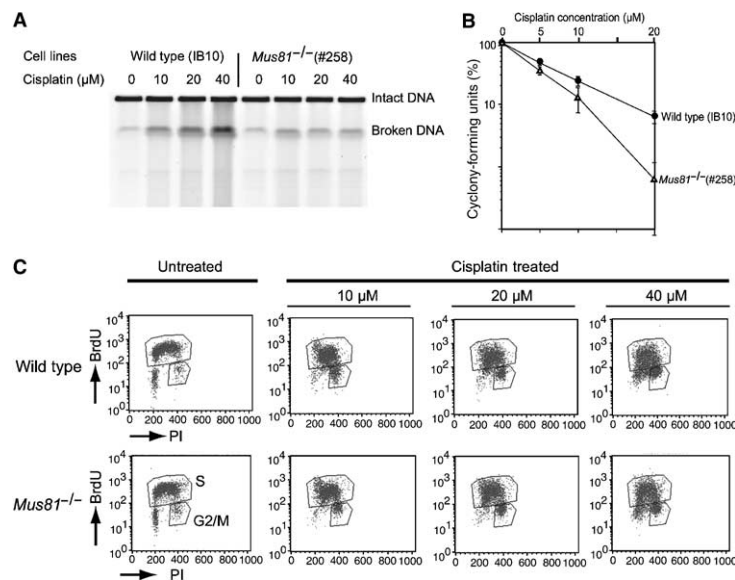
Figure 2 Analysis of cisplatin-induced DSB formation in wild-type and *Mus81*$^{-/-}$ ES cells. (**A**) Cells of the indicated genotype were treated with increasing concentrations of cisplatin for 24 h and their DNA was analyzed by PFGE. (**B**) Clonogenic survival curve of wild-type and *Mus81*$^{-/-}$ ES cells in response to increasing doses of cisplatin. (**C**) Cell cycle profiles of wild-type and *Mus81*$^{-/-}$ ES cells after continuous treatment with increasing doses of cisplatin for 24 h. Bi-parameter (BrdU and PI) FACscan plots are shown.

SCE per metaphase, whereas *Mus81*$^{-/-}$ cells showed 31.5 ± 1.9 SCE per metaphase. Interestingly, the spontaneous level of SCEs was already slightly, but significantly ($P < 0.01$) reduced in *Mus81*$^{-/-}$ cells compared to wild type from 9.9 ± 0.8 to 7.2 ± 0.5 SCEs per metaphase. Possibly, repair of replication forks stalled due to endogenous DNA damage is less likely to proceed through a DSB intermediate in the absence of Mus81.

In addition to reduced mitomycin C-induced SCEs level in *Mus81*$^{-/-}$ ES cells, evidence for a link between Mus81 and homologous recombination is also provided by the interaction between *S. cerevisiae* Mus81 and the homologous recombination protein Rad54 in a two-hybrid assay and in co-immunoprecipitation experiments (Interthal and Heyer, 2000). We asked whether a physical and genetic interaction exists between mouse Mus81–Eme1 and Rad54. Whole-cell extracts were prepared from an ES cell line that carries a Rad54 knockout allele and an HA-tagged Rad54 knock-in allele, which expresses HA-tagged and fully functional Rad54 protein from the endogenous promoter (Tan *et al*, 1999). HA-tagged Rad54 protein was precipitated with immobilized anti-HA antibodies. Immunoblotting of the precipitated samples was used to detect the presence of Mus81, the HA epitope and Rad54 (Figure 7A and B). Co-immunoprecipitation of Mus81 with Rad54 was detected. In contrast, Mus81 was not detected when the precipitation was performed using extracts prepared from an isogenic ES cell line in which HA-tagged Rad54 was absent. The interaction is likely protein-mediated, because DNA in the extracts was digested with DNase I before the immunoprecipitation.

The physical interaction between Mus81–Eme1 and Rad54 is consistent with a function of these proteins in the same ICL repair pathway. The DNA intermediate from which homologous recombination during ICL repair would be initiated is the DSB generated by Mus81–Eme1. Therefore, inactivating mutations in *Mus81* should be epistatic to mutations in *Rad54* in the context of ICL repair. To test this premise, we generated *Mus81*$^{-/-}$ *Rad54*$^{-/-}$ double knockout ES cells and compared their degree of mitomycin C sensitivity to that of either of the single mutants. *Rad54*$^{-/-}$ ES cells were about three-fold more sensitive to mitomycin C than wild-type ES cells (Figure 7C and Essers *et al*, 1997). The *Mus81*$^{-/-}$ ES cells displayed a seven-fold increase in mitomycin C sensitivity. The *Mus81*$^{-/-}$ *Rad54*$^{-/-}$ double knockout ES cells were as sensitive to mitomycin C as the *Mus81*$^{-/-}$ cells (Figure 7C). We conclude that *Mus81* is epistatic to Rad54 with respect to repair of ICLs. Consistent with this notion, mitomycin C-induced DSBs were observed in *Rad54*$^{-/-}$ ES cells, but not in *Mus81*$^{-/-}$ *Rad54*$^{-/-}$ ES cells (Figure 7D).

Discussion

A DNA ICL covalently links both strands of the DNA double helix and thus its repair requires incisions not only on both sides of the crosslink but also in both DNA strands. Previously, DSBs have been identified as intermediates in ICL repair. Here, we identify Mus81–Eme1 as a structure-specific endonuclease involved in converting ICLs to DSBs in a DNA replication-dependent manner.

ICL-inducing agents cause very heterogeneous types of DNA distortions (Dronkert and Kanaar, 2001). Therefore,
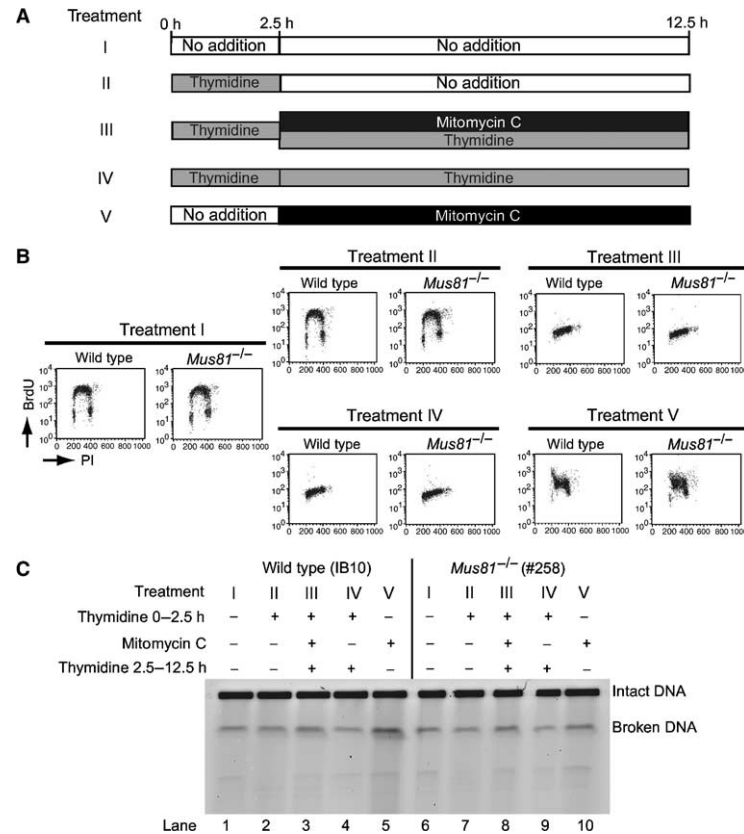
Figure 3 Inhibition of replication suppresses Mus81-dependent DSB formation in response to ICLs. (**A**) Schematic representation of the experimental protocol. Replication in wild-type and $Mus81^{-/-}$ ES cells was inhibited by incubating them in media containing 20 mM thymidine for 2.5 h. Next, the cells were treated with 2 μg/ml mitomycin C and 20 mM thymidine for 10 h (III). Control cells were either untreated (I), treated with 20 mM thymidine for 2.5 h (II) or 12.5 h (IV), or treated with 2 μg/ml mitomycin C for 10 h (V). (**B**) Cell cycle profiles of cells treated as described in panel (A) were determined by bi-parameter (BrdU and PI) FACS analysis. (**C**) Wild-type and $Mus81^{-/-}$ ES cells were treated as described above and the DSB formation was analyzed by PFGE.

recognition of ICLs posses a problem because recognition based on chemical and three-dimensional structure would require multiple recognition proteins. Instead, cells probably rely on detection methods that do not require direct recognition of the ICL, such as ICL-induced transcription or replication stalling. For cells in S phase, a replication fork stalled by an ICL can provide a branched DNA structure that triggers the required strand cleavages. However, classical excision repair pathways such as NER or base excision repair alone are not sufficient for ICL repair because these pathways have evolved to cleave only one of the two DNA strands. While it has been established that ICLs are converted into DSBs in a replication-dependent manner (Akkari et al, 2000; De Silva et al, 2000; Niedernhofer et al, 2004; Rothfuss and Grompe, 2004), the identity of nucleases responsible for this conversion had not been determined.

Mammalian cells contain at least two structure-specific endonucleases that cleave branched DNA structures: XPF-

ERCC1 and Mus81–Eme1 (Heyer et al, 2003; Heyer, 2004). XPF-ERCC1, first identified for its function in NER, prefers three-way branched junctions containing two single-stranded DNA arms, whereas Mus81–Eme1 cleaves three-way junctions with at least two double-stranded arms, such as 3′ flaps and structures resembling replication forks. $Ercc1^{-/-}$ cells are extremely sensitive to ICL-inducing agents, but the XPF–ERCC1 complex is not involved in the generation of ICL-induced DSBs and probably plays a role in another step of ICL repair (Niedernhofer et al, 2004). We have generated $Mus81^{-/-}$ ES cells to address whether Mus81 was part of the structure-specific endonuclease complex responsible for DSB formation after treatment with crosslinking agents. $Mus81^{-/-}$ cells, as well as $Eme1^{-/-}$ cells, are hypersensitive to mitomycin C and cisplatin (Figures 2B and 7C, and Abraham et al, 2003; McPherson et al, 2004; Dendouga et al, 2005). Culturing wild-type ES cells in the continuous presence of an ICL-inducing agent results in the accumulation of the cells in
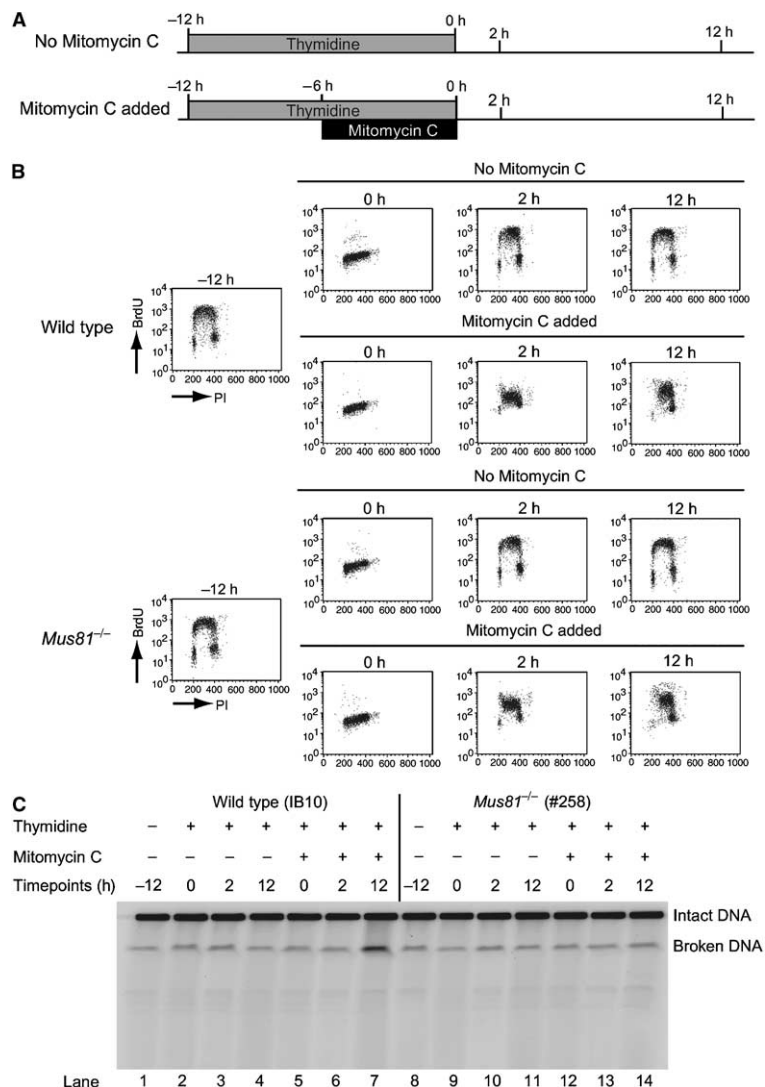
Figure 4 Mus81-dependent generation of mitomycin C-induced DSBs occurs during S phase. (**A**) Schematic representation of the experimental protocol. Wild-type and $Mus81^{-/-}$ ES cells were incubated in 5 mM thymidine for 12 h. For the last 6 h of the incubation, mitomycin C was added to a final concentration of 2 µg/ml. Control cells were incubated with thymidine-containing media only. Next, the cells were washed twice with PBS, incubated in fresh medium to allow resumption of replication, and collected at the indicated times. (**B**) Cell cycle profiles of cells treated as described in panel (A), shown as BrdU incorporation versus PI plots. (**C**) The relative amount of broken DNA in wild-type and $Mus81^{-/-}$ ES cells treated as described in panel (A) was assessed by PFGE.

S phase (Figures 1B and 2C) and in DSB formation that increases in a time- and dose-dependent manner (Figures 1C, A and 2A). By contrast, no such increase in DSB formation occurs in the absence of Mus81, even through the cells do accumulate in S phase. Inhibition of DNA replication suppresses Mus81-dependent DSBs in response to mitomycin C (Figure 3), whereas resuming replication resulted in their formation (Figure 4). Taken together, the biochemical activity of the Mus81–Eme1 complex, the mitomycin C hypersensitivity of $Mus81^{-/-}$ and $Eme1^{-/-}$ cells, and the lack of ICL-induced DSB formation in $Mus81^{-/-}$ S phase cells suggest that Mus81–Eme1 is a structure-specific endonuclease
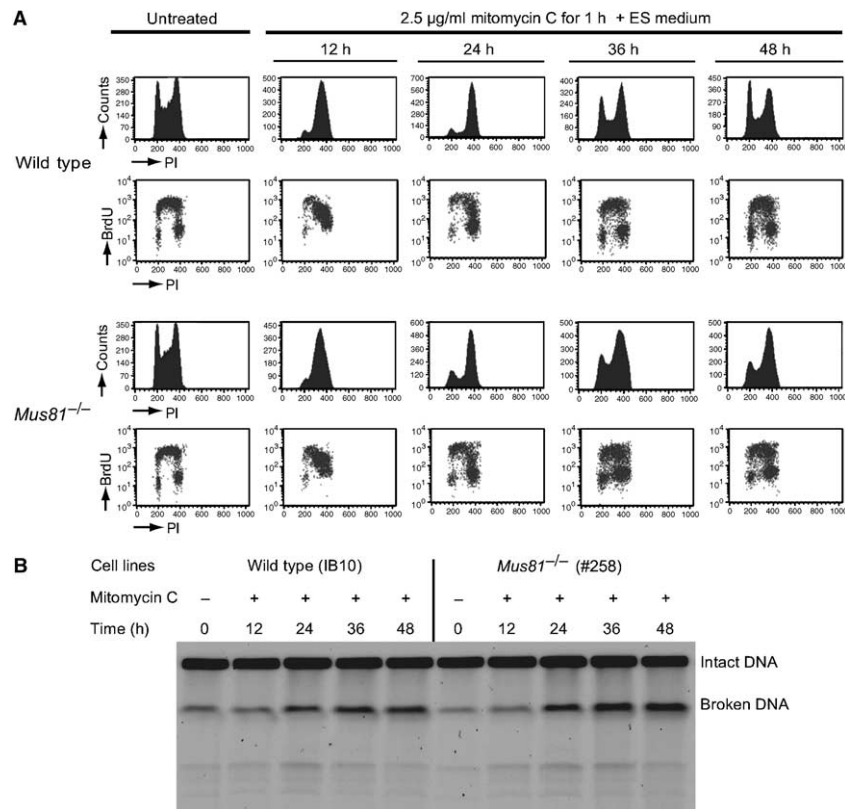
Figure 5 Analysis of DSB formation after pulse treatment of cells with mitomycin C. (**A**) ES cells of the indicated genotype were treated for 1 h with mitomycin C and continued to be incubated in media without mitomycin C for the indicated amount of time before their cell cycle profile was determined by FACS analysis. The cell count versus PI staining and BrdU incorporation versus PI profile are shown. (**B**) Wild-type and $Mus81^{-/-}$ ES cells were treated with mitomycin C for 1 h. Cells were incubated in media without mitomycin C for the indicated amount of time and the amount of broken DNA was determined by PFGE.

involved in cleaving one of the branched arms of replication forks stalled by ICL lesions.

While Mus81 is involved in cleaving replication forks stalled at ICLs, it does not seem to be responsible for dealing with DNA damage-associated replication stalling in general. After treatment with UV light, $Mus81^{-/-}$ cells accumulate a similar amount of DSBs as wild-type cells (Figure 6). Encountering DNA damage that affects only one strand, such as induced by UV light, will cause problems for a replicative polymerase but may not stop a replicative helicase. The incomplete replicated regions resulting in this case are apparently not substrates for Mus81. However, the DNA structures created, and the challenges to restarting replication, when a fork encounters an ICL are likely to be much different. Because the integrity and movement of a replication fork is determined by the presence and movement of a replicative helicase, halting this enzyme, as an ICL will, will likely cause complete disruption of fork movement. DNA synthesis will stop on both strands and the complex assem-

blies of replication proteins may disassociate from each other and their DNA templates.

While the results of our experiments reveal the involvement of Mus81–Eme1 in converting ICLs into DSBs, they also demonstrate the importance of the assay to detect these DSBs. When cells are continuously exposed to mitomycin C, they accumulate in S phase and Mus81-dependent DSBs can be detected (Figure 1). On the other hand, when they are treated with a short pulse of mitomycin C, cells do not accumulate in S phase and while DSBs are detected they are not Mus81-dependent (Figure 5), consistent with the results of a previous study (Dendouga *et al*, 2005). It is possible that unrepaired or partially repaired ICL damage, for example gaps or crosslinks between sister chromatids, are still present in G2 cells. Once such cells go through mitosis, this damage can impair proper chromosome segregation, for example as evidenced by an increase in anaphase bridging especially under conditions of reduced ICL repair (Niedernhofer *et al*, 2004), and lead to mechanical breakage
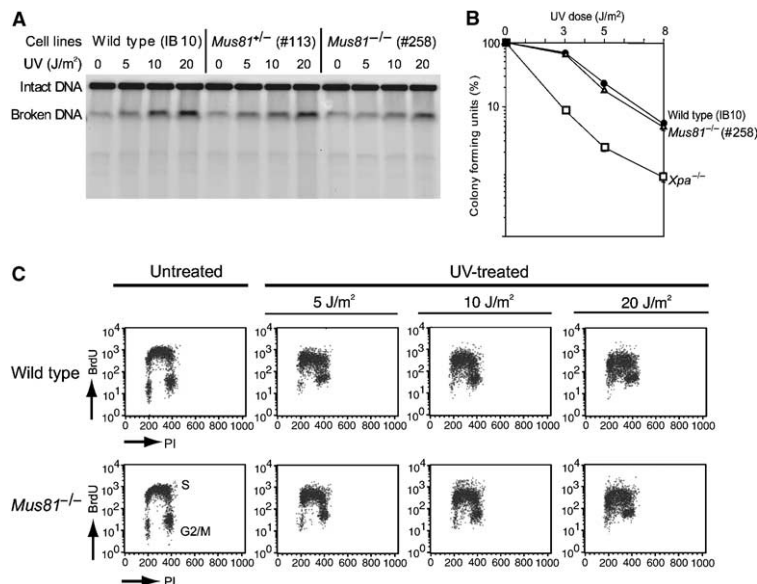
Figure 6 Analysis of UV-light-induced DSB formation in wild-type and *Mus81*$^{-/-}$ ES cells. (**A**) UV-light-induced DSB formation in wild-type, *Mus81*$^{+/-}$ and *Mus81*$^{-/-}$ ES cells as analyzed by PFGE. (**B**) Survival curve in response to UV light for wild-type, and *Mus81*$^{-/-}$ ES cells. *Xpa*$^{-/-}$ ES cells served as a control. (**C**) Cell cycle profiles of wild-type and *Mus81*$^{-/-}$ ES cells 4 h after treatment increasing doses of UV light. The BrdU incorporation versus PI profiles are shown.

of DNA molecules, both in wild-type and Mus81-deficient cells. Alternatively, the Mus81-independent breaks might occur in the subsequent S phase. The conversion of mitomycin C mono-adducts to ICLs is slow (Warren *et al*, 1998). Therefore, the ratio of ICLs to mono-adducts might be low in the pulse treatment assay because cells do not accumulate in S phase. When DNA-containing mono-adducts will be replicated in the subsequent S phase, the mono-adducts could trigger Mus81-independent DNA cleavage in a manor analogous to UV-light-induced DNA damage (Figure 6).

Our results indicate that Mus81–Eme1 is involved in cleaving a replication fork stalled by an ICL to produce a DSB, which itself is a genotoxic intermediate that has to be repaired before it causes further damage to the genome (Dronkert and Kanaar, 2001; McHugh *et al*, 2001). In mammalian cells, DSBs can be repaired through two mechanistically distinct pathways; homologous recombination and non-homologous end joining (van Gent *et al*, 2001). Homologous recombination mutants are hypersensitive to ICL-inducing agents, suggesting that recombination is the main pathway involved in DSB-associated ICL repair (McHugh *et al*, 1999; De Silva *et al*, 2000). The one-ended DSBs created by Mus81–Eme1 cleavage at a stalled replication fork (Supplementary Figure 3) are substrates for homologous recombination rather than nonhomologous end joining (Cromie *et al*, 2001). Thus, it would be advantageous if Mus81–Eme1 endonuclease would be directly linked to the recombination machinery for efficient processing of the DSBs it generates. Indeed, Mus81 has first been identified in *S. cerevisiae* through a two-hydrid interaction with the homologous recombination

protein Rad54 (Interthal and Heyer, 2000). Here we show, in mammalian cells, that the Mus81 and Rad54 proteins interact (Figure 7A) and that they are genetically involved in the same ICL survival pathway (Figure 7C). Furthermore, we show that mitomycin C-induced SCEs are reduced in the absence of Mus81. These results are consistent with the notion that the Mus81-generated DSBs are further processed by Rad54-mediated homologous recombination. The additional sensitivity of the *Mus81*$^{-/-}$ ES cells compared to *Rad54*$^{-/-}$ ES cells indicates that alternative pathways exists for repair of the ICL-induced DSBs that do not involve Rad54, consistent with the mild homologous recombination defect of *Rad54*$^{-/-}$ ES cells (Essers *et al*, 1997; Dronkert *et al*, 2000). One such alternative pathway might involve the Rad54 paralog Rad54B (Wesoly *et al*, 2006). Both Rad54 paralogs interact with Rad51, which provides the catalytic core of homologous recombination. Rad51 assembles into nucleoprotein filaments on single-stranded DNA and promotes homology recognition and DNA strand exchange, which can result in repair of DSBs (Wyman *et al*, 2004). In a possible scenario to limit the genotoxicity of the DSB intermediate in ICL repair, Rad51 could assemble on single-stranded DNA arising at the ICL-stalled DNA replication fork, before the DSB has occurred. As Rad54 in mammalian cells interacts with Rad51 upon the induction of DNA damage (Tan *et al*, 1999), it is possible that it is the Rad51 nucleoprotein filament that attracts Rad54. This notion has previously been proposed as a mechanism to target Rad54, which acts on the duplex DNA, to the intact homologous template DNA (Mazin *et al*, 2000; Solinger *et al*, 2001). As Rad54 interacts with Mus81, the structure-specific
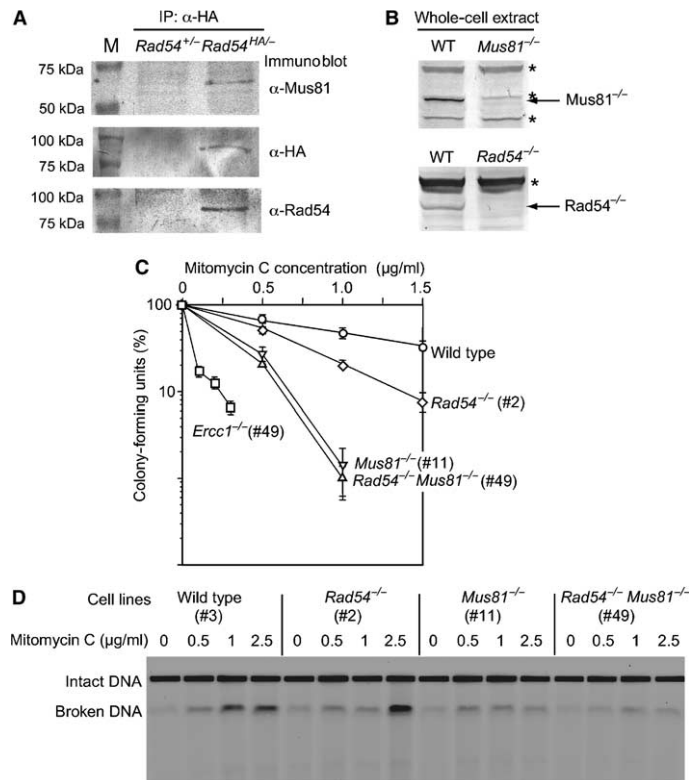
Figure 7 Analysis of relationship between Mus81 and Rad54 with respect to ICL repair. (**A**) Immunoprecipitation (IP) of Rad54 and Mus81. Using an anti-HA-antibody, HA-tagged Rad54 protein was precipitated from HA-tagged Rad54 knock-in ES cells. The precipitated material was analyzed by immunoblotting using antibodies against Mus81, HA and Rad54. As a negative control, $Rad54^{+/-}$ cells (cell line #18) were used, because the cell line is isogenic to the $Rad54^{HA/-}$ cell line, except for the HA-tag on Rad54. (**B**) Identification of the Mus81 and Rad54 proteins in the input material for the immunoprecipitation. Immunoblots using whole-cell extracts representing 1% of the material used for the immunoprecipitation. As controls for the identification of Mus81 and Rad54, extracts from $Mus81^{-/-}$ and $Rad54^{-/-}$ ES cells were used. Signals from nonspecific proteins are indicated by an asterix. (**C**) Comparison of mitomycin C sensitivity of wild-type, $Mus81^{-/-}$, $Rad54^{-/-}$ and $Mus81^{-/-}$ $Rad54^{-/-}$ ES cells. ES cells of the indicated genotype were treated with increasing doses of mitomycin C for 1 h after which the medium was refreshed. Colonies were fixed, stained and counted after 5–8 days. Error bars indicate the standard error of the mean. (**D**) Analysis of mitomycin C-induced DSB formation in wild-type, $Rad54^{-/-}$, $Mus81^{-/-}$ and $Mus81^{-/-}$ $Rad54^{-/-}$ ES cells using PFGE.

endonuclease would only get in the proximity of the stalled replication fork when the critical DSB repair proteins are already in place.

Based on the results described above, we propose a model for a Mus81-dependent ICL repair pathway (Supplementary Figure 3). ICL lesions prevent DNA unwinding required for processive replication and thereby induce stalling of replication forks. The exact structure of DNA strands at an ICL stalled fork is not known. A replicative helicase may stop some base pairs ahead of the crosslinked nucleotides. The presence of single-stranded gaps in the nascent strands will depend on the resulting mis-coordination between leading and lagging strands. Regression of the newly synthesized strands or other recombination-mediated DNA strand exchanges may be needed to assure that the yet to be replicated parental and new daughter DNA strands remain associated

for fork recovery after ICL removal. Many scenarios can be envisioned that would result in branched DNA structures that match the *in vitro* nuclease activity of Mus81–Eme1 for cleavage to a DSB. Although potentially dangerous, DSBs are needed to remove ICLs and may facilitate subsequent repair processes. A DSB may serve as an exit point for stalled replication proteins as well as a release for accumulated positive DNA supercoiling, which inhibits most DNA-binding proteins. In both cases, DSB formation would promote recruitment of repair enzymes, including incision nuclease(s). The ICL is still in place after Mus81 cleavage (Supplementary Figure 3) and therefore additional strand incisions are required for its removal. The hypersensitivity of $Ercc1^{-/-}$ and *XPF* mutant cells to ICL-inducing agents highlights the importance of this complex for ICL repair. The XPF–ERCC1 endonuclease can incise ICL-containing DNA *in vitro*

(Bessho *et al*, 1997; Kuraoka *et al*, 2000). This activity is consistent with a role in incising DNA at one side of an ICL, in the unreplicated DNA region of the cleaved fork shown in Supplementary Figure 3. Subsequently, rotating the cross-linked base out of the helix creates in effect, a single-stranded gap (Kaye *et al*, 1980; Matsumoto *et al*, 1989; De Silva *et al*, 2000). This idea is supported by the observation that ICL-induced single-stranded breaks and single-stranded gaps are decreased in XPF- and ERCC1-deficient cell lines (De Silva *et al*, 2000; De Silva *et al*, 2002; Rothfuss and Grompe, 2004). Homologous recombination between the daughter DNA molecules could re-establish a replication fork. The Mus81-generated DSB would be processed such that its 3′ end invades and pairs with the other daughter molecule to create a primer for the polymerase. DNA synthesis over the site of the crosslink would likely require a translesion polymerase to restore the duplex and eventually result in re-establishing a complete replication fork.

The coordinated cooperation of several DNA repair pathways is clearly required during Mus81-dependent repair of ICLs during S phase. Additional complexities to understanding ICL repair are provided by the possibility that other Mus81-independent ICL repair pathways must exist. For example, the ICL sensitivity of $Ercc1^{-/-}$ ES cells is much greater than that of $Mus81^{-/-}$ cells (Figure 7C). Outside of S phase, ICLs cannot be detected by stalled DNA replication, yet they will still be highly toxic owing to their interference with transcription. Recently, compelling evidence has been provided for the existence of a G1 phase ICL repair in *S. cerevisiae*, which is dependent on NER and a translesion DNA polymerase (Sarkar *et al*, 2006).

Materials and methods

Cell lines
The cell lines used in this study are described in Supplementary Table 1. The method of *de novo* isolation of ES cells is described previously (Essers *et al*, 2000). The generation of $Mus81^{-/-}$ ES cells is described in the Supplementary data. Subconfluent cultures of ES cells were treated with DNA-damaging agents or thymidine as indicated.

Detection of DSBs by pulse-field gel electrophoresis
Subconfluent cultures of wild-type, $Mus81^{+/-}$, $Mus81^{-/-}$, $Rad54^{-/-}$, $Rad54^{-/-}$ $Mus81^{-/-}$ and $Ercc1^{-/-}$ ES cells were treated with mitomycin C or cisplatin for 24 h, unless otherwise indicated. In case of UV-light treatment, cells were washed with 10 ml phosphate-buffered saline (PBS), exposed to UV light and incubated in fresh medium to allow repair and cell cycle progression for 4 h. Cells were harvested after trypsinization and agarose plugs containing 10^6 cells were prepared with a CHEF-disposable plug mold (Bio-Rad). The cells were lysed by incubation of the plugs in 1 mg/ml proteinase K in 100 mM EDTA, 0.2% sodium deoxycholate, 1% sodium lauryl sarcosine for 48 h at 37°C and then washed repetitively with 10 mM Tris–HCl, pH 8.0, 100 mM ETDA. Electrophoresis was performed for 23 h at 13°C through 0.9% agarose in Tris–borate–EDTA buffer using a Biometra Rotaphor apparatus with the following parameters: interval, 30–5 s log; angle, 120°–110° linear; 180–120 V log). The DNA was stained with ethidium bromide and visualized using a Typhoon 9200 scanner (Amersham Pharmacia Biotech). The electrophoresis conditions were specifically designed to compact lower molecular weight DNA fragments (several Mbp to 500 kbp) into a single band, while keeping high molecular weight genomic DNA in the well. The lower molecular weight DNA fragments are the results of DSBs in the chromosomal DNA. Thus, the assay allows broken DNA to be readily detected. However, in the context of DSBs arising during DNA replication stalling, the assay has limited sensitivity and is not quantitative. When a DSB occurs at a DNA replication fork, the broken DNA is still attached to the template chromosome. To detect DSBs in the assay, two relatively closely (several Mbp) spaced independent DSBs have to occur.

Flow cytometric analysis
Before collection after the various indicated treatments, ES cells were incubated with 10 μM BrdU for 5 min at 37°C, harvested by trypsynization and fixed overnight with 70% ethanol at 4°C (Smits *et al*, 2000). After the ethanol was washed away, the cells were treated with 0.1 N HCl containing 0.5 mg/ml pepsin (Merck) for 20 min at room temperature. Next, the cells were treated with 2 N HCl for 12 min at 37°C, followed by the addition of borate buffer (pH 8.5). The cells were washed with PBS containing 0.5% Tween-20 and 0.1% BSA and incubated with FITC-conjugated anti-BrdU antibodies (Becton Dickinson) for 1 h at 4°C. After washing, the cells were counterstained with a solution containing PI (10 μg/ml) and RNase (10 μg/ml) for 30 min at 37°C. The cells were analyzed on a fluorescence-activated cell sorter (Becton Dickinson) using CellQuest software.

Colony survival assays and SCE analysis
Sensitivity of ES cells to increasing doses of mitomycin C was determined as described previously (Budzowska *et al*, 2004). Briefly, ES cells of the indicated genotypes were plated in 60 mm dishes, at various dilutions. After overnight incubation, cells were treated with mitomycin C for 1 h. Subsequently, the cells were washed twice with PBS and incubated with fresh medium for 6–8 days. Cells were fixed, stained and colonies were counted. All experiments were performed in triplicate. Similar protocols were followed to determine sensitivities to cisplatin and UV light. Analysis of SCEs was carried out as described (Dronkert *et al*, 2000).

Immunoprecipitation
Subconfluent cultures of ES cells were harvested after trypsinization and lysed in IP lysis buffer (20 mM Tris–HCl, pH 7.5, 1 mM EDTA, 0.5% Triton X-100, 150 mM NaCl, 10% glycerol, protease inhibitors Complete (Roche)) for 1 h on ice. The lysate was centrifugated for 1 h at 4°C at 46 000 r.p.m. using SW60 rotor (Beckman) and the supernatant was collected into a new tube. To get rid of DNA, 2 mM $MgCl_2$ and DNase I were added and the mixture was incubated at room temperature for 15 min. An anti-HA antibody attached to an agarose matrix (Roche) was added to the lysate followed by an overnight incubation at 4°C. The precipitate was washed four times with Wash buffer (20 mM Tris–HCl, pH 7.5, 2 mM EDTA, 200 mM NaCl, 0.5 % Triton X-100).

Supplementary data
Supplementary data are available at *The EMBO Journal* Online (http://www.embojournal.org).

References

Abraham J, Lemmers B, Hande MP, Moynahan ME, Chahwan C, Ciccia A, Essers J, Hanada K, Chahwan R, Khaw AK, McPherson P, Shehabeldin A, Laister R, Arrowsmith C, Kanaar R, West SC, Jasin M, Hakem R (2003) Eme1 is involved in DNA damage processing and maintenance of genomic stability in mammalian cells. *EMBO J* **22:** 6137–6147

Adair GM, Rolig RL, Moore-Faver D, Zabelshansky M, Wilson JH, Nairn RS (2000) Role of ERCC1 in removal of long non-homo-

logous tails during targeted homologous recombination. *EMBO J* **19:** 5552–5561

Akkari YM, Bateman RL, Reifsteck CA, Olson SB, Grompe M (2000) DNA replication is required to elicit cellular responses to psoralen-induced DNA interstrand cross-links. *Mol Cell Biol* **20:** 8283–8289

Bessho T, Mu D, Sancar A (1997) Initiation of DNA interstrand cross-link repair in humans: the nucleotide excision repair system makes dual incisions 5' to the cross-linked base and removes a 22- to 28-nucleotide-long damage-free strand. *Mol Cell Biol* **17:** 6822–6830

Boddy MN, Gaillard PH, McDonald WH, Shanahan P, Yates III JR, Russell P (2001) Mus81–Eme1 are essential components of a Holliday junction resolvase. *Cell* **107:** 537–548

Branzei D, Foiani M (2005) The DNA damage response during DNA replication. *Curr Opin Cell Biol* **17:** 568–575

Budzowska M, Jaspers I, Essers J, de Waard H, van Drunen E, Hanada K, Beverloo B, Hendriks RW, de Klein A, Kanaar R, Hoeijmakers JH, Maas A (2004) Mutation of the mouse Rad17 gene leads to embryonic lethality and reveals a role in DNA damage-dependent recombination. *EMBO J* **23:** 3548–3558

Chen XB, Melchionna R, Denis CM, Gaillard PH, Blasina A, Van de Weyer I, Boddy MN, Russell P, Vialard J, McGowan CH (2001) Human Mus81-associated endonuclease cleaves Holliday junctions *in vitro*. *Mol Cell* **8:** 1117–1127

Cheng S, Sancar A, Hearst JE (1991) RecA-dependent incision of psoralen-crosslinked DNA by (A)BC excinuclease. *Nucleic Acids Res* **19:** 657–663

Ciccia A, Constantinou A, West SC (2003) Identification and characterization of the human mus81–eme1 endonuclease. *J Biol Chem* **278:** 25172–25178

Constantinou A, Chen XB, McGowan CH, West SC (2002) Holliday junction resolution in human cells: two junction endonucleases with distinct substrate specificities. *EMBO J* **21:** 5577–5585

Courcelle J, Hanawalt PC (2001) Participation of recombination proteins in rescue of arrested replication forks in UV-irradiated *Escherichia coli* need not involve recombination. *Proc Natl Acad Sci USA* **98:** 8196–8202

Cromie GA, Connelly JC, Leach DR (2001) Recombination at double-strand breaks and DNA ends: conserved mechanisms from phage to humans. *Mol Cell* **8:** 1163–1174

de Laat WL, Appeldoorn E, Jaspers NG, Hoeijmakers JH (1998) DNA structural elements required for ERCC1–XPF endonuclease activity. *J Biol Chem* **273:** 7835–7842

De Silva IU, McHugh PJ, Clingen PH, Hartley JA (2000) Defining the roles of nucleotide excision repair and recombination in the repair of DNA interstrand cross-links in mammalian cells. *Mol Cell Biol* **20:** 7980–7990

De Silva IU, McHugh PJ, Clingen PH, Hartley JA (2002) Defects in interstrand cross-link uncoupling do not account for the extreme sensitivity of ERCC1 and XPF cells to cisplatin. *Nucleic Acids Res* **30:** 3848–3856

Dendouga N, Gao H, Moechars D, Janicot M, Vialard J, McGowan CH (2005) Disruption of murine Mus81 increases genomic instability and DNA damage sensitivity but does not promote tumorigenesis. *Mol Cell Biol* **25:** 7569–7579

Doe CL, Osman F, Dixon J, Whitby MC (2004) DNA repair by a Rad22–Mus81-dependent pathway that is independent of Rhp51. *Nucleic Acids Res* **32:** 5570–5581

Doe CL, Whitby MC (2004) The involvement of Srs2 in postreplication repair and homologous recombination in fission yeast. *Nucleic Acids Res* **32:** 1480–1491

Dronkert ML, Beverloo HB, Johnson RD, Hoeijmakers JH, Jasin M, Kanaar R (2000) Mouse RAD54 affects DNA double-strand break repair and sister chromatid exchange. *Mol Cell Biol* **20:** 3147–3156

Dronkert ML, Kanaar R (2001) Repair of DNA interstrand cross-links. *Mutat Res* **486:** 217–247

Essers J, Hendriks RW, Swagemakers SM, Troelstra C, de Wit J, Bootsma D, Hoeijmakers JH, Kanaar R (1997) Disruption of mouse RAD54 reduces ionizing radiation resistance and homologous recombination. *Cell* **89:** 195–204

Essers J, van Steeg H, de Wit J, Swagemakers SM, Vermeij M, Hoeijmakers JH, Kanaar R (2000) Homologous and non-homologous recombination differentially affect DNA damage repair in mice. *EMBO J* **19:** 1703–1710

Heyer WD (2004) Recombination: Holliday junction resolution and crossover formation. *Curr Biol* **14:** R56–R58

Heyer WD, Ehmsen KT, Solinger JA (2003) Holliday junctions in the eukaryotic nucleus: resolution in sight? *Trends Biochem Sci* **28:** 548–557

Interthal H, Heyer WD (2000) MUS81 encodes a novel helix-hairpin-helix protein involved in the response to UV- and methylation-induced DNA damage in *Saccharomyces cerevisiae*. *Mol Gen Genet* **263:** 812–827

Kaliraman V, Mullen JR, Fricke WM, Bastin-Shanower SA, Brill SJ (2001) Functional overlap between Sgs1–Top3 and the Mms4–Mus81 endonuclease. *Genes Dev* **15:** 2730–2740

Kaye J, Smith CA, Hanawalt PC (1980) DNA repair in human cells containing photoadducts of 8-methoxypsoralen or angelicin. *Cancer Res* **40:** 696–702

Kuraoka I, Kobertz WR, Ariza RR, Biggerstaff M, Essigmann JM, Wood RD (2000) Repair of an interstrand DNA cross-link initiated by ERCC1–XPF repair/recombination nuclease. *J Biol Chem* **275:** 26632–26636

Langston LD, Symington LS (2005) Opposing roles for DNA structure-specific proteins Rad1, Msh2, Msh3, and Sgs1 in yeast gene targeting. *EMBO J* **24:** 2214–2223

Matsumoto A, Vos JM, Hanawalt PC (1989) Repair analysis of mitomycin C-induced DNA crosslinking in ribosomal RNA genes in lymphoblastoid cells from Fanconi's anemia patients. *Mutat Res* **217:** 185–192

McHugh PJ, Gill RD, Waters R, Hartley JA (1999) Excision repair of nitrogen mustard-DNA adducts in *Saccharomyces cerevisiae*. *Nucleic Acids Res* **27:** 3259–3266

Mazin AV, Bornarth CJ, Solinger JA, Heyer WD, Kowalczykowski SC (2000) Rad54 protein is targeted to pairing loci by the Rad51 nucleoprotein filament. *Mol Cell* **6:** 583–592

McHugh PJ, Spanswick VJ, Hartley JA (2001) Repair of DNA interstrand crosslinks: molecular mechanisms and clinical relevance. *Lancet Oncol* **2:** 483–490

McPherson JP, Lemmers B, Chahwan R, Pamidi A, Migon E, Matysiak-Zablocki E, Moynahan ME, Essers J, Hanada K, Poonepalli A, Sanchez-Sweatman O, Khokha R, Kanaar R, Jasin M, Hande MP, Hakem R (2004) Involvement of mammalian Mus81 in genome integrity and tumor suppression. *Science* **304:** 1822–1826

Niedernhofer LJ, Essers J, Weeda G, Beverloo B, de Wit J, Muijtjens M, Odijk H, Hoeijmakers JH, Kanaar R (2001) The structure-specific endonuclease Ercc1–Xpf is required for targeted gene replacement in embryonic stem cells. *EMBO J* **20:** 6540–6549

Niedernhofer LJ, Lalai AS, Hoeijmakers JH (2005) Fanconi anemia (cross)linked to DNA repair. *Cell* **123:** 1191–1198

Niedernhofer LJ, Odijk H, Budzowska M, van Drunen E, Maas A, Theil AF, de Wit J, Jaspers NG, Beverloo HB, Hoeijmakers JH, Kanaar R (2004) The structure-specific endonuclease Ercc1–Xpf is required to resolve DNA interstrand cross-link-induced double-strand breaks. *Mol Cell Biol* **24:** 5776–5787

Ogrunc M, Sancar A (2003) Identification and characterization of human MUS81–MMS4 structure-specific endonuclease. *J Biol Chem* **278:** 21715–21720

Paques F, Haber JE (1999) Multiple pathways of recombination induced by double-strand breaks in *Saccharomyces cerevisiae*. *Microbiol Mol Biol Rev* **63:** 349–404

Rothfuss A, Grompe M (2004) Repair kinetics of genomic interstrand DNA cross-links: evidence for DNA double-strand break-dependent activation of the Fanconi anemia/BRCA pathway. *Mol Cell Biol* **24:** 123–134

Sargent RG, Meservy JL, Perkins BD, Kilburn AE, Intody Z, Adair GM, Nairn RS, Wilson JH (2000) Role of the nucleotide excision repair gene ERCC1 in formation of recombination-dependent rearrangements in mammalian cells. *Nucleic Acids Res* **28:** 3771–3778

Sarkar S, Davies AA, Ulrich HD, McHugh PJ (2006) DNA interstrand crosslink repair during G1 involves nucleotide excision repair and DNA polymerase zeta. *EMBO J* **25:** 1285–1294

Smits VA, van Peer MA, Essers MA, Klompmaker R, Rijksen G, Medema RH (2000) Negative growth regulation of SK-N-MC cells by bFGF defines a growth factor-sensitive point in G2. *J Biol Chem* **275:** 19375–19381

Solinger JA, Lutz G, Sugiyama T, Kowalczykowski SC, Heyer WD (2001) Rad54 protein stimulates heteroduplex DNA formation in the synaptic phase of DNA strand exchange via specific interactions with the presynaptic Rad51 nucleoprotein filament. *J Mol Biol* **307:** 1207–1221

103

Tan TL, Essers J, Citterio E, Swagemakers SM, de Wit J, Benson FE, Hoeijmakers JH, Kanaar R (1999) Mouse Rad54 affects DNA conformation and DNA-damage-induced Rad51 foci formation. *Curr Biol* **9**: 325–328

van Gent DC, Hoeijmakers JH, Kanaar R (2001) Chromosomal stability and the DNA double-stranded break connection. *Nat Rev Genet* **2**: 196–206

Warren AJ, Maccubbin AE, Hamilton JW (1998) Detection of mitomycin C-DNA adducts *in vivo* by ^{32}P-postlabeling: time course for formation and removal of adducts and biochemical modulation. *Cancer Res* **58**: 453–461

Wesoly J, Agarwal S, Sigurdsson S, Bussen W, Van Komen S, Qin J, Van Steeg H, Van Benthem J, Wassenaar E, Baarends WM, Ghazvini M, Tafel AA, Heath H, Galjart N, Essers J, Grootegoed JA, Arnheim N, Bezzubova O, Buerstedde JM, Sung P, Kanaar R (2006) Differential contributions of mammalian Rad54 paralogs to recombination, DNA damage repair and meiosis. *Mol Cell Biol* **26**: 976–989

Whitby MC, Osman F, Dixon J (2003) Cleavage of model replication forks by fission yeast Mus81–Eme1 and budding yeast Mus81–Mms4. *J Biol Chem* **278**: 6928–6935

Wyman C, Ristic D, Kanaar R (2004) Homologous recombination-mediated double-strand break repair. *DNA Repair* **3**: 827–833

Supplemental data

The structure-specific endonuclease Mus81–Eme1 promotes conversion of interstrand DNA crosslinks into double-strands breaks

Katsuhiro Hanada, Magda Budzowska, Mauro Modesti, Alex Maas, Claire Wyman, Jeroen Essers and Roland Kanaar

Construction of Mus81 targeting vectors and generation of *Mus81$^{-/-}$* ES cells

A *Mus81* cDNA fragment was obtained from IMAGE clone 2937030. Genomic fragments hybridizing to the *Mus81* cDNA, encoding the carboxy-terminal fragment made by Eco RI and Not I digestion of the IMAGE clone DNA, were subcloned in pBluescript II KS (+) (Stratagene). The location of the intron-exon borders was determined using DNA sequence data from Celera. Two targeting vectors were made. The first one was made by inserting a cassette containing the *neomycin* resistance gene driven by the *tk* promoter between two Bgl II sites in the *Mus81* genomic DNA (see Figure 1). The second was made by inserting a *hygromycin* resistance gene expressed from the *PGK* promotor between the Bgl II sites. E14 ES cells (subclone IB10) were cultured in BRL-conditioned medium supplemented with 1000 U/ml leukemia inhibitory factor. A 10 µg aliquot of the Not I and Sal I linearized targeting vector (pBS-*GEMUS19-Neo2-2*) was electroporated into approximately 10^7 ES cells in 400 µl ES cell culture medium. Selection with 200 µg/ml G-418 was started 24 hrs after electroporation. After 8-10 days, G418-resistant clones were isolated. Screening for homologous recombinants was performed using DNA blot analysis of Kpn I-digested DNA and a 300 bp 5' external probe. Proper integration of the construct at the 3' side was confirmed using DNA blot analysis of Bam HI-digested DNA and a 1 kb 3' external probe. To obtain ES cell lines carrying a disruption in both *Mus81* alleles, a *Mus81$^{neo/+}$*-targeted ES cell line (03/04/04/#113) was electroporated with the Not I-linearized targeting vector (pBS-*GEMUS19-hyg2-2*). After selection with hygromycin B (200 µg/ml) for 8-10 days, colonies were isolated, expanded and analyzed by DNA blotting. Using the flanking probes described above ES cells lacking wild type *Mus81* alleles were identified.

Supplemental Table 1. Mouse embryonic stem (ES) cells used in this study.

Cell lines	Genotype	Notes
129/Sv genetic background		
IB10	wild type	E14 subclone, (Essers *et al.*, 1997)
03/04/04/#113	*Mus81*^{+/-}	See Materials and Methods
03/07/04/#258	*Mus81*^{-/-}	See Materials and Methods
95/08/15/#18	*Rad54*^{+/-}	(Essers *et al.*, 1997)
96/01/12/#10	*Rad54*^{-/-}	(Essers *et al.*, 1997)
98/10/02/#27 [a]	*Rad54*[HA/-]	(Tan *et al.*, 1999)
97/05/28/#49	*Ercc1*^{-/-}	(Niedernhofer et al. 2001)
129/Sv×C57BL/6 genetic background		
04/02/28/#3	wild type	*de novo* isolated (See Materials and Methods)
97/02/01/#2	*Rad54*^{-/-}	(Essers *et al.*, 2000)
97/02/01/#2.2	*Rad54*^{-/-}, *PGK-hRad54*	(Essers *et al.*, 2000)
04/05/11/#1	*Mus81*^{+/-}	*de novo* isolated (See Materials and Methods)
04/05/13/#11	*Mus81*^{-/-}	*de novo* isolated (See Materials and Methods)
05/02/03/#49 [b]	*Mus81*^{-/-} *Rad54*^{-/-}	04/05/13/#11 × p11.1-*Hyg, Pur*
05/02/03/#14 [c]	*Mus81*^{-/-}, *PGK-hMus81*	04/05/13/#11 × pPGK-*hMus81*
D2	*Rad17*[5'Δ/5'Δ]	(Budzowska *et al.*, 2004)
C57BL/6 genetic background		
Xpa	*Xpa*^{-/-}	(de Waard *et al.*, 2003)

[a] This cell line was established by gene targeting using the targeting vectors, p11.1::HA (*Rad54* with carboxy-terminal fusion of HA epitope, and *Hyg*[r]). The details of this gene targeting vector were described previously (Tan *et al.*, 1999).
[b] This cell line was established by two rounds of gene targeting (p11.1-*Hyg*, *Rad54*::*Hyg* knock-out construct and p11.1-*Pur*, *Rad54*::*Pur* knock-out construct). The details of these targeting constructs were described previously (Essers *et al.*, 1997).
[c] These cell lines were established by random integration of the expression vector, pPGK-*hMus81*, which expresses hMus81 from the *PGK* promoter.
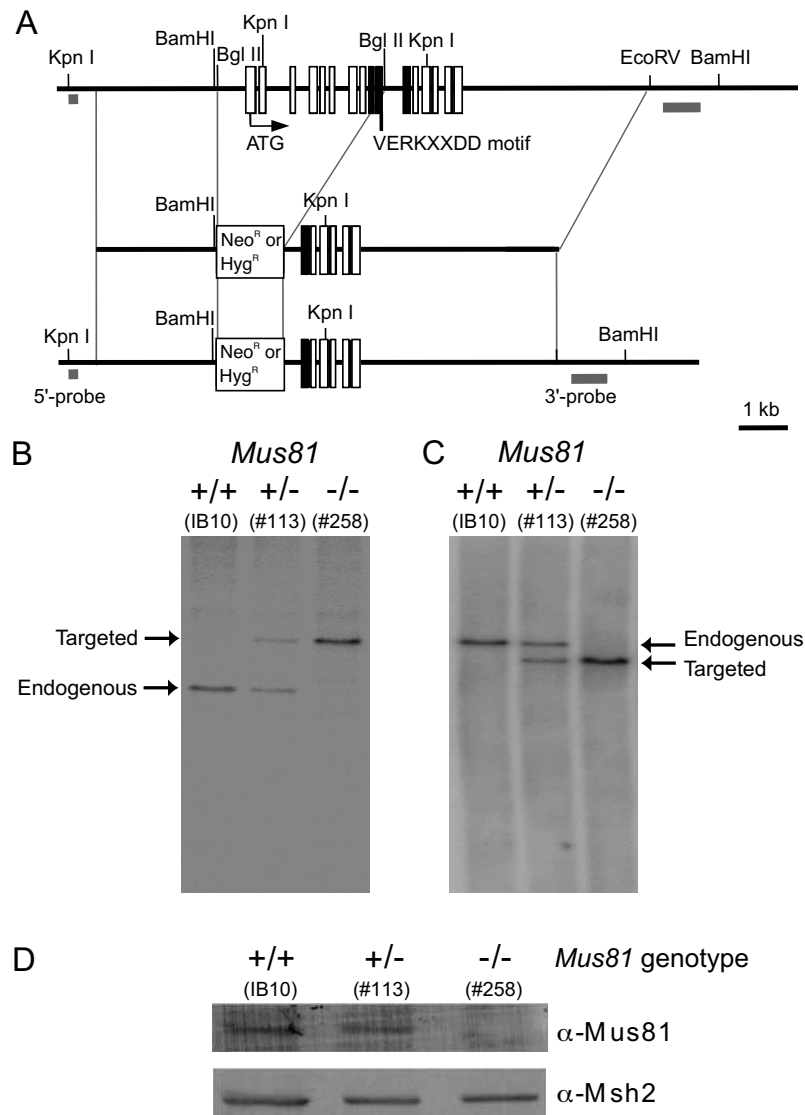
Supplemental Figure 1. Generation of Mus81$^{-/-}$ ES cells.
(**A**) Schematic representation of the mouse *Mus81* genomic locus, the gene targeting constructs and the targeted *Mus81* allele. Part of *Mus81* gene between the indicated Bgl II sites, including the start codon and the VERKXXDD nuclease motif, was replaced by an antibiotic resistance gene (either *Neo^r* or *Hyg^r*). (**B**) DNA blot analysis of wild type, *Mus81$^{+/-}$*, and *Mus81$^{-/-}$* ES cells. Kpn I-digested ES cell DNA was transferred to a membrane and hybridized with a probe flanking the *Mus81* targeting construct on 5' side. The resulting bands from the endogenous (3.5 kb) and the targeted (4.2 kb) *Mus81* locus are indicated. (**C**) DNA blot analysis using Bam HI-digested DNA and a 3'-flanking probe. The 8.8 kb and 8.0 kb bands are indicative of the endogenous and targeted *Mus81* alleles, respectively. (**D**) Immuno-blot analysis of Mus81 expression. Using an anti-Mus81 antibody, the expression of Mus81 protein was analyzed in wild type, *Mus81$^{+/-}$*, and *Mus81$^{-/-}$* ES cells. Msh2 served as a loading control.

107

Cell lines	Wild type (IB10)				*Mus81*$^{-/-}$ (#113)				*Mus81*$^{-/-}$ (#258)			
Mitomycin C (µg/ml)	0	0	2.5	2.5	0	0	2.5	2.5	0	0	2.5	2.5
F-VAD-FMK (µM)	0	10	0	10	0	10	0	10	0	10	0	10

Intact DNA

Broken DNA
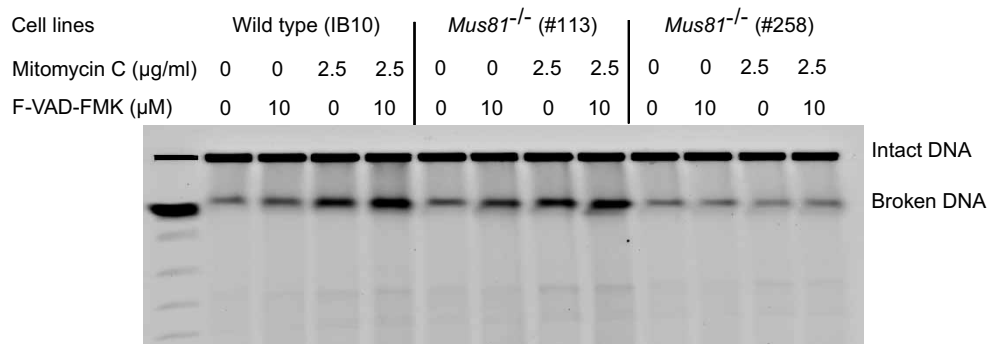
Supplemental Figure 2. Analysis of mitomycin C-induced DSB formation in wild type, *Mus81*$^{+/-}$ and *Mus81*$^{-/-}$ ES cells. Cells of the indicated genotype were incubated in the absence (-) or presence (+) of 2.5 µg/ml mitomycin C for 24 hrs, collected into agarose plugs and their DNA was electrophoresed through an agarose gel. In contrast to *Mus81*$^{-/-}$ ES cells, mitomycin C-induced DSBs could be observed in wild type and *Mus81*$^{+/-}$ ES cells. To demonstrate that the mitomycin C-induced DSBs were not due to chromosome fragmentation during apoptosis, the experiment was also performed in the presence of the Caspase 9 inhibitor V-ZAD-FMK (Gregoli and Bondurant, 1999). Under those conditions the amount of broken DNA upon mitomycin C treatment increased (compare lanes 3 and 5), indicating that mitomycin C-induced apoptosis actually decreased the signal observed. Thus, the DSBs induced by mitomycin C treatment were not due to the chromosome fragmentation during apoptosis. *Saccharomyces cerevisiae* chromosomes were used as molecular size markers in the lane on the left.
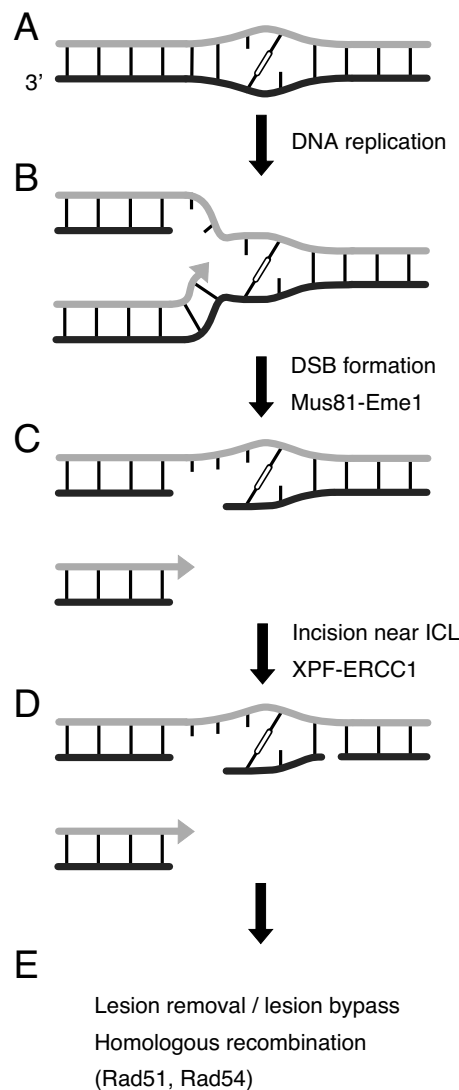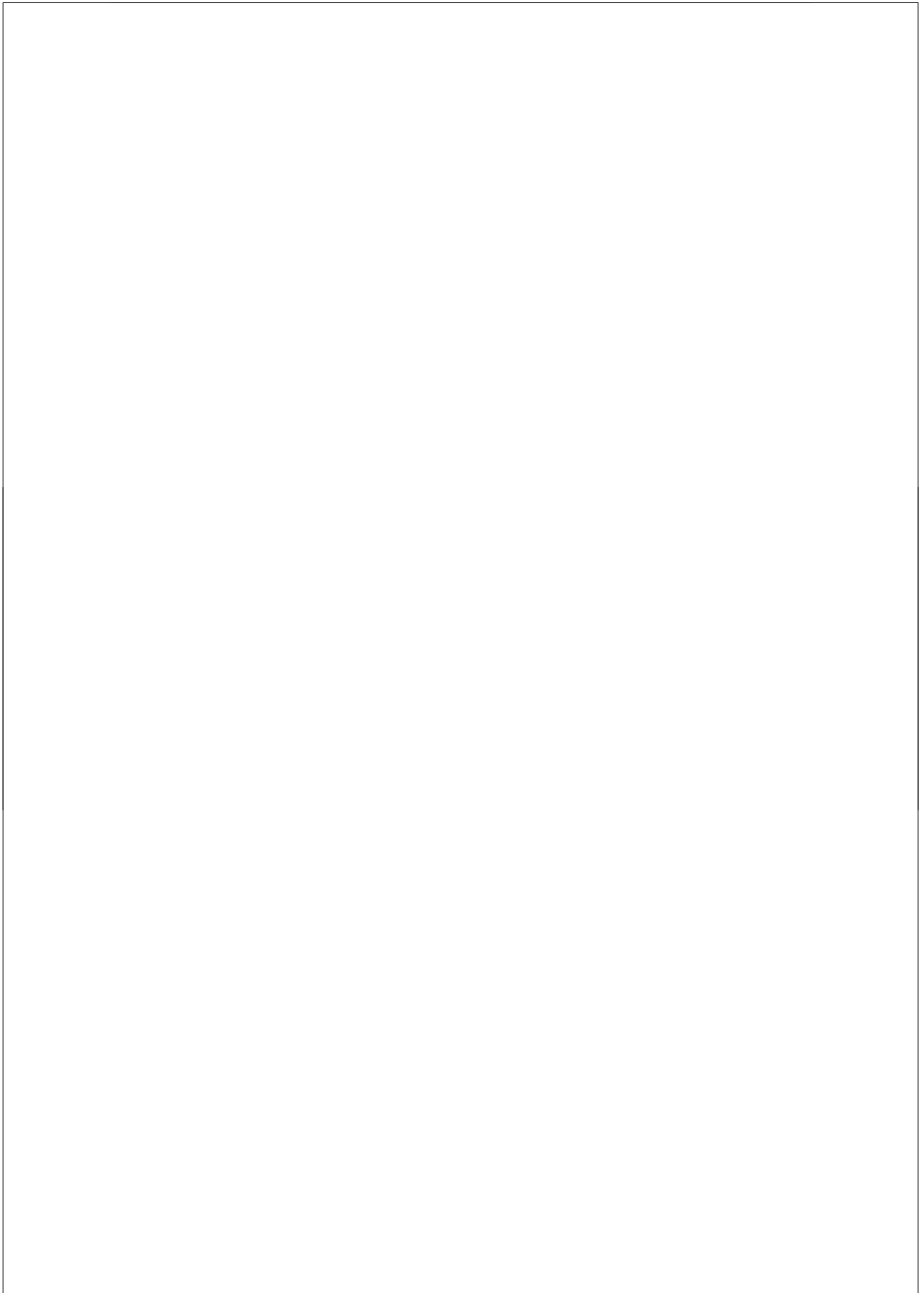
Supplemental Figure 3. Model for action of the Mus81-Eme1 and XPF-ERCC1 structure-specific endonucleases in ICL repair.
(**A**) The two strands of duplex DNA with the indicated polarity are represented by lines of different shades of gray. Basepairs and bases are indicated by the thin black lines. An ICL is depicted as the white box connecting two bases of the complementary strands. (**B**) A replication fork arriving at the ICL is stalled because the template strands cannot be unwound. The 3' end of the leading strand is indicated by the arrowhead. (**C**) The Mus81-Eme1 structure-specific endonuclease cleaves the leading strand template, resulting in a chromatid containing a double-strand end and a chromatid containing a single-strand gap as well as the ICL. (**D**) The ICL-containing chromatid is further processed by XPF-ERCC1 which incises at the replication distal side of the ICL. (**E**) The two substrates generated in this manner by the action of the two structure-specific endonucleases can now serve as substrates for homologous recombination and translesion DNA synthesis, as detailed in the text.

Supplementary References

Budzowska, M., Jaspers, I., Essers, J., de Waard, H., van Drunen, E., Hanada, K., Beverloo, B., Hendriks, R.W., de Klein, A., Kanaar, R., Hoeijmakers, J.H. and Maas, A. (2004) Mutation of the mouse Rad17 gene leads to embryonic lethality and reveals a role in DNA damage-dependent recombination. *EMBO J*, **23**, 3548-3558.

de Waard, H., de Wit, J., Gorgels, T.G., van den Aardweg, G., Andressoo, J.O., Vermeij, M., van Steeg, H., Hoeijmakers, J.H. and van der Horst, G.T. (2003) Cell type-specific hypersensitivity to oxidative damage in CSB and XPA mice. *DNA Repair (Amst)*, **2**, 13-25.

Essers, J., Hendriks, R.W., Swagemakers, S.M., Troelstra, C., de Wit, J., Bootsma, D., Hoeijmakers, J.H. and Kanaar, R. (1997) Disruption of mouse RAD54 reduces ionizing radiation resistance and homologous recombination. *Cell*, **89**, 195-204.

Gregoli, P.A. and Bondurant, M.C. (1999) Function of caspases in regulating apoptosis caused by erythropoietin deprivation in erythroid progenitors. *J Cell Physiol*, **178**, 133-143.

Niedernhofer, L.J., Essers, J., Weeda, G., Beverloo, B., de Wit, J., Muijtjens, M., Odijk, H., Hoeijmakers, J.H. and Kanaar, R. (2001) The structure-specific endonuclease Ercc1-Xpf is required for targeted gene replacement in embryonic stem cells. *EMBO J*, **20**, 6540-6549.

Tan, T.L., Essers, J., Citterio, E., Swagemakers, S.M., de Wit, J., Benson, F.E., Hoeijmakers, J.H. and Kanaar, R. (1999) Mouse Rad54 affects DNA conformation and DNA-damage-induced Rad51 foci formation. *Curr Biol*, **9**, 325-328.
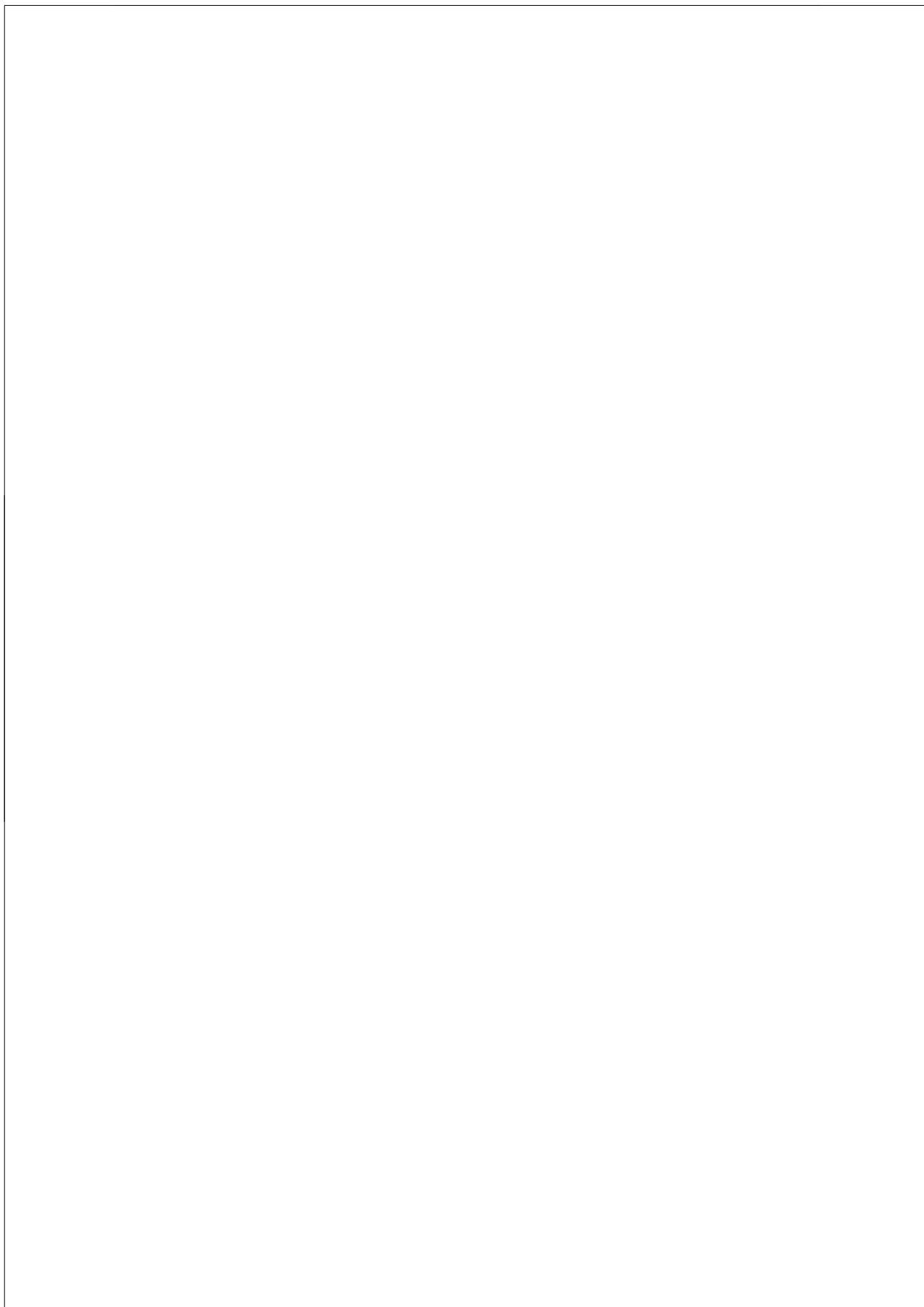
Chapter 5

The structure-specific endonuclease

Mus81 contributes to

replication restart by generating

double-strand DNA breaks

The structure-specific endonuclease Mus81 contributes to replication restart by generating double-strand DNA breaks

Katsuhiro Hanada[1,2], Magda Budzowska[1], Sally L Davies[2], Ellen van Drunen[3], Hideo Onizawa[1], H Berna Beverloo[3], Alex Maas[1], Jeroen Essers[1,4], Ian D Hickson[2] & Roland Kanaar[1,4]

Faithful duplication of the genome requires structure-specific endonucleases such as the RuvABC complex in *Escherichia coli*. These enzymes help to resolve problems at replication forks that have been disrupted by DNA damage in the template. Much less is known about the identities of these enzymes in mammalian cells. Mus81 is the catalytic component of a eukaryotic structure-specific endonuclease that preferentially cleaves branched DNA substrates reminiscent of replication and recombination intermediates. Here we explore the mechanisms by which Mus81 maintains chromosomal stability. We found that Mus81 is involved in the formation of double-strand DNA breaks in response to the inhibition of replication. Moreover, in the absence of chromosome processing by Mus81, recovery of stalled DNA replication forks is attenuated and chromosomal aberrations arise. We suggest that Mus81 suppresses chromosomal instability by converting potentially detrimental replication-associated DNA structures into intermediates that are more amenable to DNA repair.

An important challenge for all proliferating cells is to maintain genomic integrity during DNA replication so that genetic information can be faithfully transmitted to daughter cells. Damage in the template DNA, induced by exogenous or endogenous agents, interferes with DNA replication, thereby increasing the risk of genomic instability[1–4]. Among the most severe types of DNA damage are DNA double-strand breaks (DSBs), which can trigger chromosomal aberrations such as deletions, insertions and translocations[5,6]. Therefore, preventing DSBs from forming should contribute to the maintenance of genomic integrity.

Paradoxically, DSBs frequently occur at the sites of DNA replication forks[1,7]. For example, the RuvABC complex in *E. coli*, which has branch-migration and Holliday junction–cleavage activities, creates DSBs through cleavage near stalled DNA replication forks[8–10]. The broken DNA is efficiently repaired by DNA end processing involving the DNA helicase complex RecBCD, followed by RecA-mediated homologous recombination with the sister chromatid[11]. Another important function of homologous recombination is to recruit PriA and other DNA replication factors to recombination intermediates (D-loops) such that DNA replication can be re-initiated in an origin-independent manner[11–14]. Therefore, RuvABC-dependent DSB formation has been suggested to be a mechanism for recovery of stalled DNA replication forks and thereby to contribute to genomic stability[8,10]. Given the importance of maintaining genomic stability, it is

likely that eukaryotic cells have evolved similar mechanisms for the re-establishment of DNA replication forks after their progression has been impeded by lesions in the template. A subset of homologous recombination proteins are involved in break-induced replication, a recombination-dependent DNA replication process that is initiated at DSBs, in the yeast *Saccharomyces cerevisiae*[15–17]. However, it is not known whether eukaryotes contain enzymes that deliberately introduce DSBs at stalled DNA replication forks to stimulate the recovery of DNA replication.

Mus81 is the catalytic subunit of a structure-specific endonuclease that has a preference for cleaving branched DNA substrates, including structures that are reminiscent of replication and recombination intermediates such as 3′ flaps, 'Y'-shaped structures, D-loops and 'X'-shaped structures (Holliday junctions and nicked Holliday junctions)[18–25]. Mus81 forms a complex with Mms4 in *S. cerevisiae* and with Eme1 in *Schizosaccharomyces pombe*[19]. The Mus81–Eme1 complex has also been identified in mammalian cells, and it shows similar activities to those of its yeast counterparts[20,26–29]. In addition to Eme1, mammalian cells express an Eme1 homolog, named Eme2 (ref. 27). A connection between Mus81 and homologous recombination has been suggested from its interaction with the Rad54 homologous recombination protein in *S. cerevisiae*[30]. *S. cerevisiae* cells containing a mutated *mus81* gene are hypersensitive to UV light and methylmethanesulfonate (MMS), and with regard to these
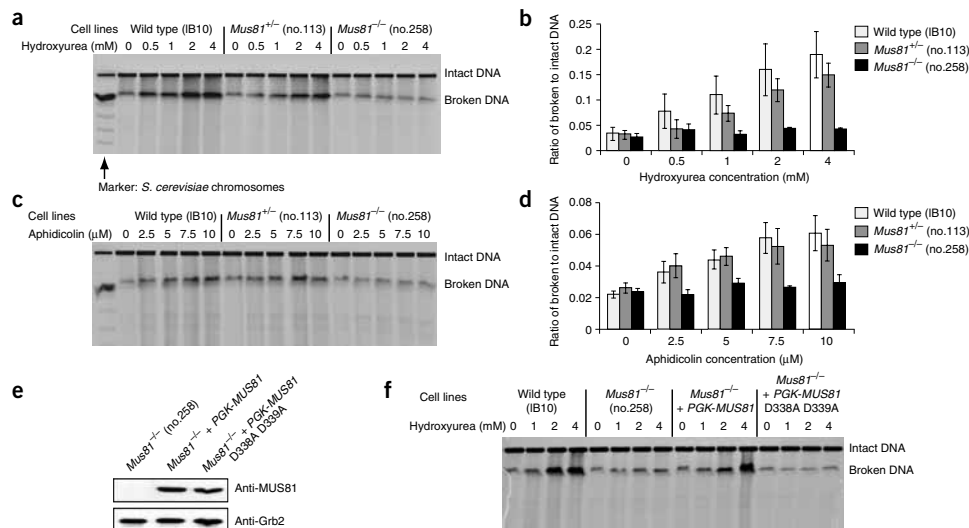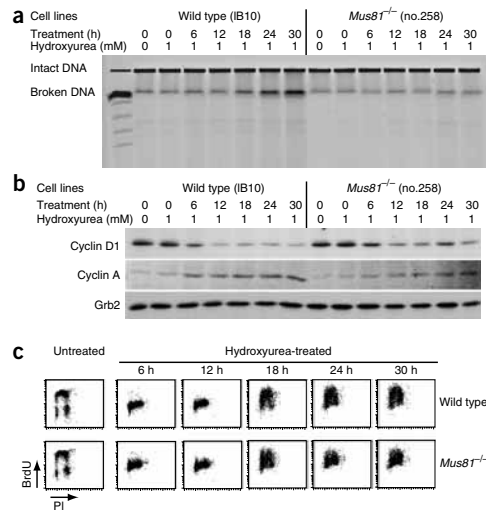
Figure 1 Analysis of DSB formation induced by DNA replication inhibitors in wild-type and *Mus81*-deficient mouse ES cells. (**a**) DSB formation in response to 24-h incubation with hydroxyurea, analyzed by PFGE. (**b**) Quantification of hydroxyurea-induced formation of broken DNA. The mean ratio of broken to total DNA from gels such as that in **a** was determined from four independent experiments. Error bars show s.e.m. (**c**) Analysis of DSB formation in response to 24-h treatment with aphidicolin. (**d**) Quantification of aphidicolin-induced formation of broken DNA. The ratio of broken to total DNA from gels such as that in **c** was determined from four independent experiments. Error bars show s.e.m. (**e**) Generation of *Mus81*−/− ES cells expressing human MUS81 cDNAs from the *PGK* promoter. *Mus81*−/− ES cells were transfected with cDNAs encoding wild-type MUS81 or nuclease-defective MUS81 containing two point mutations in the nuclease active site (D338A D339A). Clones stably expressing MUS81 were identified by immunoblotting using MUS81-specific antibodies. Antibodies to Grb2 served as a loading control. (**f**) Analysis of DSB formation in cells expressing nuclease-defective MUS81. Wild-type, *Mus81*−/− and *Mus81*−/− ES cells expressing wild-type MUS81 or MUS81 D338A D399A were incubated with hydroxyurea for 24 h and their DNA was analyzed by PFGE.

phenotypes, the *mus81* mutation is epistatic to a *rad54* mutation[30]. However, it is unlikely that Mus81–Mms4 is required for DSB repair through homologous recombination, because *mus81* mutants are not hypersensitive to γ-rays. *mms4* mutants show similar phenotypes as *mus81* mutants: sensitivity to MMS, UV light, hydroxyurea and 4-nitroquinoline-*N*-oxide. With regard to hypersensitivity to UV light and MMS, mutation of *MMS4* is epistatic to mutation of *RAD52*, which encodes another factor that is involved in homologous recombination[31]. Similarly, *S. pombe mus81* mutants show hypersensitivity to agents that impede DNA replication, such as UV light, MMS, hydroxyurea and camptothecin[19,32,33]. On the basis of the results of biochemical and genetic experiments, Mus81–Eme1 has been proposed to introduce DSBs through cleavage of stalled DNA replication forks that are subsequently repaired by homologous recombination[19,21,33]. Alternatively, on the basis of genetic experiments in *S. cerevisiae*, it is thought that Mus81–Mms4 may act downstream of homologous recombination on stalled replication-induced recombination intermediates[34]. However, physical evidence is lacking for nuclease-dependent broken chromosomal DNA in response to stalled replication and associated reestablishment of replication.

In addition to mutants in yeasts, *Mus81*- and *Eme1*-deficient mouse embryonic stem (ES) cells and a *MUS81*-decificient human cell line have been established by gene targeting[29,35–38]. Unexpectedly, neither *Mus81*- nor *Eme1*-deficient ES cells show sensitivity to UV light or

MMS. However, both *Mus81*- and *Eme1*-deficient ES cells are hypersensitive to interstrand DNA cross-linking agents such as mitomycin C and cisplatin. These results indicate that responses to stalled DNA replication forks in mammalian cells might not be identical to those in yeast, but that, at least under some specific conditions, Mus81–Eme1 could be involved in processing stalled DNA replication forks. One important observation is that both *Mus81*- and *Eme1*-deficient ES cells show higher than normal rates of chromosome instability, especially after treatment with mitomycin C[29,35–37]. In response to interstrand DNA cross-links, Mus81–Eme1 introduces DSBs. However, it is not clear whether these DSBs are important for the recovery of stalled replication[38]. Clearly, Mus81–Eme1 has a crucial role in maintaining genomic stability in the face of selective DNA lesions, but the mechanism through which Mus81–Eme1 maintains chromosomal stability has not been fully unraveled.

In this study, we addressed part of the mechanism that *Mus musculus* Mus81 uses to maintain chromosomal stability. After treatment with DNA replication inhibitors, chromosomes were analyzed in wild-type and *Mus81*−/− mouse ES cells using pulsed-field gel electrophoresis (PFGE) and DNA fiber techniques. Our results indicate that mammalian Mus81 is involved in DSB formation in response to replication inhibition by hydroxyurea and aphidicolin. In the absence of this chromosomal processing by Mus81, the recovery of stalled DNA replication forks is attenuated. We suggest that Mus81

Figure 2 Time course of DSB formation and cell-cycle analysis of wild-type and *Mus81*^{−/−} ES cells treated with hydroxurea. (**a**) Cells were treated with 1 mM hydroxyurea for the indicated times, and their DNA was analyzed using PFGE. (**b**) Cells were treated with 1 mM hydroxyurea for the indicated times and analyzed for expression of cyclin D1 and cyclin A by immuno-blotting. Grb2 was used as a loading control. (**c**) Cell-cycle profiles of wild-type and *Mus81*^{−/−} ES cells after exposure to 1 mM hydroxyurea for the indicated times were analyzed using a FACscan. Cells were pulsed-labeled with BrdU and analyzed for total DNA content by propidium iodide (PI) staining (*x*-axis) and replication status by BrdU incorporation (*y*-axis).

Mus81^{−/−} ES cells expressing a nuclease-defective version of human MUS81 (ref. 20) (**Fig. 1e,f**). By contrast, expression of a complementary DNA encoding the wild-type human MUS81 protein did result in induction of DSBs by hydroxyurea.

To confirm that the PFGE method specifically detected DSBs, we measured the amount of single-stranded DNA breaks by alkaline gel electrophoresis (**Supplementary Methods** and **Supplementary Fig. 1** online). The amount of single-stranded DNA breaks induced by the replication inhibitors was comparable for all cell lines, irrespective of their Mus81 status. To show that the DSBs induced by the replication inhibitors were not due to chromosome fragmentation during apoptosis, we also performed the experiment in the presence of the caspase-9 inhibitor Z-VAD-FMK (**Supplementary Fig. 2** online). Under those conditions, the amount of broken DNA found after treatment with hydroxyurea or aphidicolin was similar to that observed in the absence of the apoptosis inhibitor.

Next, we determined the time course of Mus81-dependent DSB induction upon replication inhibition (**Figs. 2** and **3**). If Mus81 acts on stalled replication forks or stalled replication-induced recombination intermediates, then the induction of DSBs by hydroxyurea and aphidicolin should be slow, in contrast to DSB induction by agents that directly act on DNA, such as ionizing radiation. Indeed, in wild-type ES cells cultured in the presence of 1 mM hydroxyurea or 5 μM aphidicolin, DSB induction became apparent only after 18 h and
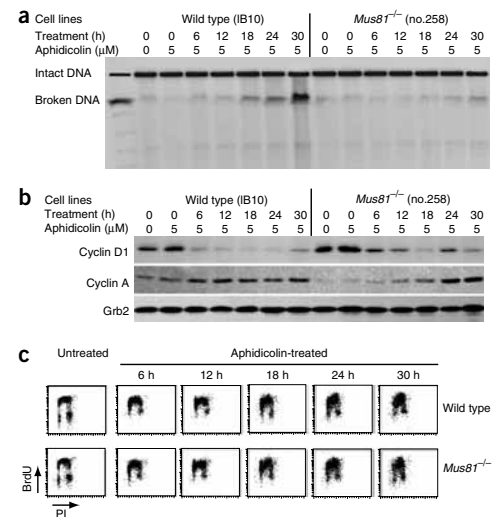
contributes to the suppression of chromosomal instability by converting potentially detrimental replication-associated DNA structures into intermediates for DNA repair.

RESULTS

DSBs induced by replication inhibitors are Mus81-dependent

To address whether the Mus81 protein is involved in cleaving stalled DNA replication forks, we treated wild-type, *Mus81*^{+/−} and *Mus81*^{−/−} ES cells with replication inhibitors and used PFGE to compare the amounts of DSBs that were induced (**Fig. 1**). We used two replication inhibitors: hydroxyurea, which inhibits ribonucleotide reductase and thereby depletes cellular dNTP pools, and aphidicolin, which is a direct inhibitor of at least five DNA polymerases, including replicative DNA polymerases α and ε. Treatment of cells with either compound results in DSBs at DNA replication sites[1,7,39]. After 24 h of continuous treatment with either hydroxyurea or aphidicolin, DSBs were induced in both wild-type and *Mus81*^{+/−} ES cells (**Fig. 1a,c**). By contrast, there was no such induction of DSBs in *Mus81*^{−/−} ES cells. Quantification of the relative amount of broken versus intact chromosomal DNA from four independent experiments revealed that whereas DSB induction by the replication inhibitors showed a concentration-dependent increase in Mus81-proficient ES cells, there was no detectable induction of DSBs in *Mus81*^{−/−} ES cells even at the highest dose of inhibitor (**Fig. 1b,d**). We detected no induction of Mus81-dependent DSB formation upon DNA replication stalling in

Figure 3 Time course of DSB formation and cell-cycle analysis of wild-type and *Mus81*^{−/−} ES cells in response to aphidicolin. (**a**) Cells were treated with 5 μM aphidicolin for the indicated times and their DNA was analyzed using PFGE. (**b**) Cells were treated with 5 μM aphidicolin for the indicated times and analyzed for expression of cyclin D1 and cyclin A by immuno-blotting. Grb2 was used as a loading control. (**c**) Cell-cycle profiles of wild-type and *Mus81*^{−/−} ES cells after exposure to 5 μM aphidicolin for the indicated times were analyzed using a FACscan. Cells were pulsed-labeled with BrdU and analyzed for total DNA content by propidium iodide (PI) staining (*x*-axis) and replication status by BrdU incorporation (*y*-axis).

Figure 4 Sensitivity of wild-type and *Mus81*$^{-/-}$ ES cells to hydroxyurea, aphidicolin and ionizing radiation. (**a**) Survival curves in response to increasing doses of hydroxyurea for wild-type, *Mus81*$^{+/-}$ and *Mus81*$^{-/-}$ ES cells. (**b**) Survival curves in response to increasing doses of aphidicolin for wild-type, *Mus81*$^{+/-}$ and *Mus81*$^{-/-}$ ES cells. (**c**) Survival curves in response to increasing doses of hydroxyurea for wild-type and *Mus81*$^{-/-}$ ES cells and for *Mus81*$^{-/-}$ ES cells expressing either wild-type or nuclease-defective (D338A D339A) human MUS81. (**d**) Survival curves in response to increasing doses of ionizing radiation for wild-type, *Mus81*$^{+/-}$ and *Mus81*$^{-/-}$ ES cells. *Rad54*$^{-/-}$ cells served as a control. Data in **a**–**d** are means of three experiments; error bars show s.e.m. (**e**) ES cells of the indicated genotype were treated with 0, 10 or 20 Gy of ionizing radiation and their DNA was analyzed using PFGE either immediately after irradiation or after a 2-h recovery period.
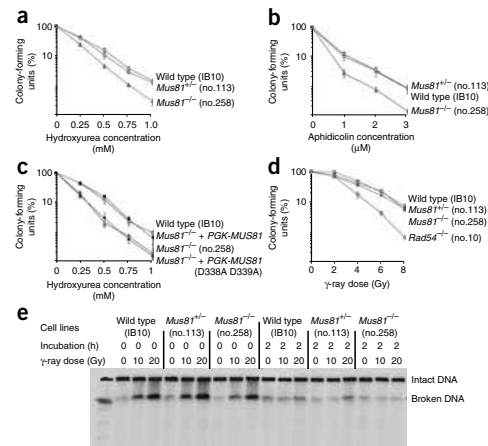
subsequently increased over time (**Fig. 2a** and **Fig. 3a**). Again, no DSBs were induced in *Mus81*$^{-/-}$ ES cells, even after 30 h of incubation with the DNA replication inhibitors. By contrast, DSBs induced by ionizing radiation appeared immediately upon irradiation and in a Mus81-independent manner (see below). Upon incubation of the cells for 2 h after irradiation, the amount of broken DNA returned to background levels in all cell lines, indicating that both the formation and the repair of DSBs induced by ionizing radiation are independent of Mus81.

To show that hydroxyurea and aphidicolin inhibited DNA replication in mouse ES cells, we analyzed the cell-cycle profile of the cells. ES cells cultured in the presence of hydroxyurea or aphidicolin accumulated in S phase, as shown by a reduction in cyclin D1 and a concomitant increase in cyclin A expression (detected by immunoblotting) (**Fig. 2b** and **Fig. 3b**). Furthermore, two-parameter FACS analysis, which assessed the replication status of the cells by comparing bromodeoxyuridine (BrdU) incorporation to their total DNA content, showed that the cells accumulated in S phase (**Fig. 2c** and **Fig. 3c**) and that the hydroxyurea treatment resulted in a more stringent replication inhibition than the aphidicolin treatment. Notably, after 18 h of incubation, the cells were able to incorporate nucleotides again in a

Mus81-independent manner. This effect was particularly apparent after hydroxyurea treatment.

To test whether the Mus81-dependent formation of DSBs upon the addition of DNA replication inhibitors is physiologically relevant, we tested the sensitivity of Mus81-proficient and Mus81-deficient ES cells to killing by hydroxyurea and aphidicolin. Cells were treated with increasing concentrations of hydroxyurea or aphidicolin for 24 h and incubated in fresh medium for 6–8 d, and their colony-forming ability was then assessed (**Fig. 4**). *Mus81*$^{-/-}$ ES cells were more sensitive to both of these drugs than wild-type or *Mus81*$^{+/-}$ ES cells (**Fig. 4a,b**), and this protective effect of Mus81 seemed to depend on the nuclease activity of Mus81 (**Fig. 4c**). Consistent with their overt lack of a DSB-processing defect upon irradiation, *Mus81*$^{-/-}$ ES cells were not sensitive to ionizing radiation (**Fig. 4d,e**). On the basis of these results, we conclude that Mus81, through its structure-specific endonuclease activity, is involved in the formation of DSBs when DNA replication forks are stalled by the replication inhibitors hydroxyurea and aphidicolin.

Reduced recovery of stalled replication in *Mus81*$^{-/-}$ ES cells

We have shown that Mus81 is involved in the formation of DSBs in response to stalled DNA replication forks. To determine whether Mus81-dependent processing influences the reactivation of stalled DNA replication forks, we measured the efficiency of replication recovery using the DNA fiber technique[40]. For this purpose, we visualized DNA replication sites using two differentially modified
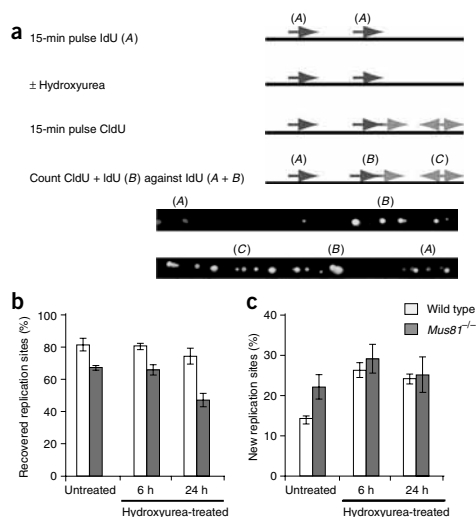

Figure 5 Recovery of DNA replication after treatment with hydroxyurea. (**a**) Outline of the protocol used to measure replication recovery after treatment with hydroxyurea, and an example of labeled replication tracks. The efficiency of DNA replication recovery was estimated by dividing the number of CldU- and IdU-containing tracks (*B*) by the total number of IdU-containing tracks (*A* + *B*). (**b**) Reduced recovery of DNA replication in *Mus81*$^{-/-}$ ES cells. Wild-type and *Mus81*$^{-/-}$ ES cells were treated with 0.5 mM hydroxyurea for 6 or 24 h. After the treatment, the cells were incubated in CldU-containing medium. Error bars show s.e.m. (**c**) Quantification of sites of newly initiated replication at the indicated times after removal of the hydroxyurea. The percentage of newly initiated replication was determined by dividing the number of CldU-containing tracks (*C*) by the number total of tracks (*A* + *B* + *C*).
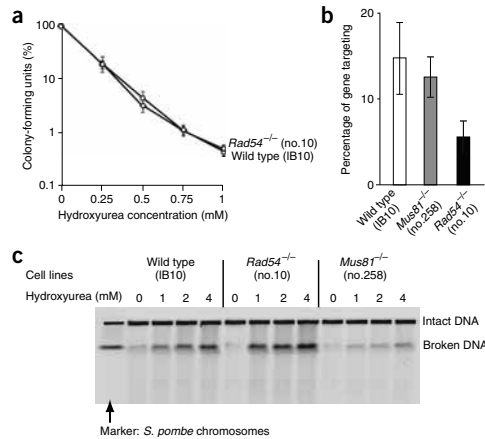
Figure 6 Response of $Rad54^{-/-}$ ES cells to hydroxyurea. (a) Survival curves in response to increasing doses of hydroxyurea for wild-type and $Rad54^{-/-}$ ES cells. (b) Determination of homologous recombination efficiency. Cells were electroporated with a DNA construct that results in GFP expression only when it homologously integrates into the $Rad54$ locus. The percentage of cells undergoing homologous gene targeting is a measure of homologous recombination efficiency and was determined by FACS analysis. Data in a and b are means of three experiments; error bars show s.e.m. (c) DSB formation in response to hydroxyurea was analyzed by PFGE. Cells were incubated with 0, 1, 2 or 4 mM hydroxyurea for 24 h and the amount of broken DNA was assessed. *S. pombe* chromosomes were run in parallel as molecular size markers in the left-hand lane.

nucleoside analogs, iododeoxyuridine (IdU) and chlorodeoxyuridine (CldU). First, DNA replication sites were labeled with IdU (15 min) and then the cells were treated with 0.5 mM hydroxyurea for 24 h to induce replication fork stalling. After the treatment, cells were washed with PBS and incubated for 15 min in fresh medium with CldU. To visualize sites of DNA replication, we prepared chromosomal DNA fragments on glass slides and used specific antibodies to detect the modified nucleosides that were incorporated into the chromosomal DNA (Fig. 5a). Tracks containing IdU (red in Fig. 5a) represent all sites of DNA replication that were active before treatment with hydroxyurea. CldU-containing tracks (green in Fig. 5a) represent the sites where DNA synthesis is still active after the removal of hydroxyurea. If this new DNA synthesis occurs at sites of previously stalled DNA replication forks, CldU-containing tracks will colocalize with IdU-containing tracks (yellow dots in Fig. 5a). We counted CldU- and IdU-containing tracks as well as the total number of IdU-containing tracks and determined the recovery of DNA synthesis from stalled DNA replication sites (Fig. 5b). In untreated wild-type ES cells, 81% ± 9.9% of IdU-containing tracks colocalized with CldU. Notably, even in the absence of external perturbation, replication recovery was reduced in $Mus81^{-/-}$ ES cells, as only 67% ± 2.9% of the IdU-containing tracks colocalized with CldU. This value is significantly lower than that that for wild-type ES cells ($P < 0.015$). After a 24-h treatment with hydroxyurea to induce replication fork stalling, 74% ± 11% of the replication sites recovered DNA synthesis in wild-type ES cells. By contrast, only 47% ± 9.4% of the replication sites recovered in the absence of Mus81. The recovery efficiency in $Mus81^{-/-}$ ES cells was significantly lower than in wild-type ES cells after 24 h of

treatment ($P < 0.002$) and was also lower than that in untreated $Mus81^{-/-}$ ES cells ($P < 0.002$). There was no significant difference in the initiation of new replication events after removal of the hydroxyurea between wild-type and $Mus81^{-/-}$ ES cells ($P = 0.56$ for the 6 h time point and $P = 0.86$ for the 24 h time point; Fig. 5c). Our results indicate that the recovery of stalled DNA replication is reduced in $Mus81^{-/-}$ ES cells.

Response of Rad54 and Rad51 to replication stalling

Interaction of Mus81 with homologous recombination, a process that has been implicated in replication restart[4,11,17], has been revealed in *S. cerevisiae* through the interaction between Mus81 and Rad54 (ref. 30). These proteins also interact in mammalian cells and seem to function in the same pathway for repair of interstrand DNA cross-links[38]. Therefore, we tested whether Rad54 is also involved in the cellular response to stalled DNA replication (Fig. 6). However, $Rad54^{-/-}$ ES cells were no more sensitive to treatment with hydroxyurea than were wild-type ES cells (Fig. 6a). Furthermore, hydroxyurea-induced DSB formation was not affected in $Rad54^{-/-}$ ES cells (Fig. 6c). Conversely, whereas Rad54 is required for the homologous recombination pathway that mediates homologous gene targeting, Mus81 is not (Fig. 6b)[35]. However, the core protein of homologous recombination, Rad51, did form foci in response to hydroxyurea treatment in a dose- and time-dependent manner (Fig. 7a). Labeling sites of DNA replication by the addition of IdU 30 min before exposure to hydroxyurea resulted in the colocalization of IdU and Rad51, as detected by antibody staining (Fig. 7b). Thus, the local accumulations of Rad51 corresponded to sites were DNA replication was occurring before the addition of hydroxyurea.

Figure 7 Rad51 focus formation and colocalization in response to hydroxyurea. (a) Rad51 focus formation. Wild-type and $Mus81^{-/-}$ ES cells were treated with the indicated concentrations of hydroxyurea, fixed at the indicated time points, stained with Rad51-specific antibodies and analyzed by immunofluorescence detection. Data are means of three experiments; error bars show s.e.m. (b) Colocalization of Rad51 with sites of stalled replication. Wild-type ES cells were labeled with IdU for 30 min, after which the cells were incubated in IdU-free medium containing 1 mM hydroxyurea. After 24 h cells were fixed, stained with IdU- and Rad51-specific antibodies and analyzed by immunofluorescence detection.
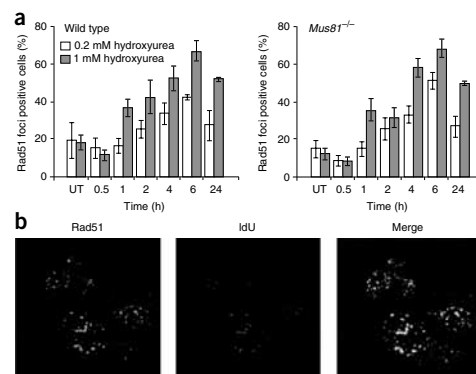
Figure 8 Chromosomal aberrations after treatment with hydroxyurea in wild-type and $Mus81^{-/-}$ ES cells. (**a**) Metaphase spreads from $Mus81^{-/-}$ ES cells treated with 0.5 mM hydroxyurea for 24 h and incubated in fresh medium for 24 h. (**b**) Frequency of chromosomal breaks and gaps after treatment with hydroxyurea. Treated cells were incubated in fresh medium with BrdU and fixed after 24 h. Chromosomes were stained with acridine orange to distinguish metaphase spreads from the first and second cell divisions. Error bars, s.d.

Mus81 prevents hydroxyurea-induced chromosomal aberrations

The hypersensitivity of $Mus81^{-/-}$ ES cells to DNA damage and their lack of hydroxyurea-induced DSB formation indicates a defective response to stalled DNA replication, which could lead to the accumulation of chromosomal abnormalities and genomic instability. We therefore compared the amounts of spontaneous and hydroxyurea-induced chromosomal aberrations in wild-type and $Mus81^{-/-}$ ES cells. Analysis of acridine orange–stained metaphase spreads revealed increased numbers of chromosomal abnormalities, including breaks, gaps, fragments, chromosomal fusions and dicentric chromosomes, in $Mus81^{-/-}$ ES cells (**Fig. 8** and **Supplementary Table 1** online). In the first metaphase after hydroxyurea treatment, chromosomal aberrations were observed in both wild-type and $Mus81^{-/-}$ ES cells. $Mus81^{-/-}$ ES cells showed more aberrations than did wild-type ES cells, but this difference was not statistically significant ($P = 0.38$). Notably, many more aberrations were present in metaphase chromosomes from the second division after hydroxyurea treatment in $Mus81^{-/-}$ ES cells than in wild-type ES cells. These results highlight an important role of Mus81 in maintaining genomic stability, especially after DNA replication problems.

DISCUSSION

To transmit genetic information accurately to daughter cells, it is vital that cells maintain genomic integrity during DNA replication. However, exogenous and endogenous DNA-damaging agents can disturb the translocation of replication forks, leading to replication fork stalling. Many enzymes involved in processing these stalled forks are known in *E. coli*[11–13,41]. For example, stalled forks can be acted upon by DNA structure–specific modifying enzymes such as the branch-migration and Holliday junction–resolution complex, RuvABC, and the helicase/nuclease complex RecBCD[8,42,43]. These enzymes generate and/or process DSBs from stalled replication forks, so that replication can be restarted in an origin-independent manner, using the homologous recombination machinery and specific replication restart proteins such as PriA[11,13,44]. In this manner, the transient DSB intermediate prevents the stalled replication fork from causing genomic instability. Much less is known about the identity of the enzymes that are involved in this process in mammalian cells. Here, we set out to investigate whether mammalian cells contain an enzyme that can introduce DSBs in response to the stalling of replication forks in a manner that would be important for the resumption of replication. Given its structure specificity, we focused on Mus81, the catalytic component of a heterodimeric endonuclease.

Mus81–Eme1 can cleave branched DNA substrates that mimic DNA replication forks and homologous recombination intermediates[19–25]. Previous studies have indicated two possible roles for Mus81–Eme1, which are not mutually exclusive. One is that Mus81–Eme1 is involved in the cleavage of homologous recombination intermediates, such as D-loops and Holliday junctions[19,23,24]. The other is that Mus81–Eme1 processes stalled DNA replication forks[19,22]. So far, only limited *in vivo* evidence of this processing has been reported, but it has been suggested that Mus81–Eme1 cleaves stalled DNA replication forks to stimulate DNA replication recovery[19,20,22,26] or acts on DNA structures generated by homologous recombination in response to stalled replication[34]. However, the mechanism by which Mus81–Eme1 maintains chromosomal stability is still unclear. Therefore, we tested whether Mus81 can generate DSBs in response to stalled forks and whether it promotes resumption of DNA replication from stalled forks and determined the type of chromosomal aberrations that accumulate in its absence in response to replication inhibitors.

DSB formation in response to stalled DNA replication forks

Treatment of cells with either hydroxyurea or aphidicolin results in the formation of DSBs at the sites of DNA replication forks[1,7,39]. Treatment with either hydroxyurea or aphidicolin for 24 h induced DSBs in both wild-type and $Mus81^{+/-}$ ES cells (**Fig. 1a,c**). However, no such induction of DSBs was detected in $Mus81^{-/-}$ ES cells. This result indicates that DSB formation is an active process and not the consequence of unprogrammed fork collapse. Moreover, this result indicates that Mus81 is essential for the formation of DSBs in response to stalled replication forks. These Mus81-dependent DSBs accumulated between 18 and 30 h after the onset of treatment with either hydroxyurea or aphidicolin (**Fig. 2a** and **Fig. 3a**), which is slow for a DNA damage response. It is reasonable to suggest that Mus81-dependent processing is a late response to the stalling of replication forks, because DSB formation introduces a risk of promoting genomic instability. Only when other attempts to overcome stalled replication, including those that do not use a DSB intermediate, have been exhausted does the Mus81-dependent pathway become activated. This notion is consistent with the observation that acute hydroxyurea exposure of *S. pombe* cells, which are hypersensitive to chronic hydroxyurea exposure, leads to dissociation of Mus81 from chromatin, thereby suppressing its activity[45]. There are multiple pathways for the recovery of DNA replication from stalled forks. ES cells, after 18 h in hydroxyurea, can initiate the incorporation of nucleotides into DNA in a Mus81-independent manner (**Fig. 2c**); this indicates that they can adapt to smaller nucleotide pools and activate replication, at least a subset of forks, through a replication restart pathway that does not require DSBs. One Mus81-independent replication restart pathway that acts at early times after fork arrest is the one that requires the BLM helicase. In the absence of BLM, a deficiency in replication restart is manifested as early as 2 h after replication arrest induced by hydroxyurea or aphidicolin[46].

Mus81-dependent recovery of stalled DNA replication forks

Although we had shown that Mus81 is involved in DSB formation in response to stalled DNA replication forks, it was unclear whether

Mus81-dependent processing is required for the repair of stalled replication forks. To address this, we measured the efficiency of DNA replication recovery using the DNA fiber technique. Previous studies have shown that the DNA fiber technology is a powerful approach by which to analyze the dynamics of DNA replication[40]. To analyze the recovery of stalled DNA replication forks, we blocked replication using hydroxyurea and then determined the efficiency of replication recovery after removal of the hydroxyurea. Notably, for untreated cells, replication recovery is lower in $Mus81^{-/-}$ ES cells than in wild-type ES cells (**Fig. 5b**). This is to be expected, as endogenous DNA damage will also lead to stalled replication forks. When $Mus81^{-/-}$ ES cells were treated with hydroxyurea for 24 h, the efficiency of replication recovery was markedly reduced compared with untreated $Mus81^{-/-}$ ES cells (**Fig. 5b**). No such difference was observed for wild-type ES cells. These results indicate that Mus81-dependent processing of stalled forks is involved in the replication recovery process. No appreciable difference in the efficiency of replication recovery was observed in $Mus81^{-/-}$ ES cells that had been exposed to hydroxyurea for only 6 h rather than 24 h (**Fig. 5b**). This observation correlates with the lack of hydroxyurea-induced DSB formation in ES cells exposed to hydroxyurea for only 6 h and is consistent with the notion that Mus81 is involved in a late-acting replication recovery process.

Recombination proteins at sites of stalled replication

In addition to promoting DSB formation during hydroxyurea- and aphidicolin-induced stalled replication, Mus81 is also involved in processing interstrand DNA cross-links into DSBs[38]. During interstrand DNA cross-link repair, Mus81 has been linked to homologous recombination–mediated DNA repair through physical and genetic interactions with Rad54 (ref. 38). However, our results reveal that Mus81 and Rad54 are not obligatory functional partners. Although $Mus81^{-/-}$ ES cells are hypersensitive to hydroxyurea (**Fig. 4a**), $Rad54^{-/-}$ ES cells are not (**Fig. 6a**). Conversely, although Rad54 is involved in homologous gene targeting[47], Mus81 does not influence this homologous recombination pathway (**Fig. 6b**)[35]. These results indicate that the subpathways of homologous recombination that require Rad54 are not vital for promoting DNA replication restart under the conditions tested here. However, homologous recombination is important in processing stalled replication forks[11]. Indeed, stalling DNA replication by treatment with hydroxyurea induces the formation of Rad51 nuclear foci at sites of stalled replication (**Fig. 7**).

DNA replication–associated chromosomal aberrations

Our results indicate that Mus81 acts on DNA structures that are formed in response to stalled DNA replication forks and generates single-ended DSBs. Although DSB formation introduces an additional risk for chromosomal integrity, it can also greatly encourage DNA break–dependent recovery of DNA replication forks, which is beneficial in preventing chromosomal aberrations. Thus, if Mus81-dependent processing is not functional under conditions that cause DNA replication forks to stall, DNA replication will be compromised (**Supplementary Fig. 3** online). Unreplicated regions will cause chromatid breaks and gaps during mitosis when the partially replicated sister chromatids are disjoined in anaphase. If these cells survive and enter the next cell cycle, their chromosomes will contain single-strand breaks and gaps, which will be converted into DSBs in S phase. At the subsequent metaphase, the number of chromosomal breaks and gaps should therefore be much higher in $Mus81^{-/-}$ ES cells than in wild-type ES cells, and this is what we observed (**Fig. 8**). This idea has also been invoked to explain why $mus81\Delta$ S. pombe cells are

not particularly hypersensitive to acute hydroxyurea exposure, compared to chronic exposure[45].

In summary, our results indicate that Mus81 is involved in reestablishing active replication forks by introducing DSBs in response to the stalling of forks *in vivo*. The chromosomal aberrations that arise in its absence can be suppressed by establishing active replication forks from the one-ended DSBs that would result from Mus81 cleavage, using homologous recombination[7,15,16,19,22,24]. Alternatively, Mus81 might not cleave the stalled forks directly, but might require homologous recombination to generate its substrate from stalled forks[34]. Our observation that replication stalling induces Rad51 foci in a Mus81-independent manner (**Fig. 7a**) is consistent with this possibility. This might limit the genotoxicity of the DSB intermediate in replication restart because Rad51, a pivotal DSB repair protein, would already be localized near the site where the nuclease activity of Mus81 is required.

METHODS

Cells and cell culture. The genotypes of the mouse ES cells used in this study are listed in **Supplementary Table 2** (online). The cells were cultured on gelatin-coated dishes in a 1:1 mixture of DMEM and buffalo rat liver (BRL) conditioned medium, supplemented with 10% (v/v) FBS (Hyclone), 0.1 mM nonessential amino acids (Biowhittaker), 50 μM β-mercaptoethanol (Sigma) and 500 U ml^{-1} leukemia inhibitory factor. We generated $Mus81^{-/-}$ ES cells expressing wild-type and nuclease-defective human MUS81 by transfecting the cells with cDNA constructs encoding wild-type and nuclease-defective MUS81 from the phosphoglycerate kinase (PGK) promoter. We analyzed isolated clones for stable MUS81 expression by immunoblotting using a monoclonal MUS81-specific antibody (ab14387, Abcam). The nuclease-defective version of MUS81 was made using PCR with the primers 5′-CGGCTAGCCGCCCTTTG CAGCAGCATCATCGACGG and 5′-AAGGGCGGCTAGCCGCTTGCGCTCC ACAATGTGATCC, which change the aspartate codons in MUS81 at positions 338 and 339 into alanine codons. Constructs were checked by DNA sequence analysis.

Miscellaneous methods. For the analysis cell-cycle phase using immunoblotting, we used the following antibodies: mouse monoclonal antibody to cyclin A (E23.1, ab38, Abcam), mouse monoclonal antibody to cyclin D1 (DCS6, cat. no. 2926, Cell Signaling Technology, Inc.) and mouse monoclonal antibody to GRB2 (cat no. 610112, BD Biosciences). Detection of Rad51 foci, FACS analysis and the homologous gene targeting assay were performed as described[29,38,48].

Pulsed-field gel electrophoresis. Subconfluent cultures of ES cells were treated with hydroxyurea or aphidicolin for 24 h or were irradiated with γ-rays (^{137}Cs source, 0.8 Gy min^{-1}). Cells were harvested by trypsinization, and agarose plugs of 10^6 cells were prepared with a CHEF disposable plug mold (BioRad). We incubated the plugs in lysis buffer (100 mM EDTA, 1% (w/v) sodium lauryl sarcosyne, 0.2% (w/v) sodium deoxycholate, 1 mg ml^{-1} proteinase K) at 37 °C for 48 h and then washed them four times in TE buffer (10 mM Tris-HCl (pH 8.0), 100 mM EDTA) before loading them onto an agarose gel. Electrophoresis was performed for 23 h at 13 °C in 0.9% (w/v) agarose containing 250 mM Tris-borate with EDTA (TBE) using a Biometra Rotaphor apparatus with the following parameters: voltage 180–120 V log; angle from 120° to 110° linear; interval 30 s to 5 s log. Under the electrophoresis conditions used, high–molecular weight genomic DNA (more than several million base pairs (bp)) remains in the well, whereas lower–molecular weight DNA fragments (several Mbp to 500 kbp) migrate into the gel and are compacted into a single band. Either S. cerevisiae or S. pombe chromosomes were run in parallel as molecular size markers. The gel was stained with ethidium bromide and analyzed using a Typhoon 9200 scanner (Amersham). Band intensities were quantified using ImageQuant 5.2 software (GE Healthcare). The amount of broken DNA was calculated as the intensity of DNA in the migrated fraction over the intensity of DNA in the well and the migrated fraction.

Replication labeling and DNA fiber spreads. Cells were labeled with 20 μM IdU for 15 min and then incubated with 50 μM thymidine for 15 min to chase

out the IdU. After pre-labeling, the cells were treated with 0.5 mM hydroxyurea for 0, 6 or 24 h, and the cells were then incubated with 100 μM CldU for 15 min. DNA spreads were made as described[41], with certain modifications. Briefly, the cells were trypsinized and resuspended in PBS at 2.5×10^5 cells per ml. The labeled cells were diluted 1:8 with unlabeled cells, and 2.5 μl of cells were mixed with 7.5 μl of lysis buffer (200 mM Tris-HCl (pH 7.5), 50 mM EDTA, 0.5% (w/v) SDS) on a glass slide. After 8 min, the slides were tilted at 15°, and the resulting DNA spreads were air-dried, fixed in 3:1 methanol/acetic acid and refrigerated overnight. The slides were treated with 2.5 M HCl for 1 h and then neutralized in 0.1 M $Na_2B_4O_7$ (pH 8.5). Slides were washed several times in PBS and were blocked in 1% (w/v) BSA and 0.1% (v/v) Tween 20. The slides were then incubated at 37 °C with the following antibodies, rinsed three times in PBS with 0.1% (v/v) Tween 20, and then washed three times for 20 min in blocking buffer between each incubation: first, for 1 h in 1:40 rat anti-bromodeoxyuridine (detects CldU; Abcam BU1/75); second, for 45 min in 1:200 Alexafluor 488-conjugated anti-rat (Molecular Probes A11006); third, for 1 h in 1:2 mouse anti-bromodeoxyuridine (detects IdU; Becton Dickinson B44). To increase the specificity, slides were washed with high-salt buffer (28 mM Tris-HCl, 500 mM NaCl, 0.5% (v/v) Tween-20). After the high-salt wash, slides were washed with PBS containing 0.1% (v/v) Tween-20 and then incubated for 45 min with Cy3-conjugated anti-mouse IgG (Sigma C-2181, 1:1800 dilution). Microscopy was carried out using a Zeiss Axioskop 2 plus microscope. The significance of the difference between the means was determined by Student's *t*-test.

Chromosome and sister-chromatid exchange analysis. Wild-type and $Mus81^{-/-}$ ES cells were exposed to 0.5 mM hydroxyurea for 24 h. The cells were washed and incubated in medium containing BrdU (10 μg ml^{-1}). After 24 h, the cells were harvested by trypsinization and prepared for analysis of metaphases as described[49]. Metaphases from spreads were scored as being in either the first or second division, on the basis of the differential staining patterns of sister chromatids with acridine orange.

Colony survival assays. The sensitivity of ES cells to increasing doses of DNA-damaging agents was determined by measuring their colony-forming ability. ES cells of the indicated genotypes were trypsinized and counted. Various cell dilutions were plated onto gelatin-coated, 60-mm dishes. After 4–16 h, cells were incubated for 24 h in drug-containing media. We determined sensitivity to ionizing radiation by comparing the colony-forming ability of ES cells after irradiation with a ^{137}Cs source. Cells were grown for 5–8 d, fixed and stained, and colony numbers were counted. All measurements were performed in triplicate.

Note: Supplementary information is available on the Nature Structural & Molecular Biology website.

1. Saintigny, Y. *et al.* Characterization of homologous recombination induced by replication inhibition in mammalian cells. *EMBO J.* **20**, 3861–3870 (2001).
2. Higuchi, K. *et al.* Fate of DNA replication fork encountering a single DNA lesion during oriC plasmid DNA replication in vitro. *Genes Cells* **8**, 437–449 (2003).
3. Saleh-Gohari, N. *et al.* Spontaneous homologous recombination is induced by collapsed replication forks that are caused by endogenous DNA single-strand breaks. *Mol. Cell. Biol.* **25**, 7158–7169 (2005).
4. Wyman, C. & Kanaar, R. DNA double-strand break repair: All's well that ends well. *Annu. Rev. Genet.* **40**, 363–383 (2006).
5. Hanada, K. *et al.* RecQ DNA helicase is a suppressor of illegitimate recombination in *Escherichia coli. Proc. Natl. Acad. Sci. USA* **94**, 3860–3865 (1997).
6. Sonoda, E. *et al.* Rad51-deficient vertebrate cells accumulate chromosomal breaks prior to cell death. *EMBO J.* **17**, 598–608 (1998).
7. Lundin, C. *et al.* Different roles for nonhomologous end joining and homologous recombination following replication arrest in mammalian cells. *Mol. Cell. Biol.* **22**, 5869–5878 (2002).
8. Seigneur, M., Bidnenko, V., Ehrlich, S.D. & Michel, B. RuvAB acts at arrested replication forks. *Cell* **95**, 419–430 (1998).
9. West, S.C. Molecular views of recombination proteins and their control. *Nat. Rev. Mol. Cell Biol.* **4**, 435–445 (2003).
10. Baharoglu, Z., Petranovic, M., Flores, M.J. & Michel, B. RuvAB is essential for replication forks reversal in certain replication mutants. *EMBO J.* **25**, 596–604 (2006).
11. Kogoma, T. Stable DNA replication: interplay between DNA replication, homologous recombination, and transcription. *Microbiol. Mol. Biol. Rev.* **61**, 212–238 (1997).
12. McGlynn, P., Al-Deib, A.A., Liu, J., Marians, K.J. & Lloyd, R.G. The DNA replication protein PriA and the recombination protein RecG bind D-loops. *J. Mol. Biol.* **270**, 212–221 (1997).
13. Xu, L. & Marians, K.J. PriA mediates DNA replication pathway choice at recombination intermediates. *Mol. Cell* **11**, 817–826 (2003).
14. Sonoda, E., Hochegger, H., Saberi, A., Taniguchi, Y. & Takeda, S. Differential usage of non-homologous end-joining and homologous recombination in double strand break repair. *DNA Repair (Amst.)* **5**, 1021–1029 (2006).
15. Kraus, E., Leung, W.Y. & Haber, J.E. Break-induced replication: a review and an example in budding yeast. *Proc. Natl. Acad. Sci. USA* **98**, 8255–8262 (2001).
16. Davis, A.P. & Symington, L.S. RAD51-dependent break-induced replication in yeast. *Mol. Cell. Biol.* **24**, 2344–2351 (2004).
17. Branzei, D. & Foiani, M. The DNA damage response during DNA replication. *Curr. Opin. Cell Biol.* **17**, 568–575 (2005).
18. Heyer, W.D., Ehmsen, K.T. & Solinger, J.A. Holliday junctions in the eukaryotic nucleus: resolution in sight? *Trends Biochem. Sci.* **28**, 548–557 (2003).
19. Boddy, M.N. *et al.* Mus81-Eme1 are essential components of a Holliday junction resolvase. *Cell* **107**, 537–548 (2001).
20. Chen, X.B. *et al.* Human Mus81-associated endonuclease cleaves Holliday junctions in vitro. *Mol. Cell* **8**, 1117–1127 (2001).
21. Kaliraman, V., Mullen, J.R., Fricke, W.M., Bastin-Shanower, S.A. & Brill, S.J. Functional overlap between Sgs1-Top3 and the Mms4-Mus81 endonuclease. *Genes Dev.* **15**, 2730–2740 (2001).
22. Whitby, M.C., Osman, F. & Dixon, J. Cleavage of model replication forks by fission yeast Mus81-Eme1 and budding yeast Mus81-Mms4. *J. Biol. Chem.* **278**, 6928–6935 (2003).
23. Osman, F., Dixon, J., Doe, C.L. & Whitby, M.C. Generating crossovers by resolution of nicked Holliday junctions: a role for Mus81-Eme1 in meiosis. *Mol. Cell* **12**, 761–774 (2003).
24. Doe, C.L., Osman, F., Dixon, J. & Whitby, M.C. DNA repair by a Rad22-Mus81-dependent pathway that is independent of Rhp51. *Nucleic Acids Res.* **32**, 5570–5581 (2004).
25. Fricke, W.M., Bastin-Shanower, S.A. & Brill, S.J. Substrate specificity of the *Saccharomyces cerevisiae* Mus81-Mms4 endonuclease. *DNA Repair (Amst.)* **4**, 243–251 (2005).
26. Constantinou, A., Chen, X.B., McGowan, C.H. & West, S.C. Holliday junction resolution in human cells: two junction endonucleases with distinct substrate specificities. *EMBO J.* **21**, 5577–5585 (2002).
27. Ciccia, A., Constantinou, A. & West, S.C. Identification and characterization of the human MUS81-EME1 endonuclease. *J. Biol. Chem.* **278**, 25172–25178 (2003).
28. Ogrunc, M. & Sancar, A. Identification and characterization of human MUS81-MMS4 structure-specific endonuclease. *J. Biol. Chem.* **278**, 21715–21720 (2003).
29. Abraham, J. *et al.* Eme1 is involved in DNA damage processing and maintenance of genomic stability in mammalian cells. *EMBO J.* **22**, 6137–6147 (2003).
30. Interthal, H. & Heyer, W.D. MUS81 encodes a novel helix-hairpin-helix protein involved in the response to UV- and methylation-induced DNA damage in *Saccharomyces cerevisiae. Mol. Gen. Genet.* **263**, 812–827 (2000).
31. Odagiri, N. *et al.* Budding yeast *mms4* is epistatic with *rad52* and the function of Mms4 can be replaced by a bacterial Holliday junction resolvase. *DNA Repair (Amst.)* **2**, 347–358 (2003).
32. Boddy, M.N. *et al.* Damage tolerance protein Mus81 associates with the FHA1 domain of checkpoint kinase Cds1. *Mol. Cell. Biol.* **20**, 8758–8766 (2000).
33. Doe, C.L., Ahn, J.S., Dixon, J. & Whitby, M.C. Mus81-Eme1 and Rqh1 involvement in processing stalled and collapsed replication forks. *J. Biol. Chem.* **277**, 32753–32759 (2002).
34. Fabre, F., Chan, A., Heyer, W.D. & Gangloff, S. Alternate pathways involving Sgs1/Top3, Mus81/Mms4, and Srs2 prevent formation of toxic recombination intermediates from single-stranded gaps created by DNA replication. *Proc. Natl. Acad. Sci. USA* **99**, 16887–16892 (2002).

35. McPherson, J.P. *et al.* Involvement of mammalian Mus81 in genome integrity and tumor suppression. *Science* **304**, 1822–1826 (2004).

36. Dendouga, N. *et al.* Disruption of murine Mus81 increases genomic instability and DNA damage sensitivity but does not promote tumorigenesis. *Mol. Cell. Biol.* **25**, 7569–7579 (2005).

37. Hiyama, T. *et al.* Haploinsufficiency of the Mus81-Eme1 endonuclease activates the intra-S-phase and G2/M checkpoints and promotes rereplication in human cells. *Nucleic Acids Res.* **34**, 880–892 (2006).

38. Hanada, K. *et al.* The structure-specific endonuclease Mus81-Eme1 promotes conversion of interstrand DNA crosslinks into double-strands breaks. *EMBO J.* **25**, 4921–4932 (2006).

39. Arnaudeau, C., Tenorio Miranda, E., Jenssen, D. & Helleday, T. Inhibition of DNA synthesis is a potent mechanism by which cytostatic drugs induce homologous recombination in mammalian cells. *Mutat. Res.* **461**, 221–228 (2000).

40. Merrick, C.J., Jackson, D. & Diffley, J.F. Visualization of altered replication dynamics after DNA damage in human cells. *J. Biol. Chem.* **279**, 20067–20075 (2004).

41. Courcelle, J., Donaldson, J.R., Chow, K.H. & Courcelle, C.T. DNA damage-induced replication fork regression and processing in *Escherichia coli*. *Science* **299**, 1064–1067 (2003).

42. Magee, T.R. & Kogoma, T. Requirement of RecBC enzyme and an elevated level of activated RecA for induced stable DNA replication in *Escherichia coli*. *J. Bacteriol.* **172**, 1834–1839 (1990).

43. Grompone, G., Ehrlich, D. & Michel, B. Cells defective for replication restart undergo replication fork reversal. *EMBO Rep.* **5**, 607–612 (2004).

44. Masai, H., Asai, T., Kubota, Y., Arai, K. & Kogoma, T. *Escherichia coli* PriA protein is essential for inducible and constitutive stable DNA replication. *EMBO J.* **13**, 5338–5345 (1994).

45. Kai, M., Boddy, M.N., Russell, P. & Wang, T.S. Replication checkpoint kinase Cds1 regulates Mus81 to preserve genome integrity during replication stress. *Genes Dev.* **19**, 919–932 (2005).

46. Davies, S.L., North, P.S. & Hickson, I.D. Role for BLM in replication-fork restart and suppression of origin firing after replicative stress. *Nat. Struct. Mol. Biol.* **14**, 677–679 (2007).

47. Essers, J. *et al.* Disruption of mouse RAD54 reduces ionizing radiation resistance and homologous recombination. *Cell* **89**, 195–204 (1997).

48. Van Veelen, L.R. *et al.* Analysis of ionizing radiation-induced foci of DNA damage repair proteins. *Mutat. Res.* **574**, 22–33 (2005).

49. Niedernhofer, L.J. *et al.* The structure-specific endonuclease Ercc1-Xpf is required to resolve DNA interstrand cross-link-induced double-strand breaks. *Mol. Cell. Biol.* **24**, 5776–5787 (2004).
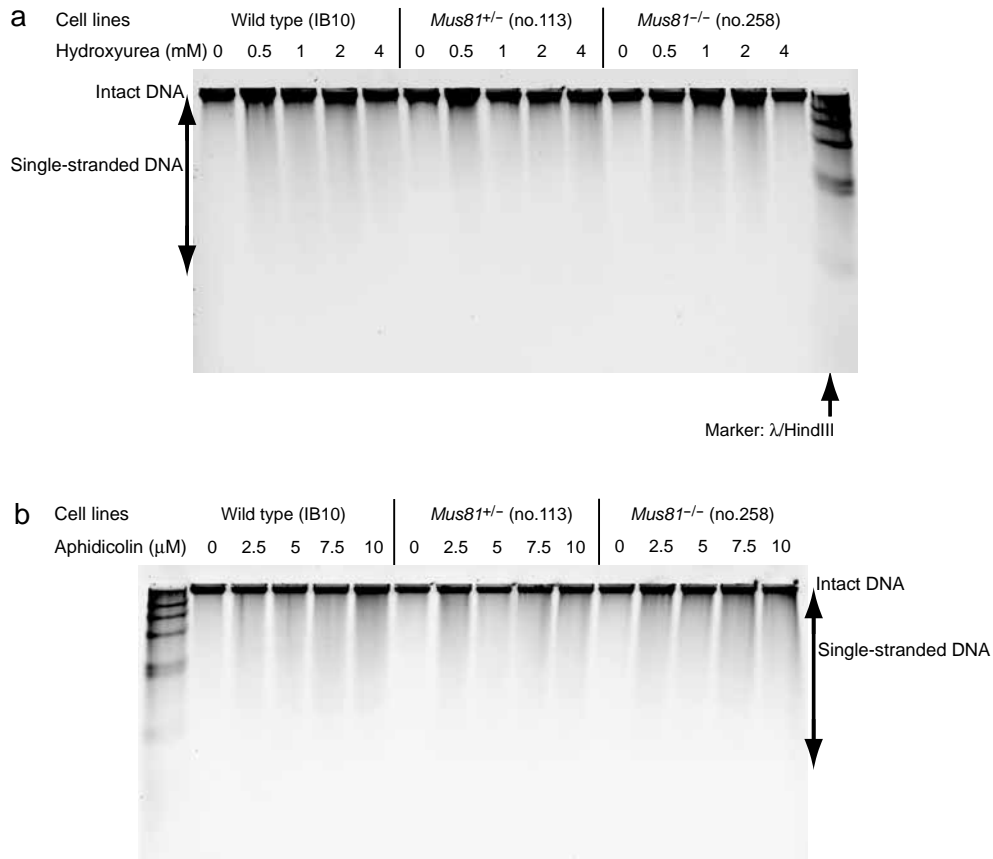
Supplemental data

The structure-specific endonuclease Mus81 contributes to replication restart by generating double-strand DNA breaks

Katsuhiro Hanada, Magda Budzowska, Sally L Davies, Ellen van Drunen, Hideo Onizawa, H Berna Beverloo, Alex Maas, Jeroen Essers, Ian D Hickson and Roland Kanaar
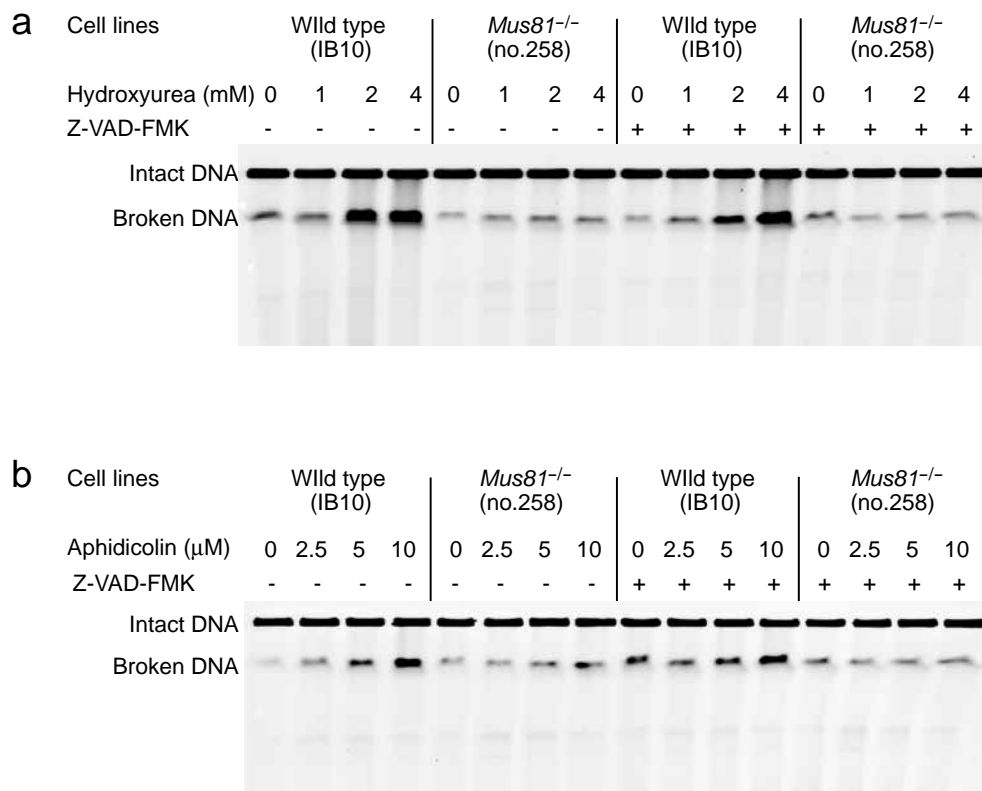
Methods

Alkaline gel electrophoresis. Samples were prepared as described for the PFGE experiments. Briefly, sub-confluent cultures of ES cells were treated with hydroxyurea or aphidicolin for 24 hrs, the cells were trypsinized, and agarose plugs of 106 cells were prepared with a CHEF disposable plug Mold (Bio-Rad). The plugs were incubated in lysis buffer (100 mM EDTA, 1% sodium lauryl sarcosine, 0.2 % sodium deoxycholate, 1 mg/ml Proteinase K) at 37 oC for 48 hrs. DNA was denatured for 45 minutes in buffer containing 0.5 M NaOH and 1.5 M NaCl. The plugs were loaded onto an alkaline gel (1% agarose in 40 mM NaOH, 1 mM EDTA), and electrophoresed for 14-16 hrs at 1 V/cm. The agarose gel was incubated in neutralization buffer (1 M Tris-HCl, 1.5 M NaCl) and DNA was stained by Syber-gold (Molecular probes).

a

Cell lines		Wild type (IB10)					Mus81+/− (no.113)					Mus81−/− (no.258)			
Hydroxyurea (mM)	0	0.5	1	2	4	0	0.5	1	2	4	0	0.5	1	2	4

Intact DNA

Single-stranded DNA

Marker: λ/HindIII

b

Cell lines		Wild type (IB10)					Mus81+/− (no.113)					Mus81−/− (no.258)			
Aphidicolin (µM)	0	2.5	5	7.5	10	0	2.5	5	7.5	10	0	2.5	5	7.5	10

Intact DNA

Single-stranded DNA

Supplementary Figure 1. Analysis of single-stranded DNA breaks in wild type, Mus81+/-, and Mus81-/- mouse ES cells using alkaline gel electrophoresis.
(**a**) Analysis of single-stranded DNA break formation in response to hydroxyurea. Cells of the indicated genotype were incubated with 0, 0.5, 1, 2, or 4 mM hydroxyurea for 24 hrs, collected into agarose plugs and their denatured DNA was separated on an alkaline agarose gel. Phage lambda DNA digested with Hind III was used as a molecular size marker in the lane on the left.
(**b**) Analysis of single-stranded DNA break formation in response to aphidicolin. Cells of the indicated genotype were incubated with 0, 2.5, 5, 7.5, or 10 µM aphidicolin for 24 hrs and their DNA was denatured and separated as described in panel **a**. Phage lambda DNA digested with Hind III was used as molecular size markers in the lane on the right.

a Cell lines

| | Wild type (IB10) | | | | Mus81$^{-/-}$ (no.258) | | | | Wild type (IB10) | | | | Mus81$^{-/-}$ (no.258) | | | |

Hydroxyurea (mM) 0 1 2 4 | 0 1 2 4 | 0 1 2 4 | 0 1 2 4

Z-VAD-FMK - - - - | - - - - | + + + + | + + + +

Intact DNA

Broken DNA

b Cell lines

| | Wild type (IB10) | | | | Mus81$^{-/-}$ (no.258) | | | | Wild type (IB10) | | | | Mus81$^{-/-}$ (no.258) | | | |

Aphidicolin (μM) 0 2.5 5 10 | 0 2.5 5 10 | 0 2.5 5 10 | 0 2.5 5 10

Z-VAD-FMK - - - - | - - - - | + + + + | + + + +

Intact DNA

Broken DNA

Supplementary Figure 2. Analysis of hydroxyurea- and aphidicolin-induced DSB formation in wild type and Mus81-/- ES cells under conditions that inhibit apoptosis.
(**a**) Cells of the indicated genotype were incubated in the presence of the indicated concentrations of hydroxyurea for 24 hrs, either in the absence (-) or presence (+) of the Caspase 9 inhibitor V-ZAD-FMK. Subsequently, cells were collected into agarose plugs and their DNA was electrophoresed through an agarose gel. The level of broken DNA upon replication inhibition is similar whether or not the apoptosis inhibitor is present. Thus, the hydroxyurea-induced DSBs are not due to chromosome fragmentation during apoptosis. (**b**) As in panel **a**, except aphidicolin was used to inhibit DNA replication rather than hydroxyurea.
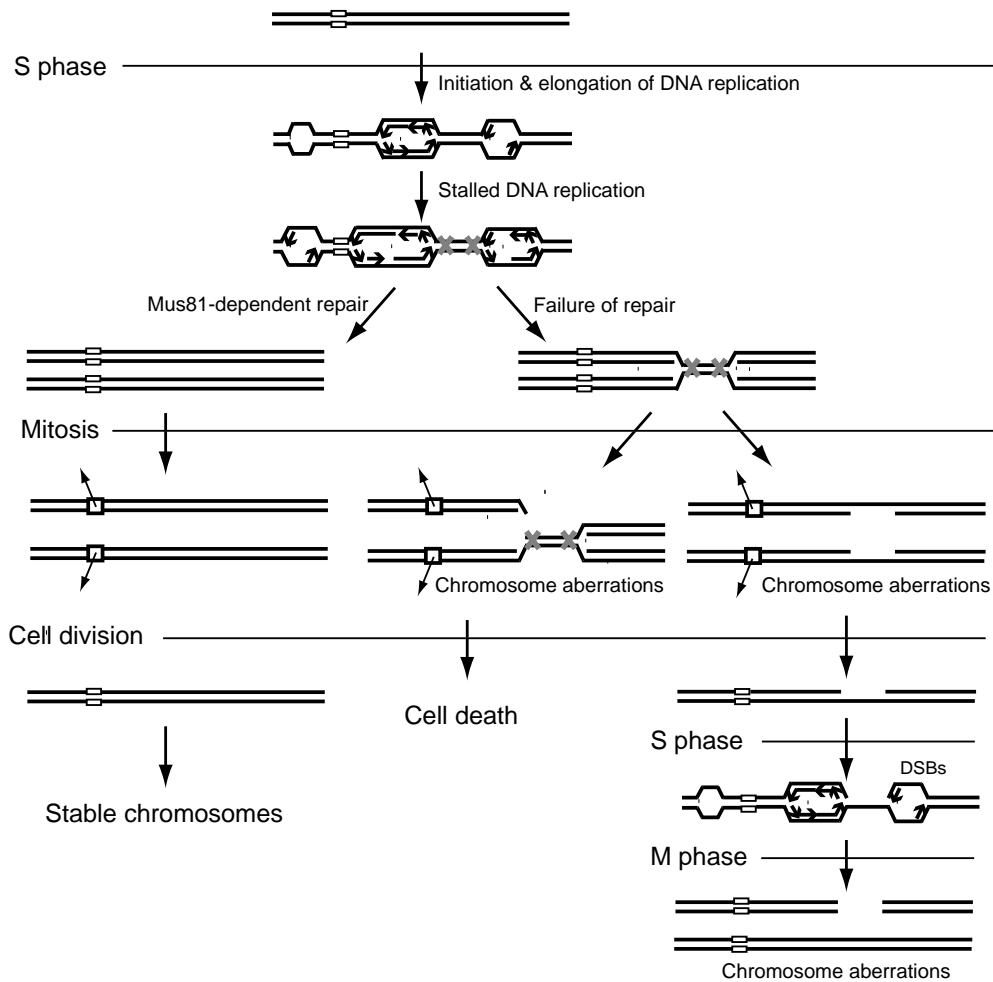
Supplementary Figure 3. A model for the role of Mus81 in chromosome maintenance.
Upon replication perturbation, a number of the stalled forks are repaired via a Mus81-dependent pathway. If the Mus81-dependent pathway is dysfunctional, unreplicated regions have the potential to result in chromatid breaks and gaps during mitosis when the partially replicated sister-chromatids are disjoined in anaphase. When some of these cells go through the next cell cycle, chromosome breaks and gaps will result.

Supplementary Table 1 Chromosomal aberrations induced by DNA replication inhibitors in Mus81$^{-/-}$ ES cells.

Genotype of ES cells	Treatment	Division	# of metaphases analyzed	Fragments	Gaps	Chromatid breaks	Chromosome breaks	Radials	Dicentrics	Rings
Wild type (IB10)	mock	1st	19	0	0	0	0	0	0	0
	mock	2nd	25	0.04	0	0.04	0.12	0	0	0
	hydroxyurea	1st	39	0.21	0.08	0	0.38	0.21	0	0.05
	hydroxyurea	2nd	27	0.07	0.22	0	0	0	0	0
Mus81$^{-/-}$ (#258)	mock	1st	20	0.05	0	0	0	0	0	0
	mock	2nd	25	0	0.08	0	0	0	0	0
	hydroxyurea	1st	64	0.69	0.25	0.02	0.20	0.30	0.03	0
	hydroxyurea	2nd	23	0.83	0.78	0	0.22	0	0	0

Listed are the numbers of aberrations per metaphase.

Supplementary Table 2 Embryonic stem cell lines used in this study.

Cell line	Genotype	Notes
IB10	129/SV: control	E14 subclone[1]
03/04/04/#113	IB10: *Mus81*[Neo/+]	[2]
03/07/04/#258	IB10: *Mus81*[Neo/Hyg]	[2]
96/01/12/#10	IB10: *Rad54*[Neo/Hyg]	[1]
98/10/02/#27	IB10: *Rad54*[Neo/HA]	[3]
C7	IB10: *Rad54*[HA/GFP]	98/10/02/#27 X 11.1*Rad54*-HA [a]
04/06/20/#9	IB10: *Mus81*[Neo/Hyg] *Rad54* [GFP/+]	03/07/04/#258 X 11.1*hRad54*-GFP [b]
07/05/14/#8	IB10: *Mus81*[Neo/Hyg] *PGK-hMUS81*	03/07/04/#258 X pPGK-*MUS81*
07/05/15/#12	IB10: *Mus81*[Neo/Hyg] *PGK-hMUS81*(D338A,D339A)	03/07/04/#258 X pPGK-*MUS81*(D338A,D339A)
04/02/28/#3	129 X B6: control	[2]
97/02/01/#2	129 X B6: *Rad54*[Neo/Neo]	[1]
04/05/13/#11	129 X B6: *Mus81*[Neo/Neo]	[2]
05/02/03/#49	129 X B6: *Mus81*[Neo/Neo] *Rad54*[Pur/Hyg]	[2]

[a, b] These cell lines were established by gene targeting. The details of gene targeting constructs were described previously[3,4].

Supplementary References
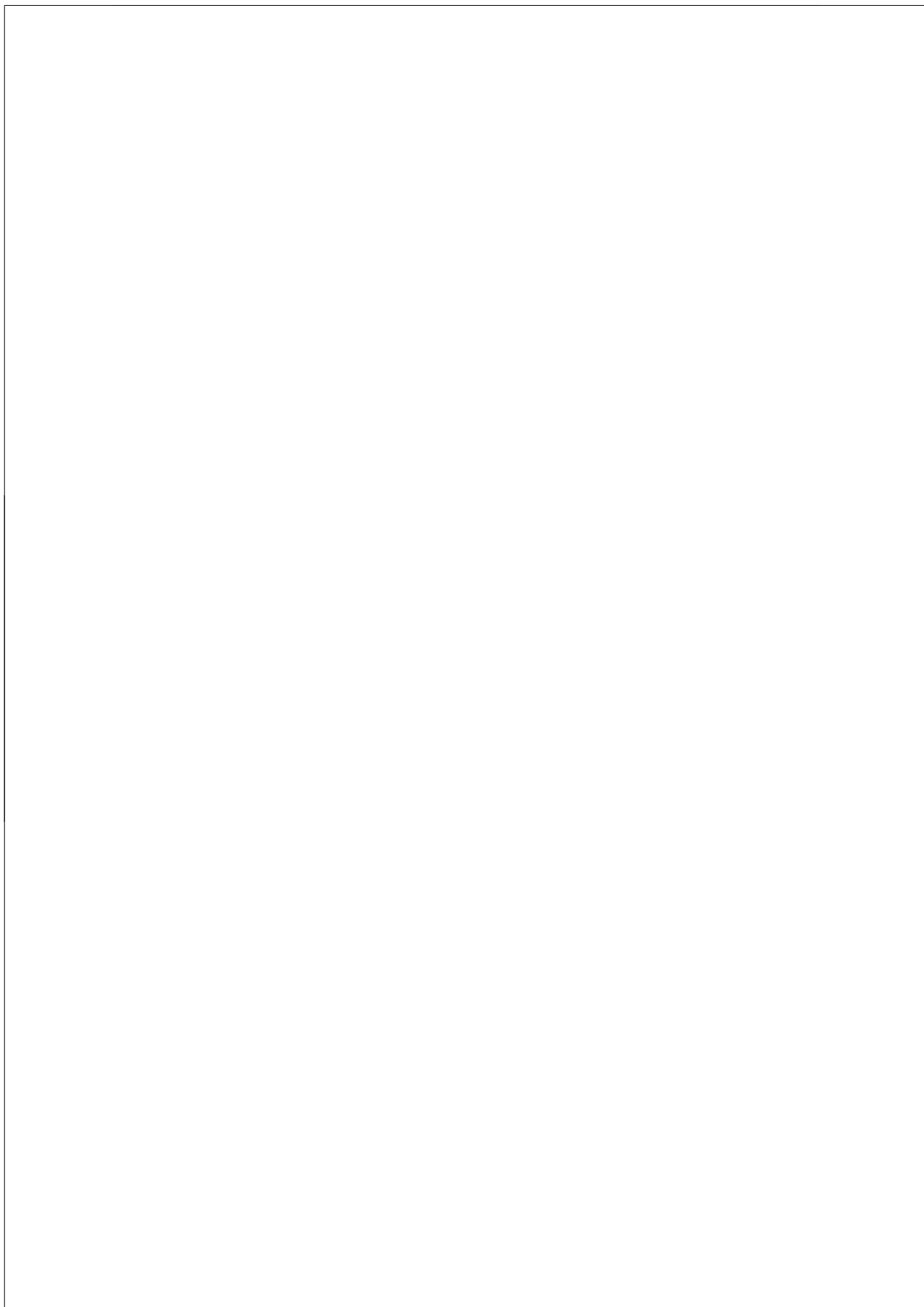
1. Essers, J. *et al*. Disruption of mouse RAD54 reduces ionizing radiation resistance and homologous recombination. *Cell* **89**, 195-204 (1997).

2. Hanada, K. *et al*. The structure-specific endonuclease Mus81-Eme1 promotes conversion of interstrand DNA crosslinks into double-strands breaks. *EMBO J.* **25**, 4921-4932 (2006).

3. Tan, T.L. *et al*. Mouse Rad54 affects DNA conformation and DNA-damage-induced Rad51 foci formation. Curr. Biol. **9**, 325-328 (1999).

4. Budzowska, M. *et al*. Mutation of the mouse Rad17 gene leads to embryonic lethality and reveals a role in DNA damage-dependent recombination. *EMBO J.* **23**, 3548-3558 (2004).

Chapter 6

RAD51AP1 is a structure-specific

DNA binding protein

that stimulates joint molecule

formation during RAD51-mediated

homologous recombination

RAD51AP1 Is a Structure-Specific DNA Binding Protein that Stimulates Joint Molecule Formation during RAD51-Mediated Homologous Recombination

Mauro Modesti,[1,5,*] Magda Budzowska,[1] Céline Baldeyron,[1,6] Jeroen A.A. Demmers,[2] Rodolfo Ghirlando,[4] and Roland Kanaar[1,3]

[1]Department of Cell Biology and Genetics
[2]Department of Biochemistry and Proteomics
[3]Department of Radiation Oncology
Erasmus MC, PO Box 2040, 3000 CA, Rotterdam, The Netherlands
[4]Laboratory of Molecular Biology, National Institute of Diabetes and Digestive and Kidney Diseases, National Institutes of Health, Bethesda, MD 20892, USA
[5]Present address: Genome Instability and Carcinogenesis, CNRS FRE 2931, 31 Chemin Joseph Aiguier, 13402 Marseille Cedex 20, France.
[6]Present address: Institut Curie, Section de Recherche, UMR218 CNRS/IC, 26 rue d'Ulm, 75248 Paris Cedex 05, France.
*Correspondence: mmodesti@ibsm.cnrs-mrs.fr
DOI 10.1016/j.molcel.2007.08.025

SUMMARY

Homologous recombination is essential for preserving genome integrity. Joining of homologous DNA molecules through strand exchange, a pivotal step in recombination, is mediated by RAD51. Here, we identify RAD51AP1 as a RAD51 accessory protein that specifically stimulates joint molecule formation through the combination of structure-specific DNA binding and physical contact with RAD51. At the cellular level, we show that RAD51AP1 is required to protect cells from the adverse effects of DNA double-strand break-inducing agents. At the biochemical level, we show that RAD51AP1 has a selective affinity for branched-DNA structures that are obligatory intermediates during joint molecule formation. Our results highlight the importance of structural transitions in DNA as control points in recombination. The affinity of RAD51AP1 for the central protein and DNA intermediates of recombination confers on it the ability to control the preservation of genome integrity at a number of critical mechanistic steps.

INTRODUCTION

DNA damage hinders the progression of DNA replication forks and can lead to fork arrest or collapse (Cox et al., 2000). To avoid these detrimental effects, cells have evolved a number of DNA damage removal or tolerance systems (Hoeijmakers, 2001). However, when these systems malfunction or DNA damage escapes detection, replication fork demise can occur, leading to the formation of single-ended DNA double-strand breaks (DSBs). These broken forks can be re-established via homologous recombination mediated by the RAD51 ATP-dependent recombinase (Krogh and Symington, 2004; Wyman and Kanaar, 2006). Through strand invasion and exchange, RAD51 catalyzes the formation of a joint molecule between the broken end and its homologous template. The joint molecule intermediate can then serve to prime DNA synthesis (Kogoma, 1997).

To facilitate the analysis of the molecular mechanism of RAD51-dependent homologous recombination, the process can conceptually be separated into three distinct phases (Kowalczykowski, 2000). During the presynaptic phase, RAD51 assembles into a nucleoprotein filament around the 3′ single-stranded (ss) overhang generated by resection of a broken double-stranded (ds) DNA end. The ATP-coordinated RAD51 nucleoprotein filament forms the active structure that supports homology recognition and strand exchange. It is during this synaptic phase that the single-end invasion intermediate (SEI), central to the RAD51-dependent homologous recombination reaction, is formed (Hunter and Kleckner, 2001). Structurally, the SEI DNA intermediate is composed of a 3′ ended single strand invaded into a homologous DNA duplex, forming a displacement loop (D loop) with a protruding ss or ds arm. Finally, heteroduplex extension and resolution can occur during the postsynaptic phase and is presumably accompanied by dissociation of RAD51 from DNA.

A number of proteins interact with the RAD51 recombinase to regulate and guide its action during each of these three mechanistically distinct phases. For instance, BRCA2, RAD54, the SWI5/SFR1 complex, RAD51B, and RAD51C are implicated during the early presynaptic phase in directing the assembly and/or stabilization of the RAD51 nucleoprotein filament (Haruta et al., 2006; Sung, 2005). Stimulation and regulation of recombinase

function in eukaryotes at the synaptic phase might be generally required. DMC1, a RAD51-related meiosis-specific recombinase, is strongly stimulated during joint molecule formation by HOP2/MND1 (Chen et al., 2004; Enomoto et al., 2006; Petukhova et al., 2005; Pezza et al., 2006). Roles for RAD54 and the XRCC3/RAD51C complex during the late phase of homologous recombination have also been identified (Liu et al., 2004; Solinger et al., 2002; Brenneman et al., 2002; Sugawara et al., 2003).

Recently, a human homolog of murine RAB22, called PIR51 for protein interacting with RAD51 and subsequently renamed RAD51AP1 (RAD51 associated protein 1), has been rediscovered in a screen for genes highly expressed in aggressive lymphomas and carcinomas (Henson et al., 2006; Kovalenko et al., 1997; Mizuta et al., 1997; Song et al., 2004; Wang et al., 2005). Downregulation of RAD51AP1 with small interfering RNA (siRNA) increases the sensitivity of human HeLa cells to the DNA interstrand crosslinker mitomycin C and results in accumulation of sister chromatid breaks in metaphase chromosomes (Henson et al., 2006). It has been postulated that RAD51AP1 plays a specific role in connecting the later stages of RAD51-dependent homologous recombination to the early response to DNA interstrand crosslinks orchestrated by the Fanconi Anemia proteins (Henson et al., 2006).

Here, we unravel a functional and mechanistic connection between RAD51AP1 and RAD51. We show that RAD51AP1 is specifically required for not only the cellular response to interstrand DNA crosslinking agents but also for the response to other DSB-inducing agents, including ionizing radiation and camptothecin. Importantly, we uncovered that RAD51AP1 exhibits a structure-specific DNA binding activity. The protein displays a selective affinity for branched-DNA structures that are central intermediates in homologous recombination. We demonstrate that RAD51AP1-mediated stimulation of D loop formation by RAD51, a pivotal step in recombination, requires both its specific physical interaction with RAD51 and its structure-specific DNA binding activity.

RESULTS

RAD51AP1 Confers Resistance to DNA Damaging Agents
Depletion of RAD51AP1 (Figure S1A in the Supplemental Data available with this article online) increased the sensitivity of HeLa cells to treatment with interstrand DNA crosslinking agents (mitomycin C or cis-platin, Figures 1A and 1B) and ionizing radiation (Figure 1C). RAD51AP1-depleted cells also showed increased sensitivity to camptothecin, a topoisomerase I inhibitor known to trigger accumulation of DSBs in S phase after passage and collapse of a replication fork (Figure 1D). Concomitant downregulation of RAD51AP1 and either RAD51 or XRCC3 did not result in an increased sensitivity of the cells to ionizing radiation or mitomycin C compared to downregulation of just RAD51 or XRCC3 (Figures 1E–1H and 1K). Thus, in terms of mitomycin C and ionizing radiation sensitivity

after downregulation, RAD51 and XRCC3 appear to be epistatic to RAD51AP1. Taken together, our results are consistent with a role for RAD51AP1 in homologous recombination-mediated DSB repair.

Spontaneous and Damage-Induced RAD51 Foci Are Apparently Unaffected by RAD51AP1 Depletion
Repair of DSBs by homologous recombination critically depends on the RAD51 homology recognition and DNA strand exchange protein (Kowalczykowski, 2000). During S phase, in the absence of exogenously induced DNA damage, RAD51 "spontaneously" accumulates to form foci detectable by immunofluorescence, presumably at sites of compromised replication forks (Tashiro et al., 1996). Upon DNA damage induction by ionizing radiation or by treatment with interstrand DNA crosslinking agents, an increase in the number of RAD51 foci is observed (Haaf et al., 1995). If RAD51AP1 would influence the activity of RAD51, they should reside at the same location, at least part of the time. Indeed, HeLa cells stably expressing GFP-RAD51AP1 (Figure S1A) displayed spontaneous RAD51AP1 foci that colocalized with RAD51 (Figure 2A). As is the case for RAD51, the number of RAD51AP1 foci increased when the cells were treated with ionizing radiation. Both spontaneous and DNA damaged induced RAD51AP1 foci were less plentiful compared to RAD51. However, most if not all, RAD51AP1 foci did colocalize with RAD51.

To determine the possible role of RAD51AP1 on the activity of the RAD51 recombinase, we asked whether RAD51AP1 depletion would affect RAD51 nuclear distribution. In RAD51AP1-depleted cells, the assembly of both spontaneous and DNA damage-induced RAD51 foci was qualitatively and quantitatively unaffected (Figures 2B–2E). This result argues, at least on the cell biological level, that assistance of RAD51-mediated homologous recombination by RAD51AP1 occurs via a different mechanism compared to the RAD51 paralogs or BRCA2, because deficiency in these recombination mediators results in the attenuation of DNA damage-induced RAD51 foci formation (Takata et al., 2000, 2001; Yuan et al., 1999).

RAD51AP1 Is an Elongated Monodisperse Monomer in Solution
Full-length recombinant human RAD51AP1 was produced in bacteria and purified to near homogeneity to determine its biochemical activities (Figure 3). Recombinant RAD51AP1 migrated slower than expected during denaturing SDS polyacrylamide gel electrophoresis under reducing conditions, because it displayed an apparent molecular weight of ~48 kDa as compared to its calculated molecular weight of 39,417 Da (Figures 3A and 3B). This retarded mobility was also observed for the endogenous protein detected in human cell extracts (Figure S1A). RAD51AP1 also behaved as a single and larger than expected entity during Sephacryl 200 gel permeation chromatography (~180 kDa, Figures 3B and 3C),
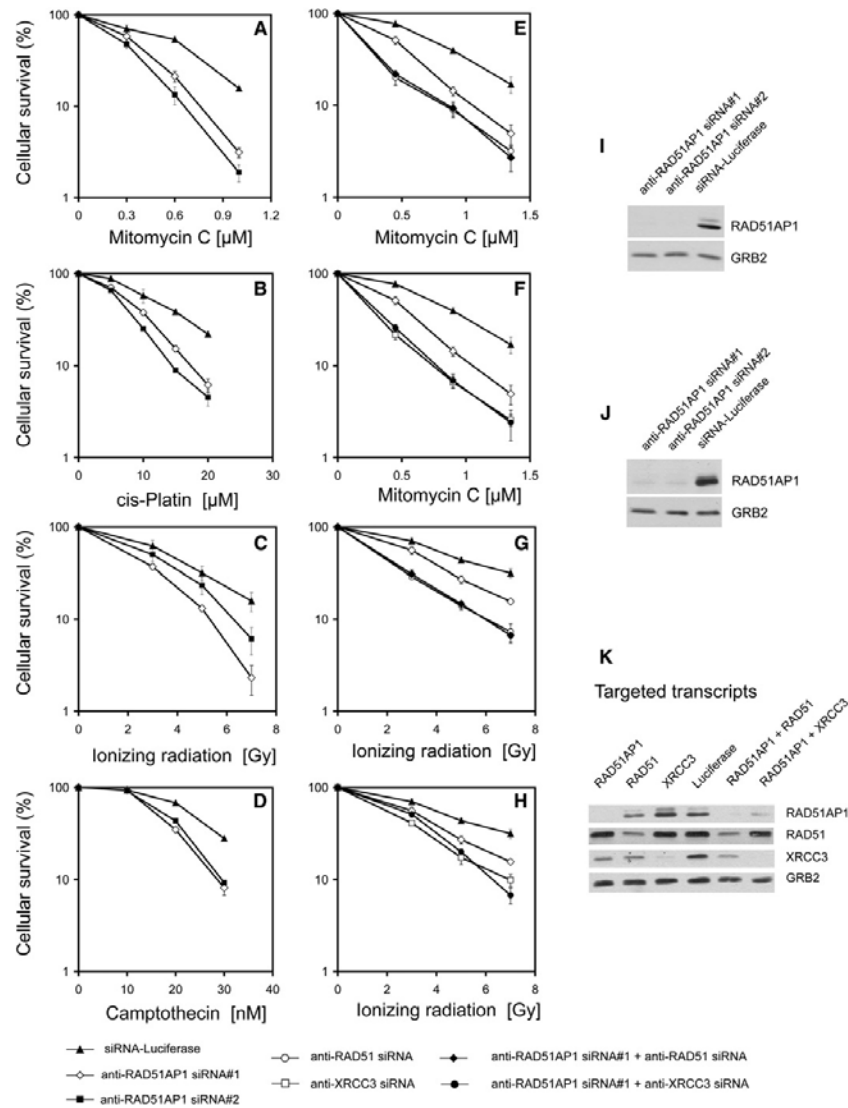
Figure 1. DNA Damage Sensitivity Profile of HeLa Cells after siRNA-Mediated Downregulation of RAD51AP1

(A–D) Survival curves in response to increasing doses of (A) mitomycin C, (B) cis-platin, (C) ionizing radiation, and (D) camptothecin. siRNA#1 and siRNA#2 are targeted against RAD51AP1, whereas siRNA-L is a control siRNA targeted against luciferase. Note that the percentage of surviving cells is plotted on a logarithmic scale.

(E) Survival curves in response to increasing doses of mitomycin C after RAD51AP1, RAD51, and their combined downregulation.

(F) Survival curves in response to increasing doses of mitomycin C after RAD51AP1, XRCC3, and their combined downregulation.

(G) Survival curves in response to increasing doses of ionizing radiation after RAD51AP1, RAD51, and their combined downregulation.

(H) Survival curves in response to increasing doses of ionizing radiation after RAD51AP1, XRCC3, and their combined downregulation.

(I and J) Relevant immunoblots detecting RAD51AP1 and the loading control GRB2. (I) and (J) show immunoblots from cell populations used in (B) and (D), and (A) and (C), respectively.

(K) Relevant immunoblots detecting RAD51AP1, RAD51, and XRCC3 and the loading control GRB2 in cell populations used in (E)–(H).

All cell survival experiments were performed in triplicate, and errors bars represent standard errors of the mean.
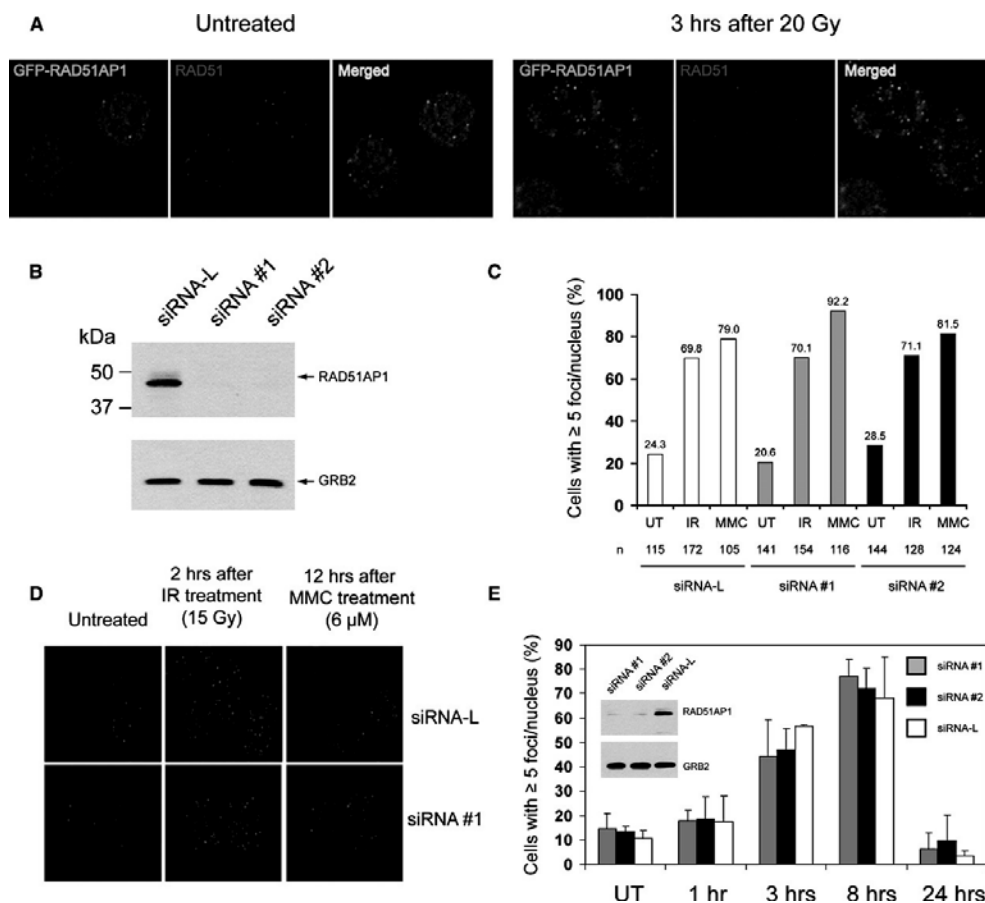
Figure 2. Spontaneous and Damage-Induced RAD51 Foci Formation Does Not Depend on RAD51AP1

(A) Colocalization of GFP-RAD51AP1 (green) and RAD51 (red, indirect immunofluorescence) into spontaneous and DNA damage-induced nuclear foci (3 hr after irradiation with 20 Gy). At least 95% of RAD51AP1 foci colocalized with RAD51 foci in both untreated and ionizing radiation treated cells.

(B) Immunoblot analysis of extracts from HeLa cells downregulated for RAD51AP1 and collected just prior to treatment with DNA damaging agents in the experiment presented in (C) and (D). Detection of GRB2 was used as loading control. siRNA#1 and siRNA#2 are targeted against RAD51AP1, and siRNA-L is a nonspecific control siRNA against luciferase.

(C) RAD51 foci formation as detected by immunofluorescence was quantified by counting the fraction of cells containing ≥ 5 foci/nucleus. UT, untreated; IR, ionizing radiation-treated; and MMC, mitomycin C-treated cells.

(D) Representative micrographs obtained by superimposing the RAD51 signal (red) onto the DAPI DNA counter stain (blue).

(E) Kinetics of RAD51 foci formation after RAD51AP1 downregulation was determined by counting the fraction of cells containing ≥ 5 foci/nucleus at the indicated time points after treatment with ionizing radiation (6 Gy). Immunoblot analysis to verify RAD51AP1 downregulation as in (B), of one of the experiments from which the data was collected, is shown as an inset. The average of two experiments is reported where error bars represent standard deviations. At least 100 cells were scored for each experimental point.

suggesting assembly of an oligomer in solution and/or an elongated monomeric structure. To distinguish between these two possibilities, sedimentation equilibrium experiments were carried out on the RAD51AP1 preparation (Figure 3D). The sedimentation profiles collected at a single loading concentration were consistent with the presence of a single ideal solute having an experimental mo-

lecular mass of 40.9 ± 0.8 kDa. This corresponds to a stoichiometry of 1.04 ± 0.02, demonstrating that the protein is both monomeric and monodisperse in solution. Consistently, a mass of 39,286 ± 6 Da corresponding exactly to the predicted mass of the polypeptide lacking the first methionine residue was measured for RAD51AP1 after electrospray ionization under relative mild conditions
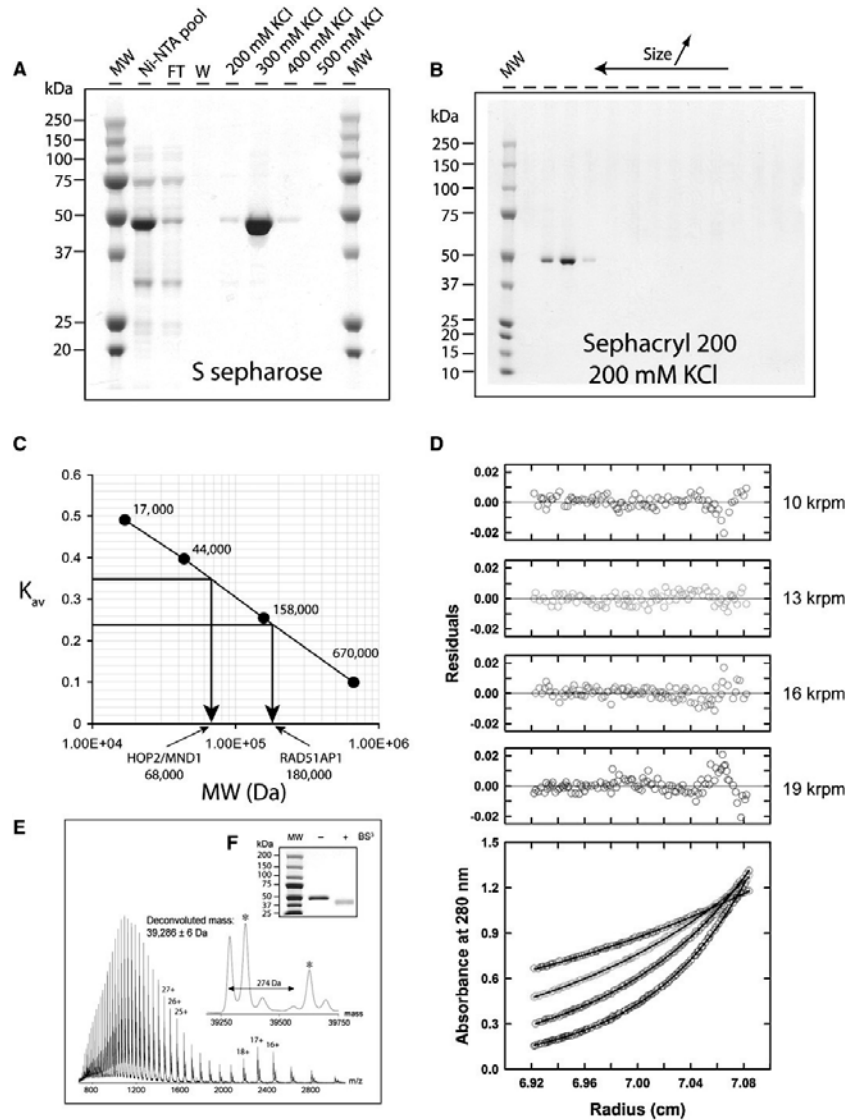
Figure 3. RAD51AP1 Is an Elongated Monodisperse Monomer in Solution
(A) Reducing SDS-PAGE gel of fractions after S Sepharose chromatography stained with Coomassie. Ni-NTA pool, fraction obtained by batch purification over Ni-NTA resin; FT, flowthrough; W, wash; and MW, molecular weight standard.
(B) Coomassie-stained reducing SDS-PAGE gel of fractions after Sephacryl 200 gel permeation chromatography.
(C) A semilog plot of the partition coefficient (K_{av}) versus molecular weight was constructed using a standard set of globular proteins to determine the apparent molecular weight of RAD51AP1. The HOP2/MND1 heterodimer with an expected mass of 50,180 Da was used as control.
(D) Sedimentation equilibrium profiles at 4.0°C plotted as a distribution of the absorbance at 280 nm versus r at equilibrium. Data were collected at 10 (red), 13 (green), 16 (pink), and 19 (blue) krpm at a loading A_{280} of 0.90. The solid lines show the best-fit global analysis in terms of a single ideal solute, with the corresponding residuals shown in the panels above the plot.

137
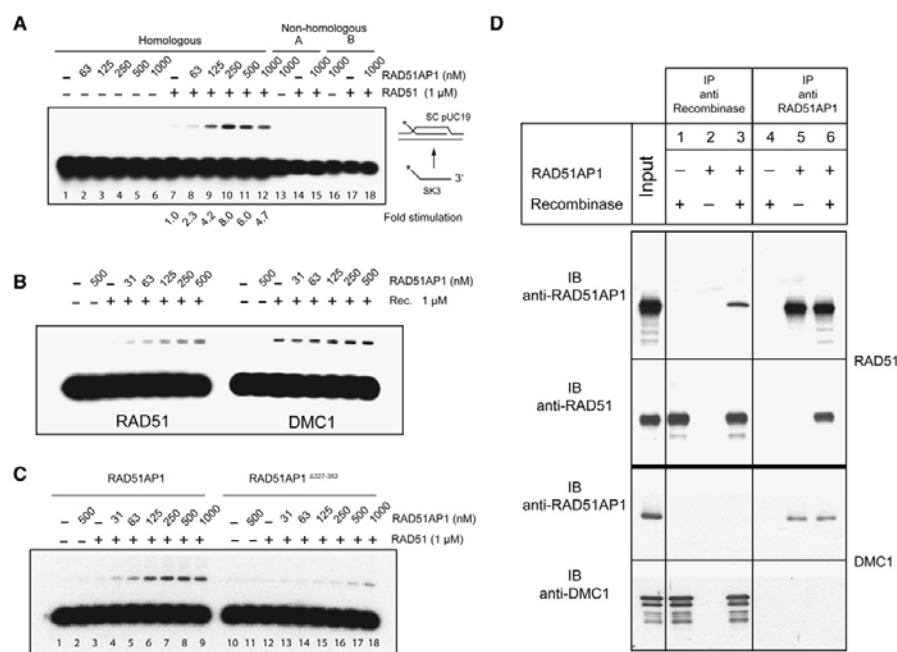
Figure 4. RAD51AP1 Specifically Stimulates D Loop Formation by RAD51

(A) Effect of RAD51AP1 in RAD51-catalyzed D loop assays with homologous invading oligonucleotide SK3 (lanes 1–12) or with nonhomologous invading oligonucleotides NHA (lanes 13–15) or NHB (lanes 16–18). Position of the radiolabel on the substrate is indicated with an asterisk. Recipient substrate was supercoiled pUC19 plasmid (SC pUC19).

(B) Effect of RAD51AP1 in RAD51 (left) or DMC1 (right) catalyzed D loop assays with homologous oligonucleotide SK3.

(C) Effect of RAD51AP1 (left) or C-terminally deleted RAD51AP1$^{\Delta327-352}$ (right) in RAD51-catalyzed D loop assays with homologous invading oligonucleotide SK3.

(D) RAD51AP1 specifically and directly binds RAD51, but not DMC1. Immunoblot analysis (IB) of RAD51AP1-RAD51 binding reactions after immunoprecipitation (IP) as indicated (upper two panels). Immunoblot analysis (IB) of RAD51AP1-DMC1 binding reactions after immunoprecipitation (IP) as indicated (lower two panels).

from an aqueous buffer (Figure 3E). The spectrum did not indicate the presence of any multimers. In addition, crosslinking of RAD51AP1 resulted in a single diffuse and faster migrating species during denaturing SDS polyacrylamide gel electrophoresis under reducing conditions with no evidence for crosslinked multimers (Figure 3F). We conclude that RAD51AP1 is likely to be an elongated protein.

RAD51AP1 Specifically Stimulates D Loop Formation by RAD51

A defining step of homologous recombination mediated by RAD51 is the formation of a joint molecule between the recombining partner DNAs into a D loop structure. Therefore, we tested whether RAD51AP1 augments this crucial activity of RAD51 in an established D loop formation assay (Bugreev and Mazin, 2004; Mazin et al., 2000) (Figure 4). Ss oligonucleotides were preincubated with RAD51 at a ratio of one RAD51 monomer per three nucleotides to allow assembly of nucleoprotein filaments. A recipient supercoiled plasmid harboring a sequence homologous to the oligonucleotide was then added to the reaction mixture to start D loop formation. Using these standard conditions and in the presence of Mg^{2+} ions and ATP, the addition of RAD51AP1 substantially stimulated D loop formation by RAD51 (Figures 4A–4C). Levels of D loop products were increased up to ∼8-fold (see Experimental Procedures for quantification). The stimulatory effect was dependent on homology (Figure 4A, lanes 13–18)

(E) Mass spectrometry of RAD51AP1 after electrospray ionization of the "native" protein in 50 mM ammonium acetate. Averaged calculated mass = 39,417 Da and experimental deconvoluted mass = 39,286 ± 6 Da, which corresponds exactly to the mass of the polypeptide minus the first methionine. The peaks marked with an asterisk represent a higher mass species and are absent when the protein is sprayed from a denaturing methanol solution, indicating a noncovalently bound adduct to the protein (data not shown).

(F) Coomassie-stained reducing SDS-PAGE gel of RAD51AP1 after BS^3 crosslinking.

and was detectable at a substoichiometric ratio of one RAD51AP1 monomer to ten RAD51 monomers. Stimulation was independent of the order of addition of RAD51 and RAD51AP1 during the first step of filament formation on the invading ss oligonucleotide (Figure S2).

Specific RAD51-RAD51AP1 Protein-Protein Interaction Is Required for the Full Extent of RAD51AP1 Stimulation of D Loop Formation by RAD51
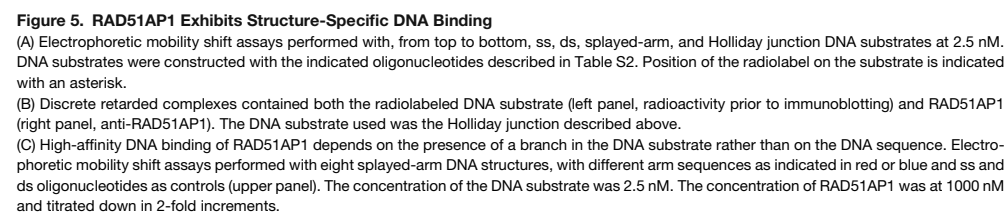
Next we tested whether the specificity of the RAD51AP1 stimulatory effect on D loop formation by RAD51 depended on a specific protein-protein interaction. Two-hybrid and coimmunoprecipitation experiments using cell extracts suggest that RAD51AP1 binds directly to RAD51 (Henson et al., 2006; Kovalenko et al., 1997, 2006; Mizuta et al., 1997). Highly purified RAD51 and RAD51AP1 free of DNA were incubated in solution, and their ability to interact was assessed by coimmunoprecipitation. RAD51AP1 directly bound to RAD51, but not to DMC1, a related ATP-dependent meiosis-specific recombinase (Bishop et al., 1992) (Figure 4D). Interestingly, under identical conditions, RAD51AP1 stimulated D loop formation by RAD51, whereas stimulation of DMC1 was less effective (Figure 4B). In contrast, addition of HOP2/MND1 to the DMC1 reaction increased the levels of D loop products (data not shown). This suggests that the stimulation of D loop formation by RAD51AP1 requires a specific and direct physical interaction between RAD51AP1 and the recombinase. To test this notion, we deleted residues 327–352, the 26 C-terminal residues of RAD51AP1 that contain a RAD51 interaction domain identified by two-hybrid experiments (Kovalenko et al., 2006). This C-terminally truncated RAD51AP1 protein lost its ability to physically interact with RAD51 in the coimmunoprecipitation assay described above (Figure 7C, lane 4) and was strongly affected in its ability to stimulate D loop formation by RAD51 (Figure 4C). However, the RAD51 D loop stimulatory ability of this truncated RAD51AP1 was not completely abolished, as a low level of stimulation was detected when the truncated RAD51AP1 was present at higher concentrations (Figure 4C, lanes 17 and 18). Likewise, a low but detectable level of stimulation of DMC1-mediated D loop formation by full-length RAD51AP1 was observed even though RAD51AP1 did not directly bind DMC1 (Figures 4B and 4D). We conclude that a physical interaction between RAD51AP1 and RAD51 is required, but not sufficient, to obtain the full extent of RAD51AP1 stimulation of D loop formation by RAD51. Therefore, we postulate that an additional activity supported by the first 326 residues of RAD51AP1 must also be involved in stimulation of RAD51-mediated D loop formation, possibly by binding to DNA.

RAD51AP1 Exhibits Enhanced Affinity for Synthetic SEI DNA Intermediates and Holliday Junctions

Because D loop formation involves a spectrum of DNA structures, including ss, ds, and branched-DNA struc-

tures, we tested whether human RAD51AP1 was able to discriminate between various DNA structures by using electrophoretic mobility shift assays employing synthetic oligonucleotide DNA substrates. Human RAD51AP1 bound both ss and ds linear DNAs, but with little specificity, as evidenced by the aggregation of protein-DNA complexes in the well at relatively high protein to DNA ratios (Kovalenko et al., 1997) (Figure 5A). DNA binding did not depend on the presence of divalent cations or a high-energy cofactor and was cooperative because only a 2-fold incremental increase in protein concentration resulted in an abrupt mobility shift of all DNA substrate in the wells of the gels. The titration experiment revealed a slightly higher affinity of RAD51AP1 for ds- compared to ssDNA. Strikingly, RAD51AP1 showed a marked preference for binding to branched-DNA substrates, including a splayed-arm branched-DNA structure and a four-way junction (Figure 5A and Figure S3). In particular, with the branched-DNA substrates RAD51AP1 formed discrete complexes, consistent with specific protein-DNA interactions. Anti-RAD51AP1 immunoblotting analysis after gel retardation demonstrated that the complexes contained both the radiolabeled DNA substrate and the RAD51AP1 protein (Figure 5B). Under the experimental conditions tested, RAD51AP1 exhibited the highest affinity for a four-way Holliday junction structure with homologous sequence at its core (Figure S3A). Assuming a 1:1 protein-DNA complex, the apparent K_Ds for the interactions with the branched-DNA substrates was estimated to be in the range of $\sim$20–50 nM (Figure S3A, lower four panels). Furthermore, the stability of RAD51AP1-Holliday junction complexes was only mildly affected at high salt concentrations (Figure S3B), suggesting that the interaction is partly electrostatic and partly hydrophobic. To rule out the possibility that the observed effect was due to a strong sequence dependence of RAD51AP1 DNA binding, we generated eight branched-DNA substrates that differed in sequence (Figure 5C). Although subtle differences in affinity could be observed, a comparison with their unbranched ss and ds derivates (Figure 5C, upper panel) revealed that the dominant feature determining formation of specific RAD51AP1-DNA complexes was the branched nature of the DNA substrate (Figure 5C, lower panel). We conclude that RAD51AP1 is a structure-specific DNA binding protein having a preference for branched-DNA structures.

Branched-DNA structures are intrinsic to intermediates in homologous recombination. They are an inherent part of the SEI DNA intermediate that is formed after strand invasion and exchange by RAD51. Given its general specificity for branched-DNA structures, we asked whether RAD51AP1 demonstrated increased affinity for specific DNA branches located within an SEI DNA intermediate (= D loop with a protruding ss or ds arm). To this end, a series of synthetic oligonucleotide DNA substrates that structurally mimic the different branched junctions in this intermediate were generated and tested for their relative RAD51AP1 affinity (Figure 6). RAD51AP1 bound the SEI

139

Figure 5. RAD51AP1 Exhibits Structure-Specific DNA Binding

(A) Electrophoretic mobility shift assays performed with, from top to bottom, ss, ds, splayed-arm, and Holliday junction DNA substrates at 2.5 nM. DNA substrates were constructed with the indicated oligonucleotides described in Table S2. Position of the radiolabel on the substrate is indicated with an asterisk.

(B) Discrete retarded complexes contained both the radiolabeled DNA substrate (left panel, radioactivity prior to immunoblotting) and RAD51AP1 (right panel, anti-RAD51AP1). The DNA substrate used was the Holliday junction described above.

(C) High-affinity DNA binding of RAD51AP1 depends on the presence of a branch in the DNA substrate rather than on the DNA sequence. Electrophoretic mobility shift assays performed with eight splayed-arm DNA structures, with different arm sequences as indicated in red or blue and ss and ds oligonucleotides as controls (upper panel). The concentration of the DNA substrate was 2.5 nM. The concentration of RAD51AP1 was at 1000 nM and titrated down in 2-fold increments.

DNA intermediate with much higher affinity than a ds linear substrate, a DNA bubble substrate, or a simple D loop without a protruding DNA strand (Figure 6A). The binding affinity of RAD51AP1 for D loop structures was slightly higher when the protruding DNA was ds rather than ss (Figure 6A and Figure S3A, lower panels on the left).

If the branch-specific DNA binding of RAD51AP1 is relevant to the mechanism by which RAD51AP1 stimulates D
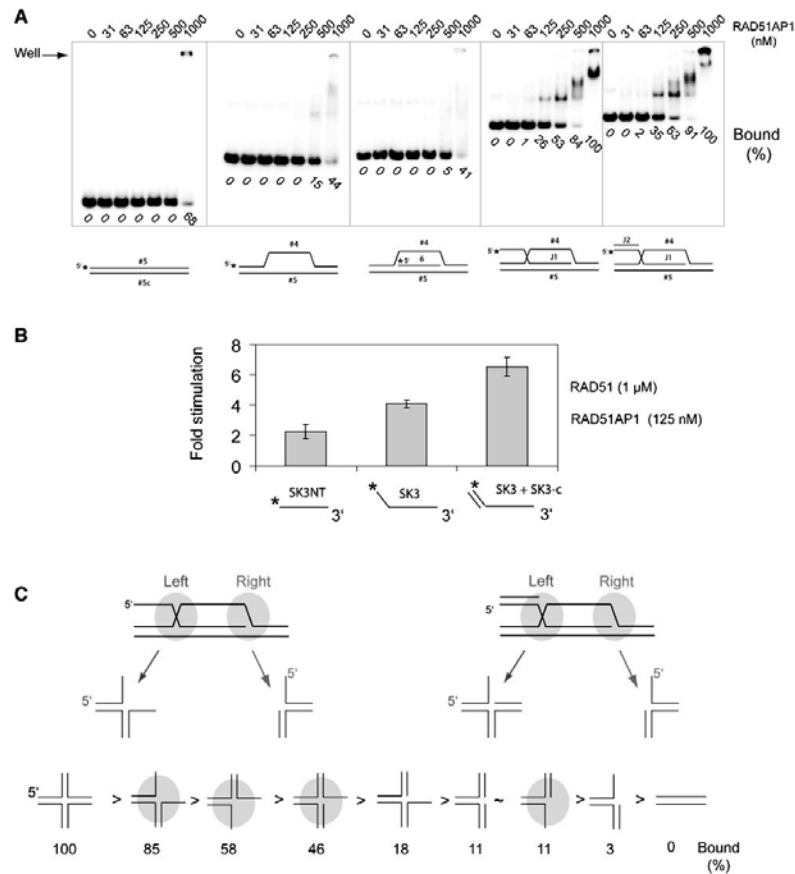
Figure 6. High-Affinity Binding of RAD51AP1 to Single-End Invasion DNA Substrates

(A) Electrophoretic mobility shift assays performed with, from left to right, linear ds, bubble, D loop, ss branch, or ds branch containing D loop DNA substrates used at 2.5 nM final concentration. Position of the radiolabel on the substrate is indicated with an asterisk.

(B) Fold RAD51AP1-mediated stimulation measured in RAD51-catalyzed D loop assays performed with an unbranched (SK3NT), ss (SK3), or ds (SK3+SK3-c) branch containing invading oligonucleotides. Averages of four experiments are plotted. Error bars represent standard deviations.

(C) Dissection of SEI DNA intermediates into their respective left and right branched sites (top). Summary of the relative affinity of RAD51AP1 for various branched-DNA substrates as measured by electrophoretic mobility shift assays (bottom). Primary data is shown in Figure S4.

loop formation by RAD51, then those D loop formation reactions involving DNA intermediates for which RAD51AP1 displays the highest affinity should be stimulated to the greatest extent. To test this prediction, we analyzed the effect of RAD51AP1 in RAD51-catalyzed D loop assays by using invading oligonucleotides, resulting in D loops without protruding arms or with ss or ds arm extensions (Figure 6B). Indeed, RAD51AP1 stimulated D loop formation to the highest extent when the invading oligonucleotide contained a nonhomologous extension, especially so when the protruding extension was ds.

The SEI DNA intermediates used in this study contain a number of distinct branched-DNA structures. For simplicity we refer to them as the "left" and "right" branched sites, as schematically depicted in Figure 6C. The results from experiments presented above (Figures 6A and 6B) suggest that RAD51AP1 might act by binding to the left branched site of the SEI DNA intermediate rather than the right branched site (Figure 6C). Oligonucleotide substrates mimicking either the isolated left or right branched sites of the SEI DNA intermediate, as well as additional branched structures, were generated, and the relative RAD51AP1 binding affinity to these substrates was determined by gel electrophoresis mobility shift assays. The results are shown in Figure S4 and summarized in Figure 6C. RAD51AP1 exhibited a clear preference for the substrates

141
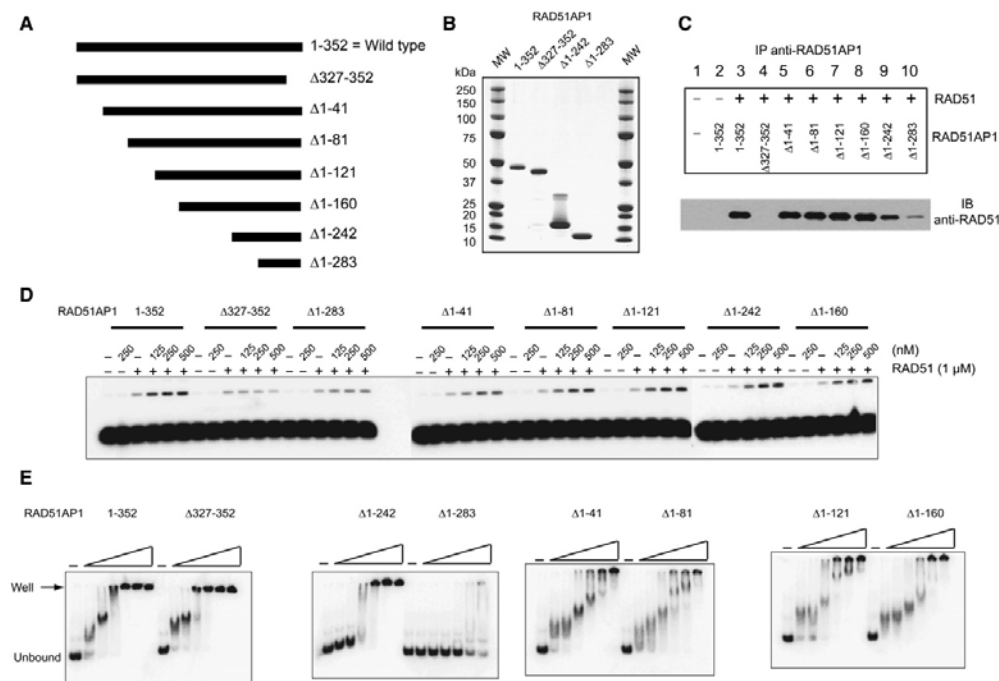
Figure 7. RAD51AP1 Deletion Mutant Analysis

(A) Scheme of the RAD51AP1 deletion variants produced for this analysis.

(B) A reducing SDS-PAGE gel stained with Coomassie containing wild-type RAD51AP1 and deletion variants Δ327–352, Δ1–242, and Δ1–283.

(C) RAD51 binding analysis of the RAD51AP1 deletions by in vitro coimmunoprecipitation as revealed by immunoblots. Anti-RAD51AP1 (R1085) was reactive against all deletion variants, including Δ327–352 (data not shown). Its effectiveness was reduced for deletion variants Δ1–242 and Δ1–283, possibly due to loss of available epitopes.

(D) Effect of RAD51AP1 deletion variants in RAD51-catalyzed D loop assays using homologous invading oligonucleotide SK3 and supercoiled pUC19 plasmid as recipient. Quantification is reported in Table S1.

(E) Analysis of the RAD51AP1 deletion variants by mobility shift assays using 5 nM of radiolabeled SEI DNA substrate with a ds protruding arm. RAD51AP1 was titrated starting at 2000 nM and diluted in 2-fold increments. Quantification is reported in Table S1.

that mimicked the left branched site of the SEI DNA intermediate. Taken together, these results suggest that the mechanism by which RAD51AP1 stimulates D loop formation by RAD51 relies on a bimodular organization of the RAD51AP1 polypeptide. The very C-terminal domain (∼30 residues) supports direct physical interaction with RAD51. Located N-terminal to this RAD51 binding domain, a second RAD51AP1 domain binds the left branched site in the SEI DNA intermediate.

Stimulation of RAD51-Mediated D Loop Formation by RAD51AP1 Depends on Both Its RAD51 and SEI DNA Intermediate Binding Activities

Because the RAD51 binding site of RAD51AP1 seems to be located at the very C terminus of the polypeptide, we generated and purified a series of N-terminal deletion mutants of RAD51AP1 to delineate the residues conferring DNA binding ability (Figures 7A and 7B and Table S1).

These N-terminally truncated RAD51AP1 polypeptides, along with the C-terminal truncation described above (Figure 4C), were tested for their ability to bind RAD51, to bind the SEI DNA intermediate, and to stimulate D loop formation by RAD51 (Figures 7C–7E and summarized in Table S1). The first 242 N-terminal residues of RAD51AP1 could be deleted without a major effect on its ability to bind RAD51, to bind the SEI DNA intermediate, and to stimulate D loop formation by RAD51. The smallest RAD51AP1 polypeptide (RAD51AP1$^{\Delta 1-283}$ containing the last 69 C-terminal residues) was defective in stimulation of D loop formation by RAD51 but still bound RAD51. Thus, the domain involved in binding to the SEI DNA intermediate is likely located between residues 243 and 326. In addition, because the truncated version RAD51AP1$^{\Delta 1-283}$ still exhibited a weak but detectable binding to the SEI DNA intermediate, at least one residue critical for RAD51AP1 DNA binding should be located within

positions 284–326. Finally, the C-terminal truncation that failed to interact with RAD51 and stimulate RAD51 D loop formation activity (Figure 4C) bound the SEI DNA intermediate in a manner similar to the wild-type RAD51AP1 (Figure 7E, first panel). We conclude that both the RAD51 binding and the structure-specific SEI DNA intermediate binding ability of RAD51AP1 are required for efficient stimulation of D loop formation by RAD51.

DISCUSSION

Homologous recombination, the exchange of DNA strands between homologous DNA molecules, is essential for preserving genome integrity and for accurate genome duplication (Hoeijmakers, 2001). A key step in homologous recombination, joint molecule formation through homology recognition and DNA strand exchange, is mediated by RAD51. To unravel the molecular mechanism of RAD51 action, it is imperative to identify protein partners of RAD51 that influence its activity in homologous recombination. The primary conclusion from the work presented here is that RAD51AP1 is a RAD51 accessory protein that specifically stimulates joint molecule formation through its structure-specific DNA interaction and its interaction with RAD51 (Figures 4–7 and Figures S2–S4). Previous experiments led to the suggestion that RAD51AP1 has a specific role in connecting RAD51 to the cellular response to DNA interstrand crosslinks mediated by the Fanconi anemia proteins (Henson et al., 2006). Our results reveal that RAD51AP1-depleted cells exhibit increased sensitivity, not only to DNA interstrand crosslinking agents but also to other DSB-inducing agents, including ionizing radiation and camptothecin (Figure 1). In addition, the results of siRNA-mediated downregulation experiments suggest that RAD51AP1 is hypostatic to the homologous recombination factors XRCC3 and RAD51 (Figure 1). Furthermore, RAD51AP1-depleted cells display a reduced level of DSB-induced gene conversion (Wiese et al., 2007 [this issue of *Molecular Cell*]; data not shown). Thus, RAD51AP1 plays a more general role during RAD51-dependent repair of DSBs.

Mechanism of RAD51AP1 Stimulation of D Loop Formation by RAD51

Our biochemical analysis reveals that RAD51AP1 specifically stimulates joint molecule formation by RAD51 (Figures 4A–4C). Because of its ability to directly bind RAD51 (Figure 4D), RAD51AP1 could potentially act during the presynaptic phase of recombination by helping the nucleation or by stabilizing the RAD51 nucleoprotein filament (Figure S5, possibility 1). We do not favor this interpretation because proteins such as BRCA2, involved in the nucleation phase (Kojic et al., 2002; Yang et al., 2005), or complexes of the RAD51 paralogs, implicated in RAD51 filament stabilization (Lio et al., 2003; Sigurdsson et al., 2001), are required for damage-induced RAD51 foci formation (Takata et al., 2000, 2001; Yuan et al., 1999). In contrast, downregulation of RAD51AP1 does not affect

damage-induced RAD51 foci formation (Figure 2). In addition, through the analyses of seven different RAD51AP1 truncation mutants, we show that binding to both branched DNA and RAD51 correlates with the ability to stimulate D loop formation (Figure 7 and Table S1). Because both of these RAD51AP1 activities are required, RAD51AP1 could come into play just before or as soon as strand exchange has initiated, i.e., after nucleation and filament extension (Figure S5, possibilities 2 and 3).

A key feature of RAD51AP1 is its enhanced affinity for the left branched site of the SEI DNA intermediate (Figure 6). This activity might allow RAD51AP1 to act as sensor or anchor during homology recognition. Once a critical level of homology is encountered during strand invasion, RAD51AP1 would anchor the RAD51 filament at the nascent branched-DNA site, thereby stabilizing the joint molecule intermediate without requiring more extensive heteroduplex DNA formation (Figure S5, possibility 3 and see below). Because this function of RAD51AP1 would require both the interaction with RAD51 and a branched-DNA structure that RAD51 generates, there is the potential for the RAD51AP1 control mechanism to be highly specific. If these two RAD51AP1 interactions are coupled, RAD51AP1 will have a preference for sites containing both features rather than RAD51-less branched-DNA structures or RAD51 ss DNA filaments free of branched DNA.

RAD51AP1 versus Other Accessory Proteins Stimulating RAD51-Mediated D Loop Formation

S. cerevisiae Rad52 stimulates the Rad51 D loop reaction by forming a stoichiometric complex with Rad51 (Arai et al., 2005). Therefore, the mode of action of Rad52 in D loop formation is likely to differ from that of RAD51AP1, because the RAD51AP1 stimulatory effect is detected at a substoichiometric ratio of close to one RAD51AP1 per RAD51 nucleoprotein filament (Figure 4). Instead, Rad52 stimulates Rad51-mediated D loop formation by acting at the presynaptic phase (Benson et al., 1998; New et al., 1998; Shinohara and Ogawa, 1998; Sung, 1997).

As opposed to Rad52, which functions at the presynaptic phase, RAD54 can stimulate joint molecule formation at the synaptic phase. Stimulation by RAD54 at this particular stage of homologous recombination involves its translocase activity that affects the topology of the ds DNA recipient and/or its chromatin structure (Heyer et al., 2006). Given that ds DNA is the substrate for RAD54 at this stage of recombination stimulation, whereas RAD51AP1 preferentially binds branched-DNA structures, RAD54 likely functions differently from RAD51AP1 in stimulating D loop formation. Interestingly, recently RAD54 has been found to promote branch migration of DNA substrates similar in structure to the left branched site of the SEI DNA intermediate (Bugreev et al., 2006). However, the relationship between RAD51AP1 binding to these structures and their branch migration by RAD54 remains to be explored.

Several features of the RAD51AP1 D loop stimulation resemble the action of the yeast, murine, or human HOP2/MND1 complex on the meiosis-specific ATP-dependent

DMC1 recombinase. HOP2/MND1 physically interacts with the recombinase and strongly stimulates its ability to form D loops when present in the reaction at a substoichiometric ratio relative to the recombinase (Chen et al., 2004; Enomoto et al., 2006; Petukhova et al., 2005; Pezza et al., 2006). However, the HOP2/MND1 DNA binding activities have not yet been investigated in great detail. Nevertheless, in vertebrate somatic cells, RAD51AP1 could represent a functional analog of the germline-specific HOP2/MND1 complex.

Although RAD51AP1 homologs are found in different vertebrates, *S. cerevisiae* does not appear to encode an obvious RAD51AP1 sequence homolog. In contrast, the proteins at the core of homologous recombination, the recombinases that mediated homology recognition and DNA strand homolog, are conserved (Krogh and Symington, 2004; Sung, 2005; Wyman and Kanaar, 2006). Absence of conservation appears to be common among regulators of homologous recombination. For example, *S. cerevisiae* does not have a BRCA2 homolog, which is critical for homologous recombination in mammals. Conversely, Rad52 is essential for homologous recombination in *S. cerevisiae* but is dispensable in murine cells. Clearly, difference in nuclear physiology among species, or even within a species but among different cell types, will require differential regulation of homologous recombination.

Potential Roles of RAD51AP1 during the Postsynaptic Phase of RAD51-Mediated Homologous Recombination

The RAD51AP1-enhanced affinity for the left branched site of the SEI DNA intermediate (Figure 6C) places it on the structure poised to re-establish a functional replication fork by either a strand cleavage or a branch migration mechanism (Figure S5, possibility 4). RAD51AP1 binding to the left branched site of the SEI DNA intermediate could affect the processing of this intermediate by, e.g., imposing a bias in resolution. Alternatively or in addition, RAD51AP1 could affect branch migration by preventing formation of extensive heteroduplex DNA, which is not necessarily a productive or beneficial reaction. Instead, it could promote unidirectional branch migration toward the 3′ end of the invaded DNA strand and thereby stimulate the formation of structures from which an active replication fork can be reassembled (Figure S5, possibility 4). In addition to binding with high affinity to the left branched site of the SEI DNA intermediate, RAD51AP1 also exhibits high affinity for four-way Holliday junctions (Figure 5 and Figures S3 and S4). An involvement of RAD51AP1 in Holliday junction resolution, not necessarily in direct association with RAD51, is possible (Figure S5, possibility 4).

Importance of Structural Transitions in DNA during RAD51-Dependent Homologous Recombination

Studies of the bacterial RecA recombinase have revealed that the ds/ss transition that is formed upon 5′ to 3′ resection of a DSB represents a critical control site where nucle-ation of nucleoprotein filaments can be initiated (Cox, 2007). The ds/ss transition appears to be an equally important control site for the assembly of eukaryotic RAD51 nucleoprotein filament. It has been proposed that BRCA2 delivers RAD51 at the ds/ss transition by a mechanism that displaces RPA (an ss DNA binding protein) from the protruding ss extension (Kojic et al., 2002; Yang et al., 2005). Our results with RAD51AP1 imply that an additional structural transition in DNA, the branched DNA of the SEI DNA intermediate, might also be an important control site during the synaptic and postsynaptic phases of RAD51-mediated homologous recombination. If RAD51AP1 promotes RAD51-mediated homologous recombination through binding to the ds/ss DNA transition upon joint molecule formation, it will be well suited to act as a key homologous recombination regulator at a number of critical mechanistic steps. First, it could displace the mediator class of accessory factors, such as BRCA2, that act at the presynaptic phase from the ds/ss transition. Second, it could regulate and direct branch migration of the structure toward productive re-establishment of replication forks, as argued above. Third, it has the potential to participate in resolution of the branched intermediate structures. In summary, the binding specificity of RAD51AP1 for central players in homologous recombination, RAD51, and branched-DNA intermediates confers the ability on RAD51AP1 to control vital steps in the preservation of genome integrity.

EXPERIMENTAL PROCEDURES

Proteins

RAD51AP1 was overexpressed in Rosetta/pLysS cells (Novagen) by induction with IPTG (1 mM final concentration) when the optical density at 600 nm reached 0.4. After 5 hr at 37°C, cells were collected by centrifugation and lysed in NiA buffer (0.5 M KCl, 10% glycerol, 20 mM HEPES-NaOH [pH 8], 2 mM Imidazole, and 1 mM PMSF). After clarification (30,000 × g for 1 hr), the lysate was incubated with Ni-NTA Sepharose resin for 1 hr and washed with NiA, with NiA + 20 mM Imidazole, and with NiA + 40 mM Imidazole. RAD51AP1 was eluted with NiA + 200 mM Imidazole. The Ni-NTA pool was diluted by addition of two volumes of SA buffer (20 mM HEPES-NaOH [pH 8], 10% glycerol, 1 mM DTT, and 1 mM EDTA) and loaded on an S Sepharose column equilibrated with SA + 150 mM KCl. The column was washed with SA + 150 mM KCl buffer, and then the salt concentration was increased in steps from 200, 300, 400, and 500 mM KCl. RAD51AP1 eluted in the 300 mM KCl fraction. Analytical Sephacryl 200 gel permeation chromatography was performed in 20 mM HEPES-NaOH (pH 8), 10% glycerol, 1 mM DTT, 1 mM EDTA, and 200 mM KCl and at a starting loading concentration of 20 μM. Globular standards (#151-1901) were from Bio-Rad. Identical results were obtained when the experiment was performed at 400 mM KCl instead of 200 mM. Human RAD51 and DMC1 were purified as described (Masson et al., 1999; Ristic et al., 2005) and stored in 300 mM KCl, 20 mM HEPES-NaOH (pH 8), 10% glycerol, 1 mM DTT, and 1 mM EDTA. Protein concentrations were measured by the Bradford method (Bio-Rad) using BSA as standard and expressed in molarity of monomer.

Materials and conditions employed for the following assays are listed in the Supplemental Data: antibodies and immunoblotting, siRNA downregulation, colony survival assays, immunofluorescence conditions, plasmid constructs, sedimentation analysis, mass

spectrometry, protein crosslinking, coimmunoprecipitation, electrophoretic mobility shift, and D loop assays.

Supplemental Data

Supplemental Data include Supplemental Results, Supplemental Experimental Procedures, Supplemental References, five figures, and two tables and can be found with this article online at http://www.molecule.org/cgi/content/full/28/3/468/DC1/.

REFERENCES

Arai, N., Ito, D., Inoue, T., Shibata, T., and Takahashi, H. (2005). Heteroduplex joint formation by a stoichiometric complex of Rad51 and Rad52 of Saccharomyces cerevisiae. J. Biol. Chem. *280*, 32218–32229.

Bishop, D.K., Park, D., Xu, L., and Kleckner, N. (1992). DMC1: a meiosis-specific yeast homolog of E. coli recA required for recombination, synaptonemal complex formation, and cell cycle progression. Cell *69*, 439–456.

Benson, F.E., Baumann, P., and West, S.C. (1998). Synergistic actions of Rad51 and Rad52 in recombination and DNA repair. Nature *391*, 401–404.

Brenneman, M.A., Wagener, B.M., Miller, C.A., Allen, C., and Nickoloff, J.A. (2002). XRCC3 controls the fidelity of homologous recombination: roles for XRCC3 in late stages of recombination. Mol. Cell *10*, 387–395.

Bugreev, D.V., and Mazin, A.V. (2004). Ca2+ activates human homologous recombination protein Rad51 by modulating its ATPase activity. Proc. Natl. Acad. Sci. USA *101*, 9988–9993.

Bugreev, D.V., Mazina, O.M., and Mazin, A.V. (2006). Rad54 protein promotes branch migration of Holliday junctions. Nature *442*, 590–593.

Chen, Y.K., Leng, C.H., Olivares, H., Lee, M.H., Chang, Y.C., Kung, W.M., Ti, S.C., Lo, Y.H., Wang, A.H., Chang, C.S., et al. (2004). Heterodimeric complexes of Hop2 and Mnd1 function with Dmc1 to promote meiotic homolog juxtaposition and strand assimilation. Proc. Natl. Acad. Sci. USA *101*, 10572–10577.

Cox, M.M. (2007). Regulation of Bacterial RecA Protein Function. Crit. Rev. Biochem. Mol. Biol. *42*, 41–63.

Cox, M.M., Goodman, M.F., Kreuzer, K.N., Sherratt, D.J., Sandler, S.J., and Marians, K.J. (2000). The importance of repairing stalled replication forks. Nature *404*, 37–41.

Enomoto, R., Kinebuchi, T., Sato, M., Yagi, H., Kurumizaka, H., and Yokoyama, S. (2006). Stimulation of DNA strand exchange by the human TBPIP/Hop2-Mnd1 complex. J. Biol. Chem. *281*, 5575–5581.

Haaf, T., Golub, E.I., Reddy, G., Radding, C.M., and Ward, D.C. (1995). Nuclear foci of mammalian Rad51 recombination protein in somatic cells after DNA damage and its localization in synaptonemal complexes. Proc. Natl. Acad. Sci. USA *92*, 2298–2302.

Haruta, N., Kurokawa, Y., Murayama, Y., Akamatsu, Y., Unzai, S., Tsutsui, Y., and Iwasaki, H. (2006). The Swi5-Sfr1 complex stimulates Rhp51/Rad51- and Dmc1-mediated DNA strand exchange in vitro. Nat. Struct. Mol. Biol. *13*, 823–830.

Henson, S.E., Tsai, S.C., Malone, C.S., Soghomonian, S.V., Ouyang, Y., Wall, R., Marahrens, Y., and Teitell, M.A. (2006). Pir51, a Rad51-interacting protein with high expression in aggressive lymphoma, controls mitomycin C sensitivity and prevents chromosomal breaks. Mutat. Res. *601*, 113–124.

Heyer, W.D., Li, X., Rolfsmeier, M., and Zhang, X.P. (2006). Rad54: the Swiss Army knife of homologous recombination? Nucleic Acids Res. *34*, 4115–4125.

Hoeijmakers, J.H. (2001). Genome maintenance mechanisms for preventing cancer. Nature *411*, 366–374.

Hunter, N., and Kleckner, N. (2001). The single-end invasion: an asymmetric intermediate at the double-strand break to double-holliday junction transition of meiotic recombination. Cell *106*, 59–70.

Kogoma, T. (1997). Stable DNA replication: interplay between DNA replication, homologous recombination, and transcription. Microbiol. Mol. Biol. Rev. *61*, 212–238.

Kojic, M., Kostrub, C.F., Buchman, A.R., and Holloman, W.K. (2002). BRCA2 homolog required for proficiency in DNA repair, recombination, and genome stability in Ustilago maydis. Mol. Cell *10*, 683–691.

Kovalenko, O.V., Golub, E.I., Bray-Ward, P., Ward, D.C., and Radding, C.M. (1997). A novel nucleic acid-binding protein that interacts with human rad51 recombinase. Nucleic Acids Res. *25*, 4946–4953.

Kovalenko, O.V., Wiese, C., and Schild, D. (2006). RAD51AP2, a novel vertebrate- and meiotic-specific protein, shares a conserved RAD51-interacting C-terminal domain with RAD51AP1/PIR51. Nucleic Acids Res. *34*, 5081–5092.

Kowalczykowski, S.C. (2000). Initiation of genetic recombination and recombination-dependent replication. Trends Biochem. Sci. *25*, 156–165.

Krogh, B.O., and Symington, L.S. (2004). Recombination proteins in yeast. Annu. Rev. Genet. *38*, 233–271.

Lio, Y.C., Mazin, A.V., Kowalczykowski, S.C., and Chen, D.J. (2003). Complex formation by the human Rad51B and Rad51C DNA repair proteins and their activities in vitro. J. Biol. Chem. *278*, 2469–2478.

Liu, Y., Masson, J.Y., Shah, R., O'Regan, P., and West, S.C. (2004). RAD51C is required for Holliday junction processing in mammalian cells. Science *303*, 243–246.

Masson, J.-Y., Davies, A.A., Hajibagheri, N., Van Dyck, E., Benson, F.E., Stasiak, A.Z., Stasiak, A., and West, S.C. (1999). The meiosis-specific recombinase hDmc1 forms ring structures and interacts with hRad51. EMBO J. *18*, 6552–6560.

Mazin, A.V., Zaitseva, E., Sung, P., and Kowalczykowski, S.C. (2000). Tailed duplex DNA is the preferred substrate for Rad51 protein-mediated homologous pairing. EMBO J. *19*, 1148–1156.

Mizuta, R., LaSalle, J.M., Cheng, H.L., Shinohara, A., Ogawa, H., Copeland, N., Jenkins, N.A., Lalande, M., and Alt, F.W. (1997). RAB22 and RAB163/mouse BRCA2: proteins that specifically interact with the RAD51 protein. Proc. Natl. Acad. Sci. USA *94*, 6927–6932.

New, J.H., Sugiyama, T., Zaitseva, E., and Kowalczykowski, S.C. (1998). Rad52 protein stimulates DNA strand exchange by Rad51 and replication protein A. Nature *391*, 407–410.

Petukhova, G.V., Pezza, R.J., Vanevski, F., Ploquin, M., Masson, J.Y., and Camerini-Otero, R.D. (2005). The Hop2 and Mnd1 proteins act in concert with Rad51 and Dmc1 in meiotic recombination. Nat. Struct. Mol. Biol. *12*, 449–453.

Pezza, R.J., Petukhova, G.V., Ghirlando, R., and Camerini-Otero, R.D. (2006). Molecular activities of meiosis-specific proteins Hop2, Mnd1, and the Hop2-Mnd1 complex. J. Biol. Chem. *281*, 18426–18434.

Ristic, D., Modesti, M., van der Heijden, T., van Noort, J., Dekker, C., Kanaar, R., and Wyman, C. (2005). Human Rad51 filaments on double- and single-stranded DNA: correlating regular and irregular forms with recombination function. Nucleic Acids Res. *33*, 3292–3302.

Shinohara, A., and Ogawa, T. (1998). Stimulation by Rad52 of yeast Rad51-mediated recombination. Nature *391*, 404–407.

Sigurdsson, S., Van Komen, S., Bussen, W., Schild, D., Albala, J.S., and Sung, P. (2001). Mediator function of the human Rad51B-Rad51C complex in Rad51/RPA-catalyzed DNA strand exchange. Genes Dev. *15*, 3308–3318.

Solinger, J.A., Kiianitsa, K., and Heyer, W.D. (2002). Rad54, a Swi2/Snf2-like recombinational repair protein, disassembles Rad51:dsDNA filaments. Mol. Cell *10*, 1175–1188.

Song, H., Xia, S.L., Liao, C., Li, Y.L., Wang, Y.F., Li, T.P., and Zhao, M.J. (2004). Genes encoding Pir51, Beclin 1, RbAp48 and aldolase b are up or down-regulated in human primary hepatocellular carcinoma. World J. Gastroenterol. *10*, 509–513.

Sugawara, N., Wang, X., and Haber, J.E. (2003). In vivo roles of Rad52, Rad54, and Rad55 proteins in Rad51-mediated recombination. Mol. Cell *12*, 209–219.

Sung, P. (1997). Function of yeast Rad52 protein as a mediator between replication protein A and the Rad51 recombinase. J. Biol. Chem. *272*, 28194–28197.

Sung, P. (2005). Mediating repair. Nat. Struct. Mol. Biol. *12*, 213–214.

Takata, M., Sasaki, M.S., Sonoda, E., Fukushima, T., Morrison, C., Albala, J.S., Swagemakers, S.M., Kanaar, R., Thompson, L.H., and Takeda, S. (2000). The Rad51 paralog Rad51B promotes homologous recombinational repair. Mol. Cell. Biol. *20*, 6476–6482.

Takata, M., Sasaki, M.S., Tachiiri, S., Fukushima, T., Sonoda, E., Schild, D., Thompson, L.H., and Takeda, S. (2001). Chromosome instability and defective recombinational repair in knockout mutants of the five Rad51 paralogs. Mol. Cell. Biol. *21*, 2858–2866.

Tashiro, S., Kotomura, N., Shinohara, A., Tanaka, K., Ueda, K., and Kamada, N. (1996). S phase specific formation of the human Rad51 protein nuclear foci in lymphocytes. Oncogene *12*, 2165–2170.

Wang, Y., Hayakawa, J., Long, F., Yu, Q., Cho, A.H., Rondeau, G., Welsh, J., Mittal, S., De Belle, I., Adamson, E., et al. (2005). "Promoter array" studies identify cohorts of genes directly regulated by methylation, copy number change, or transcription factor binding in human cancer cells. Ann. N Y Acad. Sci. *1058*, 162–185.

Wiese, C., Dray, E., Groesser, T., San Filippo, J., Shi, I., Collins, D.W., Tsai, M.-S., Williams, G.J., Rydberg, B., Sung, P., and Schild, D. (2007). Promotion of homologous recombination and genomic stability by RAD51AP1 via RAD51 recombinase enhancement. Mol. Cell *28*, this issue, 482–490.

Wyman, C., and Kanaar, R. (2006). DNA double-strand break repair: all's well that ends well. Annu. Rev. Genet. *40*, 363–383.

Yang, H., Li, Q., Fan, J., Holloman, W.K., and Pavletich, N.P. (2005). The BRCA2 homologue Brh2 nucleates RAD51 filament formation at a dsDNA-ssDNA junction. Nature *433*, 653–657.

Yuan, S.S., Lee, S.Y., Chen, G., Song, M., Tomlinson, G.E., and Lee, E.Y. (1999). BRCA2 is required for ionizing radiation-induced assembly of Rad51 complex in vivo. Cancer Res. *59*, 3547–3551.

Supplemental Data

RAD51AP1 Is a Structure-Specific DNA Binding Protein that Stimulates Joint Molecule Formation during RAD51-Mediated Homologous Recombination

Mauro Modesti, Magda Budzowska, Céline Baldeyron, Jeroen A.A. Demmers, Rodolfo Ghirlando, and Roland Kanaar

Supplemental Results

Efficient down regulation of RAD51AP1 by siRNA

To monitor levels of RAD51AP1 in cells we generated polyclonal antibodies using purified recombinant human RAD51AP1 as an antigen. The antibodies proved to be highly specific and were used to monitor the levels of RAD51AP1 in human HeLa cell extracts after siRNA-mediated down regulation. Four independent siRNAs targeted against RAD51AP1 were tested (Supplemental Figure 1A). All four RAD51AP1-directed siRNAs induced substantial reduction of RAD51AP1 intracellular levels as early as 24 hrs post-transfection. Effective down regulation was maintained for at least 72 hrs post-transfection. All subsequent RAD51AP1 down regulation experiments were performed with siRNA #1 and #2, since they resulted in a highly efficient and reproducible down regulation of RAD51AP1.

RAD51AP1 down regulation does not affect FANCD2 monoubiquitination or RAD51 expression levels

It is possible that the putative requirement for RAD51AP1 in RAD51-mediated DNA repair is indirect. RAD51AP1 could be part of the early cellular response to interstrand DNA crosslinking agents, of which FANCD2 mono-ubiquitination is a landmark event (Gurtan and D'Andrea, 2006; Henson et al., 2006). Alternatively RAD51AP1 could indirectly affect the protein levels of RAD51. However, neither the steady state levels of RAD51 nor FANCD2 monoubiquitination were affected after RAD51AP1 down regulation (Supplemental Figure 1B and C).
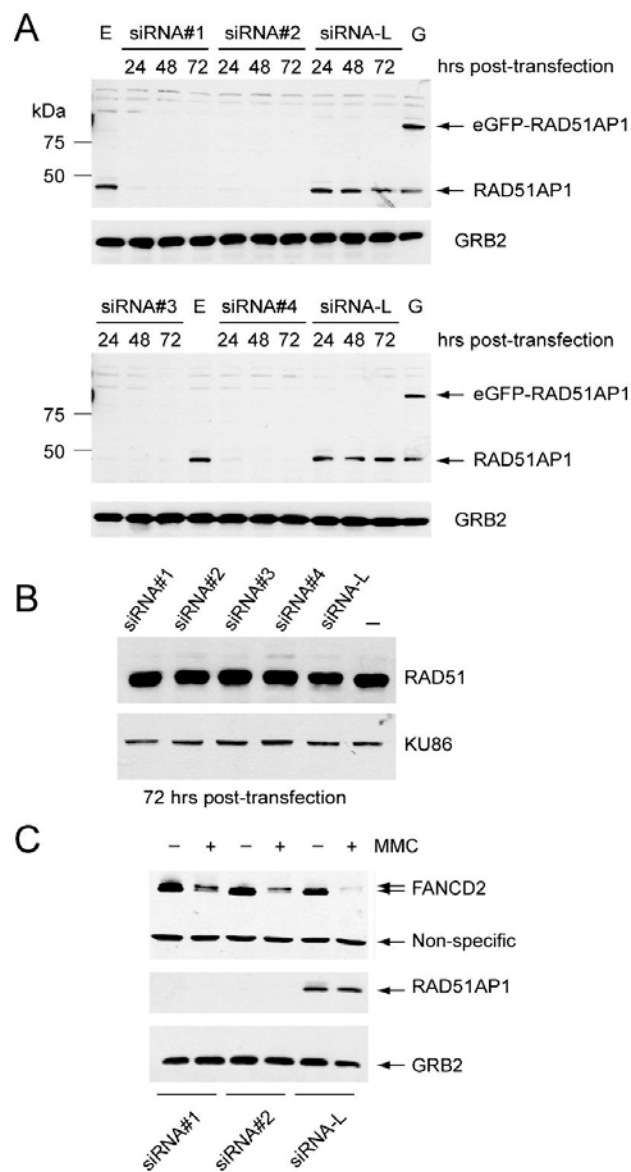
Figure S1. RAD51 levels and FANCD2 mono-ubiquitination are unaffected upon RAD51AP1 depletion.
(A) Down regulation of RAD51AP1 in HeLa cells. Lanes representing nontransfected wild type HeLa cells and HeLa cells expressing eGFP-RAD51AP1 are marked with 'E' and 'G', respectively. GRB2 detection was used as a loading control. **(B)** Levels of RAD51 72 hrs after siRNA transfection. KU86 detection served as a loading control. **(C)** Top panel: FANCD2 monoubiquitination in untreated and mitomycin C-treated cells (MMC, 3 μM mitomycin C for 24 hrs) after mock (siRNA-L) or RAD51AP1 depletion (siRNA #1 and #2). Detection of a non-specific band verified equal loading. Bottom two panels: verification of RAD51AP1 depletion using GBR2 detection as a loading control.

148

Buffer Buffer Buffer RAD51AP1 RAD51 Buffer Buffer Buffer RAD51AP1 RAD51 1st incubation

Buffer RAD51AP1 RAD51 RAD51 RAD51AP1 Buffer RAD51AP1 RAD51 RAD51 RAD51AP1 2nd incubation

| 1 | 2 | 3 | 4 | 5 | 6 | 7 | 8 | 9 | 10 |

1.0 4.8 4.7   1.0 7.8 8.1 Fold stimulation

RAD51AP1 (125 nM)   RAD51AP1 (250 nM)

RAD51 (1 µM)   RAD51 (1 µM)
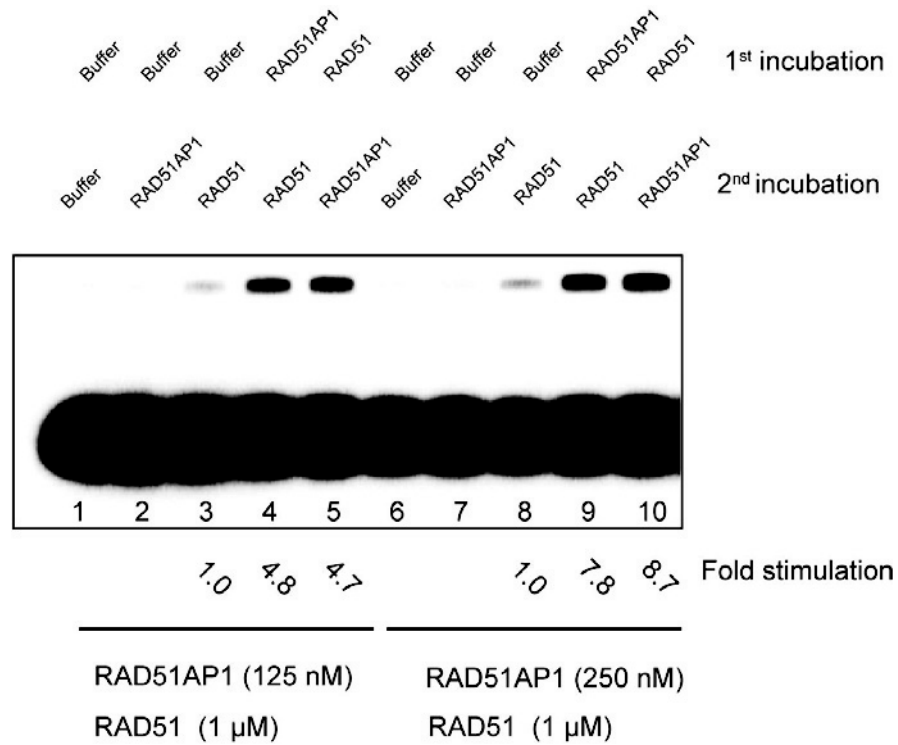
Figure S2. RAD51AP1 stimulation of D loop formation by RAD51 is independent of the order of addition during filament assembly phase.
Effect of RAD51AP1 in RAD51-catalyzed D loop assays using homologous invading oligonucleotide SK3 and supercoiled pUC19 plasmid as recipient substrate. RAD51AP1 was added either before (lanes 4 and 9) or after (lanes 5 and 10) RAD51 during the filament assembly phase prior to addition of the recipient plasmid.

149
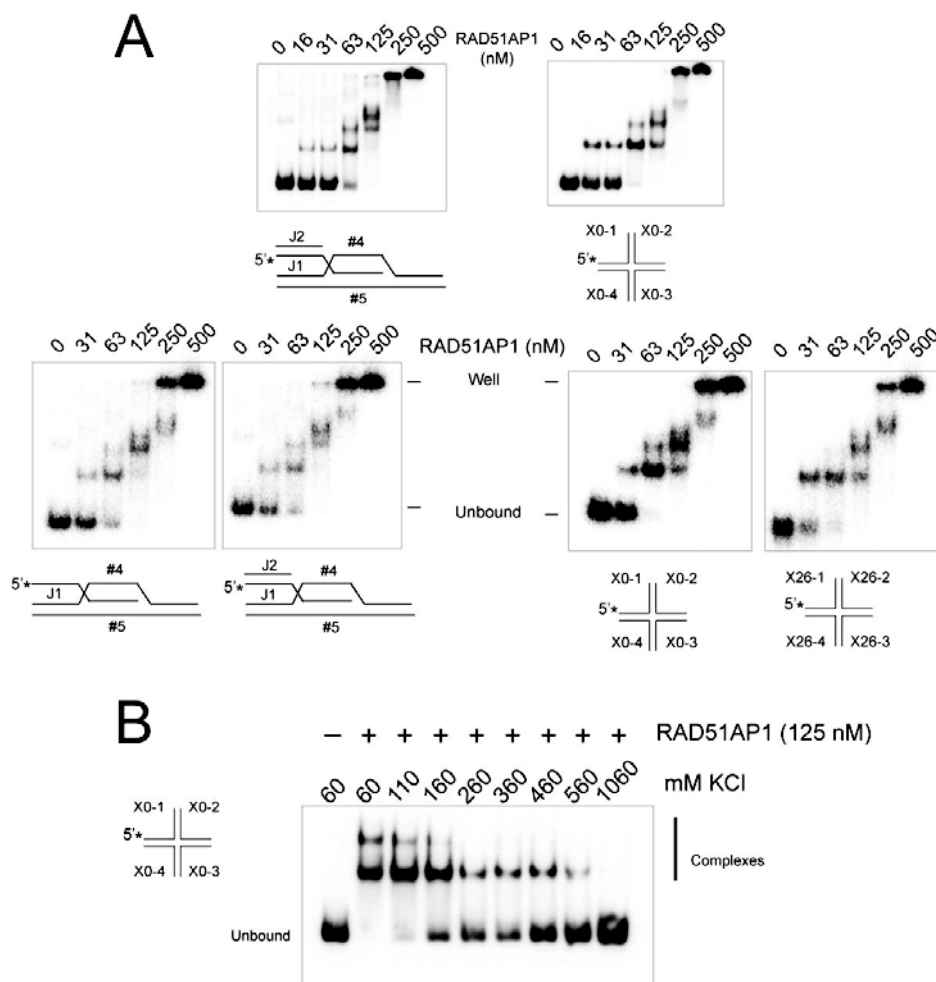
Figure S3. High affinity of RAD51AP1 for synthetic branched DNA structures.
(A) Electrophoretic mobility shift assays using 1.25 nM of SEI DNA intermediates and Holliday junction substrates constructed with the indicated oligonucleotides for which the sequences can be found in Supplemental Table 2. Holliday junction X0-1,2,3,4 contains an immobile junction due to heterologous DNA arms. Holliday junction X26-1,2,3,4 contains homologous DNA sequences at its core. The position of the radiolabel on the DNA substrates is indicated with an asterisk. **(B)** RAD51AP1 (125 nM) was incubated with the indicated Holliday junction (1.25 nM) in increasing concentrations of KCl and complexes were resolved by native acrylamide gel electrophoresis.
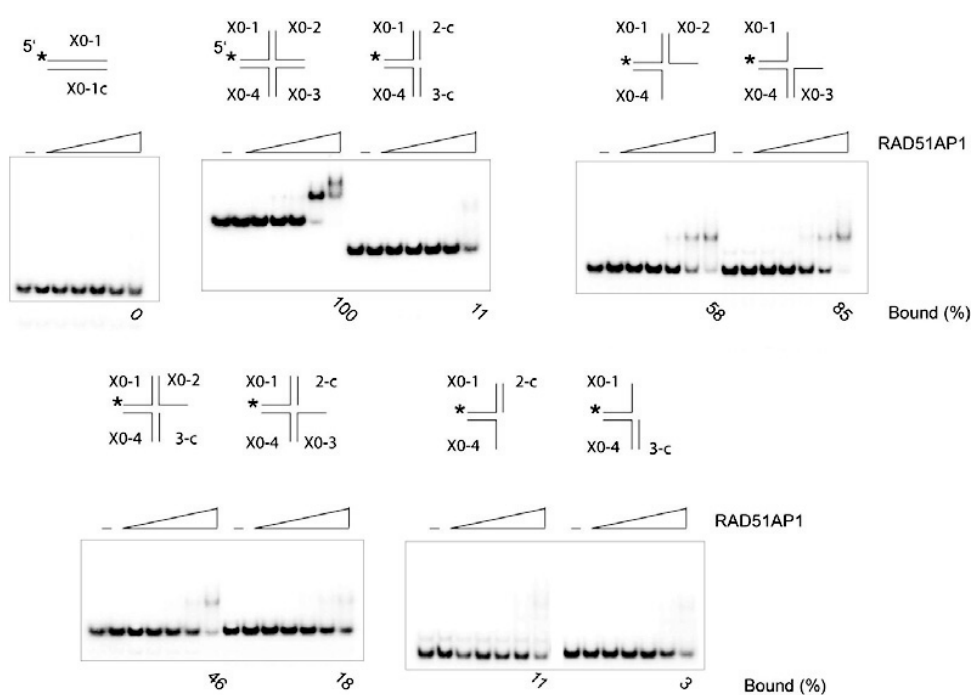
Figure S4. Affinity of RAD51AP1 for synthetic branched DNA.
Electrophoretic mobility shift assays using 2.5 nM of each DNA substrate. RAD51AP1 started at a concentration of 500 nM and was titrated down in two-fold increments. DNA substrates were constructed with the indicated oligonucleotides for which the sequences can be found in Supplemental Table 2. Position of the radiolabel on the substrates is indicated with an asterisk.
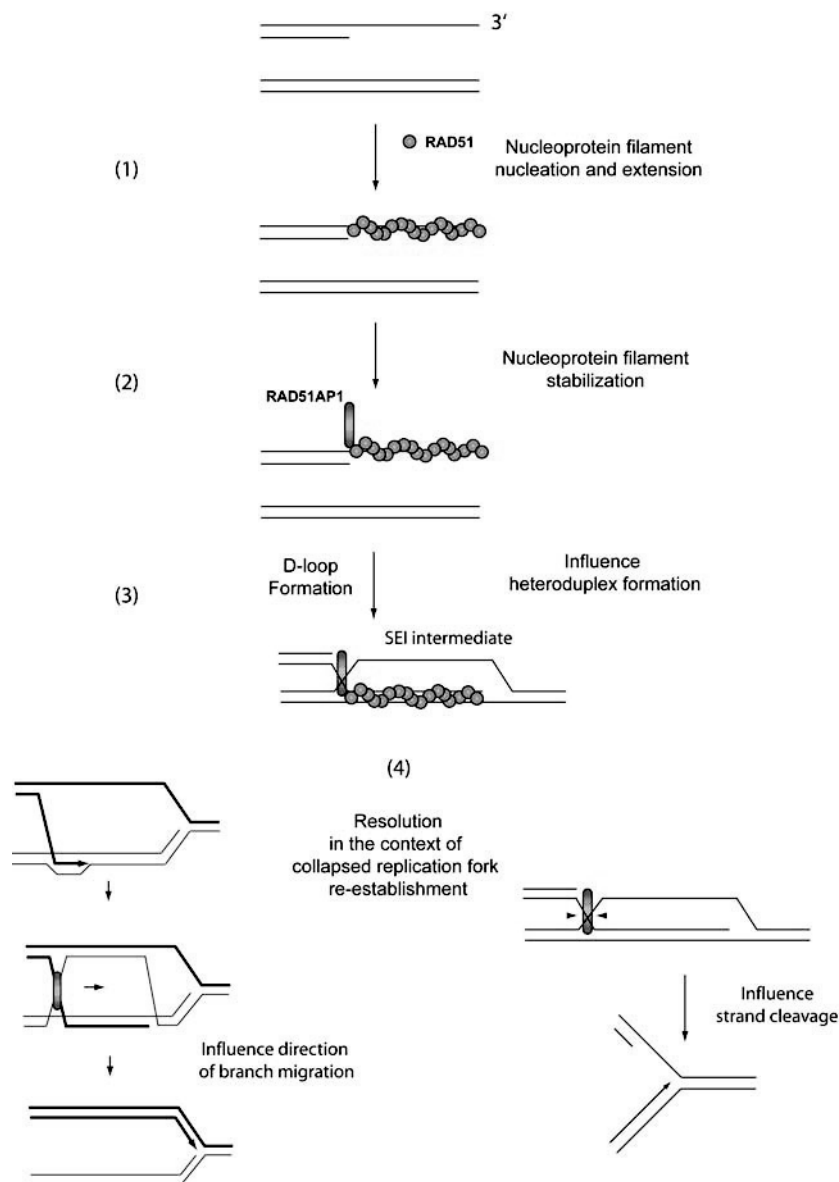
Figure S5. Possible roles of RAD51AP1 during RAD51-mediated homologous recombination.
Steps in homologous recombination for which potential roles of RAD51AP1 are considered in the Discussion. (1) RAD51 nucleoprotein filament nucleation and extension. (2) Stabilization of the RAD51 nucleoprotein filament. (3) Anchoring or sensing during homology recognition by the RAD51 nucleoprotein filament. (4) Resolution of branched intermediates by either affecting direction of branch migration or influencing strand cleavage.

Table S1. Summary of RAD51AP1 deletion mutant analysis.

Primary data is shown in Figure 7.

RAD51AP1 variant	RAD51 binding by in vitro Co-IP	SEI DNA binding by mobility shift assay bound (%) at Protein/ DNA ratio = 50	RAD51 stimulation by D loop assays fold stimulation at RAD51AP1/RAD51 ratio = 0.5
1-352 Wild type	+	100	5.6
Δ327-352	-	100	1.0
Δ1-41	+	100	4.8
Δ1-81	+	100	6.2
Δ1-121	+	100	6.4
Δ1-160	+	100	6.0
Δ1-242	+	100	6.6
Δ1-283	+	0	1.9

Supplemental Experimental Procedures

Antibodies

Rabbit polyclonal antibodies R1085 and R1086 were raised against recombinant human RAD51AP1 and purified using protein A or protein G, respectively (Eurogentec). Guinea pigs polyclonal antibodies GP9 and GP10 were raised against recombinant human RAD51AP1 (Eurogentec). Rabbit polyclonal anti-hRAD51 antibodies (#2307) were described previously (Essers et al., 2002). Mouse anti-RAD51 (#05-530) was obtained from Upstate. Mouse anti-DMC1 (ab11054), rabbit anti-DMC1 (ab18254) and rabbit anti-XRCC3 (ab6494) antibodies were obtained from Abcam. Anti-GRB2 (#610111) was obtained from BD Transduction Laboratories. Anti-KU86 (SC- 1484) was obtained from Santa Cruz Biotechnology. Anti-FANCD2 (NB100-316) was obtained from Novus Biologicals.

Immunoblotting

Cells were directly lysed with SDS sample buffer (2% SDS, 10% glycerol, 60 mM Tris-HCl (pH 6.8)). After the protein concentration was determined by the Lowry protein assay, extracts were supplemented with 0.5% ß-mercaptoethanol and 0.02% bromophenol blue. Equal loading of proteins was independently verified by probing with anti-GRB2 or anti-KU86 antibodies. After fractionation by SDS-PAGE, proteins were transferred to a nitrocellulose membrane. The blots were blocked with PBS / 3% skimmed milk / 0.2% Tween 20 and probed with primary antibodies. After washing with PBS / 0.2% Tween 20, the membranes were probed with the relevant horseradish peroxidase-conjugated secondary antibodies (Jackson Immunoresearch), and developed with ECL Western blotting detection reagents (Amersham Biosciences).

SiRNA-mediated down regulation of RAD51AP1, XRCC3 and RAD51

HeLa cells were cultured in a 1:1 mixture of Dulbecco's modified Eagle's medium (DMEM) and Ham's F10, supplemented with 10% (v/v) fetal calf serum (HyClone) and streptomycin/penicillin, at 37°C in an atmosphere containing 5% CO2. Transfection of siRNA duplexes was carried out using Lipofectamine 2000 (Invitrogen) according to the manufacturer's instructions. HeLa cells were seeded on 60 mm dishes. When confluency reached 20-30%, cultures were transfected with 200 pmoles of siRNA and 10 µl of liposomes per dish. Sense sequences of the RAD51AP1-directed siRNA were (CCUCAUAUCUCUAAUUGCAUU) (#1), (UGAACAAUCUCCGGAAAGAUU) (#2), (GCUGAAAGCAAGAAACCUAUU) (#3), and (GGAUGGCUUUAGAUGACAAUU) (#4). The sense sequence of luciferasedirected siRNA was (CGUACGCGGAAUACUUCGAdTdT). Whole cells extracts were prepared by lysing cells with SDS sample buffer at different time points after transfection. RAD51AP1 down regulation was monitored by immunoblotting. Equal loading of proteins was verified by probing for GRB2. The sense sequence of XRCC3 and RAD51-directed siRNAs were (GGACCUGAAUCCCAGAAUUUU) and (GGGAAUUAGUGAAGCCAAAdTdT), respectively.

Colony survival assays

RAD51AP1, RAD51 or XRCC3 down regulated cells were trypsinized, counted and 1000 cells were seeded onto 60 mm diameter dishes. After a 12 hrs attachment period, cells were treated with increasing doses of misogynic C (Kyowa) for 1 hr, cisplatin (Sigma) for 2 hrs and camptothecin (Sigma) for 12 hrs. Cells were subsequently washed twice with PBS and incubated in fresh media for 7-10 days, after which the colonies were fixed, stained and counted. To determine cellular survival efficiency in response to ionizing radiation, HeLa cells were irradiated with γ-rays from a ^{137}Cs source (0.75 Gy/min). Cells were grown for 7-10 days, fixed, stained, and counted. All measurements were performed in triplicate.

Immunofluorescence

HeLa cells (10 – 20% confluent cultures) were transfected with RAD51AP1-directed siRNAs and 60 hrs after transfection were seeded on glass coverslips, and allowed to attach for 12 hrs. For each transfection, an aliquot of the cells was also seeded on 60 mm dishes and lysed 24 hrs later in SDS sample buffer to verify RAD51AP1 down regulation. Cells were irradiated with a 137Cs source (0.75 Gy/min) and processed 2 hrs later, or treated with 6 µM mitomycin C and processed 12 hrs later. Cells were processed by a 2 min permeabilization step in 0.5% Triton X-100, 20 mM HEPES-KOH (pH 7.9), 50 mM NaCl, 3 mM MgCl2 and 300 mM sucrose, and then fixed in 2% paraformaldehyde for 30 min at room temperature and washed 3 times with PBS. The coverslips were further blocked with PBS containing 0.5% BSA and stained with anti-RAD51 antibodies (#2307 1:2500) for 1 hr at room temperature, washed with PBS containing 0.1% Triton X-100 and incubated with Alexa Fluor 594-conjugated goat anti-rabbit antibodies (Jackson Immunoresearch, 1:1000) for 1 hr at room temperature. The coverslips were mounted in Vectashield containing DAPI (Vector Laboratories) and analyzed with an LSM410 confocal laser-scanning microscope using a Plan-Apochromat 63X N.A. 1.40 oil immersion objective (Carl Zeiss).

Plasmids

The human RAD51AP1 open reading frame (isoform 1) was amplified from IMAGE clone 4107592 by PCR using primers 5'-CGCGGGCCCCATGGTGCGGCCTGTGAGAC and 5'-CGCGCGCTCGAGTCAATGGTGATGGTGATGGTGATGGGTGCTAGTGGCATTTGG. The PCR fragment was digested with NcoI and XhoI and subloned in between the NcoI and XhoI sites of pET28a (Novagen). The RAD51AP1 deletion constructs were generated by subcloning NcoI-XhoI fragments (all with an C-terminal His7 tag) in between the NcoI and XhoI sites of pET28a or pET16b (Novagen). The eGFP-RAD51AP1 fusion construct was generated by subcloning a BglII-XhoI fragment in between the BglII and SalI sites of peGFP-C1 (Clontech). All constructs were verified by DNA sequencing.

Equilibrium sedimentation analysis

Sedimentation equilibrium experiments were conducted at 4.0°C in a Beckman Optima XL-A analytical ultracentrifuge. Samples in 200 mM KCl, 20 mM Tris-HCl (pH 8.0), 1 mM TCEP and 5% (v/v) glycerol were loaded at an initial A280 of 0.90 (90 µM). Data were acquired at 10, 13, 16 and 19 krpm as an average of 4 absorbance measurements at a wavelength of 280 nm and a radial spacing of 0.001 cm. Equilibrium was achieved within 48 hrs. Data were analyzed globally in terms of a single ideal solute using SEDPHAT 4.3 (http://www.analyticalultracentrifugation.com/sedphat/sedphat.htm; Schuck, 2003). Excellent data fits were observed. Solution densities (ρ) were measured at 20.00°C on a Mettler-Toledo DE51 density meter and corrected to values for ρ at 4.0°C; protein partial specific volumes (*v*) were calculated in SEDNTERP (http://www.jphilo.mailway.com/).

Mass spectrometry

Purified RAD51AP1 was either buffer exchanged in a 50 mM ammonium acetate solution or dissolved in methanol at a concentration of 20 µM. Samples were introduced into a quadrupole - time-of-flight mass spectrometer (Q-ToF Ultima; Waters Inc., UK) by means of nanoflow electrospray ionization. Spectra were recorded in the positive ion mode, using a capillary voltage of 1,100 V and a cone voltage of 30 V. The deconvoluted mass was calculated using the MaxEnt 1 module in the MassLynx software (v 4.1, Waters Inc., UK).

Protein crosslinking

RAD51AP1 was buffer exchanged in a buffer containing 2 mM TCEP, 20mM HEPES-KOH (pH 8), 200 mM KCl and 1 mM EDTA. BS3 crosslinker (Pierce) was added at a final concentration of 0.625 mM to 5 µM of RAD51AP1 in a final volume of 40 µl and incubated at room temperature for 30 min. The reaction was quenched by addition of 10 µl of 1M Tris-HCl (pH 7.5) and further incubated for 30 min at room temperature. The reaction mixture was analyzed by reducing SDS-PAGE and Coomassie staining.

In vitro co-immunoprecipitation assays

RAD51 (1µg) (or DMC1) was mixed with RAD51AP1 (1µg) in a volume of 50 µl of binding buffer containing 25 mM Tris-Acetate (pH 7.5), 1 mM DTT, 5% glycerol, 3 mM Mg Acetate, 150 mM KCl and 0.5% NP40 and incubated for 30 min at room temperature. The relevant antibody was then added in a volume of 2 µl and further incubated for 30 min at room temperature. Precipitation was performed by adding 200 µl of protein G sepharose beads suspension prepared by mixing 200 µl of the original bead suspension (Amersham 17-0618-01) with 800 µl of binding buffer supplemented with acetylated BSA and casein (each at 1 mg/ml final concentration). After 1 hr at 4°C, beads were collected by centrifugation, washed six times in binding buffer and analyzed by immunoblotting with the indicated antibodies.

Electrophoretic mobility shift assays

Oligonucleotides used in this study are listed in Supplemental Table 2. Radiolabeled DNA substrates were prepared by 5' end labeling with T4 polynucleotide kinase and annealed as described (Ciccia et al., 2003). Binding reactions (10 µl) containing 20 mM Tris-HCl (pH 7.5), 120 mM KCl (unless indicated otherwise), 5% glycerol, 1 mM DTT, 2 mM EDTA, 0.1 mg/ml acetylated BSA, 0.01% Triton X100 and the indicated concentration of RAD51AP1 and DNA substrate were incubated for 30 min at room temperature. Before addition to the reaction tubes, RAD51AP1 was diluted in 20 mM Tris-HCl (pH 7.5), 300 mM KCl, 10% glycerol, 1 mM DTT, 1 mM EDTA, 0.1 mg/ml acetylated BSA. Reaction mixtures were fractionated by electrophoresis through 6% acrylamide gel in Tris-Borate buffer at 15 V/cm for 60 min unless otherwise indicated. Gels were dried on DEAE paper. Signals were captured by phosphorimaging using a Typhoon scanner and quantified using ImageQuant version 5.2 (Molecular dynamics).

D loop assays

RAD51 (1µM) (or DMC1) was incubated with the relevant 32P-labeled ss DNA (3 µM nt, see Supplemental Table 2) in buffer containing 50 mM Tris-HCl (pH 7.5), 1 mM ATP, 100 µg/ml BSA, 1 mM DTT, 2 mM MgCl2 and 30 mM KCl (added with the protein stock) in a volume of 20 µl. After 5 min at 37°C, RAD51AP1 was added at the indicated concentration in a volume of 2 µl and the reaction was further incubated for 5 min. D loop formation was initiated by addition of supercoiled pUC19 ds DNA (90 µM nt). After incubation at 37°C for 30 min, reactions were stopped by addition of 5 µl of 0.5% SDS, 50 mM EDTA, 30% glycerol. Samples were deproteinized by addition of 2 µl of proteinase K (10 mg/ml) and incubation for 15 min at 37°C. Reaction mixtures were fractionated by 0.6% agarose gel electrophoresis in Tris-Borate buffer. Gels were dried on DEAE paper. Signals were captured by phosphorimaging using a Typhoon scanner and quantified using ImageQuant version 5.2 (Molecular dynamics). Given the low levels of the intrinsic RAD51 D loop formation efficiency under Mg2+ / ATP conditions, accurate measurements of the absolute yield of product of this baseline reaction are difficult to obtain as described previously (Bugreev and Mazin, 2004).

Table S2. DNA oligonucleotides used in this study.

Oligo name	Oligo sequence 5' to 3'	design
SK3	AATTCTCATTTTACTTACCGGACGCTATTAGCAGTGGCAGATTGTACTGAG AGTGCACCATATGCGGTGTGAAATACCGCACAGATGCGT	(Mazin et al., 2000)
SK3NT	GCAGTGGCAGATTGTACTGAGAGTGCACCATATGCGGTGTGAAATACCGC ACAGATGCGT	This study
SK3-c	TAATACCGTCCGGTAAGTAAAATGAGAATT	This study
NHA	CTTTAGCTGCATATTTACAACATGTTGACCTACAGCACCAGATTCAGCAAT TAAGCTCTAAGCCATCCGCAAAAATGACCTCTTATCAAAAGGA	Communicated by Alex Mazin
NHB	ACAGCACCAGATTCAGCAATTAAGCTCTAAGCCATCCGCAAAAATGACCTC TTATCAAAAGGA	Communicated by Alex Mazin
# 4	GCCAGGGACGGGGTGAACCTGCAGGTGGGCGGCTGCTCATCGTAGGTTA GTATCGACCTATTGGTAGAATTCGGCAGCGTCATGCGACGGC	(McIlwraith et al., 2005)
# 5	GCCGTCGCATGACGCTGCCGAATTCTACCACGCTACTAGGGTGCCTTGCT AGGACATCTTTGCCCACCTGCAGGTTCACCCCGTCCCTGGC	(McIlwraith et al., 2005)
# 5-c	GCCAGGGACGGGGTGAACCTGCAGGTGGGCAAAGATGTCCTAGCAAGGC ACCCTAGTAGCGTGGTAGAATTCGGCAGCGTCATGCGACGGC	(McIlwraith et al., 2005)
# 6	AAGATGTCCTAGCAAGGCACCCTAGTAGC	(McIlwraith et al., 2005)
J1	TATGATTAGTCTAGGATTCTATTATCTATTAAGATGTCCTAGCAAGGCACCC TAGTAGC	This study

J2	AATAGATAATAGAATCCTAGACTAATCATA	This study
X0-1	GACGCTGCCGAATTCTACCAGTGCCTTGCTAGGACATCTTTGCCCACCTGCAGGTTCACCC	(Ciccia et al., 2003)
X0-2	TGGGTGAACCTGCAGGTGGGCAAAGATGTCCATCTGTTGTAATCGTCAAGCTTTATGCCGTT	(Ciccia et al., 2003)
X0-3	GAACGGCATAAAGCTTGACGATTACAACAGATCATGGAGCTGTCTAGAGGATCCGACTATCGA	(Ciccia et al., 2003)
X0-4	ATCGATAGTCGGATCCTCTAGACAGCTCCATGTAGCAAGGCACTGGTAGAATTCGGCAGCGT	(Ciccia et al., 2003)
2-c	TGGGTGAACCTGCAGGTGGGCAAAGATGTCC	(Ciccia et al., 2003)
3-c	CATGGAGCTGTCTAGAGGATCCGACTATCGA	(Ciccia et al., 2003)
X0-1c	GGGTGAACCTGCAGGTGGGCAAAGATGTCCTAGCAAGGCACTGGTAGAATTCGGCAGCGTC	This study
X0-13'	AAAGATGTCCTAGCAAGGCACTGGTAGAATTCGGCAGCGTC	This study
X26-1	CCGCTACCAGTGATCACCAATGGATTGCTAGGACATCTTTGCCCACCTGCAGGTTCACCC	(Constantinou et al., 2001)
X26-2	TGGGTGAACCTGCAGGTGGGCAAAGATGTCCTAGCAATCCATTGTCTATGACGTCAAGCT	(Constantinou et al., 2001)
X26-3	GAGCTTGACGTCATAGACAATGGATTGCTAGGACATCTTTGCCGTCTTGTCAATATCGGC	(Constantinou et al., 2001)
X26-4	TGCCGATATTGACAAGACGGCAAAGATGTCCTAGCAATCCATTGGTGATCACTGGTAGCGG	(Constantinou et al., 2001)
1	TGGGTGAACCTGCAGGTGGGCAAAGATGTCCATCTGTTGTAATCGTCAAG	This study

	CTTTATGCCGTT	
2	TGGGTGAACCTGCAGGTGGGCAAAGATGTCCACGCTAGCATGAGCATGG GATGACATGGATT	This study
3	TGGGTGAACCTGCAGGTGGGCAAAGATGTCCTTTTTTTTTTTTTTTTTTTTT TTTTTTTTTT	This study
4	TGGGTGAACCTGCAGGTGGGCAAAGATGTCCCGGCATGGACTGGGGGTA GCAGGTAGCGCAA	This study
5	ATCGATAGTCGGATCCTCTAGACAGCTCCATGTAGCAAGGCACTGGTAGA ATTCGGCAGCGT	This study
6	ATTAGGATGGATGGGGATGGGATGATGGATTCTAGCAAGGCACTGGTAGA ATTCGGCAGCGT	This study
7	ACGCAGCGCGCAGGGGGGGAGGGGGACCGCAATAGCAAGGCACTGGTA GAATTCGGCAGCGT	This study
8	ATATTTTATTTTTTTATTTTTTTTATTTTATTTTAGCAAGGCACTGGTAGAATTC GGCAGCGT	This study

Supplemental References

Bugreev, D. V., and Mazin, A. V. (2004). Ca2+ activates human homologous recombination protein Rad51 by modulating its ATPase activity. Proc. Natl. Acad. Sci. U S A *101*, 9988-9993.

Ciccia, A., Constantinou, A., and West, S. C. (2003). Identification and characterization of the human MUS81-EME1 endonuclease. J. Biol. Chem. *278*, 25172-25178.

Constantinou, A., Davies, A. A. and West, S. C. (2001). Branch Migration and Holliday Junction Resolution Catalyzed by Activities from Mammalian Cells. Cell *104*, 259-268.

Essers, J., Hendriks, R. W., Wesoly, J., Beerens, C. E., Smit, B., Hoeijmakers, J. H., Wyman, C., Dronkert, M. L., and Kanaar, R. (2002). Analysis of mouse Rad54 expression and its implications for homologous recombination. DNA Repair (Amst) *1*, 779-793.

Gurtan, A. M., and D'Andrea, A. D. (2006). Dedicated to the core: understanding the Fanconi anemia complex. DNA Repair (Amst) *5*, 1119-1125.

Henson, S. E., Tsai, S. C., Malone, C. S., Soghomonian, S. V., Ouyang, Y., Wall, R., Marahrens, Y., and Teitell, M. A. (2006). Pir51, a Rad51-interacting protein with high expression in aggressive lymphoma, controls mitomycin C sensitivity and prevents chromosomal breaks. Mutat Res *601*, 113-124.

Mazin, A. V., Zaitseva, E., Sung, P., and Kowalczykowski, S. C. (2000). Tailed duplex DNA is the preferred substrate for Rad51 protein-mediated homologous pairing. EMBO J. *19*, 1148-1156.

McIlwraith, M. J., Vaisman, A., Liu, Y., Fanning, E., Woodgate, R., and West, S. C. (2005). Human DNA polymerase eta promotes DNA synthesis from strand invasion intermediates of homologous recombination. Mol. Cell *20*, 783-792.

Schuck, P. (2003). On the analysis of protein self-association by sedimentation velocity analytical ultracentrifugation. Anal. Biochem. *320*, 104-124.

Abbreviations

aa	amino-acid		GFP	green fluorescent protein
AT	ataxia telangiectasia		Gy	Gray
ATM	ataxia telangiectasia mutated		h	human
ATP	adenosine 5'-triphosphate		HJ	Holliday Junction
ATR	ataxia telangiectasia- and Rad3-related		HR	homologous recombination
ATRIP	ATR-interacting protein		hrs	hours
bp	base pair		HU	hydroxyurea
BrdU	bromodeoxyuridine		ICL	interstrand crosslink
C-	carboxy-		IdU	iododeoxyuridine
CAK	CDK-activating kinase		kb	kilo base pairs
CCC	cell cylce checkpoint		m	mouse
cDNA	complementary DNA		MMC	mitomycin C
CDI	CDK inhibitor		MMS	methyl methanesulfonate
CDK	cyclin-dependent kinase		MRN	MRE11/RAD50/NBS1
ChIP	chromatin immunoprecipitation		N-	amino-
CIdU	chlorodeoxyuridine		NBS1	Nijmegen breakage syndrom protein 1
CPD	cyclobutane pyrimidine dimer		NER	nucleotide excision repair
Da	dalton		ORC	origin recognition complex
dCMP	deoxycytidine monophoshate		PAGE	polyacrylamide gel electrophoresis
DDK	Dbf-dependent kinase		PBS	phosphate buffered saline
D-loop	displacement-loop		PCNA	proliferating cell nuclear antigen
DNA	deoxyribonucleic acid		PCR	polymerase chain reaction
dNTP	deoxyribonucleotide triphosphate		PI	propidium iodine
DSB	doube-stranded break		PI3K	phosphatidylinositol 3-kinase
E.coli	Escherichia coli		PIKK	PI3K-like protein kinase
ES	embryonic stem		PLK1	Polo-like kinase 1
FACS	fluorescence-activated cell sorting		Pol	DNA polymerase

162

pre-RC	pre-replicative complex		SSB	single-stranded break
RFC	replication factor C		ssDNA	single-stranded DNA
RPA	replication protein A		TLS	translesion synthesis
S.cerevisiae	Sacchromyces cerevisiae		TopBP1	topoisomerase IIß binding protein 1
S.pombe	Sacchromyces pombe		UV-light	ultraviolet light
SDSA	synthesis-dependent strand annealing		XP-V	xeroderma pigmentosum variant
SEI	single-end invasion intermediate		6-4 PP	pyrimidine-(6,4)-pyrimidone adduct
SSA	single-strand annealing			

Summary

DNA is constantly damaged by exogenous and endogenous agents. If unrepaired, DNA damage can cause mutations and chromosomal aberrations, which can lead to cell dysfunction and death. In the long term, accumulated damage contributes to aging and increases the probability of malignant transformation and cancer development. Therefore, correct response to DNA damage is essential for survival and proper function of cells and organisms. The first part of **Chapter 1** describes the signaling pathways, called checkpoints, which sense DNA damage and/or replication problems and coordinate the cellular damage response. Checkpoint cascades regulate cell cycle proteins to stop or delay cell cycle progression in order to give the cell sufficient time to repair the damage. In mammalian cells checkpoint activation is controlled by two related kinases: ATM and ATR. ATM is activated mainly by DSBs in a complex process involving changes in chromatin structure, ATM acetylation and autophosphorylation, interaction with the MRN complex, and recruitment of ATM to DSBs. ATR responds to a wide range of DNA damaging agents and replication inhibition. Its activation requires cooperation of several proteins: RPA, RAD17, RAD1, RAD9, HUS1, TopBP1 and Claspin. The ATR branch of checkpoint signaling is essential for cell viability.

DNA damage is particularly dangerous when it occurs in S-phase, since lesions present in the DNA template may interfere with efficiency and precision of DNA replication. They can lead to stalling of replication forks and cause mutations, which will be inherited by daughter cells. Therefore, cells need mechanisms that would efficiently overcome replication problems. Two main pathways implicated in restarting the stalled replication forks: homologous recombination (HR) and translesion synthesis (TLS) are described in the second part of **Chapter 1**. HR uses an intact sister chromatid as a template for repair and is therefore essentially error-free. The main protein involved in catalyzing the recombination reactions in eukaryotic cells is RAD51. The action of RAD51 is regulated during every step of recombination by a number of essential accessory proteins. During the process of TLS specialized, low-fidelity polymerases are recruited to the replication forks stalled at lesions, which replicative polymerases cannot bypass. Ubiquitination of PCNA at the stalled fork induces polymerase switch, as a result of which TLS polymerases transiently gain access to the DNA template. They synthesize a short DNA fragment opposite the lesion, after which the regular polymerases can resume high-fidelity DNA replication.

The research described in this thesis addresses several aspects of the cellular response to replication problems. Chapters 2 and 3 describe the effect of Rad17 N-terminal truncation on the checkpoint signaling and DNA damage repair. Chapters 4 and 5 focus on the role of the structure-specific endonuclease Mus81 in processing stalled replication forks. Chapter 6 introduces a novel regulator of HR – RAD51AP1 and analyzes mechanisms by which it stimulates HR and promotes repair of replication-associated DSBs.

The aim of the research described in **Chapter 2** was to investigate the effect of Rad17 deletion in mice and mouse cells. The knock out strategy involved introducing a deletion in the *Rad17* locus, which would result in *Rad17* null allele. As mentioned above, ATR signaling pathway is essential for cell viability. Consistently, Rad17-

deficient embryos suffered major developmental abnormalities and died between day 8.5 and 11.5 of embryonic development. Surprisingly, embryonic stem cells isolated from 3.5 day embryos were able to use an alternative starting codon downstream of the deletion introduced in *Rad17* locus. As a result, they expressed N-terminally truncated Rad17 (5'Δ Rad17), lacking the first 78 amino acids. Although the Rad17$^{5'\Delta/5'\Delta}$ cells were viable, they were hypersensitive to a wide range of DNA damaging agents, including ionizing radiation, UV-light, mitomycin C (MMC), methyl methanesulfonate, and hydroxyurea. The hypersensitivity was not caused by a checkpoint defect, since both wild type and Rad17$^{5'\Delta/5'\Delta}$ cells were equally able to delay cell cycle progression after treatment with ionizing radiation and MMC. This data suggested that Rad17, in addition to its role in checkpoint signaling, might be directly involved in DNA damage processing and/or repair. The hypersensitivity of Rad17$^{5'\Delta/5'\Delta}$ cells to many different damaging agents indicates that Rad17 could be involved in a step shared by many repair pathways. Interestingly, homologous gene targeting was drastically reduced in Rad17$^{5'\Delta/5'\Delta}$ cells. It suggests that Rad17 could play a role in HR-mediated repair of stalled replication forks. However, the exact role of Rad17 in this process remains speculative.

In **Chapter 3** the response of Rad17$^{5'\Delta/5'\Delta}$ cells to replication inhibition was investigated in more detail. Rad17$^{5'\Delta/5'\Delta}$ cells were hypersensitive to hydroxyurea, aphidicolin, camptothecin and etoposide, all of which cause replication fork stalling by different mechanisms. Consistently with our previous observations, Rad17$^{5'\Delta/5'\Delta}$ cells did not show a checkpoint dysfunction resulting in premature entry into mitosis. In contrast, Rad17$^{5'\Delta/5'\Delta}$ cells treated with replication inhibitors and subsequently allowed to resume cell cycle progression stayed longer in G2 phase compared to wild type cells. They also showed prolonged checkpoint activation, as measured by Chk1 phosphorylation, and accumulated more HU-induced DSBs that wild type cells. This data further supports the possibility that Rad17 is directly involved in recovery of stalled replication forks.

Chapter 4 describes the role of Mus81 in the cellular response to crosslinking agents. Repair of interstrand crosslinks (ICLs) and restart of replication forks stalled by ICLs is a complex process, which requires cooperation of distinct repair pathways and involves generation of DSBs as intermediates. The latter process is replication-dependent, which suggests that DSB might be formed at the sites of stalled replication forks. A likely candidate for generating these DSBs is Mus81/Eme1 complex. It is a structure specific endonuclease, which cleaves branched DNA structures resembling replication and recombination intermediates. Indeed, the data presented in Chapter 4 shows that the formation of MMC- and cisplatin-induced DSBs, as measured by pulsed field gel electrophoresis, is inhibited in Mus81-deficient cells. Mus81$^{-/-}$ cells were hypersensitive to both MMC and cisplatin, indicating that Mus81-mediated DSB formation promotes cell survival after treatment with crosslinking agents. However, since DSBs are dangerous DNA lesions, they should be processed correctly and efficiently to avoid further DNA damage. Interestingly, immunoprecipitation experiments and survival assays indicate that Mus81 interacts both physically and genetically with HR protein Rad54. This interaction could serve to limit the toxicity of Mus81-generated DSBs by channeling them directly into HR-mediated repair.

The evidence presented in **Chapter 5** shows that Mus81 is involved in

166

generating DSBs in response to replication inhibition caused by hydroxyurea and aphidicolin. In contrast to wild type cells, Mus81-deficient cells failed to induce DSBs after treatment with both of these agents. Mus81$^{-/-}$ cells were hypersensitive to hydroxyurea and aphidicolin, indicating that Mus81-dependent DSB formation is physiologically relevant. Consistent with this notion, the recovery of replication forks stalled by hydroxyurea treatment, measured using the DNA fiber technique, was reduced in Mus81$^{-/-}$ cells. These cells also showed increased levels of hydroxyurea-induced chromosomal abnormalities, which included gaps, breaks and chromosomal fusions. This data suggests that Mus81 plays an important role in maintaining genomic stability following replication problems.

Chapter 6 describes a novel protein, RAD51AP1, involved in regulating RAD51-mediated HR and shows that RAD51AP1 is required for efficient cellular response to interstrand DNA crosslinking agents and other DSB-inducing agents, including ionizing radiation and camptothecin. Analysis of RAD51 foci formation indicates that RAD51AP1 affects HR differently than mediators identified so far. Depletion of RAD51AP1 did not affect RAD51 foci formation, while cells deficient in XRCC3 or in another HR mediator - BRCA2 failed to induce RAD51 foci after DNA damage. *In vitro* experiments show that RAD51AP1 physically interacts with RAD51. It is also a structure-specific DNA-binding protein, which has a selective affinity for branched-DNA structures that are obligatory intermediates in homologous recombination. RAD51AP1 stimulates joint molecule formation catalyzed by RAD51, and both RAD51 and DNA binding is required for the stimulation.

Samenvatting

Het DNA in onze cellen wordt continu beschadigd door exogene en endogene factoren. Indien deze beschadigingen niet gerepareerd worden, kunnen ze mutaties en chromosomale afwijkingen veroorzaken. Dit kan leiden tot abnormaal functioneren van de cel en celdood. Op de lange termijn draagt geaccumuleerde schade bij aan veroudering en verhoogt het de kans op kwaadaardige transformatie en de ontwikkeling van kanker. Daarom is een correcte reactie op DNA-schade essentieel voor de overleving en de juiste functie van cellen en organismen. Het eerste deel van **Hoofdstuk 1** beschrijft de signaaltransductieroutes, checkpoints (controlepunten) genaamd, die DNA-schade en/of replicatieproblemen detecteren en de cellulaire response hierop coördineren. Deze checkpoint routes reguleren celcycluseiwitten om de progressie door de celcyclus te stoppen of te vertragen, zodat de cel voldoende tijd krijgt om de schade te repareren. In zoogdiercellen staat checkpoint activering onder de controle van twee gerelateerde kinases: ATM en ATR. ATM wordt met name geactiveerd door dubbelstrengs breuken (DSB) in een ingewikkeld proces waarbij veranderingen in de chromatine structuur, acetylering en autofosforylering van ATM, interactie met het MRN complex en de migratie van ATM naar DSB, betrokken zijn. ATR reageert op een ruim scala aan factoren die het DNA beschadigen en de replicatie remmen. Voor de activering van ATR is de samenwerking van verschillende eiwitten nodig, zoals RPA, RAD17, RAD1, RAD9, HUS1, TopBP1 en Claspin. De ATR tak van checkpoint-signalering is ook essentieel voor de overleving van de cellen.

DNA-schade is in het bijzonder gevaarlijk tijdens S-fase, aangezien dan een beschadiging in het DNA de efficiency en nauwkeurigheid van de DNA-replicatie kan beïnvloeden. Dit kan leiden tot het vastlopen van replicatievorken maar ook tot mutaties die door de dochtercellen worden geërfd. Daarom hebben cellen mechanismen nodig die deze replicatieproblemen helpen te voorkomen. Homologe recombinatie (HR) en translesie synthese (TLS), de twee voornaamste processen die betrokken zijn bij het opnieuw opstarten van vastgelopen replicatievorken, worden beschreven in het tweede deel van **Hoofdstuk 1**. HR gebruikt het intacte zuster-chromatide als een soort mal voor reparatie van de schade en werkt daardoor vrijwel foutloos. In eukaryote cellen is RAD51 het centrale eiwit dat betrokken is bij de katalyse van deze recombinatiereacties. De werking van Rad51 wordt tijdens elke stap van de recombinatie gereguleerd door verschillende andere essentiële eiwitten. Tijdens het proces van TLS worden gespecialiseerde, maar zeker niet foutloze, polymerases aangetrokken naar de vastgelopen replicatievorken, waar de reguliere DNA-polymerases zijn gestopt. Ubiquitinering van PCNA bij de vastgelopen replicatievorken leidt tot een omschakeling van de polymerases, waardoor de TLS-polymerases tijdelijk toegang krijgen tot het DNA. Deze speciale polymerases synthetiseren dan een kort DNA- fragment tegenover de beschadiging, waarna de reguliere polymerases de betrouwbare DNA-replicatie kunnen hervatten.

Het onderzoek, zoals beschreven in dit proefschrift, behandelt verschillende aspecten van de cellulaire respons op replicatieproblemen. In de hoofdstukken 2 en 3 wordt het effect van deletie van een deel van de N-terminus van Rad17 op checkpoint-signaaltransductie en DNA-schadeherstel beschreven. Hoofdstukken 4 en 5 richten zich op de functie van het structuurspecifieke Mus81-endonuclease tijdens het verwerken van vastgelopen replicatievorken. In hoofdstuk 6 wordt een

nieuwe regelaar van HR, RAD51AP1, geïntroduceerd en worden de mechanismen geanalyseerd waarmee dit eiwit HR stimuleert en bijdraagt aan het herstel van DSB, die tijdens de replicatie ontstaan.

Hoofdstuk 2 beschrijft het onderzoek van het effect van een deletie in Rad17 in muizen en muizencellen. De 'knock out'-strategie bestond uit het introduceren van een deletie in de *Rad17* locus, wat zou resulteren in een niet functioneel *Rad17* allel. Zoals eerder beschreven is de ATR-signaaltransductieroute essentieel voor de celgroei. Hiermee overeenkomend hebben Rad17-deficiente embryo's grote ontwikkelingstoornissen en overlijden ze tussen dag 8.5 en 11.5 van de embryonale ontwikkeling. Verrassend was dat de embryonale stamcellen, geïsoleerd van 3.5 dag oude embryo's, gebruik konden maken van een alternatief startcodon, wat gelegen was na de geïntroduceerde deletie in de *Rad17* locus. Ten gevolge hiervan brachten ze een alternatief Rad17 eiwit tot expressie dat de eerste 78 aminozuren mist (5'D Rad17). De Rad17$^{5'\Delta/5'\Delta}$ cellen leefden, maar waren wel overgevoelig voor een groot scala aan reagentia die DNA schade veroorzaken, inclusief ioniserende straling, UV-licht, mitomycine C, methyl methanesulfonate, and hydroxyurea. Aangezien zowel de wildtype als de Rad17$^{5'\Delta/5'\Delta}$ cellen de celcyclusprogressie na de behandeling met ioniserende straling en mitomycine C konden vertragen, werd deze overgevoeligheid niet veroorzaakt door een defect in het checkpoint. Deze data suggereren dat Rad17, naast een rol in checkpoint-signalering, mogelijk ook direct betrokken is bij de verwerking of reparatie van de DNA-schade. De overgevoeligheid van Rad17$^{5'\Delta/5'\Delta}$ cellen voor zoveel verschillende DNA-schade-veroorzakende reagentia laat zien dat Rad17 betrokken kan zijn in een stap die gedeeld wordt door meerdere herstelroutes. Het was interessant om te zien dat homologe 'gene targeting' dramatisch verminderd was in Rad17$^{5'\Delta/5'\Delta}$ cellen. Dit wijst erop dat Rad17 een rol zou kunnen spelen in de reparatie van vastgelopen replicatievorken door HR. De exacte functie van Rad17 in dit proces blijft echter speculatief.

In **Hoofdstuk 3** wordt de respons van Rad17$^{5'\Delta/5'\Delta}$ cellen op de remming van de replicatie meer in detail beschreven. Rad17$^{5'\Delta/5'\Delta}$ cellen waren overgevoelig voor hydroxyurea, aphidicolin, camptothecin en etoposide, welke allemaal het vastlopen van replicatievorken veroorzaken. In overeenstemming met de eerdere bevindingen lieten Rad17$^{5'\Delta/5'\Delta}$ cellen geen ontregeld checkpoint zien, wat tot een vroegtijdige mitose zou leiden. Rad17$^{5'\Delta/5'\Delta}$ cellen die eerst behandeld waren met replicatieinhibitors, en vervolgens de celcyclusprogressie weer hervatten, bleven echter langer in G2 fase dan de controlecellen. Ze lieten ook een verlengde activering van het checkpoint zien, gemeten door Chk1-fosforylering, en hoopten meer HU-geïnduceerde DSB op dan de controlecellen. Deze bevindingen ondersteunen de mogelijkheid dat Rad17 direct betrokken is bij het herstel van vastgelopen replicatievorken.

In **Hoofdstuk 4** wordt de functie van Mus81 beschreven in de cellulaire respons op stoffen die crosslinking van het DNA veroorzaken. Het herstel van 'interstand crosslinks' (ICLs) en het opnieuw opstarten van replicatievorken die zijn vastgelopen door ICLs is een ingewikkeld proces, waarvoor de samenwerking van verschillende herstelroutes nodig zijn. Tijdens dit proces worden DSB gegenereerd op een manier die afhankelijk is van replicatie, wat suggereert dat DSB gevormd kunnen worden op plaatsen waar replicatievorken vastlopen. Het Mus81/Eme1-

complex is een mogelijke kandidaat voor het genereren van deze DSB. Mus81/Eme1 is een structuurspecifiek endonuclease dat speciale DNA-structuren knipt, die op structuren lijken die tijdens replicatie en recombinatie ontstaan. De data, beschreven in Hoofdstuk 4, laten inderdaad zien dat de vorming van MMC- en cisplatin-geïnduceerde DSB, gemeten met behulp van pulse-field gel elektroforese, wordt geremd in cellen die geen Mus81 hebben. Deze cellen zijn overgevoelig voor zowel MMC als cisplatin. Dit wijst erop dat DSB-vorming, gekatalyseerd door Mus81, helpt in de overleving van cellen na behandeling met reagentia die crosslinks veroorzaken. Maar omdat DSB gevaarlijke DNA-beschadigingen zijn, moeten ze echter wel op een correcte en efficiënte manier verwerkt worden om verdere DNA-schade te voorkomen. Immunoprecipitatie-experimenten lieten zien dat Mus81 bindt aan het HR eiwit Rad54 en uit overlevingsproeven blijkt dat deze eiwitten in dezelfde route functioneren. Deze interactie zou ervoor kunnen zorgen dat de toxiciteit van DSB, gegenereerd door Mus81, wordt beperkt door deze DSB direct door te sturen naar DNA-reparatie door HR.

Het resultaat van het onderzoek, gepresenteerd in **Hoofdstuk 5,** laat zien dat Mus81 betrokken is bij het genereren van DSB door de remming van de replicatie door hydroxyurea en aphidicolin. In tegenstelling tot normale cellen kunnen Mus81-deficiente cellen geen DSB genereren na behandeling met deze reagentia. Cellen die geen Mus81 hebben zijn overgevoelig voor hydroxyurea en aphidicolin, wat het belang van de vorming van DSB door Mus81 laat zien. Het herstel van replicatievorken, die zijn vastgelopen door behandeling met hydroxyurea, gemeten door de 'DNA fiber'-techniek, is verminderd in Mus81-deficiente cellen, wat in overeenstemming is met de eerdere data. Deze cellen laten ook meer chromosomale afwijkingen, zoals gaten, breuken en chromosomale fusies, na de behandeling met hydroxyurea zien. Deze data geven de aanwijzing dat Mus81 een belangrijke rol speelt bij het behouden van de stabiliteit van het genoom na replicatieproblemen.

In **Hoofdstuk 6** wordt RAD51AP1 beschreven: een nieuw eiwit betrokken bij de regulatie van HR door RAD51. De resultaten laten zien dat RAD51AP1 nodig is voor de cellulaire respons op interstrand DNA crosslinking reagentia en andere reagentia die DSB induceren, inclusief ioniserende straling en camptothecin. Analyse van de vorming van RAD51-foci (eiwit accumulaties/ophopingen op beschadigd DNA) laat zien dat RAD51AP1 HR op een andere manier beïnvloedt dan de tot nu toe geïdentificeerde regulerende eiwitten. Het verlagen van cellulaire RAD51AP1 niveau had geen effect op de vorming van RAD51 foci, terwijl cellen zonder XRCC3 of BRCA2, een andere regulator van HR, geen RAD51 foci kunnen vormen. Experimenten in de reageerbuis laten zien dat RAD51AP1 en RAD51 een interactie aangaan. RAD51AP1 is een eiwit dat aan speciale structuren van het DNA bindt en heeft een specifieke affiniteit voor vertakte DNA structuren die ontstaan tijdens het proces van HR. RAD51AP1 stimuleert joint-molecuulvorming door RAD51, waarvoor zowel binding aan RAD51 als DNA nodig zijn.

Vertaling: Veronique Smits
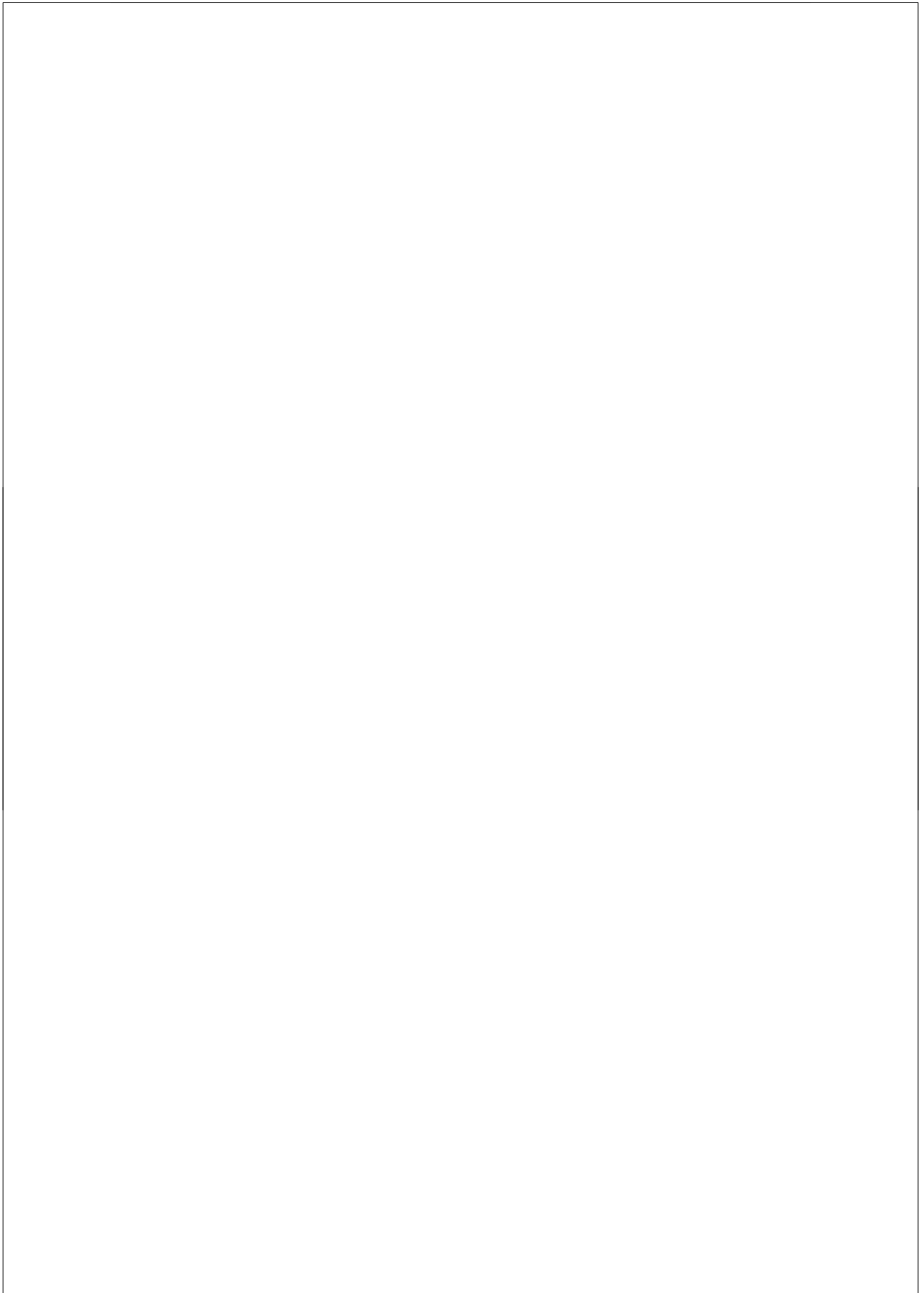
Curriculum Vitae

Name   Magdalena Budzowska

Birth date   24 August 1978

Birth place   Krakow, Poland

Education and Research
_____

March 2007   Postdoctoral fellow in the Kanaar laboratory,
- present   Department of Cell Biology and Genetics, Erasmus
                        Medical Center, Rotterdam, the Netherlands.

November 2002   PhD student at the Department of Cell Biology and
- Ferbruary 2007   Genetics, Erasmus Medical Center, Rotterdam, the
                        Netherlands.
                        Promotors: professor Roland Kanaar and professor Jan
                        Hoeijmakers

September 2001   Master student at the Institute of Genetics and
– March 2002   Microbiology, Ludwig Maximilians University, Munich,
                        Germany.
                        Supervisor: professor Wolfhard Bandlow

Ferburary 2001   Exchange student at the Institute of Genetics and
- June 2001   Microbiology, Ludwig Maximilians University, Munich,
                        Germany.

October 1997   Student of biotechnology at the Jagiellonian University,
– June 2002   Krakow, Poland

September 1993   Secondary School in Bielsko-Biala and Krzeszowice,
– June 1997   Poland

List of publications

Modesti M, **Budzowska M**, Baldeyron C, Demmers JA, Ghirlando R, Kanaar R (2007) RAD51AP1 is a Structure-Specific DNA Binding Protein that Stimulates Joint Molecule Formation during RAD51-Mediated Homologous Recombination.
Mol Cell, 28: 468-81

Hanada K, **Budzowska M**, Davies SL, van Drunen E, Onizawa H, Beverloo HB, Maas A, Essers J, Hickson ID, Kanaar R (2007) Involvement of the structure-specific endonuclease Mus81 in double-strand DNA break-dependent replication restart.
Nat Struct Mol Biol, 14: 1096-104

Hanada K, **Budzowska M**, Modesti M, Maas A, Wyman C, Essers J, Kanaar R (2006) The structure specific endonuclease Mus81-Eme1 promotes conversion of interstrand DNA crosslinks into double-strands breaks.
EMBO J. 25: 4921-32
K. Hanada and M. Budzowska contributed equally to this work

Budzowska M, Jaspers I, Essers J, de Waard H, van Drunen E, Hanada K, Beverloo B, Hendriks RW, de Klein A, Kanaar R, Hoeijmakers JH, Maas A (2004) Mutation of the mouse Rad17 gene leads to embryonic lethality and reveals a role in DNA damage-dependent recombination.
EMBO J. 23: 3548-58.

Niedernhofer LJ, Odijk H, **Budzowska M**, van Drunen E, Maas A, Theil AF, de Wit J, Jaspers NG, Beverloo HB, Hoeijmakers JH, Kanaar R (2004) The structure-specific endonuclease Ercc1-Xpf is required to resolve DNA interstrand cross-link-induced double-strand breaks.
Mol Cell Biol. 24: 5776-87.

Rutzler M, Reissaus A, **Budzowska M**, Bandlow W (2004) SUT2 is a novel multicopy suppressor of low activity of the cAMP/protein kinase A pathway in yeast.
Eur J Biochem. 271: 1284-91

Acknowledgements

Acknowledgements

Thinking of my time in the Department of Genetics I feel very grateful for everything I experienced here and all the people I have met. I have learned a lot and changed a lot and I would like to thank everybody who has been part of this process and part of my life here.

First of all I would like to thank my promotors, without whom this PhD project would not be possible.

Jan, I admire your enthusiasm for science, your ability to extract interesting points and questions from any presented topic, and the ability to make people think, all of which made discussions with you an excellent experience. I was also impressed by your way of managing conflicts and I have learned a lot from it.

Being a PhD student is not always easy and a good environment is essential to stay motivated and keep going. Roland, I found such environment in your lab. You have given me the opportunity to develop and it is difficult to express how grateful I am for this. Thank you for your constant support, excellent supervision and for always having time to discuss experiments and ideas. Also many thanks for your enormous patience in correcting my thesis and my incurable spelling mistakes. I am surprised you did not get confused by all my versions of "camtothecin" ☺. Being in your lab was a great experience. Thank you!

When I now think back to my first year in Rotterdam, I am amazed how ignorant I was at that time. And I owe many thanks to Alex for being there to answer my questions and to help me when I was completely lost in the department, for teaching me how to work with mammalian cells, and for providing me with knowledge which later I could build on. I am sorry about the problems we had later and I am happy things are working out well in your new lab.

Many thanks to the members of my promotion committee, especially Claire, Harry and Titia, for critically reading the manuscript and for the comments that helped to improve it.

I would like to thank all the present and past lab members: Sheba, Berina, Eddy, Humberto, Dejan, Kris, Hanny, Jeroen, Maurice, Aude, Mike, Céline, Linda, Jaqueline, Gusia, Paula, Martijn, Sari, Ellen and Iris for the friendly atmosphere, help and support. It was a pleasure working with you!

Especially many thanks to Cecile, for always being there, ready to drop whatever you were doing and help people out.

I had a great time in lab 659 thanks to Veronique, Joyce, Mauro, Daniël, Edward, Esther, Katsu and Kumiko. Thank you for great atmosphere, for all the jokes and (scientific) discussions, for helping me to keep my spirits up when I was panicking before presentations, and even for constantly insisting that it is all my fault ☺.